

Exploring the Structure, Function & Regulation of the Human Glucagon-Like Peptide-1 Receptor

Thesis submitted for the degree of Doctor of Philosophy
at the University of Leicester

by

Yan Huang MD, M.Sc.

Department of Cell Physiology and Pharmacology
University of Leicester

September 2010

Exploring Structure, Function & Regulation of the Human Glucagon-like Peptide-1 Receptor

Glucagon-like peptide-1 (GLP-1) enhances glucose-dependent insulin secretion and promotes β -cell function *via* its receptor (GLP-1R), which therefore is a validated target for the treatment of type 2 diabetes. Due to difficulties with peptide therapeutics, it is important to find small-molecule GLP-1R agonists. This leads to a need to understand the structure, function and regulation of the receptor, particularly, differences between agonisms mediated by GLP-1 (orthosteric agonist) and small molecules.

The GLP-1R contains a putative N-terminal signal peptide sequence, which is assessed here by recombinantly expressing several epitope-tagged GLP-1R constructs in HEK293 cells. The findings demonstrate that the GLP-1R is expressed predominately at the plasma membrane and also slightly cytosolic. Only fully glycosylated, mature form of the receptor is able to traffic to the cell surface and performs the function. The signal peptide sequence of the GLP-1R is essential for synthesis. After fulfilling the function, this sequence is cleaved and thus not part of the mature protein. The cleavage of signal peptide is critical for processing and trafficking of the GLP-1R. Based on one of these constructs generated here, a cell line (HEK293: GLP-1R-EGFP) with stable expression of the visible GLP-1R is established, which allows observations and determinations for ligand-mediated receptor internalisation in real time.

Compound 2 (6,7-dichloro-2-methylsulfonyl-3-*N-tert*-butylaminoquinoxaline) has been described as a GLP-1R allosteric modulator and agonist. Findings here that compound 2-mediated agonisms on both the wild-type (WT) GLP-1R and the mutant with removal of the N-terminal domain provide direct evidence for the allosteric agonism. Interestingly, compound 2-mediated cAMP response is enhanced by orthosteric antagonist exendin 9-39, but the latter inhibits receptor internalisation mediated by compound 2.

Recently, it has been hypothesised that the binding of GLP-1 allows a sequence of NRTFD (Asn⁶³-Asp⁶⁷) in the N-terminus of the GLP-1R to interact with another part of the receptor and cause agonism. This was examined here by generating receptor mutants and synthetic peptides. Findings here that Asp⁶⁷ plays a key role in stabilising the N-terminal structure of the GLP-1R and thus is critical for processing and trafficking of the receptor protein do not support such hypothesis although synthetic NRTFD mediates a weak and partial agonism on the WTGLP-1R.

ACKNOWLEDGEMENTS

Firstly, I would like to thank my supervisor Dr Gary Willars for letting me grab this PhD study opportunity. Thank you for your trust, encouragement and support in the supervision throughout my PhD study. Thank you so much for the great deal of time you have spent on preparation for my talks. Thank you for your patience when correcting each piece of my writing. Thank you also for your contribution to the successful publications.

I am also very grateful for the support of industrial supervisor, Dr Graeme Wilkinson (AstraZeneca, Alderley Park, U.K.). Thanks also go to Dr Alastair Brown (AstraZeneca, Alderley Park, U.K.) for the support during industrial visits to Alderley Park.

I would like to acknowledge my committee members Prof. Andrew Tobin and Dr Terry Herbert for their contributions towards this project. Thanks also go to Prof. John Challiss for encouragement and support.

Special thanks go to two of my colleagues who were with me for almost the entire journey, Karen and Caroline. Karen, I was so lucky to be working on the same project as you. It provided the perfect chance to learn brilliant lab techniques and organisation skills from you. Caroline, you were always willing to go the extra mile to help with anything. Thanks also go to group members Khalad and Neil.

I would also like to thank Sophie and all my friends in CPP that I have made. Your never ending support astounds me.

I would also like to thank Mum and Dad for supporting my PhD study by releasing me from child care, cooking and housework. My Amy and Sam, you are both the best gift from God; and were my lucky charms when it came to completing my PhD study.

Naichang, thank you so much for supporting me by your love. This PhD study might still be only a dream if it wasn't for your encouragement and contribution. Thank you for the advice of selecting stable cell line clones. Thank you for being with me and taking over my part of responsibility for the family to allow me concentrate on my study. Thank you for endless cups of tea and for allowing me to get in at midnight after work.

Without these people, this thesis would never have been possible. Thank you.

ABBREVIATIONS

[³ H]-NMS	[N-methyl- ³ H]-scopolamine methylchloride
[Ca ²⁺] _i	intracellular calcium concentrations
ΔSP	signal peptide-deleted
AC	adenylyl cyclase
ALLN/MG101	acetyl-L-leucyl-L-leucyl-L-norleucinal
ANOVA	analysis of variance
AP-2	adaptor protein-2
APS	ammonium persulphate
ATP	adenosine-5'-triphosphate
AZ	AstraZeneca
BMI	body mass index
bp	base pair
BSA	bovine serum albumin
cAMP	cyclic adenosine monophosphate
CD26	cluster of differentiation 26
cGMP	cyclic guanosine monophosphate
CHO	Chinese hamster ovary cell line
CP	Cambridge Peptides Ltd
C-peptide	connecting peptide
CRD	cysteine-rich domain
CREB	cAMP response element binding protein
CRF	corticotropin-releasing factor
CRF-R ₁	corticotropin-releasing factor receptor 1
C-terminal	carboxy-terminal
DAG	diacylglycerol
DMEM	Dulbecco's Modified Eagle Medium
DNA	deoxyribonucleic acid
dNTP	deoxyribonucleotide triphosphate
Dol-P	dolichol phosphate
DPP-IV	dipeptidyl peptidase IV
dsDNA	double-stranded DNA

DTT	dithiothreitol
ECL	extracellular loop
EDTA	ethylenediaminetetraacetic acid
EGFP	enhanced green fluorescence protein
EGFP-GLP-1R-HA	N-terminal EGFP-tagged and C-terminal HA-tagged GLP-1R
ELISA	enzyme-linked immunosorbent assay
Endo H	endoglycosidase H
Epac	cAMP-regulated guanine nucleotide exchange factors
ER	endoplasmic reticulum
FBS	foetal bovine serum
FPG	fasting plasma glucose
FRT	flippase recognition target
FSK	forskolin
G $\beta\gamma$	β - and γ - subunits complex of heterotrimeric G-proteins
G418	Geneticin
GABA _B	γ -aminobutyric acid type B receptor
GAPs	GTPase-activating proteins
GDP	guanosine diphosphate
GEF	nucleotide exchange factor
GFP	green fluorescent protein
GI	gastrointestinal
GIP	glucose-dependent insulinotropic polypeptide
Glc	glucose
GlcNAc	<i>N</i> -acetylglucosamine
GLP-1	glucagon-like peptide 1
GLP-1R	glucagon-like peptide 1 receptor
GLP-1R-EGFP	C-terminal EGFP-tagged GLP-1R
GLP-1R-HA	C-terminal HA-tagged GLP-1R
GLP-2	glucagon-like peptide 2
GnRH-R	gonadotropin-releasing hormone receptor
GPCR	G protein-coupled receptor
GPT	<i>N</i> -acetylglucosaminyl phosphate transferase
GRK	G protein-coupled receptor kinase

GRPP	glycintin-related pancreatic C-peptide
GTP	guanosine triphosphate
G α	α -subunit of heterotrimeric G-proteins
HA	hemagglutinin
HA-GLP-1R	N-terminal HA-tagged GLP-1R
HA-GLP-1R-EGFP	N-terminal HA-tagged and C-terminal EGFP-tagged GLP-1R
HbA1c	Glycosylated haemoglobin
HBS	HEPES buffered saline
HBSS	Hank's Balanced Salt Solution
h-core	hydrophobic core
HEK293	human embryonic kidney 293 cell line
HEK293:EGFP	HEK293cells with the stable expression of EGFP
HEK293:GLP-1R-EGFP	HEK293 cells with stable expression of C-terminal EGFP-tagged GLP-1R
HEK293Flp-In:WTGLP-1R	HEK293Flp-In cells with stable expression of the wild-type GLP-1R
HH	hypogonadotropic hypogonadism
IBMX	isobutylmethylxanthine
ICC	immunocytochemistry
ICL	intracellular loop
IDDM	insulin-dependent diabetes mellitus
IDF	International Diabetes Federation
IFG	impaired fasting glycaemia
IGT	impaired glucose tolerance
Ins(1,4,5)P ₃	inositol-1,4,5-trisphosphate
IP1	intervening peptide-1
IP2	intervening peptide-2
IPTG	5-bromo-4-chloro-3-indolyl-beta-D-galactopyranoside
IRS-1	insulin receptor substrate-1
IRS-2	insulin receptor substrate-2
IVGTT	intravenous glucose tolerance tests
KHB	Krebs-HEPES buffer
KHB-BSA	KHB containing 0.1% w:v BSA
LB	Luria-Bertani

M ₃	subtype-3 muscarinic acetylcholine receptors
Man	mannose
MAPK	mitogen-activated protein kinase
MCS	multiple cloning site
MG101/ALLN	acetyl-L-leucyl-L-leucyl-L-norleucinal
MG132	benzyloxycarbonyl-L-leucyl-L-leucyl-L-leucinal
MPGF	major proglucagon fragment
mRNA	messenger RNA
NAM	negative allosteric modulator
NCBI	National Centre for Biotechnology Information
NCKX	Na ⁺ /Ca ²⁺ -K ⁺ exchanger
Neo _r	neomycin-resistance cassette
NHS	National Health Service
NICE	National Institute for Health and Clinical Excellence
NIDDM	non-insulin-dependent diabetes mellitus
NMS	scopolamine methylchloride
NP-40	nonyl phenoxyethoxyethanol
nRTK	non-receptor tyrosine kinase
NSB	non-specific binding
N-terminal	amino-terminal
OGTT	oral glucose tolerance test
PAM	positive allosteric modulator
PBS	phosphate buffered saline
PC	prohormone convertase enzyme
PCR	polymerase chain reaction
PDE	phosphodiesterase
PKA	protein kinase A
PKB	protein kinase B
PKC	protein kinase C
PLC	phospholipase C
PMSF	phenylmethylsulfonyl fluoride
PNGase F	peptide N-glycosidase F
PtdIns(4,5)P ₂	phosphatidylinositol-4,5-bisphosphate

PTH	parathyroid hormone
PTHrP	parathyroid hormone-related peptides
PVDF	polyvinylidene fluoride
RE	restriction endonuclease
RNA	ribonucleic acid
RNC	ribosome-nascent-chain
rpS6	ribosomal protein S6
RSK	ribosomal S6 kinase
RT	room temperature
RT-PCR	reverse transcription polymerase chain reaction
S6K1	p70 S6 protein kinase
sem	standard error of the mean
SP	signal peptide sequence
SR	SRP receptor
SRP	signal recognition particle
T _a	annealing temperature
TCA	trichloroacetic acid
TEMED	N, N, N', N'-tetramethylethylenediamine
TM	transmembrane domain
VGCC	voltage-gated calcium channel
WHO	the World Health Organization
WT	wild-type
X-gal	isopropyl thiogalactoside

PUBLICATIONS

Peer-reviewed publications:

Huang Y, Wilkinson GF, Willars GB (2010) Role of the signal peptide in the synthesis and processing of the glucagon-like peptide-1 receptor. *Br J Pharmacol.* 159(1):237-51.

Coopman K, **Huang Y**, Johnston N, Bradley SJ, Wilkinson GF and Willars GB (2010) Comparative Effects of the Endogenous Agonist GLP-1 7-36 Amide and a Small Molecule Ago-allosteric Agent 'Compound 2' at the GLP-1 Receptor. *J Pharmacol Exp Ther.* **334**:795-808.

Book contribution:

Huang Y and Willars GB (2010) Generation of Epitope-Tagged GPCRs. Willars GB and Challiss RAJ (Eds) Receptor Signal Transduction Protocols. Methods in Molecular Biology Series. Vol. 259. Humana Press. Totowa, New Jersey.

Abstracts:

Huang Y, Wilkinson GF and Willars GB (2009) Orthosteric- and allosteric-agonist mediated internalisation of the glucagon-like peptide-1 receptor (GLP-1R): inhibition by an orthosteric antagonist, British Pharmacology Society 3rd Focused Meeting on Cell Signalling, 20 - 21 April 2009, Leicester. Poster presentation

Huang Y, Wilkinson GF and Willars GB (2008). British Pharmacology Society 2008 Winter Meeting, 16 - 18 December 2008, Brighton. Poster presentation

Contents

ACKNOWLEDGEMENTS	i
ABBREVIATIONS.....	ii
PUBLICATIONS.....	vii
CHAPTER 1 General introduction	1
1.1 Type 2 diabetes.....	1
1.1.1 <i>Background</i>	1
1.1.2 <i>Pathophysiology and causes</i>	3
1.1.3 <i>Signs, symptoms and diagnosis</i>	5
1.1.4 <i>Approaches and goals for the treatment of type 2 diabetes</i>	10
1.2 GLP-1 in type 2 diabetes	12
1.2.1 <i>Incretin hormones</i>	12
1.2.2 <i>Synthesis and secretion of GLP-1</i>	15
1.2.3 <i>Biological activities of GLP-1</i>	18
1.2.4 <i>GLP-1-based therapies in type 2 diabetes</i>	21
1.3 GPCRs in drug discovery	24
1.3.1 <i>Classification and the common structure of GPCRs</i>	25
1.3.2 <i>Signal transduction by G-proteins</i>	30
1.3.3 <i>Internalization and desensitization of GPCRs</i>	35
1.3.4 <i>Allosteric modulation of GPCRs</i>	38
1.4 Molecular characterization of the GLP-1R	39
1.4.1 <i>Residues required for ligand binding and stabilizing the structure of the receptor</i>	42
1.4.2 <i>The regions involved in receptor activation and internalization</i>	43
1.4.3 <i>Signal transduction by the GLP-1R in pancreatic β-cells</i>	45
1.5 Aims of the project	46
chapter 2 Materials and Methods	48
2.1 Materials	48
2.1.1 <i>Water</i>	48
2.1.2 <i>Standard laboratory chemicals, reagents and consumables</i>	48
2.1.3 <i>Peptides, enzymes, primers, and antibodies</i>	49
2.1.4 <i>Specific reagents and kits</i>	50
2.1.5 <i>Radioisotopes and materials for scintillation counting</i>	51
2.1.6 <i>Vector and plasmid constructs</i>	51
2.1.7 <i>Bacterial strains</i>	53
2.1.8 <i>Mammalian cell lines</i>	54

2.2	Bacterial cell culture.....	55
2.2.1	<i>Growth and multiplication</i>	55
2.2.2	<i>E. coli stock</i>	56
2.3	Bacterial transformation for amplifying vectors and GLP-1R constructs.....	56
2.3.1	<i>Preparation of competent DH5α</i>	56
2.3.2	<i>Transformation procedure using competent DH5α</i>	57
2.4	Preparation of plasmid DNA	57
2.5	Quantification of DNA by absorbance	59
2.6	PCR cloning of GLP-1R sequences	60
2.6.1	<i>Design of primers</i>	60
2.6.2	<i>Performing PCRs on a thermocycler</i>	63
2.7	Restriction digest of plasmids and DNA fragments	64
2.8	Agarose gel electrophoresis of DNA.....	65
2.9	Purification of DNA fragments from solution or agarose gel	66
2.10	DNA ligation	67
2.11	Synthesis of the HA-tag sequence by annealing two complementary primers	68
2.12	Generating mutated GLP-1R constructs.....	70
2.13	Automated DNA sequencing.....	72
2.14	Mammalian cell culture.....	73
2.14.1	<i>Growth and maintenance</i>	73
2.14.2	<i>Cell subculture</i>	73
2.14.3	<i>Cell counting and viability determination</i>	74
2.14.4	<i>Freezing cells for storage</i>	75
2.14.5	<i>Resuscitation of frozen cells</i>	75
2.15	Transfection of GLP-1R constructs.....	75
2.16	Selection and isolation of G418-resistant colonies	77
2.17	Determination of protein concentration (Bradford assay).....	77
2.18	Biotinylating cell surface proteins.....	78
2.19	Immunoblotting	79
2.19.1	<i>Sample preparation</i>	79
2.19.2	<i>SDS-polyacrylamide gel electrophoresis (SDS-PAGE)</i>	79
2.19.3	<i>Semi-dry electrophoretic transfer of proteins</i>	80
2.19.4	<i>Immunoblotting</i>	81

2.20	Glycosidase treatments	82
2.20.1	<i>Sample preparation</i>	82
2.20.2	<i>Treatment procedure</i>	82
2.21	Tunicamycin treatment	83
2.22	RT-PCR	83
2.22.1	<i>Preparation of total RNA</i>	83
2.22.2	<i>Procedure of RT-PCR</i>	85
2.23	Live-cell imaging of EGFP-tagged GLP-1Rs and determination of receptor internalization.	85
2.23.1	<i>Cell preparation</i>	85
2.23.2	<i>Confocal microscopy</i>	86
2.24	Generation and measurement of cAMP	87
2.24.1	<i>Generation of cAMP by intact cells</i>	87
2.24.2	<i>Generation of cAMP using cell membranes</i>	87
2.24.3	<i>cAMP assay</i>	89
2.25	Determination of ligand binding affinity of the GLP-1R.....	89
2.25.1	<i>Membrane preparation</i>	90
2.25.2	<i>Radioligand binding assay</i>	90
2.25.3	<i>Data analysis</i>	91
2.26	Radioligand binding assay in intact cells	91
2.26.1	<i>Binding assay in intact cells with the expression of GLP-1Rs</i>	91
2.26.2	<i>Binding assay in intact cells with the expression of M₃</i>	92
2.26.3	<i>Data analysis</i>	93
2.27	General data analysis	93
CHAPTER 3	GENERATION AND CHARACTERIZATION OF EPITOPE TAGGED GLP-1RS	95
3.1	Introduction	95
3.2	Strategies for generating epitope-tagged GLP-1R constructs	101
3.2.1	<i>C-terminal epitope-tagged GLP-1R constructs</i>	101
3.2.2	<i>The GLP-1R constructs containing an N-terminal HA-tag</i>	107
3.2.3	<i>The N-terminal EGFP-tagged and C-terminal HA-tagged GLP-1R (EGFP-GLP-1R-HA) construct</i>	112

3.3	Results	115
3.3.1	<i>Visualisation of EGFP-tagged GLP-1Rs in HEK293 cells</i>	115
3.3.2	<i>Immunoreactivity of epitope-tagged GLP-1Rs</i>	117
3.3.3	<i>Similar pharmacologic properties of epitope-tagged GLP-1Rs except EGFP-GLP-1R-HA in HEK293 cells</i>	122
3.3.4	<i>Stable expression of GLP-1R-EGFP in HEK293 cells</i>	126
3.3.5	<i>Cell surface expression of the GLP-1R-EGFP requires N-linked glycosylation</i>	132
3.4	Discussion.....	135
3.4.1	<i>Expression profile of the GLP-1R in HEK293 revealed by different epitope-tagged constructs</i>	135
3.4.2	<i>The role of N-linked glycosylation in the trafficking of GLP-1R</i>	138
3.4.3	<i>Tunicamycin treatment for inhibiting N-linked glycosylation</i>	142
CHAPTER 4 THE SIGNAL PEPTIDE OF THE GLP-1R.....		145
4.1	Introduction.....	145
4.2	Results.....	150
4.2.1	<i>Predicting cleavage of the signal peptide of GLP-1R constructs using the SignalP 3.0 server</i>	150
4.2.2	<i>Expression of full-length GLP-1Rs</i>	156
4.2.3	<i>Full-length EGFP-tagged GLP-1Rs lack cell surface fluorescence and function</i>	158
4.2.4	<i>Receptor expression requires the signal peptide sequence of the GLP-1R</i> ..	161
4.2.5	<i>Increasing the positive charge within the N-terminus partially recovers the expression and function of the ΔSPGLP-1Rs</i>	171
4.3	Discussion.....	176
4.3.1	<i>The signal peptide is required for biosynthesis of the GLP-1R</i>	176
4.3.2	<i>Cleavage of the GLP-1R signal peptide</i>	180
CHAPTER 5 A SMALL-MOLECULE AGONIST AND A POTENTIAL ENDOGENOUS AGONIST OF THE GLP-1R.....		186
5.1	Introduction.....	186
5.2	Results.....	195
5.2.1	<i>Signalling mediated by compound 2</i>	195
5.2.2	<i>Candidate sequences in the GLP-1R as an endogenous agonist</i>	203
5.2.3	<i>Activation of the WTGLP-1R by synthetic peptides representing potential endogenous agonist sequences</i>	204
5.2.4	<i>Signalling and regulation of mutated GLP-1Rs</i>	214
5.2.5	<i>Receptor internalization mediated by different ligands in HEK293 cells with stable expression of the GLP-1Rs</i>	228

5.3	Discussion	237
5.1.1	<i>Summary</i>	237
5.1.2	<i>Allosteric agonism of compound 2 at the GLP-1R</i>	239
5.1.3	<i>The endogenous agonist of the GLP-1R</i>	243
5.1.4	<i>Asp⁶⁷ in the processing and trafficking of the GLP-1R</i>	247
CHAPTER 6 FINAL DISCUSSION.....		250
6.1	Summary of results	250
6.2	Discussion and implications for further research.....	252
REFERENCES.....		258

CHAPTER 1 General Introduction

Glucagon-like peptide 1 (GLP-1) is released from intestinal L-cells in response to nutrient ingestion and has a number of antidiabetogenic effects, particularly enhancing glucose-dependent insulin release from pancreatic β -cells. All of the biological effects of GLP-1 are mediated *via* a member of the G-protein-coupled receptor (GPCR) superfamily, the GLP-1 receptor (GLP-1R), which has, therefore, become a validated target for the treatment of type 2 diabetes.

1.1 Type 2 diabetes

1.1.1 Background

Diabetes mellitus is a metabolic disorder of multiple aetiologies characterized by chronic hyperglycaemia with disturbances of carbohydrate, fat and protein metabolism resulting from defects in insulin secretion, insulin action, or both (WHO Consultation, 1999). Recent estimates indicate that the world prevalence of diabetes among adults (aged 20-79 years) is 6.4%, affecting 285 million adults in 2010, which will rise to 7.7%, and 439 million adults by 2030 (Shaw et al., 2010). In the UK, there are currently 2.75 million people diagnosed with diabetes and this is estimated to be more than 4 million by 2025. In addition to this, there are over 500,000 undiagnosed diabetics in the UK (Diabetes, UK, 2010). Diabetes remains the leading cause of blindness, end-stage renal disease and non-traumatic lower-limb amputation, and one of the major causes of cardiovascular disease due to microvascular complications and an increased risk of macrovascular complications (ischaemic heart disease, stroke and peripheral vascular disease) (Zimmet et al., 2001; Schwarz et al., 2007). Diabetes is not only associated

with reduced life expectancy and diminished quality of life but is also a tremendous burden on health care costs. In the UK, the NHS spends £1m per hour, 10% of its yearly budget (a total exceeding £9 billion), for treating diabetes and its complications (Diabetes, UK, 2010).

Currently diabetes mellitus is classified into four categories including type 1, type 2, other specific types and gestational diabetes (**Table 1.1**; Kuzuya and Matsuda, 1997), of which type 2 is the most common form, accounting for approximately 90% of all cases of diabetes (Tierney et al., 2002). Since patients with any form of diabetes may require insulin treatment at some stage of their disease, the WHO has recommended that the terms "insulin-dependent diabetes mellitus (IDDM)" and "non-insulin-dependent diabetes mellitus (NIDDM)" are no longer used, although they appeared in earlier classifications of diabetes and have been accepted widely (WHO Consultation, 1999).

Table 1.1. Aetiological classification of disorders of glycaemia

Types	Description and subtypes
Type 1	<p>β-cell destruction, usually leading to absolute insulin deficiency.</p> <ul style="list-style-type: none"> • Autoimmune diabetes mellitus • Idiopathic
Type 2	Ranging from predominantly insulin resistance with relative insulin deficiency to a predominantly secretory defect with or without insulin resistance
Other specific types	<ul style="list-style-type: none"> • Genetic defects of β-cell function • Genetic defects in insulin action • Diseases of the exocrine pancreas • Endocrinopathies • Drug- or chemical-induced • Infections • Uncommon forms of immune-mediated diabetes • Other genetic syndromes sometimes associated with diabetes
Gestational diabetes	Carbohydrate intolerance resulting in hyperglycaemia of variable severity with onset or first recognition during pregnancy.

Adapted from (WHO Consultation, 1999)

1.1.2 Pathophysiology and causes

Insulin is a hormone that is produced by β -cells in islet of Langerhans in the pancreas to regulate a variety of processes but particularly energy balance and glucose metabolism in the body (Rhodes and White, 2002; Benedict et al., 2004). Glucose is liberated from dietary carbohydrate such as starch or sucrose by hydrolysis within the small intestine, which is then absorbed into the blood. Elevated concentrations of glucose in blood stimulate the release of insulin. Depending on the target tissue, insulin has important effects on glucose metabolism, including the facilitation of glucose entry into muscle, adipose and several other tissues and the stimulation of the liver to store glucose in the form of glycogen. When insulin is absent or present at an insufficient concentration within the circulation, insulin-sensitive cells within the body are unable to take up glucose, and start to use alternative fuels such as fatty acids for energy. Consequently, after a meal, insulin released into the bloodstream in response to the increased glucose levels helps glucose removal from the blood and therefore decreases blood glucose levels (**Figure 1.1a**). When blood glucose levels are reduced, insulin release from the pancreas is turned down. In normal individuals, such a regulatory system helps to keep blood glucose levels in a tightly controlled range. For patients with diabetes, insufficient insulin results in hyperglycemia (Unger and Parkin, 2010).

An absolute lack of insulin, usually secondary to a destructive process affecting the insulin producing β -cells in the pancreas, underlies the development of type 1 diabetes. In contrast to this, the initial problem of type 2 diabetes is insulin resistance due to the inability of insulin-dependent cells (mostly the cells of muscle and fat tissues) to respond to insulin in an appropriate and efficient manner (Unger and Parkin, 2010). At this stage, the normal pancreatic β -cell response to such insulin resistance is compensatory insulin hypersecretion in order to maintain normoglycemia (β -cell compensation). In subjects that develop type 2 diabetes, this is followed by a decline of

insulin secretory capacity despite hyperglycemia (β -cell failure) (Leahy, 2005). Therefore, it is increasingly being realized that type 2 diabetes only develops in insulin-resistant subjects with the onset of β -cell dysfunction (Prentki and Nolan, 2006; Campbell, 2009).

The majority (estimated 60% to 90%) of patients with type 2 diabetes are obese, and obesity itself causes or aggravates insulin resistance (Muoio and Newgard, 2008). Obesity or weight gain can increase the risk for developing diabetes by greater than ninetyfold (Anderson et al., 2003). The body mass index (BMI) is the most widely used diagnostic tool to identify weight problems, which is defined as the individual's body weight divided by the square of the height (kg/m^2) (Eknoyan, 2008). The WHO regards a BMI of greater than 25 as overweight and above 30 as obese (BMI Classification). Weight management appears to be the primary therapeutic task for most patients with type 2 diabetes, aiming to lower the BMI to below 25 (Hollander, 2007). However, many of those who are not obese by traditional weight criteria (with a BMI of 18.5 to 24.9) may have an increased percentage of body fat distributed predominantly in the abdominal region (Venables and Jeukendrup, 2009), which may increase the risk of type 2 diabetes development by 2.4-fold (Cassano et al., 1992).

Risk factors for developing type 2 diabetes are also associated with diet, sedentary lifestyle and genetics (Bazzano et al., 2005). Emerging evidence shows that low-fat vegetarian and vegan diets are associated with weight loss, increased insulin sensitivity, and improved cardiovascular health and therefore have potential advantages for the management of type 2 diabetes (Barnard et al., 2009; Risérus et al., 2009). Physical activity results in a higher rate of insulin-stimulated glucose disposal at a defined insulin dose (Bazzano et al., 2005; Davis et al., 2009). In addition, having relatives (especially first-degree) with type 2 diabetes increases the risk of developing type 2 diabetes very

substantially. Recently, the insulin receptor substrate-1 (IRS-1) gene was associated with type 2 diabetes, insulin resistance and hyperinsulinemia in a large-scale study involving the screening of some 14,000 people in different countries (Rung et al., 2009).

1.1.3 Signs, symptoms and diagnosis

1.1.3.1 Signs and symptoms

Type 2 diabetes often develops slowly from a condition of pre-diabetes, and symptoms may not be apparent for years. The characteristic symptoms can develop because of hyperglycemia or high levels of glucose in the blood, which include dehydration, blurred vision, excessive thirst and increased fluid intake (polydipsia), followed by excessive urine production (polyuria). In diabetes, insulin-dependent cells are partially or fully unable to use glucose for fuel and therefore switch over to metabolizing fat as a fuel source. This process requires the use of more energy, which leads to excessive eating (polyphagia), weight loss and lethargy (Cooke and Plotnick, 2008). In addition, hyperglycemia makes it more difficult for the body to resist and fight infections and to heal, resulting in frequent infections, especially skin infections and open, slow healing sores (Setacci et al., 2009).

Serious long-term complications of diabetes include cardiovascular disease, nerve dysfunction, microvascular damage e.g., chronic renal failure and retinal damage (which can lead to blindness), impotence and poor healing (Setacci et al., 2009). The mechanisms underlying the development of such complications are not entirely clear but are associated with prolonged hyperglycaemia (Blonde, 2009). For those patients with the disease controlled inappropriately, serious acute complications may occur. Hypoglycaemia is caused by mis-administrated insulin or oral medications. Diabetic

ketoacidosis, results from a shortage of insulin; in response the body switches to burning fatty acids and producing acidic ketone bodies that cause dehydration and most of the symptoms and complications (Kitabchi and Nyenwe, 2006). Hyperglycemia hyperosmolar state is the end result of a sustained osmotic diuresis, and is characterized by severe hyperglycemia, hyperosmolarity, and dehydration, but without significant ketoacidosis (Stoner, 2005).

1.1.3.2 Diagnostic criteria of plasma glucose

Diabetes is diagnosed by recurrent or persistent hyperglycaemia which is demonstrated by any one of: a) a fasting plasma glucose (FPG) level $\geq 7.0\text{mM}$; b) plasma glucose $\geq 11.1\text{mM}$ two hours after a 75g oral glucose load (2h plasma glucose) as measured by an oral glucose tolerance test (OGTT) and; c) random plasma glucose concentration $\geq 11.1\text{mM}$. Two pre-diabetic states are also diagnosed: a) patients have FPG levels between 6.1 and 6.9mM and 2h plasma glucose (if measured) $< 7.8\text{mM}$ are considered to have impaired fasting glycaemia (IFG); b) patients with FPG $< 7.0\text{mM}$ and 2h plasma glucose $> 7.8\text{mM}$ (but $< 11.1\text{mM}$) are considered to have impaired glucose tolerance (IGT), (WHO/IDF Consultation, 2006).

1.1.3.3 Glycosylated haemoglobin (HbA1c)

Glycosylation of haemoglobin occurs when normal haemoglobin is exposed to high plasma levels of glucose, in which glucose irreversibly binds to haemoglobin in a non-enzymatic pathway and forms HbA1c (Bookchin and Gallop, 1968). Glycosylation of haemoglobin is primarily used as a treatment-tracking test, reflecting average blood glucose levels over the preceding approximately 90 days (Rahbar et al., 1969). Measurement can be performed at any time of the day and does not require any special

preparation, e.g., fasting. It has been recommended that HbA1c is measured for both: a) checking blood glucose control in people who might be pre-diabetic and; b) monitoring blood glucose control in patients with diabetes (Koenig et al., 1976). Although not used for diagnosis, an elevated level of HbA1c of 6.0% (of hemoglobin A) or higher (the 2003 revised U.S. standard) is considered abnormal by most laboratories. The current recommended goal for HbA1c in patients with diabetes is <7.0%, which is considered an index of good glycaemic control, although some guidelines are stricter (<6.5%). People with diabetes who have HbA1c levels within this range have a significantly lower incidence of complications, including retinopathy and nephropathy (Sniderman et al., 2007; Genuth, 2006).

1.1.3.4 Proinsulin and C-peptide

Insulin is synthesized in significant quantities only in β -cells of the pancreas. The insulin mRNA is translated as a single chain precursor with 110 residues, namely preproinsulin, and removal of its signal peptide (**Chapter 4**) during insertion into the endoplasmic reticulum (ER) generates proinsulin. Almost no preproinsulin exists in the cell although it is the primary translation product of the insulin gene since removal of the signal peptide is not a separate step (Hou and Min, 2009). Proinsulin (representing residues 25 to 110 of the insulin cDNA sequence, **Figure 1.1b**) is synthesized in the ER, where it is folded and its disulfide bonds are oxidized. It is then transported to the Golgi apparatus where it is packaged into secretory vesicles, and where it is processed by a series of proteases to form mature insulin by removal of 4 basic residues and the connecting peptide (C-peptide, **Figure 1.1b**, Goodge and Hutton, 2000). Mature insulin (39 residues) consists of two domains, an N-terminal B chain and a C-terminal A chain connected by disulfide bonds. When the β -cell is appropriately stimulated, insulin,

along with C-peptide, are secreted from the cell by exocytosis and diffuse into islet capillary blood.

To investigate the pathophysiology of diabetes mellitus, insulin measurements are essential in various dynamic tests, such as OGTT or intravenous glucose tolerance tests (IVGTT), to determine the insulin response of the pancreas and the degree of insulin resistance. However, insulin measurements may be complicated by cross-reactivity with partially degraded insulin, proinsulin and split forms of proinsulin. Immune complexes of these molecules are especially problematic in patients who have developed anti-insulin antibodies through administration of animal insulin. In contrast, C-peptide has a longer half-life than insulin (2-5 times longer) and thus higher concentrations of C-peptide persist in the peripheral circulation, and these levels fluctuate less than insulin. Thereby plasma C-peptide concentration is considered to reflect pancreatic insulin secretion more reliably than the level of insulin itself, and has been used as semiquantitative marker of β -cell secretory activity (Vezzosi et al., 2007).

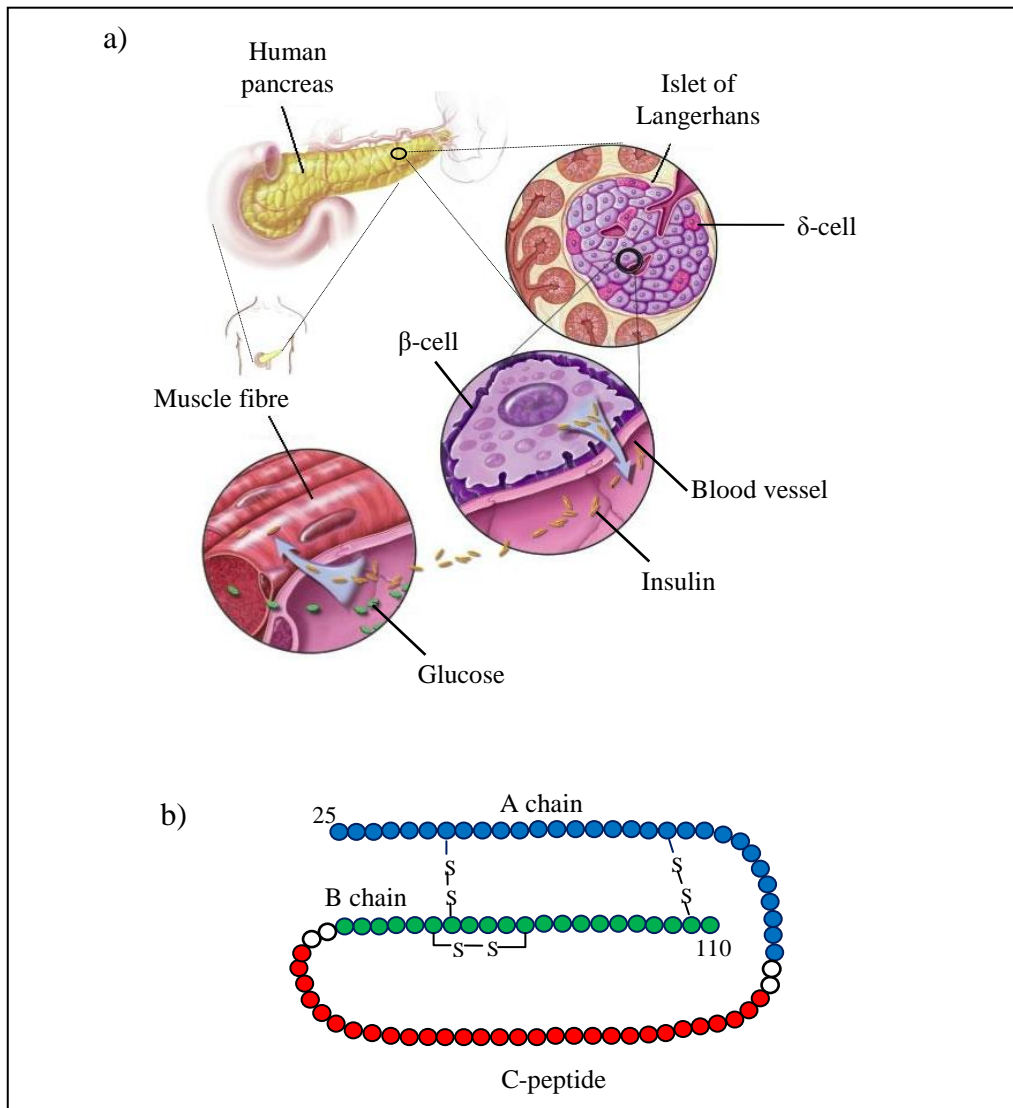


Figure 1.1 Processing and secretion of insulin. Insulin is secreted from β -cells in the islets of Langerhans and helps target insulin-sensitive cells including muscle cells to utilize glucose (a). The primary translation product of the insulin gene is preproinsulin, a peptide of 110 amino acids, which is processed to proinsulin by proteases to remove the signal peptide (the first 24 amino acids), then to insulin by removal of C-peptide (b). The B chain of insulin is represented in green, the C-peptide in red, and the A chain in blue. The blank circles indicate the basic residues that are the cleavage site for conversion from proinsulin to insulin. Picture (a) adapted from <http://2.bp.blogspot.com>.

1.1.4 Approaches and goals for the treatment of type 2 diabetes

It has been demonstrated that more intensive blood glucose control, generally determined by HbA1c levels, can delay or prevent the development and progression of complications of type 2 diabetes (Blonde, 2009). Therefore, tight control of blood glucose, with a target HbA1c level of 6.5–7.5%, for the management of diabetes has been recommended as well as control of other risk factors such as hypertension and dyslipidaemia (NICE Short Clinical Guideline 87, 2009). Initial treatment in the patient with type 2 diabetes often begins with non-pharmacological interventions including a change in diet, exercise and weight loss (when appropriate), which are expected to promote overall health through optimal nutrition and enhance insulin sensitivity to improve blood glucose control. Classic pharmacological approaches for type 2 diabetes treatment include oral hypoglycaemic agents (**Table 1.2**) and insulin injection. Oral hypoglycaemic agents reduce plasma glucose levels by one or more methods: increasing insulin secretion; reducing insulin resistance or; delaying glucose absorption by the gut (Wright, 2009). In many cases, it is gradually difficult to achieve adequate blood glucose control by treatment with single or even dual oral antihyperglycaemic agents (Swinnen et al., 2009). Insulin therapy is introduced when control of blood glucose by oral antidiabetic agents remains or becomes inadequate (fails to maintain to HbA1c <7.5%) (Meneghini, 2009). However, insulin therapy is associated with potential risks of several adverse effects, particularly, hypoglycaemia, weight gain and probable increased risk of colorectal cancer (Chiasson, 2009). This, together with route of administration (most commonly subcutaneous injection) contribute to low adherence and a reluctance to maintain intensive insulin therapy in many patients, (Hamnvik and McMahon, 2009). Thus, these classic treatment modalities for type 2 diabetes are often

unsatisfactory and there is an imperative need for new classes of glucose-lowering agents such as incretin-based therapies to preserve normal physiological responses to food intake and which have the potential to facilitate treatment intensification, encourage adherence and improve glycaemic control (see below).

Table 1.2. Type and dosages of oral hypoglycemic agents

Class	Drug	Dosage	Doses per day
Secretagogues*			
Sulfonylureas	Chlorpropamide	100-500 mg	1
	Glipizide	5-40 mg	1-2
	Glyburide	1.5-20 mg	1-2
	Glimepiride	1-8 mg	1
Non sulfonylureas	Nateglinide	180-360 mg	2-4
	Repaglinide	0.5-16 mg	2-4
Insulin Sensitizers‡			
Biguanides	Metformin	500-2,250 mg	2
Thiazolidinediones	Pioglitazone	15-45 mg	1-2
	Rosiglitazone	4-8 mg	1-2
Agents That Delay Carbohydrate Absorption§			
Alpha-glucosidase inhibitors	Acarbose	25-300 mg	3
	Miglitol	25-300 mg	3
Combination Agents	Rosiglitazone and Metformin‡	4-8 mg/ 1,000-2,000 mg	2
	Metformin and Glyburide*‡	1.25-10 mg/ 500-2,000 mg	1-2
	Metformin and Glipizide*‡	2.5-10 mg/ 500-2,000 mg	1-2

* Stimulates β -cells.

‡ Stimulates glucose uptake by muscle and adipose tissue and reduces the liver's glucose output.

§ Delays absorption of glucose by the gut.

Table adapted from Nathan et al., 2008.

1.2 GLP-1 in type 2 diabetes

1.2.1 *Incretin hormones*

Incretins are gastrointestinal hormones with hypoglycaemic effects that were originally extracted from the gut mucosa (Perley and Kipnis, 1967). The incretin concept was developed when it was observed that glucose administered orally promotes a significantly greater insulin response than glucose infused intravenously, despite the same plasma glucose responses (**Figure 1.2ai**; Creutzfeldt and Ebert, 1985; Nauck et al., 1986). Two major incretins, namely glucose-dependent insulinotropic polypeptide (GIP) and GLP-1, together are thought to be responsible for up to 70% of the insulin secretion from the β -cells of the islets of Langerhans following a meal. This is known as the incretin effect (**Figure 1.2aii**). Type 2 diabetic patients have an impaired incretin effect, suggesting a role for incretin hormones or their actions in the pathogenesis of type 2 diabetes (**Figure 1.2b, i-iii**; Nauck et al., 1989; Zander et al., 2002; Knop et al., 2007).

The GIP gene is expressed mainly in K-cells, which are enterochromaffin cells of the proximal small intestine (enteroendocrine duodenal and jejunal mucosa). The release of the 42-amino acid hormone, GIP, is stimulated by enteral glucose, lipids and products of meal digestion in a concentration-dependent manner (Schirra et al., 1996). However, GIP has not been considered a suitable candidate for therapeutic development for the treatment of type 2 diabetes, because: a) GIP concentrations in patients with type 2 diabetes are either normal, or slightly increased in response to a meal (Vilsbj rnsen et al., 2002; Holst et al., 2004) and; b) GIP infusion does not reduce plasma glucose concentrations in patients with type 2 diabetes (Matuszek et al., 2007). In contrast,

patients with type 2 diabetes, especially obese subjects, have decreased GLP-1 responses (Toft-Nielsen et al., 2001; Kjems et al., 2003; Knop et al., 2008). To date, whether reduced GLP-1 secretion is a primary phenomenon in the pathogenesis of diabetes or a consequence of diabetes is unclear. First-degree relatives of patients with type 2 diabetes have normal GLP-1 secretion in response to oral glucose and meals, suggesting that the GLP-1 secretion abnormality seen in diabetes may be acquired (Nyholm et al., 1999; Nauck et al., 2004). In addition, GLP-1 is able to stimulate glucose-dependent insulin secretion under hyperglycaemic conditions in type 2 diabetes (Nauck et al., 1993; Holst et al., 2009; Salehi et al., 2010). Furthermore, exogenous GLP-1 administration leads to a normalisation of hyperglycaemic conditions (Nauck et al., 1993; 2009; Ratner et al., 2010). Therefore, GLP-1-based strategies appear an interesting treatment potential for type 2 diabetes (Gallwitz, 2010).

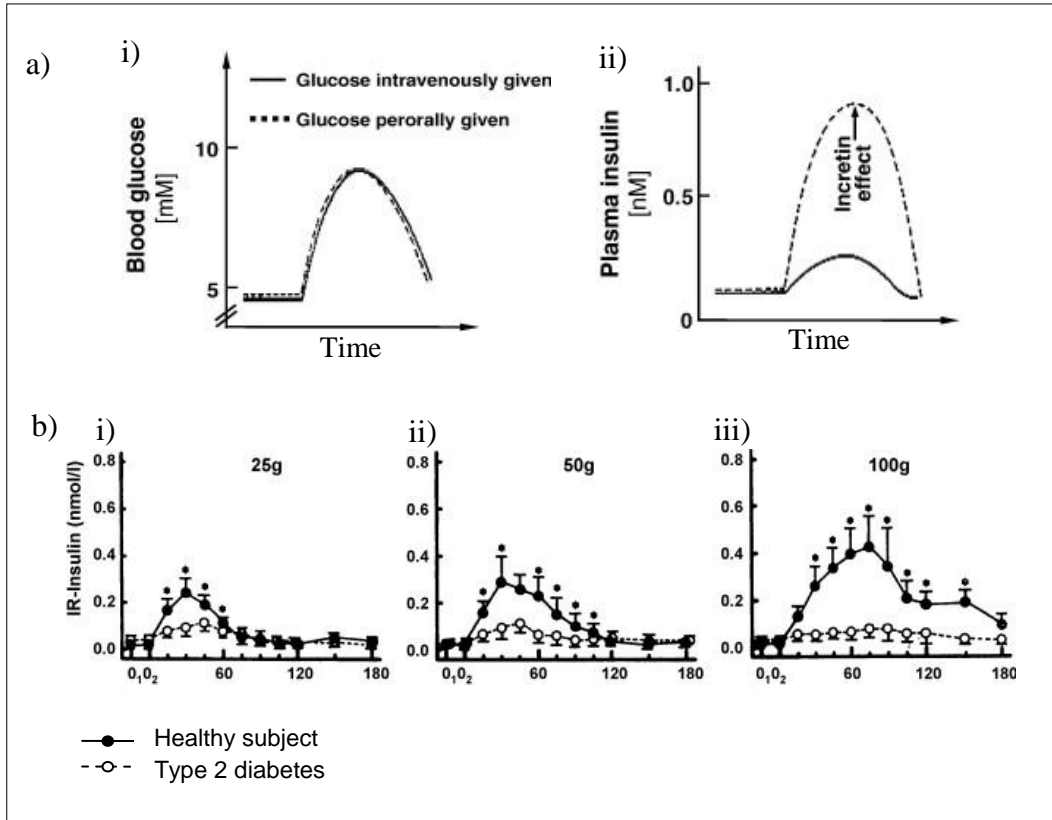


Figure 1.2. The incretin effect in healthy subjects and patients with diabetes. After glucose was given perorally or intravenously as indicated, the plasma glucose responses were identical (a, i), whereas a greater insulin response occurred in response to an oral glucose load compared to intravenous glucose administration (a, ii). This is the incretin effect. After oral-administration of 25g (b, i), 50g (b, ii) or 100g (b, iii), the insulin secretory response was measured by radioimmunoassay. 0₁-0₂: glucose infusion time. Plasma insulin levels in patients with diabetes were lower than in healthy subjects (b). From Nauck et al., 1986.

1.2.2 Synthesis and secretion of GLP-1

In mammals, GLP-1 is synthesized from proglucagon in intestinal L-cells, which are localised predominately in the lower part of the small intestine (Mojsov et al., 1986). The proglucagon gene (**Figure 1.3a**) is expressed in both the pancreatic α -cells and the intestinal L-cells, but the post-translational processing differs markedly in these two tissues (Orskov et al., 1986; 1987; Hoslt 2007). In intestinal L-cells, the molecule is processed to GLP-1, glucagon-like peptide-2 (GLP-2), intervening peptide-2 (IP2), oxyntomodulin and glicentin (Orskov et al., 1989; Thim and Moody, 1981) by prohormone convertase enzyme (PC) 3 (also known as PC1 or PC1/3; Thomas et al., 1991; Holst et al., 2010) (**Figure 1.3c**). In α -cells of the pancreas, proglucagon is cleaved by PC2 (Rouille et al., 1994) to glucagon, glicentin-related pancreatic C-peptide (GRPP), intervening peptide-1 (IP1) and major proglucagon fragment (MPGF; Mojsov et al., 1986), (**Figure 1.3b**). However, emerging evidence suggests that pancreatic α -cells can also adapt to produce GLP-1 under the condition of recombinant expression of PC3 (Wideman et al., 2006; 2007; 2009).

In the secretory vesicles, GLP-1 is further processed to the non-amidated peptide GLP-1 7-37, and the N-terminally truncated and the C-terminally amidated GLP-1 7-36 amide (Kreymann et al., 1987, **Figure 1.3d**). Both are active forms of GLP-1 and released (predominately GLP-1 7-36 amide) into the circulation very quickly after meal ingestion, in which, fat, carbohydrates and protein all seem to be powerful stimulators of GLP-1 secretion (Reimann, 2010). However, GLP-1 only has a short duration of action due to a rapid proteolytic degradation by the enzyme dipeptidyl peptidase IV (DPP-IV). The fragments GLP-1 9–36 amide and GLP-1 9-37 have been identified as

products of GLP-1 cleavage by DPP-IV action both *in vitro* and *in vivo* (Mentlein et al., 2009). This process is so quick that only <25% of GLP-1 secreted from the gastrointestinal (GI) tract enters the portal vein in an active form prior to reaching the liver (Reimann, 2010). Further degradation occurs rapidly within the liver (40–50% of the remaining GLP-1). Thus, it is estimated that most of the circulating postprandial GLP-1 (~85%) is GLP-1 9-36 amide or GLP-1 9-37 (**Figure 1.3d**, Abu-Hamdah et al., 2009). This rapid degradation continues *via* circulating DPP-IV, and limits the total half-life of GLP-1 to 1–2 min (Mentlein et al., 2009).

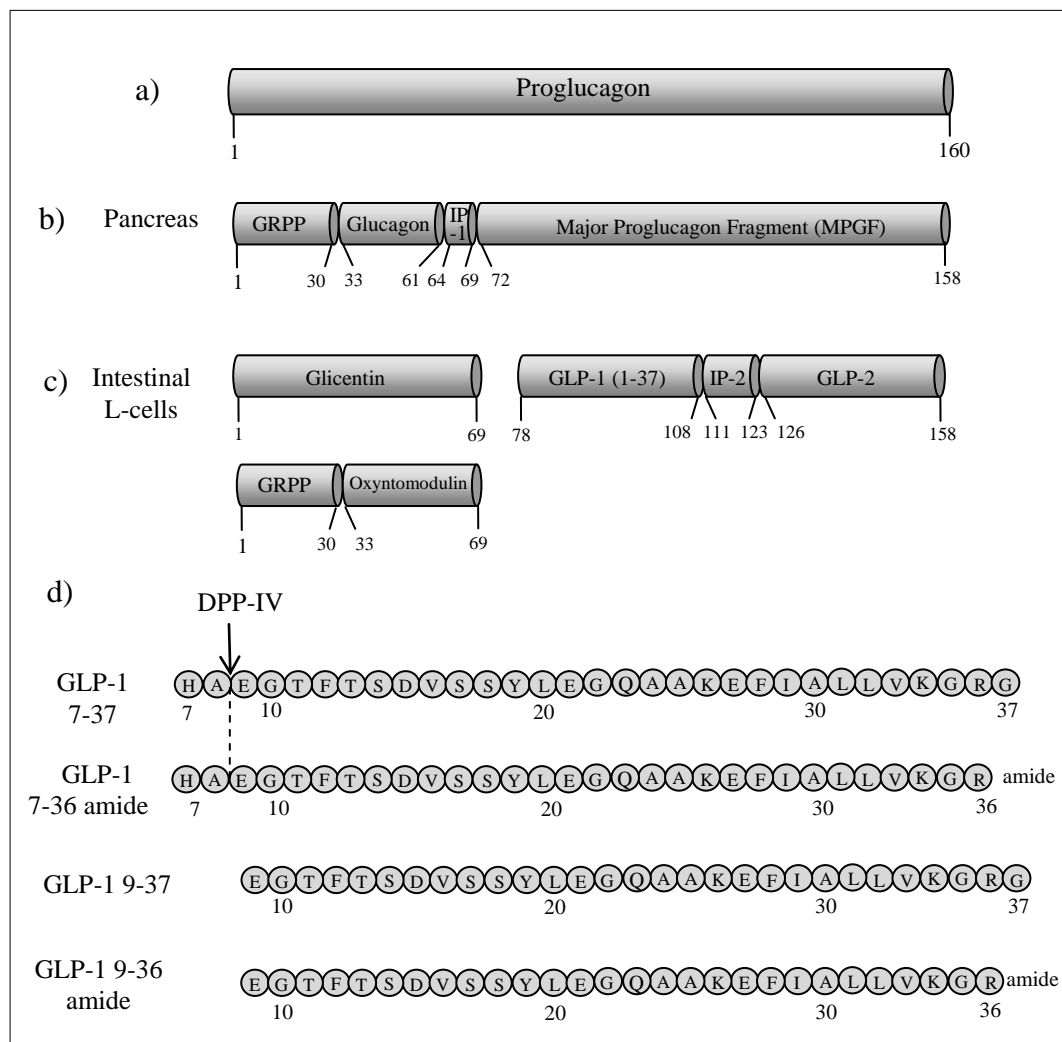


Figure 1.3. The post-translational processing of proglucagon and GLP-1. In the pancreas, proglucagon (a) is cleaved to glucagon, GRPP, IP1 and MPGF by PC2, which comprise amino acids 33-61, 1-30 and 72-158 of proglucagon, respectively (b). In the intestinal L-cells proglucagon is processed by PC3 to GLP-1, GLP-2, IP2, oxyntomodulin and glicentin which are composed of amino acids 78-107, 126-158, 111-123 and 33-69 of proglucagon respectively (c). GLP-1 7-37 and GLP-1-36 amide are the active forms of GLP-1 in the body, which are quickly cleaved by DPP-IV into inactive GLP-1 9-37 and GLP-1 9-36 amide, respectively, as indicated (d). The cleavage site is indicated by the arrow and continued by the dashed line. Picture adapted from Hoslt, 2007.

1.2.3 Biological activities of GLP-1

GLP-1 has numerous actions in different tissues through binding to a Family B GPCR, the GLP-1R (**Figure 1.4**). Structurally-related members of the glucagon family of peptides such as GLP-2, glucagon, and GIP do not exhibit cross-reactivity at the GLP-1R at physiologically relevant concentrations (Holst, 2007). The human GLP-1R gene is transcribed in pancreatic islets, lung, brain, stomach, intestine, heart, kidney and liver but not in skeletal muscle or adipose tissue of most species. (Wei and Mojsov, 1995; Bullock et al., 1996; Gupta et al., 2010).

In the pancreas, GLP-1 enhances insulin secretion from islet β -cells and suppresses glucagon secretion from islet α -cells (**Figure 1.4**; Rayner, 2001). Both actions occur in a glucose-dependent manner (De Marinis et al., 2010). Evidence, at least in animal models and cell lines, has shown that GLP-1 promotes β -cell proliferation and neogenesis, while preventing apoptosis (Li et al., 2005; Cunha et al., 2009; Quoyer et al., 2010). In the GI tract, GLP-1 delays gastric emptying and acts as a postprandial satiety signal through neurohormonal networks that signal the brain to suppress appetite and food intake (Schirra et al., 1997; Kim et al., 2009). Most likely, both the enteric and the central nervous systems are important transducers of GLP-1 action, which involves triggering of the gut-to-brain and the brain-to-periphery axis where nutrients regulate the release of GLP-1 and activate the tightly regulated enteric and cerebral neuronal circuits (Hayes et al., 2009; Burcelin et al., 2009). GLP-1Rs are expressed in the heart and vasculature of both rodents and humans and growing evidence has suggested that GLP-1 may play an important role in the cardiovascular system. Pharmacological application of GLP-1 or GLP-1R agonists demonstrates a number of

protective effects including reduction of systolic blood pressure, beneficial effects on myocardial ischaemia in animal models and positive effects on left ventricular function in heart failure (Grieve et al., 2009). Recently the GLP-1R was reported to be present on human hepatocytes and play a direct role in decreasing hepatic steatosis *in vitro* by modulating elements of the insulin signalling pathway (Gupta et al., 2010) (**Figure 1.4**).

Interestingly, emerging evidence suggests insulin-like actions of GLP-1 9-36 amide and GLP-1 9-37, metabolites of GLP-1, on liver, heart and vasculature (Tomas and Habener, 2010). Since these fragments of GLP-1 have a strongly reduced activity on the classical GLP-1R of β -cells, it has been proposed that a different receptor and a novel pathway might be involved but this have not been confirmed by experimental evidence (Tomas and Habener, 2010).

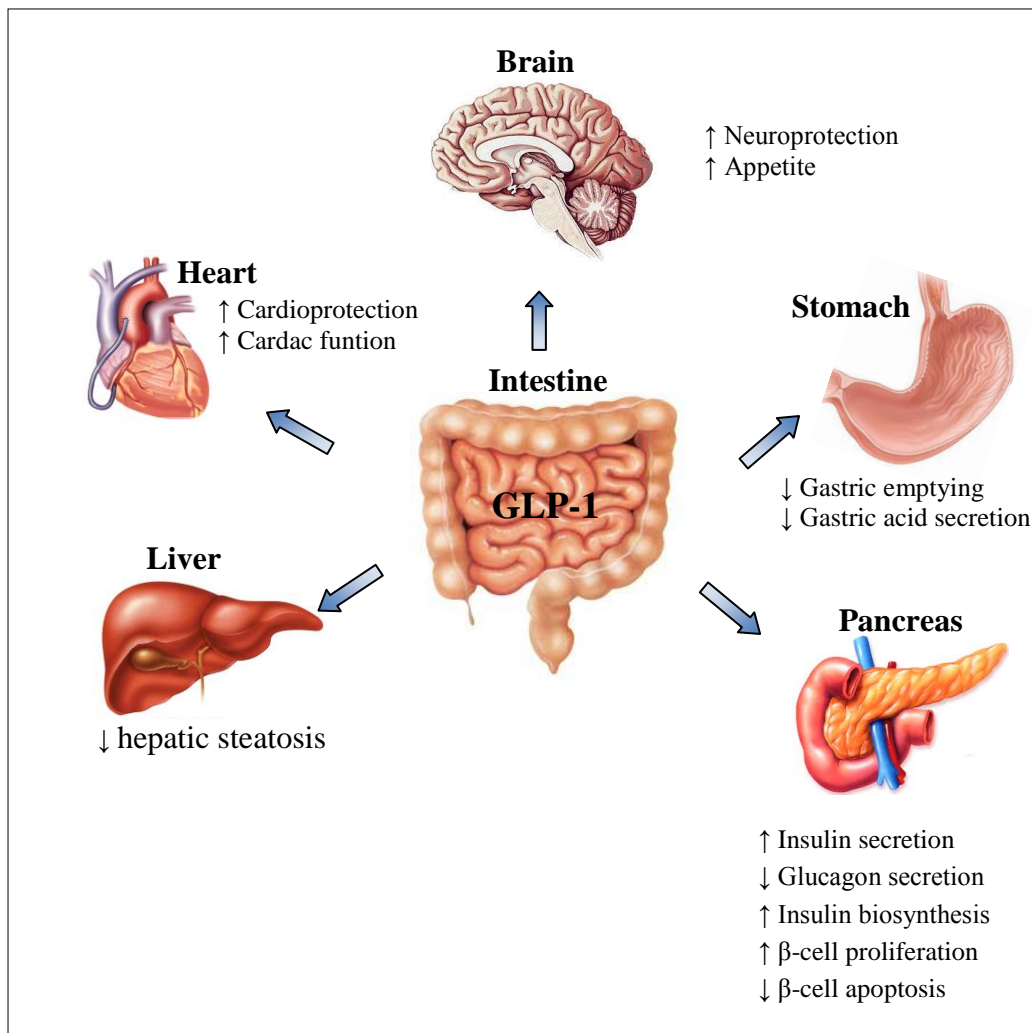


Figure 1.4. Biological activities of GLP-1. The main actions of GLP-1 are in the pancreas, where it stimulates insulin secretion and inhibits glucagon secretion in a glucose-dependent manner. In addition, GLP-1 slows gastric emptying, decreases food intake by increasing satiety and has a range of other physiological actions as indicated in the diagram. From De Leon et al., 2006.

1.2.4 GLP-1-based therapies in type 2 diabetes

The pharmacological actions of GLP-1 have been the basis of the development of two novel substance classes for type 2 diabetes therapies. Firstly DPP-IV inhibitors inhibit the degradation of GLP-1 by this enzyme (Gallwitz, 2010) and secondly GLP-1R agonists (GLP-1 mimetics) mimic the physiologic actions of native GLP-1 but with considerably longer half-lives due to resistance to DPP-IV.

1.2.4.1 Oral DPP-IV inhibitors

DPP-IV, also known as adenosine deaminase complexin G-protein 2 or CD26 (cluster of differentiation 26), is an antigenic enzyme expressed on the surface of most cell types and is associated with immune regulation, signal transduction and apoptosis. It cleaves X-proline (or alanine) dipeptides from the N-terminus of polypeptides. The substrates of this enzyme include growth factors, chemokines, neuropeptides, and vasoactive peptides (Mentlein et al., 2009). DPP-IV inhibitors have been shown to elevate active GLP-1 levels 2-3-fold by providing up to 90% inhibition of plasma DPP-IV activity over 24 hours *in vivo* and have the additional advantage of an oral route of administration (Charbonnel et al., 2006). Currently, there are three DPP-IV inhibitors (saxagliptin, sitagliptin and vildagliptin) licensed in Europe for use in patients with type 2 diabetes (Khunti and Davies, 2010). These agents significantly decrease fasting and postprandial glucose levels and also reduce HbA1c by approximately 0.5–1.0% (Gilbert and Pratley, 2009; Gallwitz, 2010). Sitagliptin and vildagliptin have also been reported to improve markers of β -cell function and to reduce systolic blood pressure (Deacon and Holst, 2006). A low incidence of hypoglycaemia has also been observed, which may be explained by the fact that the effects of GLP-1 on insulin secretion are glucose-

dependent and the counter-regulatory release of glucagon in response to hypoglycaemia is preserved even in the presence of pharmacological concentrations of GLP-1 (Pratley and Salsali, 2007). However, no weight loss is observed in patients treated with DPP IV inhibitors (Niswender, 2010). Since DPP-IV is expressed on many cell types including lymphocytes and has many diverse functions, long-term inhibition of this enzyme could be expected to have side effects (Yu et al., 2010). Indeed, experimental evidence shows an increased risk of infections and a tendency towards a higher incidence of some tumours, supporting the possibility of adverse immunological and oncological effects (Stulc and Sedo, 2010).

1.2.4.2 Long-acting, injectable peptide GLP-1R agonists

As the cleavage of GLP-1 by DPP-IV occurs between residues Ala and Glu, a conservative substitution of alanine in position 2 with, e.g. valine (A2V) is sufficient to stabilize the GLP-1 molecule against DPP-IV and does not affect the biological activity of the peptide (Deacon et al., 1998). However, the stabilized molecule is eliminated quickly in the kidneys with a half life of 4-5 min, which is still unsuitable for a drug. Exendin-4, isolated from the saliva of the Gila Monster (*Heloderma suspectum*), is a peptide with about 50% sequence homology to GLP-1 and a full agonist for the GLP-1R. Exendin-4 is stable against DPP-IV, and is eliminated in the kidneys exclusively by glomerular filtration, resulting in a longer half-life *in vivo* (Mikhail, 2008). Exenatide (Amylin Corporation and Lilly) is synthetic exendin-4 and has an *in vivo* half-life in the range of 5-6h (compared to the 1-2min half-life of GLP-1) (Robles and Singh-Franco, 2009). Exenatide has been approved for the treatment of type 2 diabetes in both Europe and the U.S., and is currently administered as a subcutaneous injection (10µg, twice

daily) for use as monotherapy in subjects not achieving adequate glycemic control on lifestyle modification alone or one or more oral agents (van Genugten et al., 2009). Based on the structure of native human GLP-1, Liraglutide (NovoNordisk) has been developed with modifications including an amino acid substitution and an attachment of a C16 acyl chain bound non-covalently to albumin, which therefore prevents both renal elimination and degradation by DPP-IV (Drucker et al., 2010). Liraglutide has a half-life of approximately 11–13h after administration and has been licensed for the treatment of type 2 diabetes in Europe for once-daily subcutaneous injection (Montanya and Sesti, 2009).

Similar to native GLP-1, exogenous GLP-1R agonists control blood glucose through regulation of islet function, principally by the stimulation of insulin secretion and inhibition of glucagon secretion in a glucose-dependent manner (Mikhail, 2008). Exenatide and Liraglutide significantly reduce HbA1c levels (by approximately 0.8–1.5% of hemoglobin A), and both fasting and postprandial glucose levels with very low rates of hypoglycaemia (Edavalath and Stephens, 2010). In contrast to treatment with DPP-IV inhibitors, which are weight neutral, Exenatide and Liraglutide reduce body weight by approximately 2–3kg, possibly by inhibition of gastric emptying, increased feelings of satiety and reduced food intake (Horton et al., 2010). They also reduce blood pressure and plasma lipid profiles in subjects with type 2 diabetes, raising the hope that long-term treatment with these agents may reduce the incidence of cardiovascular events (Buse et al., 2009). Furthermore, both Exenatide and Liraglutide have shown positive effects on β -cell function including increased insulin secretion in preclinical and clinical studies, which may indicate inhibition or reversal of progression (Pratley, 2008). Additionally, Exenatide appears to have some extra-pancreatic effects. For

example, it increases glucose transport in muscle, and increases the expression of the glucose transporter and glycogen synthesis in liver (Zheng et al., 2009).

The most common adverse events of GLP-1 agonists are gastrointestinal, in which dyspepsia or nausea are the most frequent during treatment with Liraglutide or Exenatide respectively (Buse et al., 2009). This may result from delayed gastric emptying and the adverse effects tend to decline with continued administration (Gallwitz, 2010). Rare cases of acute pancreatitis have been reported with Exenatide and Liraglutide but their clinical significance remains unclear (Drucker et al., 2010). Furthermore, as peptides these agents can be antigenic with approximately 40% of patients treated with Exenatide and 0-13% of those treated with Liraglutide developing antibodies against the GLP-1R agonist (Gilbert and Pratley, 2009). However, the Exenatide antibodies neither cross-react with human GLP-1 nor have any obvious effect on glycaemic control over a period of 3 years (Gallwitz, 2010). In addition to these potential problems, the relatively short half-life and the required subcutaneous administration route has focussed much effort on the development of longer-acting GLP-1R agonists, especially non-peptide, orally bioavailable small molecule GLP-1R modulators for therapeutic purposes.

1.3 GPCRs in drug discovery

The GLP-1R belongs to the largest superfamily of cell surface receptors, namely GPCRs, which are also known as seven transmembrane receptors. GPCRs constitute more than 800 members of the human genome that respond to a plethora of signals, including light, odours, pheromones, peptide hormones and neurotransmitters, and vary in size from photons and ions to small molecules, peptides and large proteins. As a

consequence of the pervasive involvement of GPCRs in many physiological and pathological processes, and the success of drug development programmes, GPCRs are the most common targets of medical therapeutics, representing nearly 50% of drugs for humans that are on the market (Millar and Newton, 2010). The success of such therapeutics has driven research to develop a greater understanding of these targets and their interaction with drugs to enable novel drug discovery.

1.3.1 Classification and the common structure of GPCRs

Members of the GPCR superfamily share a common membrane topology: a single polypeptide chain of up to 1100 residues passing through the plasma membrane of the cell seven times, which results in the formation of an extracellular N-terminal domain, an intracellular C-terminal domain and seven transmembrane α -helices connected by three extracellular loops (ECLs) and three intracellular loops (ICLs) (**Figure 1.6**). Classically, the mammalian members of the GPCR superfamily have been divided into three families: A, B and C (Kristiansen, 2004).

Family A, the rhodopsin-like family, is the largest family of GPCRs comprising of 672 members, including 388 odorant receptors and accounts for nearly 85% of all GPCR genes (Millar and Newton, 2010; Heilker et al., 2009). The receptors of this family are characterized by short N-termini (without any conserved domains) and several highly conserved amino acids in the seven transmembrane bundle. There is usually a disulfide bridge that connects ECL1 and ECL2 (Jacoby et al., 2006). In addition, most receptors in this family have a palmitoylated cysteine residue in the intracellular C-terminal domain. The crystal structure of rhodopsin (Palczewski et al., 2000) has indicated that the transmembrane domains of Family A receptors are 'tilted' and 'kinked' (**Figure 1.6a**). This has been followed by the solving of the structures of

the β_2 -adrenergic, β_1 -adrenergic, and the A_{2A} -adenosine receptors (Millar and Newton, 2010). Comparison of these four Family A GPCR structures reveal that the transmembrane domains are strikingly similar and the docked small molecule ligands are also fairly similar in occupying much the same space in the transmembrane cluster pocket, although adenosine docks somewhat more superficially (Hanson and Stevens, 2009). However, the structures of the ECL2 are quite divergent. In rhodopsin, the top of the transmembrane cluster seems to be occluded by the N-terminus and ECL2 domains, whereas the top of the transmembrane cluster appears to be open in the other receptors with ECL2 positioned to one side (Hanson and Stevens, 2009) (**Figure 1.5**).

Family B, the Secretin family, is a small family of GPCRs consisting of 15 known hormone peptides receptors and 35 orphan receptors in humans (Kristiansen, 2004; Bonner, 2010). The known hormone peptide ligands of Family B GPCRs include, calcitonin, parathyroid hormone (PTH)/parathyroid hormone-related peptides (PTHrP), vasoactive intestinal peptide, corticotropin-releasing factor (CRF) and many peptide hormones from the glucagon hormone family (glucagon, GLP-1, GLP-2, GIP, secretin and growth hormone releasing hormone) (Harmar, 2001). This family of receptors is characterized by a relatively long N-terminal tail and a network of three conserved cysteine disulfide bridges which stabilize the N-terminal structure (**Figure 1.6b**). The present study will focus on the GLP-1R in this family.

Family C, the Glutamate family, form the other small family of GPCRs in humans. This family contains 24 members including metabotropic glutamate receptors, γ -aminobutyric acid type B ($GABA_B$) receptors and calcium-sensing receptors, GPRC5 receptors and 7 Family C orphan receptors (IUPHAR database, Accessed on 2010-09-01). The majority of Family C receptors are characterized by very large N- and C-terminal tails, a putative disulfide bridge connecting ECL1 and ECL2, together with a

very short and well-conserved ICL3 (**Figure 1.6c**). The ligand binding site is located in the N-terminal domain, which is often described as a venus fly trap. Most Family C GPCRs, except the GABA_B receptors, contain a cysteine-rich domain with nine conserved cysteine residues, which links the venus fly trap to the seven transmembrane domains (Bräuner-Osborne et al., 2007).

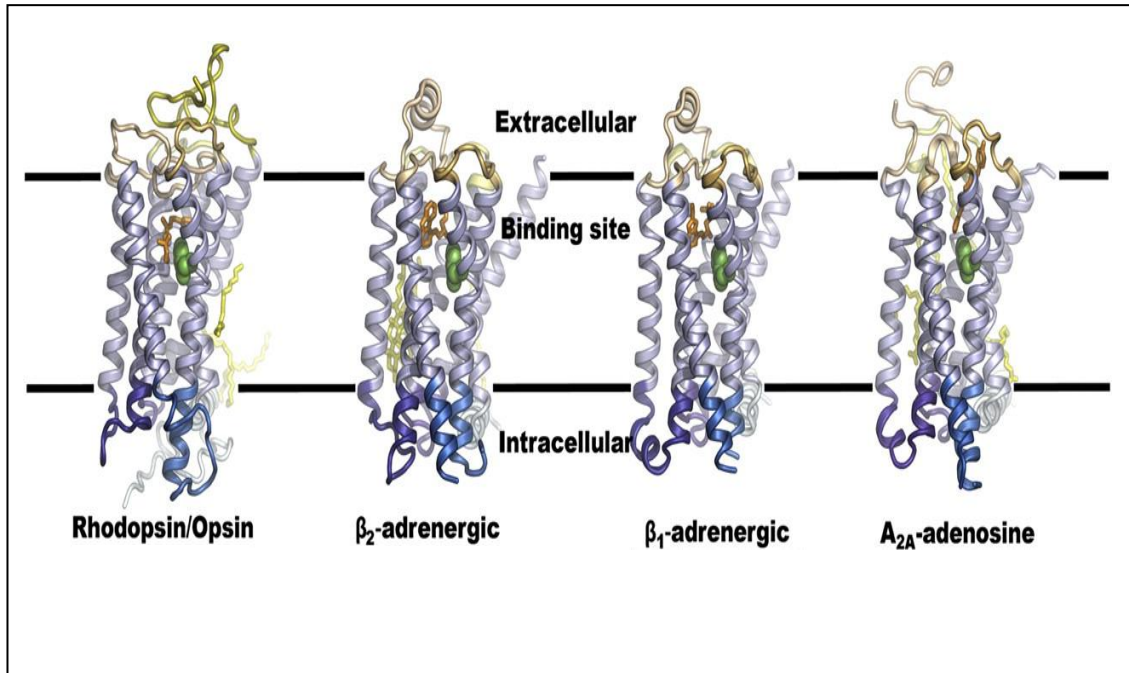


Figure 1.5. Transmembrane view of the available crystal structures of GPCRs. To date four crystal structures: rhodopsin/opsin; β_2 -adrenergic; β_1 -adrenergic and; adenosine A_{2A} receptors have become available as indicated. All structures are shown with the same orientation. Transmembrane helices are shown in purple, intracellular regions are shown in blue and extracellular regions are shown in brown. The ligands are shown in orange, and bound lipids are shown in yellow. These crystal structures show similar relative positions of the transmembrane domains and location of the ligand-docking sites with the adenosine analogue occupying a slightly more superficial position. Picture adapted from Hanson and Stevens, 2009.

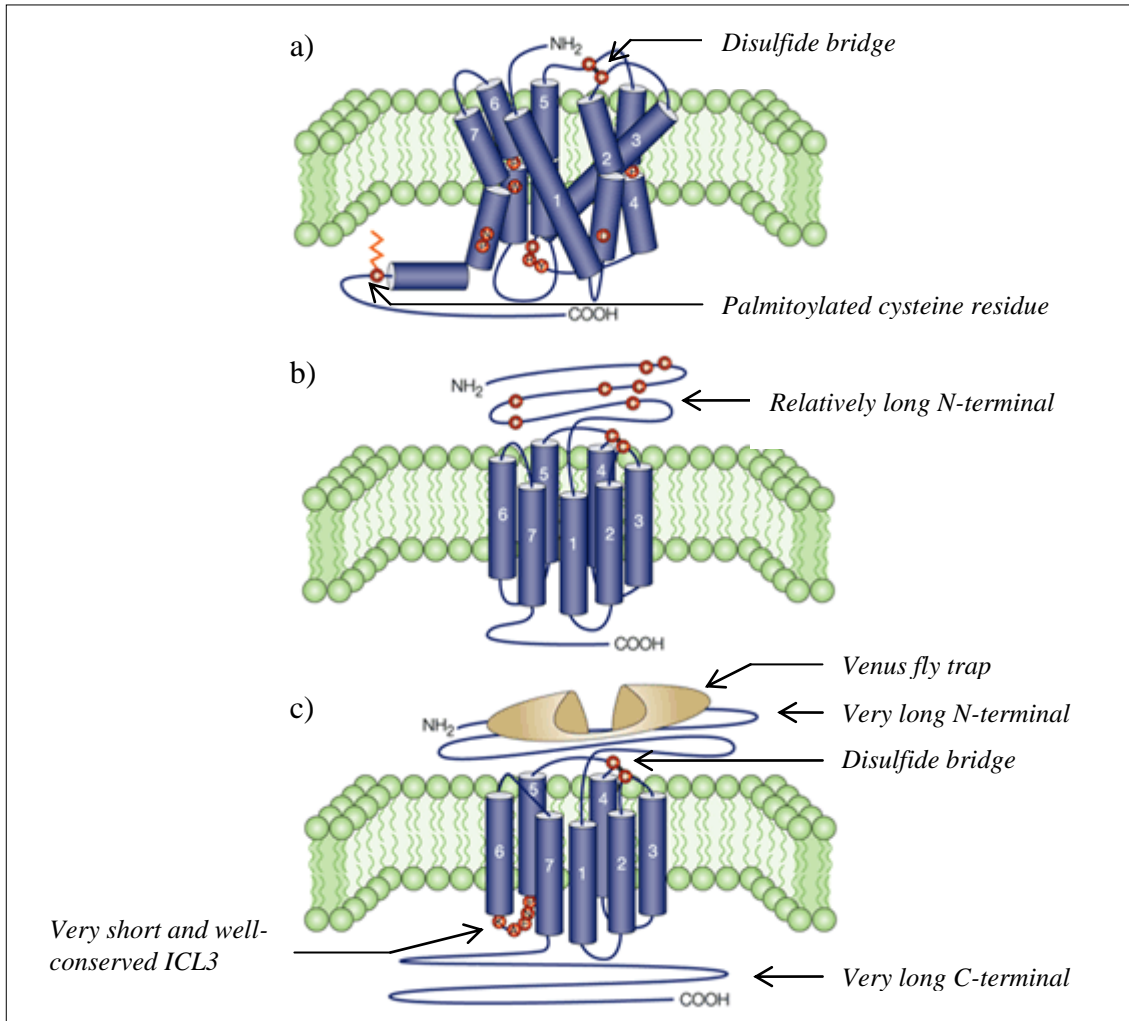


Figure 1.6. Molecular structure of GPCRs. All GPCRs share the seven transmembrane α -helices which are connected by three extracellular loops (ECL1, ECL2 and ECL3) with an extracellular NH_2 terminal and three intracellular loops (ICL1, ICL2 and ICL3) with an intracellular COOH -terminal. Red balls represent residues. **a) Family A GPCR.** The receptor is 'tilted' and 'kinked' with a disulfide bridge that connects ECL1 and ECL2 and a palmitoylated cysteine residue in the intracellular C-terminal domain. **b) Family B GPCR.** These receptors contain a relatively long N-terminal tail and a network of conserved disulfide bridges. **c) Family C GPCR.** Characterized by very large N- and C-terminal tails, a putative disulfide bridge connecting ECL1 and ECL2, together with a very short and well-conserved ICL3. The ligand-binding domain, located in the amino terminus is often described as being like a Venus fly trap. Picture adapted from George et al., 2002.

1.3.2 Signal transduction by G-proteins

Typically, GPCRs mediate their intracellular signalling through G-proteins (hence GPCRs) although in recent years more and more G-protein-independent signalling pathways have been defined (Tuteja, 2009). In G-protein signalling pathways, GPCRs regulate the activity of G-proteins which in turn regulates the activity of an intracellular effectors system. G-proteins are the go-between proteins but were actually called G-proteins because of their interaction with the guanine nucleotides guanosine triphosphate (GTP) and guanosine diphosphate (GDP, see below). There are two main classes of G-proteins, heterotrimeric G-proteins and monomeric (small) G-proteins (e.g., Ras, Rho and Rab families). Both classes of G-proteins are involved in intracellular signal transductions but heterotrimeric G-proteins generally initiate physical interactions with GPCRs (Cabrera-Vera et al., 2003) and therefore are focused on here.

1.3.2.1 Heterotrimeric G-proteins

The heterotrimeric G-proteins are composed of three subunits: α , β and γ , with molecular masses of ~39-45, 35-39, and 6-8 kDa, respectively. The α -subunit ($G\alpha$) binds guanine nucleotides while the β - and γ - subunits remain together as a $G\beta\gamma$ -complex. $G\alpha$ -subunits consist of two domains, a GTPase domain involved in the binding and hydrolysis of GTP, and an α -helical domain that buries the GTP within the core of the protein (Cabrera-Vera et al., 2003). Up to now, there exist at least 28 different $G\alpha$ -subunits that are the products of 19 different genes and splice variants. Based on the degree of primary sequence similarities of α -subunits, the heterotrimeric G-proteins have been categorised into four families: $G\alpha_s$, $G\alpha_{i/o}$, $G\alpha_{q/11}$, $G\alpha_{12/13}$. The γ -

subunits interact with the β -subunits through an N-terminal coil and make extensive contacts along the base of the β -subunits (Cabrera-Vera et al., 2003).

1.3.2.2 Typical activation and regulation of G-proteins

Following a similar principal to an activation/inactivation cycle, all heterotrimeric G-proteins allow specific transmission of signals into cells (Cabrera-Vera et al., 2003). When GDP is bound to $G\alpha$, the complex associates with $G\beta\gamma$ to form an inactive $\alpha\beta\gamma$ trimer (**Figure 1.7.1**). On the binding of agonist, the receptor (**Figure 1.7.2**) becomes activated and creates a conformational change resulting in increased affinity for the G-protein (**Figure 1.7.2**). The binding of receptor with $G\alpha$ -GDP allows the receptor to function as a guanine nucleotide exchange factor (GEF), the $G\alpha$ -subunit then exchanging GDP for GTP (**Figure 1.7.3**). This exchange in the guanine nucleotides leads to a reduction in the affinity of α -subunits for $G\beta\gamma$ and the dissociation of the heterotrimer (**Figure 1.7.4**). The active G-protein forms once $G\alpha$ -GTP is released from $G\beta\gamma$, and the dissociated subunits can then activate or inhibit different effector proteins such as enzymes and ion channels, resulting in rapid changes in the concentration of intracellular signalling molecules (e.g., cAMP). Typically, the active state of the G-protein terminates when the $G\alpha$ hydrolyses the attached GTP to GDP by its inherent GTPase activity, allowing it to re-associate with $G\beta\gamma$ and become inactive (**Figure 1.7.1**) (Cabrera-Vera et al., 2003).

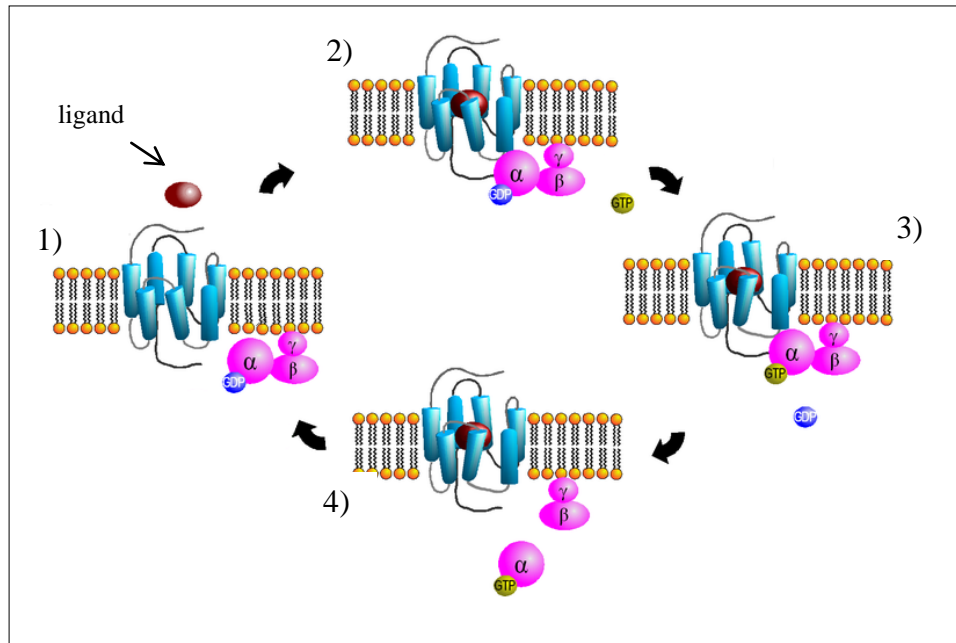


Figure 1.7. Activation cycle of G-proteins by GPCRs. In the inactive conformation, the $G\alpha\beta\gamma$ heterotrimer is probably dissociated from a GPCR and the $G\alpha$ -subunit is bound with GDP (1). Activation of receptors by an agonist induces a conformational change in the receptor, allowing it to interact with the G-protein, leading to the formation of a high-affinity agonist-receptor-G-protein complex (2). This allows the receptor to act as a GEF for the α -subunit, stimulating the exchange of GDP for GTP (3). Upon binding of GTP, the $G\alpha$ -subunit dissociates from the $G\beta\gamma$ -subunit and these proteins are released from the receptor (4). Dissociated $G\alpha$ - and $G\beta\gamma$ -subunits then interact with a variety of effector proteins. The signal is terminated by the intrinsic ability of $G\alpha$ -subunits to hydrolyze attached GTP to GDP, which is enhanced by GTPase-accelerating G-proteins (GAPs). The formation of $G\alpha$ -GDP allows it to re-associate with $G\beta\gamma$ to start a new cycle (1). Picture adapted from <http://luur.lub.lu.se/luur?func=downloadFile&fileOID=548213>.

An activated heterotrimeric G-protein dissociates into the $G\alpha$ -subunit and $G\beta\gamma$ complex, both of which have an independent capacity to signal forward through the activation or inhibition of effectors. Members of the $G\alpha_s$ family couple to and activate adenylate cyclase (AC) to increase intracellular cAMP levels, which activates both protein kinase A (PKA) and cAMP-regulated guanine nucleotide exchange factors (Epac; **Figure 1.8**; Bos, 2003). The $G\alpha_{i/o}$ family inhibit AC and trigger other signalling events, e.g., inwardly rectifying potassium channels (GIRKs: activated by $G\beta\gamma$ complex; **Figure 1.8**) (Vilardaga et al., 2009). The members of the $G\alpha_{q/11}$ family activate phospholipase C (PLC), resulting in the intramembrane hydrolysis of phosphatidylinositol-4,5-bisphosphate ($\text{PtdIns}(4,5)\text{P}_2$) to inositol-1,4,5-trisphosphate ($\text{Ins}(1,4,5)\text{P}_3$) and diacylglycerol (DAG). DAG increases the activity of classical and novel isoforms of protein kinase C (PKC), and $\text{Ins}(1,4,5)\text{P}_3$ triggers the release of Ca^{+2} ions from intracellular stores (**Figure 1.8**) (Cordeaux and Hill, 2002). The two members of the $G\alpha_{12/13}$ family regulate the Rho GTPases family, which has been shown to regulate many aspects of intracellular actin dynamics (Heasman and Ridley, 2008). $G\beta\gamma$ complexes are also important signalling molecules in their own right. They can activate a large number of effectors directly including ion channels, phospholipases, phosphoinositide kinases, and the Ras/Raf/ERK (extracellular signal-regulated kinase) pathways (Jacoby et al., 2006). These $G\beta\gamma$ complexes are often from $G\alpha_{i/o}$ -coupled GPCRs, although not exclusively. The specific function of individual $G\beta\gamma$ complexes is not fully explored although some specificity has been reported (Vilardaga et al., 2009).

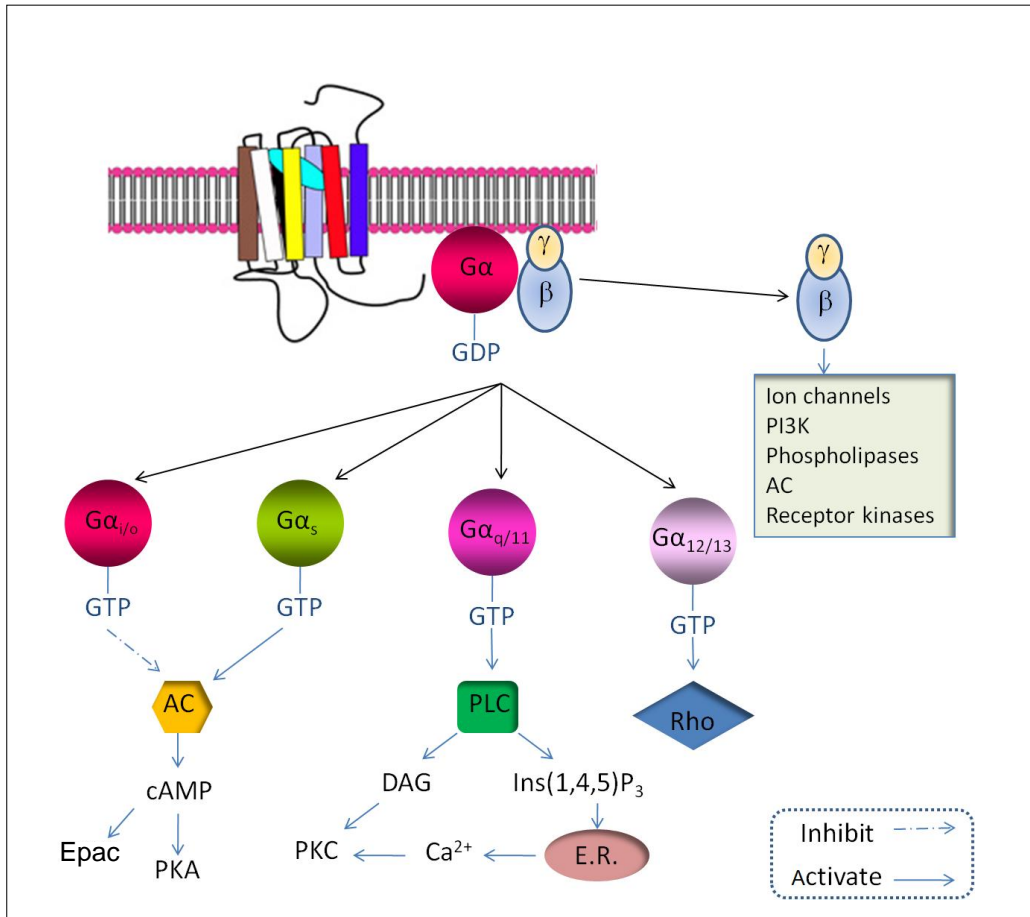


Figure 1.8. Diversity of G-protein signal transduction. A GPCR is activated by binding of a specific ligand. The ligand-bound receptor then activates a G-protein that dissociates into the G_{α} -subunit and $G_{\beta\gamma}$ complex, both of which have an independent capacity to signal forward through the activation or inhibition of effectors. G_{α_s} increases the enzymatic activity of AC which catalyzes the conversion of ATP to cAMP. The latter activates protein kinase A (PKA) and cAMP-regulated guanine nucleotide exchange factor (Epac). The activation of $G_{\alpha_{i/o}}$ inhibits AC activity. The released $G_{\beta\gamma}$ complex is also able to regulate some effectors and signal forward. The activation of $G_{\alpha_{q/11}}$ activates PLC which initiates subsequent formation of DAG and IP₃ (Ins(1,4,5)P₃). These second messengers then activate PKC, either directly (DAG), or indirectly *via* the release of internally stored Ca²⁺. PKC and Ca²⁺ activate different downstream effectors. $G_{\alpha_{12/13}}$ activates Rho proteins.

1.3.3 Internalization and desensitization of GPCRs

For most GPCRs, a loss of functional response, known as desensitization, can occur when receptors are exposed to repeated or continuous agonist stimulation. Desensitization is cell specific and dependent upon both the expression and subcellular localization of specific components that regulate the desensitization processes. Three general mechanisms are associated with desensitization of GPCRs: 1) receptor phosphorylation; 2) receptor internalization or sequestration; and 3) receptor downregulation (Gray and Roth, 2002). Agonist-induced receptor phosphorylation often results in the most rapid desensitization. In this process, conformational changes occurring on agonist binding lead to phosphorylation of various serine or threonine residues of ICL3 and/or the C-terminal tail by GPCR kinases (GRKs) (Tobin, 2008). This facilitates β -arrestin binding and promotes receptor uncoupling from their cognate heterotrimeric G-proteins. (Moore et al., 2007; Marchese et al., 2008; Jalink and Moolenaar, 2010). Receptor desensitization can also occur in a GRK-independent manner through phosphorylation of different serine/threonine sites (also of ICL3 and the C-terminal tail) by second messenger-dependent protein kinases, e.g. PKA and PKC (Benovic et al., 1985; Ferguson, 2001).

In addition to the role in GPCRs desensitization, β -arrestins promote receptor internalization involving clathrin and adaptor protein-2 (AP-2) (Doherty and McMahon, 2009). Internalization of components of the plasma membrane, associated ligands and fluid, is also called endocytosis, which is a fundamental process in eukaryotic cells. Once β -arrestin is bound to a GPCR, it undergoes a conformational change allowing it to serve as a scaffoldin G-protein for an adaptor complex AP-2, which in turn recruits clathrin. If enough receptors in the local area recruit clathrin in this manner, they aggregate and the membrane buds inwardly as a result of interactions between the molecules of clathrin, in a process called opsonization. Once the pit has been pinched off the plasma membrane due to the actions of amphiphysin and dynamin, it is now an

endocytic vesicle. Following release of the vesicles into the cytoplasm as clathrin-coated vesicles, the coated vesicles fuse with early endosomes. After targeting to the endosomal compartment, the adapter molecules and clathrin dissociate and GPCRs can be either rapidly dephosphorylated and recycled back to the plasma membrane or targeted to lysosomes for degradation (**Figure 1.9**). Thus, receptor trafficking is critical for regulation of the temporal and spatial aspects of GPCR signalling. Indeed, internalization controls the density of the receptor at the cell surface, signal termination and propagation as well as receptor resensitization (Wolfe and Trejo, 2007).

At any point in this process, the β -arrestins may also recruit other proteins such as the non-receptor tyrosine kinase (nRTK), c-src, which may initiate activation of ERK1/2, or other mitogen-activated protein kinases (MAPKs) signalling through, for example, phosphorylation of the small GTP-ase, Ras, or recruit the proteins of the ERK cascade directly (i.e. Raf-1, MEK, ERK-1/2) at which point signalling is initiated due to their close proximity to one another. Another target of c-src is the dynamin molecules involved in endocytosis. Dynamins polymerize around the neck of an incoming vesicle, and their phosphorylation by c-src provides the energy necessary for the conformational change allowing the final 'pinching-off' from the membrane (Doherty and McMahon, 2009).

Although for most GPCRs, including the β_2 -adrenoceptor, internalization involves clathrin-dependent endocytosis pathways, some GPCRs, including the endothelin A receptor, are internalised via a clathrin-independent endocytosis pathways (Pelkmans et al., 2001). For example, endocytosis can occur through structures coated with the caveolin protein (Okamoto et al., 1998). However, this caveolae-mediate endocytosis is also dependent upon dynamin and responsible for endocytosis of some proteins that partition into cholesterol-rich membrane domains, especially in endothelial cells (Sandvig et al., 2008).

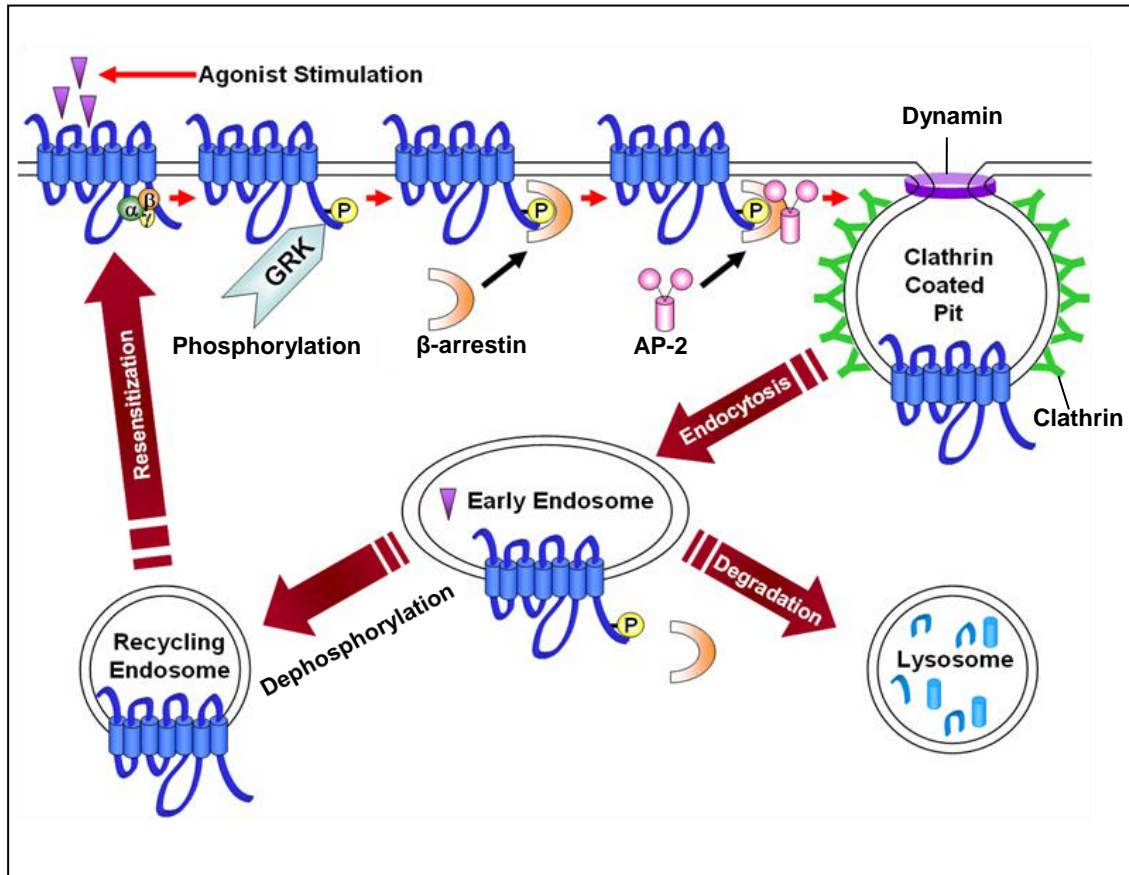


Figure 1.9. Clathrin-dependent internalization of GPCRs. The current model for agonist-induced internalization of GPCRs is based primarily on the β_2 -adrenoceptor receptor and other GPCRs. Following activation, receptors are phosphorylated by kinases, e.g., GRKs, resulting in rapid desensitisation due to G-protein uncoupling. G-protein uncoupling is further promoted by the binding of arrestins to the phosphorylated third intracellular loops and C-terminal tails of agonist-activated GPCRs. In addition, arrestins promote the targeting of desensitized receptors to clathrin coated pits for internalization by the interaction of the C-terminal portions of arrestin with both the clathrin heavy chain and the β_2 -adaptor subunit of AP-2. The dynamin induces neck formation of coated pits and their release into the cytoplasm as clathrin-coated vesicles. These coated vesicles fuse with early endosomes where the receptors may be dephosphorylated by specific phosphatases and recycled back to the plasma membrane fully resensitized or targeted to lysosomes for degradation. Picture adapted from Strachan et al., 2009.

1.3.4 Allosteric modulation of GPCRs

Distinct from the orthosteric binding site, which accommodates endogenous ligands such as hormones and neurotransmitters, allosteric binding site(s) have been revealed in GPCRs from all three major Families (i.e. A, B and C) (May and Christopoulos, 2003). Allosteric modulators bind to an allosteric site where they stabilize a receptor conformation that can result in an increase or decrease in the affinity of the receptor for the orthosteric agonist and/or a change in the efficacy of the orthosteric ligand, without directly activating the receptor (Bridges and Lindsley, 2008). Therefore, allosteric modulators are often termed positive allosteric modulators (PAMs) or negative allosteric modulators (NAMs) respectively (De amici et al., 2010). Allosteric sites may represent novel drug targets as there are a number of advantages in using allosteric modulators as therapeutic agents compared to classical orthosteric ligands. For example, allosteric binding sites on GPCRs do not need to face the same evolutionary pressure as orthosteric sites to accommodate an endogenous ligand and are therefore more diverse (Urban et al., 2007). Therefore greater GPCR selectivity may be obtained by targeting allosteric sites, which is particularly useful for GPCRs where selective orthosteric therapy has been difficult because of sequence conservation of the orthosteric site across receptor subtypes (Kenakin and Miller, 2010). In addition, these modulators may have a limited level to their effect, irrespective of the administered dose and thus have a decreased potential for toxic effects. Furthermore, if an allosteric modulator does not possess appreciable efficacy, it can provide another powerful therapeutic advantage over orthosteric ligands, namely the ability to selectively tune up or down tissue responses only when the endogenous agonist is present (Kenakin, 2009). Finally, allosteric binding sites (even of receptors for large peptides) can be targeted with low-

molecular-weight ligands that have the potential for oral bioavailability (Schwartz and Holst, 2006).

Some small-molecules bind to the allosteric site of the GPCR and function as both allosteric modulators and as agonists even in the absence of orthosteric ligand. Such allosteric ligands have been termed ago-allosteric ligands or modulators and have become novel targets in drug discovery for GPCRs with endogenous hormone agonists (Bridges and Lindsley, 2008). Clearly, signalling *via* the receptor that is mediated by ago-allosteric modulators opens the door to understand specific receptor conformations and binding dynamics. The present study has investigated the allosteric agonism of the GLP-1R which may provide further into the activation and regulation of this receptor.

1.4 Molecular characterization of the GLP-1R

The gene for the human GLP-1R is localized to the short arm of chromosome 6 (6p21) (Stoffel et al., 1993) and encodes a sequence of 463 amino acids (Van Eyll et al., 1994; Brubaker and Drucker 2002) (**Figure 1.10**). Like other members of Family B GPCRs (Thorens and Widmann, 1996), the GLP-1R (**Figure 1.10**) is predicted by Uniprot (<http://expasy.org/uniprot/P43220>) to contain a large hydrophilic, extracellular (N-terminal) domain of 122 residues with a putative signal peptide (**see Chapter 3**); seven hydrophobic transmembrane domains (TM1 to TM7) that are connected by hydrophilic extracellular and intracellular loops (ECL1, ECL2, ECL3 and ICL1, ICL2, and ICL3) and; an intracellular (C-terminal) domain (**Table 1.3**).

Table 1.3. The amino acid sequence of the GLP-1R segments

Amino acids Length (from - to)	Description	Amino acids Length (from to)	Description
23 (1-23)	Putative SP	122 (24-145)	NT
23 (146-168)	TM 1	8 (169-176)	ICL1
20 (177-196)	TM 2	31 (197-227)	ECL1
25 (228-252)	TM 3	12 (253-264)	ICL2
24 (265-288)	TM 4	15 (289-303)	ECL2
26 (304-329)	TM 5	22 (330-351)	ICL3
21 (352-372)	TM 6	15 (373-387)	ECL3
21 (388-408)	TM 7	55 (409-463)	CT

SP, signal peptide; TM, transmembrane domain; ICL, intracellular loop; ECL, extracellular loop; NT, N-terminal domain; CT, C-terminal domain. From <http://expasy.org/uniprot/P43220>

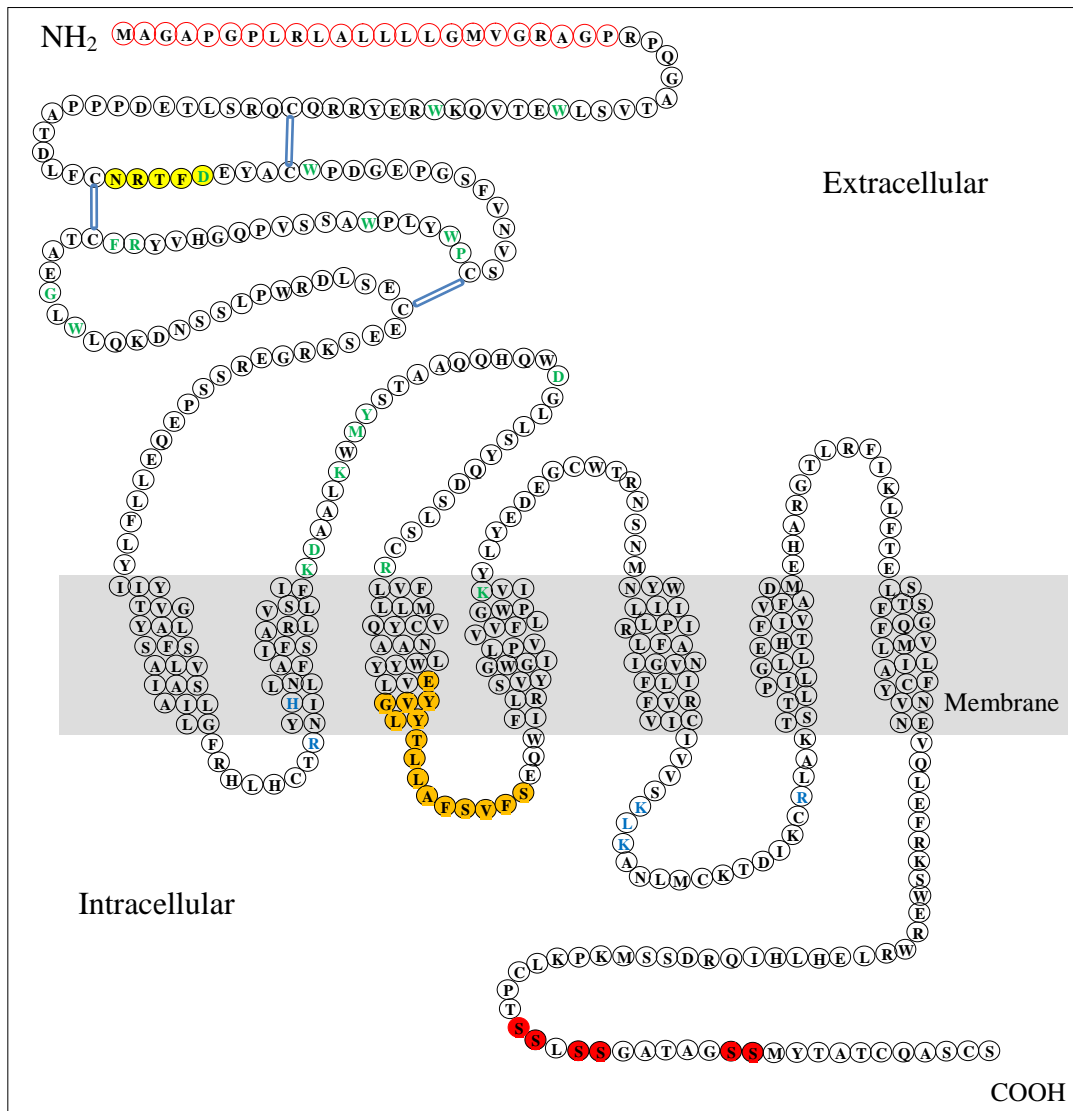


Figure 1.10. The amino acid sequence of the GLP-1R. The sequence of the putative signal peptide (1-23, see **Chapter 3**) is in red circles. Residues in green are residues involved in ligand binding (see **Section 1.10**) and; in blue are involved in receptor activation (see **Section 1.6**). The sequence highlighted in yellow represents the potential endogenous agonist (see **Chapter 5**), which interacts with another part of the GLP-1R upon the binding of GLP-1, resulting in receptor activation (Dong et al., 2008); in orange is the classical caveolin-1 binding motif (Syme et al., 2006), residues in red represent PKC phosphorylation sites (Widmann et al., 1997). The double blue lines represent the conserved disulfide bridges between Cys⁴⁶ and Cys⁷¹, Cys⁶² and Cys¹⁰⁴, and between Cys⁸⁵ and Cys¹²⁶ (see **Section 1.3.5.1**; Bazarsuren et al., 2002).

1.4.1 Residues required for ligand binding and stabilizing the structure of the receptor

Based on the current binding model of Family B GPCRs (Hoare, 2005), the C-terminal of the ligand is thought to interact with the N-terminal domain of the GLP-1R, which acts as an affinity trap to promote interaction of the N-terminal of the ligand with the transmembrane domains of the receptor to provide activation and stimulate intracellular signalling. This is reflected in the residues that have been identified as important for binding of GLP-1 (**Figure 1.10**).

The N-terminal domain of the GLP-1R contains six conserved cysteine residues, which form a disulfide-binding network with links between Cys⁴⁶ and Cys⁷¹, Cys⁶² and Cys¹⁰⁴, and between Cys⁸⁵ and Cys¹²⁶ (Bazarsuren et al., 2002, **Figure 1.10**). The presence of these extracellular cysteine residues is highly conserved among Family B receptors, thus highlighting their structural importance. In addition, Asp⁶⁷, Trp⁷², Pro⁸⁶, Arg¹⁰², Gly¹⁰⁸ and Trp¹¹⁰ in the sequence of the GLP-1R, are also conserved across Family B GPCRs, in which the importance of Trp⁷², and Trp¹¹⁰ for ligand binding has been confirmed by site-direct mutagenesis (Wilmen et al., 1997; Xiao et al., 2000). The recent crystal structure of the GLP-1R extracellular domain has shown that all of these conserved residues are centrally positioned. For example, Asp⁶⁷ is localized at the centre and forms intramolecular interactions, directly interacting with Trp⁷² and Arg¹²¹, and indirectly interacting with Arg¹⁰² via a water molecule (Runge et al., 2008). Asp⁶⁷ also interacts with Tyr⁶⁹ and Ala⁷⁰ while Arg¹⁰² is sandwiched between the side chains of Trp⁷² and Trp¹¹⁰. These interactions, together with Gly¹⁰⁸ stabilize the structure of the N-terminal domain (Runge et al., 2008). Pro⁸⁶ plays a critical structural role for the formation of the ligand binding site (Runge et al., 2008; **Figure 1.10**).

Among seven tryptophan residues in the N-terminal domain of the GLP-1R, substitution of Trp³⁹, Trp⁷², Trp⁹¹, Trp¹¹⁰, or Trp¹²⁰ by Ala in the full-length rat GLP-1R results in complete loss of binding of GLP-1, whereas substitution of Trp⁸⁷ had no apparent effect on binding or activation (Wilmen et al., 1997). However, the role of Trp³³ for binding is still unclear. Trp¹²⁰ is not involved in ligand binding but appears to play a structural role by forming a well defined surface-exposed hydrophobic cluster together with Phe⁸⁰, Tyr¹⁰¹, Phe¹⁰³ and Leu¹¹¹ (Runge et al., 2008; **Figure 1.10**).

Recently, the sequence NRTFD corresponding to Asn⁶³-Asp⁶⁷ in the N-terminal of the GLP-1R has been described as a potential endogenous agonist, which interacts with another part of the receptor upon the binding of GLP-1 and causes agonism (Dong et al., 2008). This has been examined in the present study and discussed in detail in **Chapter 5**.

Besides the N-terminal domain, the region encompassing TM1 through to TM3 is also required for ligand binding. For example, mutation of Thr¹⁴⁹ in TM1 and Lys¹⁹⁷, Asp¹⁹⁸, Lys²⁰², Met²⁰⁴ and Tyr²⁰⁵ Asp²¹⁵ or Arg²²⁷ in ECL1 remarkably decreases ligand binding affinity (Xiao et al., 2000; Lopez de Maturana and Donnelly, 2002; Lopez de Maturana et al., 2004; Beinborn et al., 2005). Particularly, the positively charged residue Lys²⁸⁸ in TM3, conserved at the equivalent position in all other Family B GPCRs, is important for the interaction with the N-terminal of GLP-1 (Al-Sabah and Donnelly, 2003; **Figure 1.10**).

1.4.2 The regions involved in receptor activation and internalization

Specific determinants of the GLP-1R for efficient coupling to G-proteins are located mainly in ICL3 and the junction of TM5 and ICL3 (Takhar et al., 1996). Three

alanine substitution mutations, Val³²⁷, Ile³²⁸ or Val³³¹, at the junction of TM5 and ICL3 result in significantly lower GLP-1-stimulated cAMP production without reductions in receptor expression. These residues, along with Lys³³⁴ in ICL3, are thought to form a hydrophobic face that directly contacts the G-protein (Mathi et al., 1997). In addition, different domains in ICL3 of the GLP-1R are responsible for specific G-protein-coupling (Hallbrink et al., 2001). For example, the N-terminal half of ICL3 is responsible for coupling to G α_s to generate cAMP, while the C-terminal half is reportedly able to stimulate G α_i /G α_o G-proteins (Hallbrink et al., 2001). Indeed, a single amino acid substitution in the N-terminal portion of the ICL3 domain at either Lys³³⁴, Leu³³⁵ or Lys³³⁶ results in a dramatic reduction in the cAMP response to GLP-1, indicating that this region is required for the efficient coupling of GLP-1R to G α_s and AC (Takhar et al., 1996), in which the position of Lys³³⁴ appears the most important. The substitution of Arg³⁴⁸ by Gly near the C-terminal of ICL3 also almost abolishes cAMP production as well as decreasing receptor affinity (Heller et al., 1996). Moreover, analysis of the first and second intracellular loops revealed only one mutation contained within ICL1, Arg¹⁷⁶ substituted by Ala, results in reducing GLP-1-mediated stimulation of cAMP without altering receptor expression (Mathi et al., 1997). The substitution of His¹⁸⁰ by Arg in TM2, causes a decrease in both affinity for GLP-1 and the potency of cAMP production (**Figure 1.10**).

It has been reported that internalization of the GLP-1R is mainly mediated by clathrin-coated pits and associated with three PKC phosphorylation sites (441/442, 444/445 and 451/452) in the C-terminal domain of the receptor (Widmann et al., 1997; **Figure 1.10**). In addition, the serine- and threonine-rich sequences (in the length of 33 amino acids) in the C-terminal domain of the GLP-1R are necessary for achieving

efficient internalization (Widmann et al., 1996; Vázquez et al., 2005a). However, a recent report suggests that internalization of the GLP-1R upon agonist stimulation in pancreatic β -cells is mainly by a caveolae-dependent endocytic pathway, in which the sequence ²⁴⁷EGVYLYTLLAFSVF²⁶⁰ in ICL2 of the GLP-1R is the classical caveolin-1 binding motif (Syme et al., 2006; **Figure 1.10**).

1.4.3 Signal transduction by the GLP-1R in pancreatic β -cells

In β -cells, most of the actions of GLP-1 through the GLP-1R are secondary to the formation of cAMP and its insulinotropic activity is strictly glucose dependent (Holst, 2007). By the binding of GLP-1, the GLP-1R is typically coupled to AC *via* $G\alpha_s$, resulting in generation of cAMP (Thorens, 1992; Coopman, 2010). This leads to activation of PKA and Epac2 (also known as cAMP-GEFII), two major regulators of insulin secretion (Kashima, et al., 2001; Ozaki, et al., 2000), and to a plethora of subsequent events including altered ion channel activity, elevation of intracellular calcium concentrations ($[Ca^{2+}]_i$) and enhanced exocytosis of insulin-containing granules (Holz, 2004). In the presence of stimulatory levels of glucose and GLP-1, Ca^{2+} influx through the activation of L-type voltage-gated calcium channels (L-type VGCC) feeds-forward into mobilization of Ca^{2+} from intracellular stores by Ca^{2+} -induced Ca^{2+} release through PKA- and Epac2-dependent mechanisms (*via* IP_3 or ryanodine receptors). Closure of K^+ channels resulting in subsequent depolarization of the plasma membrane and opening L-type VGCC for Ca^{2+} influx, is mediated *via* phosphorylation by PKA in an ADP-dependent manner (Holst, 2007). The elevation of $[Ca^{2+}]_i$ triggers the exocytotic response with further potentiation by increased cAMP levels through the acceleration of granule mobilization and an increase in the pool of granules available for

release (Holst and Gromada, 2004). In addition, sustained elevations of cAMP induce nuclear translocation of the catalytic subunit of the cAMP-dependent protein kinase, presumably leading to activation of cAMP response element binding-protein (CREB) and likely cell proliferation and survival. The phosphorylation by PKA is thought to activate CREB and its interaction with the coactivator TORC2 (transducer of regulated CREB activity) to enhance insulin receptor substrate-2 (IRS-2) gene expression leading to activation of the serine-threonine kinase Akt (also known as PKB) (Jhala et al., 2003). PKB has been reported to act as an essential mediator to link GLP-1 signalling to the intracellular machinery that modulates β -cell growth and survival (Wang et al., 2004). Furthermore, as a key component of the translational machinery in eukaryotic cells (Meyuhas, 2008), the activation of ribosomal protein S6 (rpS6) has been reported to act as a positive key regulator of β -cell mass and glucose homeostasis in animal models (Ruvinsky et al., 2005). Besides the two recently reported rpS6 kinases, p70 S6 protein kinase (S6K1) and p90 ribosomal S6 kinase (RSK) (Hui et al., 2003; Buteau et al., 2004; Roux et al., 2007; Elghazi and Bernal-Mizrachi, 2009), PKA has also been identified more recently as one of rpS6 kinases in β -cells (Moore et al., 2009).

1.5 Aims of the project

Several anti-diabetic therapies targeting the orthosteric site the GLP-1R are currently available for type 2 diabetes. However, peptide therapies are costly and there are difficulties associated with the route and frequency of administration. Thus, novel therapies are required, such as small molecule agonists, most likely targeting allosteric sites on the receptor. Such allosteric ligands offer a number of potential benefits over the currently available therapeutics, e.g. oral bioavailability. In the face of demand for

novel therapeutics to treat type 2 diabetes and the fact that the GLP-1R is a well-validated target, there is a clear need to develop more understanding of the regulation and function of this receptor. This could involve, for example, improved understanding of the synthesis, processing, trafficking and signalling of the receptor including an understanding of allosteric versus orthosteric agonism and the role of the recently identified putative endogenous agonist.

As part of this project, there was a need to develop cellular tools that would allow the signalling and regulation of the receptor to be assessed. One aspect of the field that hampers further studies is the lack of high-quality receptor antibodies and the ability to visualise the receptors in live cells. The initial aims were, therefore, to develop epitope-tagged receptors that could be used for immune recognition of the receptors to allow both immunoblotting and receptor visualisation. Thoughts about possible locations of the epitope-tag within the GLP-1R lead to the realisation that little was known of the role and fate of the putative signal peptide and a series of studies were designed to determine whether this was cleaved or formed part of the mature protein and to further examine the role of the signal peptide in the synthesis and trafficking of the receptor. With these tools in place the aim was then to explore signalling and events such as agonist-mediated receptor internalization and particularly agonism by the recently described small-molecule, ago-allosteric modulator of the GLP-1R, 'compound 2'. Studies were also designed to examine the putative endogenous ligand of the GLP-1R represented by Asn⁶³-Asp⁶⁷ in the N-terminal domain of the receptor.

CHAPTER 2 Materials and Methods

2.1 Materials

2.1.1 Water

Water used to make solutions was ultra pure (18M Ω quality) obtained through ELGA System (ELGA Labwater, Marlow, U.K.). Unless specifically noted, for all cell culture and molecular biology (except RNA) experiments, the ultra pure water was autoclaved at a temperature of 121°C for 15min. For all RNA experiments, RNase-free water was used without autoclaving and this was supplied by Sigma Aldrich (Poole, U.K.).

2.1.2 Standard laboratory chemicals, reagents and consumables

General laboratory chemicals and consumables were supplied by either Sigma Aldrich (Poole, U.K.) or Fisher Scientific (Loughborough, U.K.) unless mentioned specifically. All mammalian cell culture reagents including various culture media, phosphate buffered saline (PBS), foetal bovine serum (FBS), Geneticin (G418) and Hygromycin B were purchased from Invitrogen (Paisley, U.K.). Glass coverslips (diameter 25mm, or 18 \times 18mm) and cell culture plasticwares were purchased from VWR International (Lutterworth, U.K.). Agarose powder was purchased from Geneflow Ltd (Fradley, U.K.). Sterile plastic loops (diameter 5mm), Sterilin petri dishes (diameter, 10cm; single vent), syringe filters (0.2 μ m) and RNase-, DNase-, DNA-, pyrogens- and PCR (polymerase chain reaction) inhibitor-free microcentrifuge tubes (1.5mL or 2.0mL) were supplied by Appleton Woods (Birmingham, U.K.).

2.1.3 Peptides, enzymes, primers, and antibodies

The peptide ligands of the GLP-1R, GLP-1 7-36 amide, exendin-4 and exendin 9-39 were supplied by Bachem (Weil am Rhein, Germany). The small peptides WET, FDE and NRTFD were synthesized by Cambridge Peptides Ltd (Royston, U.K.).

Rat IgG monoclonal anti-HA antibody was purchased from Roche (Basel, Switzerland). Rabbit IgG polyclonal anti-GFP antibody was purchased from Abcam (Cambridge, U.K.). Rabbit IgG polyclonal anti-myc-tag antibody and goat anti-rabbit IgG, HRP-linked antibody was purchased from New England Biolabs (Hitchin, U.K.). Goat anti-rat IgG, HRP-linked antibody was obtained from Sigma-Aldrich (Poole, U.K.).

All restriction endonucleases (REs), T₄ DNA ligase, Taq and Vent polymerase (for cloning PCR), peptide N-glycosidase F (PNGase F), endoglycosidase H (Endo H) and the relevant working buffers and supplements were purchased from New England Biolabs (Hitchin, U.K.). PfuUltra high-fidelity DNA polymerase for generating mutated GLP-1Rs was obtained from Stratagene (Amsterdam Zuidoost, The Netherlands). Transcriptor Reverse Transcriptase for creating single stranded DNA from an RNA template was purchased from Roche Diagnostic Ltd (West Sussex, U.K.). All primers including dT₁₂₋₁₈ for reverse transcription and that for PCR, generating point mutations or annealing were supplied by Invitrogen (Paisley, U.K.). RNase A used to remove RNA from plasmid DNA preparations and DNase I for the elimination of DNA from RNA preparations prior to RT-PCR (reverse transcription PCR) were supplied by Sigma-Aldrich (Poole, U.K.).

2.1.4 Specific reagents and kits

Lipofectamine 2000 for transfection, TRIzol reagent for RNA isolation, dNTPs for PCR and DNA ladder (1kb plus, 100bp-12kp range) were purchased from Invitrogen (Paisley, U.K.). GelRed used for staining DNA in agarose gels was purchased from Cambridge Bioscience (Cambridge, U.K.).

Pre-stained protein molecular size markers used for immunoblotting (10-250kDa range) were from BioRad (CA, U.S.A.). Bradford reagent for protein determination and the cAMP phosphodiesterase (PDE) inhibitor isobutylmethylxantine (IBMX) was supplied by Sigma-Aldrich (Poole, U.K.). The AC activator, forskolin (FSK) was obtained from Ascent Scientific Ltd (Weston-Super-Mare, U.K.). Proteasome and cathepsin K inhibitor, benzyloxycarbonyl-L-leucyl-L-leucyl-L-leucinal (MG132) and proteasome and calpain 1 inhibitor, acetyl-L-leucyl-L-leucyl-L-norleucinal (ALLN or MG101) were purchased from Merck (Nottingham, U.K.). EZ-Link Sulpho-NHS-Biotin (where NHS stands for N-hydroxysuccinimide) and immobilized NeutrAvidin were obtained from Pierce (Northumberland, U.K.). Acrylamide/*bis*-acrylamide stock solution (30%, *w:v*) was purchased from National Diagnostics (U.K.) Ltd (Hessle, U.K.). Polyvinylidene fluoride (PVDF) transfer membrane was purchased from Millipore (U.K.) Ltd (Watford, U.K.). ECL⁺ reagents were from Amersham Biosciences (GE Healthcare U.K. Ltd, Chalfont, U.K.). QIAGEN plasmid mini kits and QIAquick gel extraction kits from QIAGEN (Crawley, U.K.) were used for plasmid and fragment DNA preparation. NucleoBond Xtra Midi kits for large scale plasmid DNA preparation were purchased from Fisher Scientific (Loughborough, U.K.). QuickChange kits used to generate the mutant GLP-1Rs were from Stratagene (Amsterdam Zuidoost, The Netherlands).

2.1.5 Radioisotopes and materials for scintillation counting

[2,8-³H]-adenosine 3', 5'-cyclic phosphate, ammonium salt ([³H]-cAMP; 42Ci/mmol) was obtained from Amersham Biosciences (GE Healthcare U.K. Ltd, Chalfont, U.K.). [¹²⁵I]-GLP-1 7-36 amide (2200Ci/mmol), [N-methyl-³H]-scopolamine methylchloride ([³H]-NMS; 81Ci/mmol), Emulsifier Safe scintillation fluid, Whatman GF/B glass fibre filters and other materials, including 6mL scintillation vials (Pico-vials/6) were purchased from Perkin Elmer LAS (U.K.) Ltd (Beaconsfield, U.K.).

2.1.6 Vector and plasmid constructs

A plasmid is a double stranded circular DNA molecule which is capable of replicating independently from the chromosomal DNA (Lipps, 2008). Vectors are genetic engineering-made plasmids which are able to carry and multiply (make many copies of) or express particular genes (Russell and Sambrook, 2001). A DNA construct is a plasmid that contains the gene sequence encoding a protein of interest, which has been inserted into a vector and which can be "transplanted" into a target tissue or cell. Series of plasmids were used in the present study, which included both vectors and constructs.

2.1.6.1 pcDNA3.1(+)

The popular and versatile mammalian expression vector pcDNA3.1(+) (5.4kb) from Invitrogen (Paisley, U.K.) was used to generate HA-tagged GLP-1R constructs. This vector contains an ampicillin resistance gene with an upstream bacterial promoter for selection in *Escherichia (E.) coli*. and a neomycin resistance gene for selection of stable cell lines. Several restriction recognition sites in the multiple cloning site (MCS), including *NheI*, *BamHI*, *XhoI*, *XbaI* were used for cloning GLP-1R sequences.

2.1.6.2 pEGFP-N1 and pEGFP-C1

pEGFP-N1 and pEGFP-C1 (Clontech, Oxford, UK), encoding variant GFP (enhanced GFP; EGFP) for brighter fluorescence and higher expression in mammalian cells, were used to generate EGFP-tagged GLP-1Rs. In both of them, sequences flanking EGFP have been converted to a Kozak sequence to further increase the translation efficiency in eukaryotic cells (Kozak, 1987) while stop codons were located at the end of either EGFP (pEGFP-C1) or the MCS (pEGFP-N1). In order to express a GLP-1R sequence as a fusion to the C-terminus of EGFP in pEGFP-C1 and N-terminus of EGFP in pEGFP-N1, *NheI-XhoI* and *BglIII-SalI* sites were used respectively to ensure the GLP-1R gene was in the same reading frame as EGFP. In addition to this, both vectors contain a neomycin-resistance cassette (Neo_r) to allow stably transfected eukaryotic cells to be selected using G418 and; a bacterial promoter upstream which expresses kanamycin resistance in *E. coli*.

2.1.6.3 pcDNA5FRT/WTGLP-1R

A mammalian expression construct, pcDNA5FRT/WTGLP-1R, was a kind gift from AstraZeneca (Alderley Park, Macclesfield, U.K.). This was generated by inserting a DNA sequence encoding the wild-type human GLP-1R (Accession, NP_002053; Version, NP_002053.3; GI:166795283; Gene ID: 2740 GLP1R) into a Flp-In (**Section 2.1.8.2**) expression vector, pcDNA5FRT (Invitrogen, Paisley, U.K.). This plasmid construct was used as the starting template for generating epitope-tagged GLP-1R constructs.

2.1.6.4 Myc-WTGLP1R and Myc-ΔNTGLP-1R

Mammalian expression constructs, Myc-WTGLP-1R and Myc-ΔNTGLP-1R were the kind gift from Dr D Donnelly (University of Leeds, U.K.). These constructs were generated from pcDNA3 (similar to pcDNA3.1; Invitrogen, Paisley, U.K.). The mammalian expression cassette of Myc-WTGLP-1R contains the influenza hemagglutinin (HA) signal peptide, myc-tag, the wild-type human GLP-1R (Ala²¹-Stop⁴⁶⁴; Accession, NP_002053; Version, NP_002053.3; GI:166795283; Gene ID: 2740 GLP1R), in order from the N-terminus to the C-terminus. Although in this sequence the putative signal peptide (Tyr²-Pro²³) has been partially removed (excluding residues from -3 to -1 of the predicted cleavage site), the remaining sequence encoding the GLP-1R is identical to that of pcDNA5FRT/WTGLP-1R. Similarly, Myc-ΔNTGLP-1R also generated in pcDNA3 and contains the influenza HA signal peptide and a myc-tag. However, the sequence encoding the GLP-1R is only from Glu¹³⁸ until Stop⁴⁶⁴ inclusive, thus the N-terminal domain of the receptor has been removed (Arg²⁴-Ile¹⁴⁵ is predicted as the N-terminal domain of the GLP-1R, see **Table 1.3**). These two constructs were used to explore the role of the N-terminal domain of the GLP-1R in ligand binding with different ligands.

2.1.7 Bacterial strains

E. coli are a common inhabitant of the human colon and can easily be grown in suspension culture in a nutrient medium. Two *E. coli* strains were used as the host to amplify plasmid DNA in the present study.

2.1.7.1 DH5α

DH5α (Invitrogen, Paisley, U.K.) was used to make competent cells for plasmid

DNA transformation (**Section 2.3.1**) in routine cloning and subcloning. DH5 α does not contain any antibiotic resistant gene and hence cannot be selected until transformation with a plasmid carrying an antibiotic resistant gene.

2.1.7.2 XL1-Blue

Ready-made XL1-Blue supercompetent cells (Stratagene, Amsterdam Zuidoost, The Netherlands) were used for DNA transformation in the generation of mutated GLP-1Rs. This strain is tetracycline resistant and has been improved for insert stability. It also allows blue-white colour screening for recombinant DNA (Bullock et al., 1987; Woodcock et al., 1989), in which both isopropyl thiogalactoside (X-gal) and 5-bromo-4-chloro-3-indolyl-beta-D-galactopyranoside (IPTG) are required.

2.1.8 Mammalian cell lines

2.1.8.1 HEK293 cells

HEK293 (human embryonic kidney 293) cells are extremely easy to work with since they are relatively easy to both culture and transfect. In the present study, HEK293 cells were used for both transient and stable expression of GLP-1R constructs.

2.1.8.2 Flp-In system based stable cell lines

The Flp-In-293 and Flp-In-CHO cell lines (Invitrogen, Paisley, U.K.) were generated from HEK293 and Chinese hamster ovary (CHO), respectively, which contain a single integrated FRT (Flippase Recognition Target) site in the transcriptionally active genomic locus. Co-transfection of Flp-In-293 or Flp-In-CHO cells with a Flp-In expression vector (e.g., pcDNA5FRT) containing a gene of interest

and the Flp recombinase vector (pOG44, Invitrogen, Paisley, U.K.) allows a insertion of Flp-In expression construct into the genome at the integrated FRT site *via* site-specific DNA recombination mediated by Flp recombinase. Consequently, the resulting stable cell lines can have homogeneous levels of gene expression as integration of the Flp-In expression construct (hygromycin resistant) is presumed to target to the same locus in every cell. HEK293Flp-In:pcDNA5FRT, HEK293Flp-In:WTGLP-1R and CHOFlp-In:WTGLP-1R were generated using Flp-In system by AstraZeneca (Alderley Park, Macclesfield, U.K.), which stably express either the empty vector (pcDNA5FRT) or the pcDNA5FRT/WTGLP-1R (**Section 2.1.6.3**) respectively.

2.1.8.3 HEK293:M₃ cells

HEK293:M₃ cells were previously generated on HEK293 cells (Tovey and Willars, 2004), which stably express human subtype-3 muscarinic acetylcholine receptors (M₃).

2.2 Bacterial cell culture

2.2.1 Growth and multiplication

E. coli were grown at 37°C either in Luria-Bertani (LB) broth (1% *w:v* tryptone, 0.5% *w:v* yeast extract, and 1% *w:v* NaCl) with shaking at 220-230rpm or on a solid support using LB agar (1% *w:v* tryptone , 0.5% *w:v* yeast extract, 1% *w:v* NaCl and 1.5% *w:v* agar) plates. Either ampicillin (100µg/mL) or kanamycin (50µg/mL) were use as appropriate.

2.2.2 *E. coli* stock

To make the *E. coli* stock, 600µL of fresh overnight culture and 300µL of 50% (v:v) glycerol were mixed gently in sterile 2mL cryotubes. Vials were then stored at -80°C. To grow cells from a glycerol stock, the frozen cells were scraped with a sterile plastic inoculating loop and streaked onto a fresh LB agar plate containing appropriate antibiotics. The plate was then incubated inverted at 37°C overnight and stored at 4°C until use.

2.3 Bacterial transformation for amplifying vectors and GLP-1R constructs

Bacterial transformation is the process by which host bacterial cells (e.g., *E. coli*) take up plasmid DNA. Bacteria able to take up DNA are referred to as "competent".

2.3.1 Preparation of competent *DH5α*

The method for preparing competent *DH5α* was based on soaking the cells in cold CaCl₂ (Mandel and Higa, 1970). A loop of glycerol stock was inoculated into 5mL LB broth. After incubating overnight at 37°C with shaking (220rpm), 2mL culture was inoculated into 200mL of pre-warmed LB broth containing 1mM glucose. Culture was then continued until mid-log phase with an OD₆₀₀ of 0.25-0.35. Cells were harvested by centrifugation at 3,500g for 15min at 4°C and the pellet gently resuspended in 20mL chilled MgCl₂ (100mM) and incubated on ice for 20min. After centrifugation as above, the pellet was gently resuspended in 20mL chilled CaCl₂ (100mM) and incubated on ice for a further 20min. Following collection of the bacteria as above, the pellet was finally

gently resuspended in 6mL of 100mM CaCl₂ containing 13.3% glycerol and stored at –80°C in 50µL aliquots.

2.3.2 Transformation procedure using competent DH5α

A 50-100µL aliquot of competent DH5α was thawed on ice for 10 min. A 5-10ng aliquot of plasmid DNA or 7.5µL of ligation reaction (**Section 2.10**) was then added and incubated on ice for a further 10min. The DNA/cell mixture was then heat-shocked at 42°C for 90s and immediately placed on ice for 2min. The cells were then incubated at 37°C in 1mL of SOC medium (0.5% *w:v* yeast extract, 2% *w:v* tryptone, 10mM NaCl, 2.5mM KCl, 10mM MgCl₂, 10mM MgSO₄, 20mM glucose). Transformed cells (30-100µL) were spread onto a 10cm LB agar plate containing appropriate antibiotics and incubated at 37°C overnight. The plates were then sealed with Nescofilm and stored inverted at 4°C.

2.4 Preparation of plasmid DNA

Since transformation is coupled with antibiotic selection, bacteria can be selected for incorporation of the plasmid DNA, from which the latter can be easily prepared in various scales (e.g., miniprep for ~20µg DNA, midiprep for ~100µg and maxiprep for ~500µg). For different steps of the cloning process (or generating mutated) GLP-1Rs, plasmids were prepared differently. Minipreps were conducted for a small amount of a DNA (~20µg) either using a commercial kit or “home-made” (see below). These were sufficient for either preliminary RE digest (to select DNA clones containing an expected insert) or confirming a potential construct (either by DNA sequencing or accurate restriction site analysis). In addition to this, midpreps using commercial kits were performed to amplify expression plasmids (~100µg) for transfections.

When using QIAGEN plasmid mini kits or NucleoBond Xtra Midi kits (which can achieve a yield of ~300-500µg from each midiprep) to prepare plasmids, the manufacturer's protocols were followed. However, the minipreps without any commercial kit were performed using a modified protocol based on the QIAGEN manual. Briefly, each of approximately 4 to 10 individual colonies were picked from an LB plate and inoculated into a single sterile 15mL tube containing 3mL LB broth with appropriate antibiotics. After growing overnight at 37°C with shaking (220 rpm), 1mL of cells were transferred from each culture into a clean 1.5mL microfuge tube. The remaining portion of the cultures were retained and stored at 4°C. The cells in each microfuge tube were centrifuged at 4500g, 2min, room temperature (RT). The pellet was resuspended in 100µL of buffer P1 (50mM Tris-HCl, pH 8.0, 10mM Ethylenediaminetetraacetic acid (EDTA), 100µg/mL RNase A) and vortexed until completely dissolved. The reaction was incubated for 5min at RT. A 500µL aliquot of fresh buffer P2 (200mM NaOH, 1% SDS) was then added, the tube mixed by inversion and incubated at RT for 5min. Then 500µL of chilled buffer P3 (3M potassium acetate, pH 5.5) was added, the tube mixed and incubated on ice for 10min. After centrifuging at 16,500g, 30min, 4°C, the supernatant was immediately transferred into a clean 1.5mL microfuge tube, 0.7 volumes of isopropanol added to precipitate the DNA and mixed by inversion. The tubes were centrifuged at 16,500g, 30min, 4°C, followed by carefully pouring off the supernatant, the tube washed with 0.5mL of ice-cold 70% ethanol and re-pelleted. After briefly air-drying, the DNA was finally dissolved in 40µL TE buffer (10mM Tris, pH 8.0, 1mM EDTA) and stored at -20°C until a preliminary RE digestion.

2.5 Quantification of DNA by absorbance

After plasmid DNA preparation, the yield and quality of DNA was determined by measuring absorbance at wavelengths of 260nm and 280nm. An absorbance of 1 at 260nm corresponds to a concentration of 50µg/mL double-stranded DNA (dsDNA). The DNA concentration was thus calculated using **Equation 2.1**. The samples were measured again at OD_{260nm} and OD_{280nm} at a further 1:2 dilution (*w:w*) with H₂O whenever the concentration >1.0 µg/µL to ensure that the measurement was within the linear range of the instrument (generally 0.1–1.0 OD units). The quality of DNA was determined by OD_{260nm}/OD_{280nm}, where a value of 1.7-2.0 indicated relatively pure DNA. Values below this range suggested the presence of protein and/or membrane fractions (Russell and Sambrook, 2001) and therefore the plasmid was prepared again.

Equation 2.1

$$\text{dsDNA Concentration } (\mu\text{g}/\mu\text{L}) = \text{OD}_{260\text{nm}} \times \text{df} \times 50/1000$$

where: OD, optical density; df, dilution factor (e.g., 1:200)

2.6 PCR cloning of GLP-1R sequences

PCR was applied for cloning GLP-1R gene sequences, in which Vent (a heat-stable DNA polymerase) enzymatically assembles a new DNA strand from nucleotides using pcDNA5FRT/WTGLP-1R as the template and appropriate DNA primers (also referred to oligos or oligonucleotides) to initiate DNA synthesis.

2.6.1 Design of primers

The primers used for cloning the full-length or signal peptide-deleted (Δ SP) GLP-1R genes are shown in **Figure 2.1**. These primers consisted of RE sites flanking with extra bases and at least 15bp of the sequence encoding a certain region of the GLP-1R including either a start codon (ATG) or stop codon (TAG) if applicable. In order to increase the efficiency of translation and hence overall expression of the product gene, a Kozak sequence, 'GCCACC' (Kozak, 1995), was also inserted before the start codon. When cloning the HA-tagged GLP-1R, a 15 base pairs (bp) length HA sequence was included in each primer as shown in **Figure 2.2**.

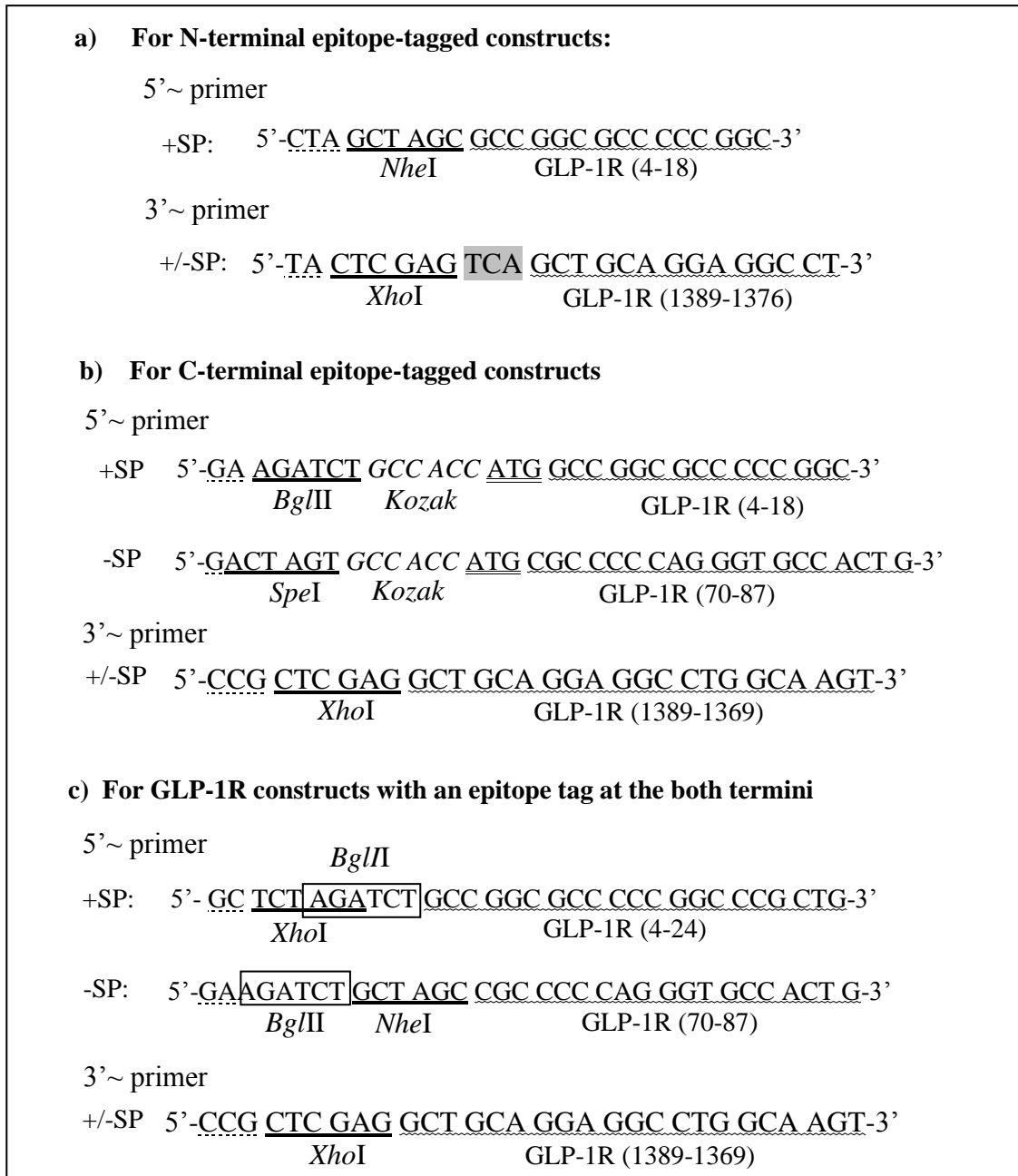


Figure 2.1. Primers for cloning GLP-1R sequences. The 5'~primers were designed differently for cloning the GLP-1R either with (+) or without (-) the putative signal peptide sequence (SP) while the 3'~primers were same for either +SP or -SP. Bases in italics represent the Kozak sequence and on a solid underline represents the RE sites as indicated. The flanking bases are on a dashed underline, the start codon on the double underline, the stop codon in a shaded box and the coding sequence of the GLP-1R on a waved underline.

2.6.2 Performing PCRs on a thermocycler

The PCR mixture was set up in a PCR tube with a total volume of 50 μ L, which contained 1 μ L of the thermostable DNA polymerase Vent (2,000unit/mL), 5 μ L of 10 \times ThermoPol reaction buffer, 1 μ L (0.5 μ g/ μ L) of each 5'~ and 3'~ primers, 1 μ L of 10mM dNTPs (10nM), 0.4 μ g plasmid DNA template (pcDNA5FRT/WTGLP-1R) and an appropriate volume of H₂O.

All PCRs for cloning a GLP-1R sequence proceeded for 30 cycles with denaturation, annealing and extension included in each cycle on the thermocycler with a heated lid (Techne Inc., Burlington, NJ, U.S.A.). The denaturation was carried out at 95°C for 1min in the first cycle and for 30s in subsequent cycles. The temperature used for the annealing step (T_a) was calculated using **Equation 2.2**. The annealing was performed for 1min in each cycle. The extension temperature was 72°C. The extension time was 3min and 10min for the last cycle. The reaction tubes were placed in the thermocycler and the following protocol run: (i) 1 cycle of 95°C for 30s; (ii) 29 cycles of 95°C for 30s, 55-57°C (T_a) for 1min and 72°C for 3min; (iii) 1 cycle of 95°C for 30s, T_a for 1min and 72°C for 10min then hold at 4°C until PCR tubes were removed from the thermocycler and stored at -20°C.

Equation 2.2

$$T_a (^{\circ}\text{C}) = 61.8^{\circ}\text{C} + [41^{\circ}\text{C} \times \Sigma(\text{G}+\text{C}) - 675^{\circ}\text{C}] / \Sigma(\text{A}+\text{T}+\text{G}+\text{C}) - 5^{\circ}\text{C}$$

where : $\Sigma(\text{A}+\text{T}+\text{G}+\text{C})$ is the total number of the bases in the primer; $\Sigma(\text{G}+\text{C})$ is the number of the bases G and C in the primer sequence.

2.7 Restriction digest of plasmids and DNA fragments

Restriction digest is the process of cutting DNA molecules into smaller pieces with REs that recognize specific sequences (RE sites) in the DNA molecule. In the present study, restriction digests were performed for preparing DNA fragments (pieces of dsDNA) with sticky ends for either ligation (see below) or RE site analysis. To prepare a linear vector or insert for ligation, 2 μ g purified DNA (plasmid or purified PCR product) were digested in a 50 μ L reaction mixture, which contained 5 μ L 10 \times enzyme-specific buffer, 10U enzyme (10U/ μ L or 20U/ μ L), 0.5 μ L of 100 \times BSA (10mg/mL) and an appropriate volume of H₂O. The mixture was incubated at 37°C for 2h to prepare an insert or 3h to prepare a vector in a water bath (or 16-20h, 37°C for digestion of PCR product in a thermal cycler; Techne Inc., Burlington, NJ, U.S.A.). Double-RE digestions were performed in one step when the conditions (temperature and buffer) for both enzymes permitted. Otherwise, two separate digestions were carried out with a DNA purification (**Section 2.2.9**) in between. After digestion, the target fragments were identified and separated by agarose gel electrophoresis (**Section 2.2.8**) followed by DNA extraction (**Section 2.2.9**).

Diagnostic digestion was performed under the same conditions as above with the exception that the total reaction volume was 20 μ L and contained 0.5 μ g DNA, 2 μ L 10 \times appropriate enzyme buffer, 3U enzyme (10U/ μ L or 20U/ μ L), 0.2 μ L of 100 \times BSA (10mg/mL) and an appropriate amount of H₂O. The digested DNA was also identified by agarose gel electrophoresis but without DNA extraction afterwards.

To perform the preliminary diagnostic digestion for the plasmid products from minipreps without using any commercial kit, the RE digest mixture was prepared in a

pool. For example, 120 μ L of mixture was prepared and mixed in a microfuge tube for digesting 6 DNA clones, which containing 12 μ L of 10 \times NEBuffer (type depending on REs), 1.2 μ L of 100 \times BSA, 15 units of each (of two) REs and an appropriate volume of H₂O. To each of 6 pre-labelled microfuge tubes, 19 μ L of mixture was transferred and 1 μ L of plasmid DNA from each clone added. A relatively short digest (\leq 2h) was then conducted at 37 $^{\circ}$ C to avoid DNA damage caused by the RNase and DNase that remained in the “home-made” DNA samples.

2.8 Agarose gel electrophoresis of DNA

DNA fragments, including original PCR products, digested PCR products and digested plasmids, were separated and identified by agarose gel electrophoresis. Depending on the length of the dsDNA, 0.38-0.5g agarose powder was mixed with 50mL TAE buffer (Tris/Acetate/EDTA: 0.4M Tris acetate, 0.01M EDTA, pH 8.3) and heated in a microwave oven until completely dissolved to make a 0.76-1.0% agarose gel. A 0.25 μ L aliquot of GelRed to allow visualisation of the DNA was added into the gel after cooling the solution to about 60 $^{\circ}$ C. The gel was then poured into a casting tray containing a comb to form the sample wells, (which was removed after the gel had solidified) and allowed to solidify at RT. The gel was inserted horizontally into an electrophoresis chamber and just covered with TAE buffer. Samples containing DNA mixed with 10 \times loading buffer (50% v:v glycerol, 2% v:v Ficoll (hydrophilic polysaccharide), 50mM EDTA and 5% w:v bromophenol blue prepared in sterile water) were then pipetted into the sample wells in the gel. A 1.0kb Plus DNA ladder (0.6 μ g/lane) was used to estimate the size of the DNA fragments in the samples. The gel

was run at 120-160 volts for 40min, removed from the tank and placed on the UV trans-illuminator to read or photograph using a digital camera.

2.9 Purification of DNA fragments from solution or agarose gel

Using the manufacturer's protocol, QIAquick gel extraction kits were used to purify DNA fragments from either agarose gel or solution (e.g., RE digestion or PCR mixture), thereby allowing the removal of dNTPs, primers, nucleotides, enzymes, mineral oil, salts, agarose, GelRed and other impurities from DNA samples.

To extract DNA from an agarose gel, the band of interest was excised using a clean scalpel under the UV trans-illuminator and weighed in a 1.5mL microfuge tube of known weight. The gel band was incubated in a volume of QG buffer (μL) equivalent to three times the gel weight (μg) at 50°C with periodic mixing for 10min or until the gel fragment was dissolved. Isopropanol was then added at a volume (μL) equivalent to the gel weight (μg), the sample mixed and applied to a QIAquick column. This was centrifuged for 1min at 16,500g, the flow-through discarded and 0.5mL of buffer QC added to the column, which was then centrifuged (1min, 16,500g). The column was washed by the addition of 0.75mL of buffer PE and further centrifugation (1min, 16,500g). The flow-through was discarded and the QIAquick column centrifuged (1min, 16,500g) again. This step completely removed residual ethanol. DNA was then eluted with 50 μL of TE buffer (10mM Tris, pH 8.0, 1mM EDTA) for final constructs or H_2O for DNA fragments and collected by centrifugation (1min, 16,500g).

To extract DNA fragments from an RE digestion or PCR mixture, 150 μ L of QG buffer and 50 μ L isopropanol were added. The mixture was applied to the QIAquick column and the processes described above followed.

2.10 DNA ligation

Ligation, catalysed by T4 DNA ligase, was conducted to join DNA fragments (inserts and linear vectors) containing cohesive (sticky) ends by covalent bonds. To generate epitope-tagged GLP-1R constructs, insert(s) from different sources such as PCR products (**Section 2.6**), annealed primers (**Section 2.11**) or existing constructs and a vector prepared from a commercial plasmid were recombined into a new DNA molecule. Since the optimum ratio can range between a 1:1 to 10:1 molar ratio of insert:vector for a ligation, 0.5 μ L of vector and 4 μ L of insert were used for all two-part ligations, in which each insert and vector were prepared by RE digest from 2 μ g DNA (**Section 2.7**). The total reaction volume of a ligation was 20 μ L. In addition to 4 μ L of insert DNA and 0.5 μ L of vector DNA, the reaction also contained 1 μ L of T4 DNA ligase, 2 μ L 10 \times T₄ ligation buffer and an appropriate volume of H₂O. The contents were mixed by tapping the tube gently and collected at the bottom of the tube by brief centrifugation (1500g, 1s). The reaction was carried out at RT for 3h. An aliquot of 7.5 μ L was then transformed directly into 50 μ L of *DH5 α* competent cells followed by selection using ampicillin resistance conferred by the vector (**Section 2.3**).

2.11 Synthesis of the HA-tag sequence by annealing two complementary primers

To introduce an HA-epitope tag sequence to the C-terminus of the GLP-1R (GLP-1R-HA), two complementary primers were annealed to form a dsDNA fragment with sticky ends, which was then ligated with a DNA fragment encoding the full-length hGLP-1R gene and a linear vector to form a new recombinant DNA plasmid. For annealing, each primer contained an HA-tag incorporating an *XhoI* RE site at the N-terminus, *XbaI* RE site at the C-terminus, an additional *Sall* RE site (for future use) and an extra base immediately before the *XbaI* site to make a stop codon TAG. (**Figure 2.3**). The annealing mixture with total volume of 20 μ L in a PCR tube contained 10mM Tris (pH 8.0), 50mM NaCl, 1mM EDTA and 2 μ g of each primer in H₂O. The tube was then placed in a thermocycler and the following protocol run: (i) heat to 95°C and maintain for 2min; (ii) slowly cool to 25°C over 45-60min (e.g., 1.5°C/min) and maintain for 10min; (iii) hold at 4°C until the tube removed. After spinning briefly in a microfuge (1500g, 1s) to draw all the moisture from the lid, the tube was kept on ice or at 4°C until use.

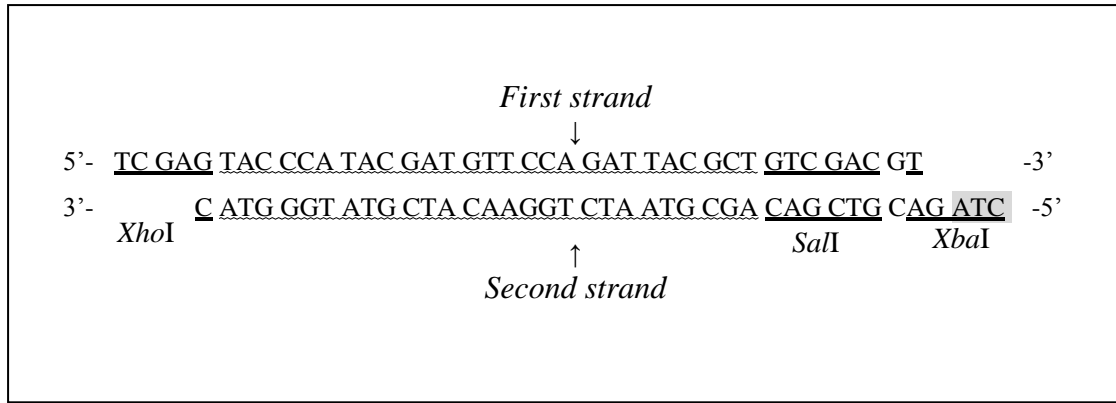


Figure 2.3. The expected product of annealing two complementary primers encoding an HA-tag. Two complementary primers (First strand and Second strand) were designed to generate a dsDNA fragment with sticky ends through annealing. Bases with a solid underline represent RE sites, bases in a shaded box represent the stop codon (the complementary bases are TAG).

2.12 Generating mutated GLP-1R constructs

Mutant GLP-1Rs were generated using the QuikChange Site-Directed Mutagenesis Kit based on PCR with modifications of the manufacture's guide. Point mutations at Ala²¹, Glu³⁴, Asp⁶⁷ and Arg¹⁰² in the hGLP-1R were introduced *via* PCR primers (**Table 2.1**). The template was either the GLP-1R-HA or GLP-1R-EGFP (C-terminal EGFP-tagged GLP-1R) construct (generated in the present study), for which only ~20ng was applied in each PCR to avoid the possibilities of too much original template (supercoiled dsDNA, *i.e.*, the non-mutated DNA) remaining in the PCR product. Unlike PCRs for cloning GLP-1R sequences (target length ~1400bp), all PCRs for generating point mutations (target length ~6100-6400bp) were performed for 25 cycles, with an annealing at 55°C, an extension at 68°C for 7.5min, in which the PCR mixture contained 0.8µL of template DNA and 1µL of PfuUltra polymerase (2.5U/µL), 5µL of 10× reaction buffer, 0.4µL of each primer (0.5µg/µL), 1µL of dNTPs (10nM) and 41.4µL H₂O. A *DpnI* (10U) digestion at 37°C for 1h was conducted directly in the amplification reaction following PCR to digest the parental supercoiled dsDNA. A 1µl aliquot of *DpnI*-treated DNA was added into 50µl of XL1-Blue supercompetent cells in a prechilled 14mL BD Falcon polypropylene round-bottom tube and the transformation procedure followed as described previously (**Section 2.3.2**). Bacterial plates were then stored inverted at 4°C until that the plasmid DNAs in colonies were isolated for automated DNA sequencing using QIAGEN plasmid mini kits (**Section 2.4**).

Table 2.1 Primers for generating mutated GLP-1R constructs

Mutation	DNA sequence		Primers (from 5' to 3')
	Wild-type	Mutation	
A21R	61 GCC 63	61 <u>AGA</u> 63	5'~ CTC GGG ATG GTG GGC AGG <u>AGA</u> GGC CCC CGC CCC CAG G 3'~ CCT GGG GGC GGG GGC <u>CTC TCC</u> TGC CCA CCA TCC CGA G
E34R	100 GAG 102	100 <u>AGG</u> 102	5'~CTG TGT CCC TCT GGA <u>GGA</u> CGG TGC AGA AAT G 3'~CAT TTC TGC ACC GTC <u>CTC</u> CAG AGG GAC AGA
E34A	100 GAG 102	100 <u>GCG</u> 102	5'~ CTG TGT CCC TCT GGG <u>GGA</u> CGG TGC AGA AAT G 3'~ CAT TTC TGC ACC GTC <u>GCC</u> CAG AGG GAC ACA G
D67A	199 GAT 201	199 <u>GCT</u> 201	5'~ GCA ACC GGA CCT TCG <u>CTG</u> AAT ACG CCT GCT G 3'~ CAG CAG GCG TAT TCA <u>GCG</u> AAG GTC CGG TTG C
D67R	199 GAT 201	199 <u>CGT</u> 201	5'~ GCA ACC GGA CCT <u>TCC</u> GTG AAT ACG CCT GCT GG 3'~ CCA GCA GGC GTA TTC <u>ACG</u> GAA GGT CCG GTT GC
D67R, R102D	304 CGG 306	304 <u>GAC</u> 306	5'~ CAG GGC CAC GTG TAC <u>GAC</u> TTC TGC ACA GCT GAA GG 3'~ CCT TCA GCT GTG CAG AAG <u>TCG</u> TAC ACG TGG CCC TG
D67E	199 GAT 201	199 <u>GAA</u> 201	5'~ GCA ACC GGA CCT TCG <u>AAG</u> AAT ACG CCT GCT G 3'~ CAG CAG GCG TAT <u>TCT</u> TCG AAG GTC CGG TTG C

Bases on underline represent mutation coding sequences.

2.13 Automated DNA sequencing

The sequence of the insert in all recombinant plasmids containing the wild-type or mutated hGLP-1R gene were confirmed by automated sequencing (Protein and Nucleic Acid Characterisation Laboratory, University of Leicester, Leicester, U.K.). The automated DNA sequencing was conducted by a Biosystems 3730 Analyzer based on fluorescently labelling DNA fragments with a cycle sequencing protocol (Rosenblum et al., 1997). All plasmid DNAs subjected to sequencing were prepared with the Qiagen mini-prep kit (Section 2.4). Since common challenges of DNA sequencing include poor quality in the first 15-40 bases of the sequence and deteriorating quality of sequencing traces after 700-900 bases, all the primers for sequencing contained 21 bases of vector sequences which were located at least 50 nucleotides away from the insert in the construct (Table 2.2). In addition to this, the sequencing was performed from the both sides of the insert to ensure full-length sequencing of the GLP-1R (~1400bp) and small epitope tags (e.g., HA-tag, 27bp). The homology of the DNA sequence was determined using BLAST, a program supported by the National Centre for Biotechnology Information (NCBI) at <http://www.ncbi.nlm.nih.gov/BLAST/>.

Table 2.2 Primers for automated DNA sequencing

Sequencing direction	Sequence	Vector and location
5' to 3'	5'-GTCTATATAAGCAGAGCTGG-3'	pEGFP-N1 (550-569)
3' to 5'	5'-CCCGTGGTGGGGCCACTTGT-3'	pEGFP-N1 (739-720)
5' to 3'	5'-GCCGCCGGGATCACTCTCGG-3'	pEGFP-C1 (1290-1309)
3' to 5'	5'-CACCTCCCCCTGAACCTGAA-3'	pEGFP-C1 (1490-1471)
5' to 3'	5'-AGGCGTTTTGCGCTGCTTCGC-3'	pcDNA3.1(+) (409-433)
3' to 5'	5'-ACTAGAAGGCACAGTCGAGGC-3'	pcDNA3.1(+) (1220-1201)

2.14 Mammalian cell culture

2.14.1 *Growth and maintenance*

Wild-type HEK293 cells were routinely cultured in growth medium which was Dulbecco's Modified Eagle Medium (DMEM, containing 4.5g/L glucose) supplemented with 10% FBS. Flp-In system based stable cell lines (**Section 2.1.8.2**) were maintained in the same medium but containing 100 μ g/mL hygromycin. The HEK293:M₃ cell line and the cell lines generated in the present including HEK293:GLP-1R-EGFP (HEK293 cells with stable expression of C-terminal EGFP-tagged GLP-1R) and HEK293:EGFP (HEK293 cells with stable expression of EGFP) were maintained in the same growth medium but containing 200 μ g/mL G418. All cells were maintained at 37°C in a 5% CO₂ humidified environment.

2.14.2 *Cell subculture*

Adherent monolayers of cells in different containers were detached for subculture once they reached 70-90% confluence. After the growth medium was aspirated, the cells were washed gently with an appropriate volume of PBS. All traces of FBS were removed by slowly rocking the container back and forth. A 0.5-2.5mL (depending on the size of the container) aliquot of trypsin-EDTA (0.05% *w:v* trypsin, 0.04% *w:v* EDTA in PBS) was added and spread by slowly rocking the container back and forth to cover all of the cells. After being left at RT for 2min, trypsination was terminated by adding growth medium at a volume equivalent to 5-fold that of the trypsin-EDTA. The cell suspension was then centrifuged at 140g for 5min at RT and resuspended in fresh growth medium and counted (**Section 2.14.3**). An appropriate amount of cells were then

transferred into a new cell culture container and cultured under the same conditions as above.

2.14.3 Cell counting and viability determination

Following trypsinisation of adherent monolayers (see above), cells in suspension were counted to determine either growth rates or to set up cultures at appropriate cell concentrations. A haemocytometer (0.100mm×0.0025mm², Sigma-Aldrich, Poole, U.K.) was used for cell counting. After the cell suspension was mixed by gentle pipetting, 0.6mL of the suspension was removed and mixed thoroughly with 0.4mL of 0.5% (w:v) trypan blue in a 1.5mL microfuge tube. A 20µL aliquot was loaded carefully onto a clean haemocytometer. The cells in the four large corner squares of the grid were counted. The cell concentration was calculated using **Equation 2.3**. With trypan blue staining, dead cells take up the dye and appear blue under the microscope, while living cells exclude trypan blue and appeared colourless. The percentage of non-viable cells (in blue) can therefore be calculated. Only when viability was >95% were cells used for experiments.

Equation 2.3

Total number of cells/mL = the average number of cells in one large square × 10⁴ × df

where: df is dilution factor.

2.14.4 Freezing cells for storage

Cells were grown to 60-70% confluence in T-75 flasks and harvested as described in **Section 2.14.2**. After centrifugation (140g, 5min, RT), the cells were resuspended in 1mL of freezing medium (10%, v:v, Dimethyl sulfoxide (DMSO) in FBS) and transferred into a sterile 2.0mL cryotube. These cryotubes were then placed in a special container (Nalgene, NY, U.S.A.), filled with isopropanol, and kept in a -80°C freezer for at least 4h. The cryotubes were then stored in liquid nitrogen until resuscitation.

2.14.5 Resuscitation of frozen cells

Once removed from the liquid nitrogen, the frozen cells in cryotubes were immediately thawed at 37°C (in a water bath) for 1-2min to minimise any damage to the cell membranes. The cells were then transferred into one 30mL sterile universal containing 10mL of pre-warmed growth medium (37°C) by pipetting gently and then centrifuged (140g, 3min, RT). The cells were resuspend in a T-75 flask containing 14mL pre-warmed growth medium and cultured under normal growth conditions (**Section 2.14.1**).

2.15 Transfection of GLP-1R constructs

Transfection is the process of deliberately introducing nucleic acids into eukaryotic cells by non-viral methods. All GLP-1R constructs generated in the present study were finally introduced into wild-type HEK293 cells by transfection. HEK293 cells grown in different containers (24-, or 6-well plates, T-25 or 75 flasks or 10cm diameter tissue culture dishes) at approximately 80-90% confluence were transfected using

Lipofectamine 2000 following the manufacturer's protocol. The cells were plated one day before transfection and allowed to attach overnight. An appropriate amount of plasmid DNA, e.g., 0.5 μ g per well of 24-well plates, 2.0 μ g per well of 6-well plates or 12 μ g per T-75 flask or 10cm dish, was gently diluted with an appropriate amount of serum-free media, e.g., 250 μ L per well of a 6-well plate or 1.5mL per T-75 flask. In the same volume of serum-free media as that used for the DNA dilution, an appropriate amount of Lipofectamine 2000 was diluted (e.g., 2.0 μ L per well of 24-well plates, 10 μ L per well of 6-well plates or 60 μ L per T-75 flask or 10cm diameter dish) and incubated at RT for 5min. These two dilutions were then combined and incubated at RT for a further 20min. The DNA-Lipofectamine 2000 complex was then added to the cells in plates or flasks, followed by a gentle mixing. Wherever was required, the total amount of DNA and Lipofectamine 2000 required for transfection were prepared as a pool before adding appropriate amounts to each well. For example, for transfection in a 24-well plate, 12 μ g DNA was diluted in 1200 μ L of serum-free media and 48 μ L Lipofectamine 2000. After combining, 100 μ L of the DNA-Lipofectamine 2000 complex was added to each well and mixed as above. After transfection, the cells were then cultured under normal growth conditions (**Section 2.14.1**) and the medium was changed after 6h.

To establish HEK293 cell lines with a stable expression of the GLP-1R-EGFP or EGFP, the transfection was performed in a 10cm diameter tissue culture dish as described above. After 6h, the transfected cells were transferred into four new 10cm diameter dishes and grown under normal conditions.

2.16 Selection and isolation of G418-resistant colonies

From the day following transfection, cells with stable expression were selected by G418 (1mg/mL) in growth medium and the medium changed every 72h until the diameters of surviving single colonies (G418-resistant colonies) were 2-3mm. The colonies for collecting were then clearly labeled on the underside the plates. After the medium was aspirated, the cells on the plates were washed carefully with 10mL PBS. Labeled colonies were then covered individually by trypsin-EDTA soaked cloning discs for 5min at RT. The cloning discs with cells were then transferred to 24-well dishes and the same G418 selection was continued for the cells in each well until >60% confluence. The cells were then transferred to 6-well plates for further selection.

2.17 Determination of protein concentration (Bradford assay)

Protein standards were prepared by diluting BSA (1mg/mL) in 0.1M NaOH to the working concentrations of 0, 25, 50, 100, 125, 250, 375, 500, 625, 750 and 1000 μ g/mL. Bradford reagent was diluted (1:2, *v:v*) with H₂O. All the protein test samples were also appropriately diluted with 0.1M NaOH (e.g., 500 μ L for each well of 24-well plates). A 10 μ L aliquot of each protein test sample or standard was added to a test tube (5mL) followed by 1mL of diluted Bradford reagent. After mixing thoroughly by vortex, the reactions were incubated at RT for 20min. The absorbance was measured at 595nm using a spectrophotometer (WPA UV 1101, Biotech Photometer, Cambridge, UK). Standard curves were fitted using GraphPad Prism (GraphPad Software Inc., San Diego, CA, U.S.A.). The unknown protein concentrations were calculated by interpolation of the standard curve.

2.18 Biotinylating cell surface proteins

HEK293:GLP-1R-EGFP cells were grown to 90% confluence on 10cm diameter tissue culture plates and rinsed three times with 8mL ice-cold PBS. Biotinylation was then performed based on a previously described method (Alken et al., 2005). Briefly, the plates were incubated with 2mL of ice-cold PBS containing 0.5mg/mL EZ-Link Sulpho-NHS-Biotin for 30min at 4°C with gentle rocking. The biotin solution was replaced by 4mL ice-cold PBS containing 100mM glycine and the plate incubated for 10min at 4°C with gentle agitation to remove any unbound biotin. Cells were then washed with ice-cold PBS three times and lysed by the addition of 2mL lysis buffer (10mM Tris, *pH* 7.4; 10mM EDTA, *pH* 8.5; 1% *v:v* NP-40 (nonyl phenoxyethoxyethanol); 0.1% *w:v* SDS; 150mM NaCl; 12mM deoxycholic acid; 0.5mM phenylmethylsulfonyl fluoride (PMSF)) for 20min at 4°C with vigorous shaking occasionally. Lysates were transferred to microfuge tubes and centrifuged at 16,000g for 20min to sediment nucleic acids and debris. A 50µL aliquot of NeutrAvidin agarose resin was added to the cell lysate and incubated for 1.5h at RT with occasional vortexing. The beads were then pelleted by centrifugation at 16,000g for 5s and washed three times with 1mL washing buffer 1 (500mM NaCl, 1mM EDTA, 0.5% *v:v* Triton X-100, 0.1% *w:v* SDS and 50mM Tris/HCl, *pH* 8.0) and once with 1mL washing buffer 2 (500mM NaCl, 1mM EDTA, 0.5% *v:v* Triton X-100, 0.1% *w:v* SDS and 50mM Tris/HCl, *pH* 7.4). The proteins were separated from the beads by incubation in 300µL Laemmli buffer (62.5mM Tris-HCl, *pH* 6.8, 2% *w:v* SDS, 20% glycerol, 5% *v:v* 2-mercaptoethanol) for 30min at RT with occasional shaking. The solution was centrifuged at 16,000g for 10min, the supernatant diluted in equal volumes of loading

buffer (2% *w:v* SDS, 5% *v:v* glycerol, 50mM Tris, *pH* 7.0, and 0.005% *w:v* bromophenol blue) and frozen at -80°C until analysis.

2.19 Immunoblotting

2.19.1 Sample preparation

The cells were grown to 90% confluence in 6-well plates. After medium was removed, the cells were washed twice with ice-cold PBS and lysed by incubation with 400µL of ice-cold lysis buffer (**Section 2.18**) for 15min on ice. Material was harvested using a cell scraper and transferred into a microfuge tube and gently mixed on a rocker in a cold room (4°C) for 15min. After centrifugation at 16,000g for 15min at 4°C, the supernatant was collected and stored at -20°C in aliquots. A 10µL aliquot of each sample was retained to measure the protein concentration as describe previously (**Section 2.17**). Immediately before loading, each lysate sample was diluted to 1µg/µL with ice-cold lysis buffer and 5× sample loading buffer (10% *w:v* SDS, 50% *v:v* glycerol, 200mM Tris-HCl, *pH* 6.8, 0.5M DTT (Dithiothreitol) and 0.01% *w:v* bromophenol blue).

2.19.2 SDS-polyacrylamide gel electrophoresis (SDS-PAGE)

A 7.5mL aliquot of separating gel (8% *w:v* acrylamide; 375mM Tris-HCl, *pH* 8.8; 0.1% *w:v* SDS; 0.1% *w:v* ammonium persulphate (APS); 0.06% *v:v* N, N, N', N'-tetramethylethylenediamine (TEMED)) was mixed gently and poured in between two glass plates separated by two vertical 1.5mm spacers of a Mini-PROTEAN electrophoresis system (Bio-Rad, Hemel Hempstead, U.K.). An overlay of isopropanol was immediately layered on top of the gels to provide a flat interface. After

polymerisation of the gels (~30min), the isopropanol was removed and the separating gel was briefly rinsed with H₂O. The stacking gel (5% w:v acrylamide; 126mM Tris-HCl, pH 6.8; 0.1% w:v SDS; 0.1% w:v APS; 0.06% v:v TEMED) was poured onto the gels. A comb was then loaded to form loading wells and the gels left to polymerise at RT for a minimum of 30min. Immediately before use, the combs were removed and the wells rinsed with H₂O.

The gels were placed into a Mini-PROTEAN vertical gel electrophoresis apparatus. The gel tank was half-filled with running buffer (25mM Tris-HCl pH 8.6, 192mM glycine and 0.1% w:v SDS) and the upper loading tank was filled with running buffer to cover the electrodes. Up to 30µL of samples were loaded into each well (10µL for HA blotting, 20µL for EGFP and 30µL for biotinylated samples). Up to 8µL Bio-Rad protein standards were loaded, usually on one side of the gel. Electrophoresis was carried out at 90V until the loading dye had concentrated at the top of the separating gel. The voltage was then increased to 120V until the tracking dye reached the bottom of the gel (approximately 90min).

2.19.3 Semi-dry electrophoretic transfer of proteins

Proteins were transferred from the gels to a PVDF membrane using a "semi-dry" method. PVDF membrane was cut to the size of the separating gel, soaked in methanol for 15s and in H₂O for 2min. The membrane was then equilibrated in transfer buffer (40mM glycine, 48mM Tris, 0.0375% w:v SDS, 20%, v:v methanol) for 5min. After electrophoresis, the gel was carefully removed, the stacking gel removed and the separating gel soaked in transfer buffer. The filter paper was pre-cut to the size of the gel and pre-wetted with transfer buffer. A typical blotting sandwich was made by

placing PVDF on the top of 4 of sheets pre-wet/pre-cut filter paper, the gel on top of this and 4 more sheets of filter paper. Transfer was carried out for 30min at 15V using a POWER PAC 300 (Bio-Rad, Hemel Hempstead, U.K.).

2.19.4 Immunoblotting

Once transfer was completed, the PVDF membrane was soaked in methanol for 15s and air-dried for at least 15min. The membrane was then blocked in 5% *w:v* fat free milk prepared in Tris buffered saline with Tween-20 (TBST, 0.05% *v:v* Tween-20; 50mM Tris, *pH* 7.5; 500mM NaCl) for 1h on a rocker at RT and incubated in 5mL of 5% milk-TBST containing a appropriately diluted primary antibody (**Table 2.3**) at 4°C with gentle rocking overnight. After washing with 20mL of TBST for three times over a 30min period, the membrane was incubated in 10mL 5% milk-TBST diluted secondary antibody (**Table 2.3**) for 1h at RT with gentle rocking. The membrane was then washed again for 3 times in 20mL of TBST over a 30min period.

Table 2.3. Antibodies used in immunoblotting for testing differently tagged GLP-1Rs

The GLP-1R for testing	Primary antibody	Secondary antibody
HA	Rat IgG monoclonal anti-HA (1:1000 dilution)	Goat anti-rat IgG, HRP-linked (1:1000 dilution)
EGFP	Rabbit IgG polyclonal anti-GFP (1:50,000 dilution)	Goat anti-rabbit IgG, HRP-linked (1:3000 dilution)

An enhanced chemiluminescent method was used to detect bound antibody according to the manufacturer's recommendations. Briefly, the membrane was covered with the enhanced chemiluminescence reagent and incubated for 5min at RT. The blot was then removed from the solution, excess reagent removed and wrapped in Clingfilm being careful to avoid air bubbles. The membrane was exposed to Kodak MXB film for 10s to 30min and processed in an automated film developer (Hyper processor; Amersham, Little Chalfont, U.K.).

2.20 Glycosidase treatments

2.20.1 Sample preparation

The cells were grown to confluence in 6-well plates. After washing with ice-cold PBS, the cells were harvested with a cell scraper in 500 μ L cold PBS and transferred into a 1.5mL microfuge tube. Cells were centrifuged at 200g for 2min at 4°C and resuspended in 1mL of homogenization buffer (1mM EDTA, 10mM Tris-HCl, 1mM PMSF, and 200 μ g/mL benzamidine, pH 7.4). After incubation on ice for 15min, cells were sonicated with a Sonifier Ultrasonic Cell Disruptor (Branson, CT, U.S.A.) at 10% amplitude for 3 \times 1s with 1min interval between. The lysate was centrifuged at 120g for 10min at 4°C to pellet nuclei and unbroken cells. The post-nuclear supernatant fractions were diluted with ice-cold homogenization buffer to 2 μ g/ μ L and stored at -20°C in aliquots.

2.20.2 Treatment procedure

An aliquot of 5 μ L cell lysate was used for each treatment following the manufacturer's instructions with slight modifications. Briefly, the initial denaturation

step was performed in a total volume of 15 μ L containing 0.05% w:v SDS at RT for 30min. Proteins were then treated with 500 units of either PNGase F or Endo H in a 20 μ L reaction containing 1% v:v NP-40 and either 1 \times G7 or G5 reaction buffer, respectively, for 60min at 37°C. Reactions were stopped by addition of 5 μ L of 5 \times sample loading buffer (**Section 2.19.1**). Proteins were then subjected to immunoblotting as described previously (**Section 2.19**).

2.21 Tunicamycin treatment

The stable HEK293:GLP-1R-EGFP cells in T-75 flasks were cultured to 50% confluency before tunicamycin treatment. The cells were washed once with pre-warmed PBS and cultured in fresh media containing 0.1 μ g/mL tunicamycin for 80h. Media was changed at 40h. Cells were then harvested (**Section 2.14.2**) and transferred into 6-well plates in the absence or presence of coverslips and grown in fresh media containing 0.2 μ g/mL tunicamycin for 60h followed by 0.4 μ g/mL tunicamycin for a further 40h. Finally, the cells grown on coverslips were subjected to live cell imaging (**Section 2.23.2**) while the cells in 6-well plates without coverslips were lysed and harvested for immunoblotting as described above (**Section 2.19.4**).

2.22 RT-PCR

2.22.1 Preparation of total RNA

At appropriate times following transfection, cells at approximately 90% confluency in 10cm diameter tissue culture dishes were washed with ice-cold PBS and the total RNA extracted using TRIzol reagent following the manufacturer's instructions with slight modifications. After adding 1mL TRIzol reagent, the resulting suspensions

were transferred to microfuge tubes and cells fully lysed by trituration ten times through a 23-gauge needle. Samples were incubated at RT for 5min to allow complete dissociation of the nucleoprotein complexes. Then 200 μ L of chloroform was added and tubes shaken vigorously for 15s and incubated at RT for 2–3 min before centrifugation (12,000g, 15min, 4°C). The upper aqueous phase was transferred to a clean microfuge tube and the RNA precipitated by addition of isopropanol (500 μ L). After incubating at RT for 10 min and centrifugation (12,000g, 10min, 4°C), the RNA pellet was washed with 1mL of 75% v:v ethanol and collected by centrifugation (7,500g, 5min, 4°C). After briefly air drying, the RNA was dissolved in 100 μ L H₂O and treated with DNase I (1000U/mL, 30min, 37°C). The RNA was purified by addition of 1mL TRIzol, repeating the procedure outline above and finally re-suspending in 100 μ L H₂O and stored in aliquots at -80°C.

The concentration of resulting RNA was measured by absorbance using a method similar to that used for determining of DNA (**Section 2.5**) with the exception that the RNA concentration was calculated using **Equation 2.4**. An absorbance value of 1 at 260nm corresponds to a concentration of 40 μ g/mL for RNA.

Equation 2.4

$$\text{RNA Concentration } (\mu\text{g}/\mu\text{L}) = \text{OD}_{260\text{nm}} \times \text{df} \times 40/1000$$

where: OD, optical density; df, dilution factor (e.g., 1:200 dilution)

2.22.2 Procedure of RT-PCR

Following the manufacturer's instructions, 3µg of total RNA from each extraction was used as template for reverse transcription with 0.5µL (10U) Transcriptor Reverse Transcriptase using 1µL of dT₁₂₋₁₈ (0.5µg/µL) as the primer in a total reaction volume of 20µL. PCRs were then performed in a 50µL volume containing 1µL cDNA template (from reverse transcription) 1µL (0.5U) of Taq DNA polymerase, 5µL of 10× ThermoPol reaction buffer, 1µL (0.5µg/µL) of each 5'~ and 3'~ primers, 1µL of 10mM dNTPs (10nM), and an appropriate volume of H₂O for 25 cycles as described previously (**Section 2.6.2**). The primers for both full-length and signal peptide-deleted versions of the receptor were used to clone the gene encoding the GLP-1R immediately after the putative signal peptide until the end of the receptor. These were 5'-CGC CCC CAG GGT GCC ACT G-3' and 5'-GCT GCA GGA GGC CTG GCA AGT-3'.

2.23 Live-cell imaging of EGFP-tagged GLP-1Rs and determination of receptor internalization.

2.23.1 Cell preparation

The HEK293 cells transiently or stably transfected with EGFP-tagged GLP-1Rs or EGFP were grown in monolayers on 0.1% poly-D-lysine hydrobromide-coated coverslips for at least 24h to allow adherence. Coverslips were then rinsed with Krebs-HEPES buffer (KHB, 118.6mM NaCl, 4.7mM KCl, 1.2mM MgSO₄, 1.2mM KH₂PO₄, 4.2mM NaHCO₃, 10mM HEPES, 1.3mM CaCl₂, 11.7mM glucose, pH 7.4) at 37°C and mounted in a perfusion chamber containing KHB heated to 37°C with a Peltier unit. The chamber volume was 0.5mL and where required was perfused at 5mL/min. To label the plasma membrane, 50µL of 0.05% w:v trypan blue in KHB was added to the chamber

containing 450 μ L of KHB. To monitor ligand-induced receptor internalization, ligand at the required concentration was added directly to the bath containing the coverslip.

2.23.2 *Confocal microscopy*

Cells were imaged using an UltraVIEW confocal microscope (PerkinElmer LAS, Beaconsfield, Bucks., U.K.) with a 60 \times oil-immersion objective lens and a 488nm Kr/Ar laser line. Emitted light was collected above 510nm for the fluorescent emission of EGFP or above 560nm for trypan blue and images were captured using a CCD camera.

For determining receptor internalization, images were captured before the ligand was added (basal, 0min) and at 2.5, 5, 10, 20, 30, 40, 50 and 60min after adding. For at least 6 individual cells in each experiment (i.e. each coverslip), fluorescence intensity was measured at a region of the plasma membrane and within the cytosolic compartment and a measure of internalization derived using **Equation 2.5**. Alternatively, images were recorded continually at a rate of approximately 3 frames per minute from ~5s before adding the ligand until 60min after.

Equation 2.5

$$\text{Internalisation (\%)} = [1 - (F_m_t / F_c_t) / (F_m_b / F_c_b)] \times 100\%$$

where F_m is membrane fluorescence, F_c is cytoplasmic fluorescence, t is time and b is basal (0min). F_{m_b} and F_{c_b} represent these parameters under basal conditions at the start of the experiment.

2.24 Generation and measurement of cAMP

2.24.1 *Generation of cAMP by intact cells*

The cAMP was extracted from intact cells using a method identical to that for the extraction of IP₃ (Willars and Nahorski, 1995). Cell monolayers in 0.1% poly-D-lysine hydrobromide pre-coated 24-well tissue culture plates were washed twice with 1mL of KHB and then equilibrated at 37°C for 10min with 500µL KHB containing 0.1% w:v BSA (KHB-BSA) either with (+) or without (-) IBMX (500µM). Buffer was then replaced with 500µL KHB-BSA (+/- 500µM IBMX) containing agonist at the required concentration. Following further incubation at 37°C for the required time, buffer was removed and reactions terminated with 400µL of ice-cold 0.5M trichloroacetic acid (TCA). Tissue culture plates were left at 4°C for at least 15 min and 50µL of 10mM EDTA (pH 7.0) added to 400µL aliquots, followed by 500µL of a freshly prepared 1:1 v:v mixture of tri-n-octyl-amine and 1,1,2-trichloro-trifluoro-ethane. After vortexing, samples were left at RT for 15min then microfuged (16,000g, 2min) and 200µL of the upper aqueous phase was taken, to which 50µL of 60mM NaHCO₃ was added. Samples were stored at 4°C until assay of cAMP (<3 days). Protein content of wells (typically 150-250µg) was assessed by Bradford assay (**Section 2.17**) in separate wells after digesting the cells with 0.1M NaOH.

2.24.2 *Generation of cAMP using cell membranes*

Membranes were prepared from cells either with or without the stable expression of receptors using a previously described method (Coopman et al., 2010). Briefly, confluent cell monolayers in T-175 flasks were washed with pre-warmed HEPES buffered saline (HBS; 154mM NaCl, 10mM HEPES, pH 7.4), incubated in ~8mL

harvesting buffer (154mM NaCl, 10mM HEPES and 5mM EDTA, pH 7.4) at 37°C for 10min and harvested by centrifugation (500g, 5min, 4 °C). The pellets prepared from the cells of four T-175 flasks were resuspended in 10mL ice-cold solubilization buffer (10mM HEPES, 10mM EDTA, pH 7.4). After incubation on ice for 15min, cells were sonicated with a Sonifier Ultrasonic Cell Disruptor on ice at 50% amplitude for 3×5s with 1min intervals and centrifuged (40,000g, 4°C, 15min). The pellets were resuspended in ice-cold resuspension buffer (10mM HEPES, 0.1mM EDTA, pH 7.4) at 2mg/mL protein and stored at -80°C in aliquots.

Agonist-mediated generation of cAMP from membrane preparation was determined using a modification of a previously described method (Dimitriadis et al., 1991). Generation of cAMP was initiated by addition of 20µg (20µL) membranes to form a 80µL reaction volume (final concentration: 10mM HEPES, 12mM MgCl₂, 60mM NaCl, 1.2mM EDTA, 1.2% w:v BSA, 480µM ATP, 2mM IBMX, pH 7.4) containing 10µM GTP (final concentration) and ligand. Incubations were continued for 5min at 30°C (in a water bath with shaking) and terminated by addition of 100µL of 1M TCA. Reactions were left on ice for at least 20min and 20µL of 10mM EDTA (pH 7.0) added, followed by 250µL of a freshly prepared 1:1 v:v mixture of tri-n-octyl-amine and 1,1,2-trichloro-trifluoro-ethane. After vortexing, samples were left at RT for 15min then microfuged (16,000g, 2min) and 120µL of the upper aqueous phase was taken. This was neutralized by addition of 60mM NaHCO₃ (30µL). Samples were stored at 4°C until assay of cAMP (<3 days).

2.24.3 cAMP assay

The cAMP content was determined using a radioreceptor assay with binding-protein purified from calf adrenal glands (Brown et al., 1971). The assay was conducted in single 50µL aliquots of duplicate cAMP generations in a final volume of 300µL (25mM Tris-HCl, 1mM EDTA, pH 7.5) at 4°C with bovine adrenal cortical binding protein (~0.6mg per tube) and [³H]-cAMP (specific activity 42Ci/mmol, 8.4nCi per tube) as radioligand. Authentic cAMP was used as a standard with non-specific binding (<10% of total) defined by 5µM cAMP. Following a 90min incubation, 250µL ice-cold charcoal (0.5% w:v charcoal, 0.2% w:v BSA, 25mM Tris-HCl, 1mM EDTA, pH 7.5) was added to each tube. After vortexing, all the reactions were incubated at 4°C for a further 12min then microfuged (16,000g, 4min, 4°C). An aliquot of 400µL supernatant was counted by liquid-scintillation spectrometry in 4.2mL Safeflour scintillant.

The cAMP content was determined by interpolation of a standard curve and related to protein. Concentration-response curves were fitted using Prism (GraphPad Software Inc., San Diego, CA, U.S.A.) by a standard four-parameter logistic equation and EC₅₀ values determined.

2.25 Determination of ligand binding affinity of the GLP-1R

The affinity of the radioligand, [¹²⁵I]-GLP-1 7-36 amide (2200Ci/mmol) for the GLP-1R was determined by homologous competition binding assays on membranes prepared from cells with the stable or transient expression of GLP-1Rs based on a previously described method (Bylund et al., 2004).

2.25.1 Membrane preparation

Membranes for binding experiments were prepared from confluent monolayers of cells in 80cm² flasks using the same method as described for cAMP generation (**Section 2.24.2**) but on a relatively small scale. Hence, instead of using a 50mL centrifuge tube, the membrane was harvested in 2.0mL microfuge tubes (30,000g, 10min, 4°C), resuspended and stored in ice-cold resuspension buffer at 1mg/mL protein, -80°C in 100µL aliquots.

2.25.2 Radioligand binding assay

Binding assays were carried out in round-bottomed 5mL clear polystyrene test tubes in a total volume of 100µL with the component parts diluted in Hank's Balanced Salt Solution (HBSS; 1.26mM CaCl₂, 0.493mM MgCl₂, 20mM HEPES, 0.1% w:v BSA, pH 7.4). Experiments were conducted such that ligand depletion was <10% and where possible, approximately 2000 c.p.m. were bound maximally. Membranes (12.5µg), [¹²⁵I]-GLP-1 7-36 amide (final concentration 0.1nM) and GLP-1 7-36 amide at a range of concentrations (1µM-1pM) were added to the tubes. Binding was allowed to proceed to equilibrium by incubating at RT for 3h. Membranes were then collected on Whatman GF/B glass fibre filters pre-soaked in 0.5% v:v polyethyleneimine using a Millipore vacuum manifold washed through with 2% w:v BSA. Ice-cold wash buffer (2mL; 25mM HEPES, 1.5mM CaCl₂, 1mM MgSO₄, 100mM NaCl, pH 7.4) was added to one tube at a time and immediately poured onto the membrane under vacuum. The tube was then washed with a further 2mL wash buffer, which was added to the filter. Membranes were then collected and allowed to dry. Bound radioactivity was then determined using a gamma-counter.

2.25.3 Data analysis

Competition binding curves were constructed assuming one class of binding site and K_d and B_{max} values of GLP-1 7-36 amide determined using standard analysis of homologous competition binding data (GraphPad Software Inc., CA, U.S.A.). For each of the receptors, total bound [125 I]-GLP 7-36 amide (c.p.m.) was plotted against the concentration (\log_{10} M) of unlabelled GLP-1 7-36 amide.

2.26 Radioligand binding assay in intact cells

Radioligand binding assays were performed in intact cells to determine cell-surface receptor expression after the cells were treated with different ligands of the GLP-1R (e.g. GLP-1 7-36 amide, exendin 9-39 and compound 2). The cells stably expressed either the GLP-1R (HEK293Flp-In-WTGLP-1R) or the human muscarinic M_3 receptor (HEK293: M_3) (Tovey and Willars, 2004).

2.26.1 Binding assay in intact cells with the expression of GLP-1Rs

Two preliminary experiments were conducted before this binding assay to confirm experiment conditions. Firstly, the cells with the stable expression of the GLP-1R-EGFP growing on coverslip were incubated with 100nM GLP-1 7-36 amide at 4°C overnight. No receptor internalization was detected in these cells by confocal imaging (**Section 2.23.2**). Secondly, different washes at 37°C with either KHB-BSA (pH 2.0) for 50s, (pH 4.0) for 2min or (pH 6.0) for 10min were performed after incubating the HEK293:GLP-1R-EGFP cells with 100nM exendin 9-39 for 1h. In these washes, pH 4.0 for 2min was sufficient to remove any bound exendin 9-39 and didn't interfere with the binding assay. Therefore, binding assays to determine cell-surface expression of the GLP-1R was conducted on cells expressing GLP-1R constructs at 4°C to prevent receptor

internalization during the binding assay. After appropriate treatments with ligands (**Chapter 5**), cell monolayers with 25-30% confluence (to reduce ligand depletion) in 24-well plates were washed with 1mL of KHB-BSA (pH 7.4 unless specifically noted) for 5min at 37°C and washed with 1mL of KHB-BSA (pH 4.0) for a further 2min at 37°C. The cells were then carefully washed with 1mL of ice-cold KHB-BSA and equilibrated in 1mL of the same buffer at 4°C for 10min. Buffer was then replaced with 600µL KHB-BSA containing 0.27nM [¹²⁵I]-GLP-1 7-36 amide. Non-specific binding (NSB) was determined in the presence of 1µM GLP-1 7-36 amide. Following overnight incubation at 4°C, buffer was removed and cells briskly washed twice with 1mL of ice-cold KHB-BSA. 250µL of NaOH (0.2M) was then added to each well and left for ~15min before transfer into 5mL clear polystyrene test tubes. Wells were washed with 0.25mL of HCl (0.2M) and this was added to the tube containing the same sample. Radioactivity was then determined using a gamma-counter. After this, 20µL of mixture from each tube was transferred into a clean 1.5mL microfuge and protein content was estimated by Bradford assay (**Section 2.17**).

2.26.2 Binding assay in intact cells with the expression of M₃

Radioligand binding assays were also conducted on intact HEK293 cells with stable expression of the human muscarinic M₃ receptors using [N-methyl-³H]-scopolamine methylchloride ([³H]-NMS, 81Ci/mmol), an antagonist of muscarinic receptors. The binding was performed for 1h at 37°C. Briefly, after appropriate treatments, monolayers of cells with ~50% confluence in 24-well plates were washed with 1mL of pre-warmed KHB-BSA and equilibrated in 1mL of the same buffer at 37 °C for 10min. Buffer was then replaced with 1mL KHB-BSA containing 0.2nM [³H]-NMS. NSB was determined

in the presence of the muscarinic receptor antagonist, atropine (2 μ M). Following 1h incubation at 37°C, buffer was removed and cells briskly washed twice with 1mL of ice-cold KHB-BSA. For cell digestion, 0.5mL of NaOH (0.1M) was added to each well and incubated at RT for 15-20min. The cell lysate were transferred into scintillation vials. Wells were washed with 0.5mL of HCl (0.1M) and this was added to the scintillation vial containing the same sample. After mixing by gentle shaking, 100 μ L from each vial was transferred into a clean 1.5mL microfuge tube and kept safely at 4°C for determination of protein content. To the scintillation vials, 5mL of scintillant was added and thoroughly vortexed. Radioactivity was then determined using a scintillation counter and protein content was estimated by Bradford assay (**Section 2.17**).

2.26.3 Data analysis

Specific binding of the ligands ([¹²⁵I]-GLP-1 7-36 amide or [³H]-NMS) to the receptor was calculated as the difference between total binding and NSB. For intact cell binding assays, the bound radioactivity was related to the cellular protein. Data were then plotted in Graphpad Prism as a percentage of radioligand specifically bound to receptors in un-treated cells.

2.27 General data analysis

All data shown are expressed as the mean \pm sem of at least three experiments (unless otherwise stated). Where representative data are presented, experiments were performed at least 3 times. All linear (e.g. protein concentration curve) and nonlinear (e.g. concentration-response curves and homologous competition binding data) curves were fitted using Prism (GraphPad Software Inc., San Diego, CA, U.S.A.). Where

statistical analyses were require, the format of the data was taken into account in the selection of an appropriate test. An unpaired Student's t-test was used for direct comparison of a test value with a control, where two groups were used. Statistical significance of differences between multiple groups was determined using either one-way analysis of variance (ANOVA) or two-way ANOVA with an appropriate post test, for multiple comparisons. Statistical significance in either cases was considered for $p < 0.05$.

CHAPTER 3 Generation and Characterization of

Epitope Tagged GLP-1Rs

3.1 Introduction

With the exception of the opsins, functional GPCRs are located at the plasma membrane and transduce signals into the cell following agonist binding. However, they are synthesized in the ER and therefore require export from the ER and passage through the Golgi apparatus. During their migration, receptors undergo post-translational modifications to attain their mature status at the plasma membrane (Duvernay et al., 2005). This procedure used to be considered as a default, un-regulated secretory pathway. Although the precise molecular mechanism underlying such processes are not completely characterized, the progress achieved over the past few years has revealed that the export of GPCRs from the ER and trafficking to the cell surface is highly regulated. For example, glycosylation may play an important role in receptor maturation and cell surface translocation (Duvernay et al., 2005; Achour et al., 2008).

Glycosylation, along with methylation, sulfation, phosphorylation and lipid addition are the principal post- (or co-) translational protein modifications performed in higher eukaryotes. Glycoproteins make up at least 50% of all human proteins (Apweiler et al., 1999). It is likely that most plasma membrane proteins including GPCRs and secretory proteins are glycosylated. This process results in the addition of one or more carbohydrate chains, namely glycans or oligosaccharides to these proteins. Two major types of glycosylation occur in the body: *N*-linked glycosylation to the amide nitrogen of asparagine side chains and *O*-linked glycosylation to the hydroxy oxygen of serine and threonine side chains. Compared with *N*-linked glycosylation, *O*-linked is less well understood and this may occur at any serine or threonine residue with no single

common core or consensus protein sequence (Brooks, 2009; An et al., 2009). In contrast, *N*-linked glycosylation initiates in the lumen of the ER by adding a glycan core unit $\text{Glc}_3\text{Man}_9\text{GlcNAc}_2$ (Glc, glucose; Man, mannose; GlcNAc, *N*-acetylglucosamine) co-translationally to the nascent polypeptide chain at the asparagine within a sequence of Asn-X-Ser/Thr, termed a sequon, in which X could be any amino acid except phenylalanine (Marshall, 1974; Elbein, 1987). After coupling to the polypeptide chain in the ER, terminal glucose residues are immediately removed by glucosidases and oligomannoses are formed (Helenius and Aebi, 2001; **Figure 3.1a**). Some but not all of the oligomannose *N*-glycans then undergo further extensive post-translational modifications to form complex *N*-glycans or hybrid *N*-glycans (**Figure 3.1b**) during the trafficking of the glycoproteins from the ER through the Golgi apparatus (Balzarini, 2007; Varki et al., 2009). Some oligomannose *N*-glycans retained in the ER and become one of the final products of *N*-linked glycosylation. Hybrid *N*-glycans are formed in the medial-Golgi as the result of incomplete action of α -mannosidase II, which cannot be further processed to complex *N*-glycans (Varki et al., 2009). Glycans can be removed from glycoproteins by some bacterial enzymes. For example, PNGase F can release oligomannose, hybrid, and complex *N*-glycans from asparagine (**Figure 3.1b**) and Endo H can remove oligomannose and hybrid *N*-glycans, but not complex *N*-glycans between the two core GlcNAc residues, leaving one GlcNAc attached to asparagine. (**Figure 3.1**).

Proteins undergoing *N*-linked glycosylation are structurally diverse as the sugar composition and the number and size of branches in the sugar tree varies among glycans bound to the protein. Thus glycosylation may play a variety of important roles in many cellular events ranging from structural to signalling and recognition. For example, emerging evidence reveals that the initial *N*-linked glycosylation in the ER plays a role in protein folding, oligomerization, quality control, sorting, and transport (Varki et al.,

2009). In the Golgi apparatus, the glycans acquire more complex structures to obtain maturation and potentially play a new set of functions in glycoproteins including conformation, solubility, trafficking and antigenicity (Helenius and Aebi, 2001; Hendriks et al., 2004; Jensen et al., 2010). Therefore, understanding these *N*-glycan pathways is important. Indeed, *N*-glycans have been used as tags to localize a glycoprotein or to follow its movement through the cell and defects in *N*-glycan synthesis has been found to lead to a variety of human diseases (Varki et al., 2009).

N-linked glycosylation occurs for most GPCRs. However, the role of glycosylation varies from receptor to receptor. For example, *N*-linked glycosylation is essential or important for receptor cell surface expression of many GPCRs including the vasoactive intestinal peptide-1 receptor (Convineau, 1994), the follicle-stimulating hormone receptor (Davis et al., 1995), the angiotensin II receptor subtype I (Deslauriers, 1999), gastrin-releasing peptide receptor (Benya et al., 2001), the relaxin receptor (Kern et al., 2007), μ -opioid receptor (Ge et al., 2009) and melanocortin 2 receptor (Roy et al., 2010). In contrast, for some GPCRs including the histamine H₂ receptor (Fukushima *et al.*, 1995), muscarinic M₂ acetylcholine receptor (van Koppen and Nathanson, 1990) and the neuropeptide S receptor (Clark et al., 2010) *N*-linked glycosylation is not responsible for receptor cell surface expression. Therefore, the extent and influence of glycosylation in the properties of mature GPCRs are variable and unpredictable. Three *N*-linked glycosylation sites are predicted at Asn⁶³, Asn⁸², Asn¹¹⁵ in the N-terminal domain of the human GLP-1R (NetNGlyc 1.0 Server, <http://www.cbs.dtu.dk/services/NetNGlyc/>). It is also known that the rat GLP-1R protein is glycosylated (Goke *et al.*, 1994; Widmann *et al.*, 1995). However, further experimental verification is required to determine the characteristics of glycosylation and its role in the processing, trafficking and function of the GLP-1R.

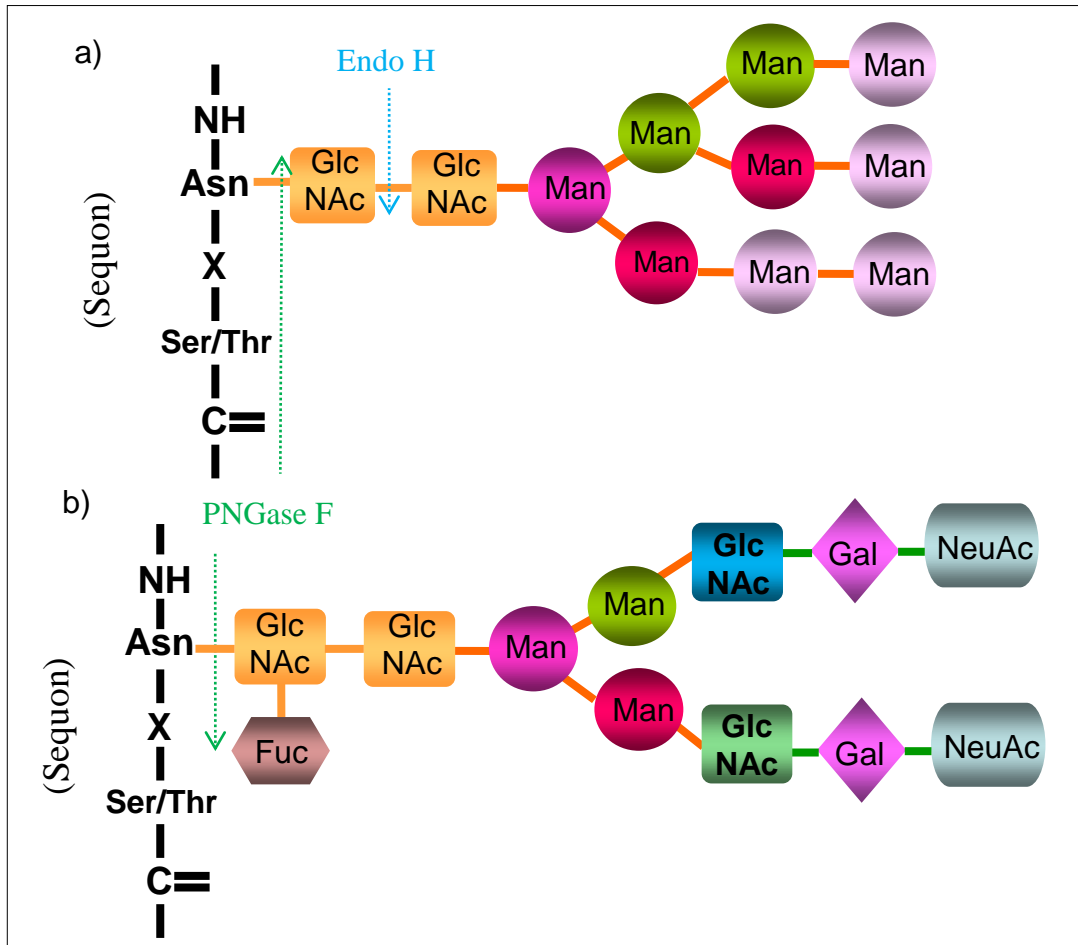


Figure 3.1. Common core sugar sequences of N-linked glycosylation. All N-glycans share an N-linked glycosylation that begins in the ER lumen. Immediately after, oligosaccharides ($\text{Glc}_3\text{Man}_9(\text{GlcNAc})_2$) are uniquely added to asparagine in a sequon (Asn-X-Ser/Thr), all three glucose residues and a variable number of mannose residues (1-4) are removed to generate oligomannoses ($\text{Man}_{5-9}(\text{GlcNAc})_2$) (a). During trafficking from the ER through the Golgi apparatus, glycans are modified extensively and glycosylation is completed in the trans-Golgi cisternae, in the form of a complex N-glycan (b) or hybrid (a mixture of oligomannose and GlcNAc) (not shown). The cleavage sites of the glycosidases are indicated: endoglycosidase H (Endo H) in blue and peptide N-glycosidase F (PNGase F) in green. Man, mannose; Glc, glucose; Gal, galactose; Fuc, fucose; GlcNAc: N-acetylglucosamine; NeuAc, N-acetylneuraminic acid.

Epitope tagging has been utilized extensively in the study of GPCR expression, trafficking, function and regulation, in which the addition of a small antigenic peptide, known as an epitope tag, into a GPCR sequence and hence the resulting product can be recognised by an antibody against the epitope tag (McIlhinney, 2004). Small epitope tags (≤ 10 residues) such as Flag- HA-, His- and Myc-tags have been inserted into many GPCRs without affecting ligand binding, function or the processing and trafficking of the receptor and thus applied commonly. Tags are mainly inserted at the N-terminus of the receptor, potentially to allow monitoring of cell surface expression by, for example, immunocytochemistry (ICC) or enzyme-linked immunosorbent assay (ELISA) (Böhme and Beck-Sickinger, 2009). In addition to this, green fluorescent protein (GFP) tags enable the direct visualisation of dynamic receptor intracellular trafficking processes and internalisation with a number of advantages including: no need for antibodies, low phototoxicity, high photo-bleaching-resistance, low background fluorescence and fluorescence that is stable to all steps of ICC (Kallal and Benovic, 2000; Böhme and Beck-Sickinger, 2009). However, a GFP-tag is relatively large in molecular size large (238 residues, ~ 27 kDa) and hence has the potential to influence properties of the receptors. This may depend on the localization of the GFP-tag. Unfortunately, it seems that there is no general rule for the location of a GFP-tag within a GPCR. Thus, while some studies reveal that a C-terminal GFP-tag is preferable to an N-terminal one (Ivic et al., 2002; Limon et al., 2007; Rodrigues et al., 2009), others show the opposite (Perret et al., 2003; McDonald et al., 2007). N-terminal GFP-tagging is ideal if the tagging does not disturb the natural features of a receptor, particularly as the use of pH-dependent GFP variants can provide additional information about subcellular trafficking (Ashby et al., 2004).

Although anti-GLP-1R antibodies have been raised against different regions (e.g., the N-terminus and C-terminus) of the GLP-1R (Widmann et al, 1995; Vahl et al, 2007, Shu et al., 2009), antibodies of sufficient quality for immunoblotting or immunofluorescence are often difficult to obtain for GPCRs in general. Indeed our laboratory has used a number of commercially available antibodies against the GLP-1R with little success. Further, the present study involved mutagenesis of the GLP-1R which may also affect the ability of antibodies to recognize the receptor. Consequently, epitope-tagging was required for the present study to provide strong immunoreactivity in both mutated and wild-type GLP-1Rs. In addition, an appropriate EGFP-tag would allow not only monitoring of the subcellular localization but also examination of the real-time movement of the GLP-1R. This tagging must not, however, change the properties of the receptor. Surprisingly, before starting this work, there was little available information about epitope tagging the GLP-1R from the published literature. In mammalian cells, the GLP-1R has been tagged with Flag- and His-tags at the N-terminus (Vázquez et al, 2005) and with a GFP-tag at either terminus (Salapatek et al., 1999; Xiao et al., 2000; Syme et al., 2006; Bavec and Ličar, 2009). However, since there was no comparison between untagged and tagged receptors or between receptors with tags in different locations (e.g., N-terminus and C-terminus), it was difficult to assess the best option for epitope-tagging the GLP-1R. In this chapter, a series of strategies were used to insert one or more epitope-tag sequences into the receptor. A variety of constructs were generated (more than ten) with an HA-tag and/or EGFP-tag at the terminus of the GLP-1R. These constructs were compared to the untagged, wild-type receptor, in aspects including receptor processing, trafficking and function. Based on this, a stable cell line was established allowing functional expression of a GLP-1R

that could be easily visualized and used to determine membrane targeting and the role of *N*-linked glycosylation.

3.2 Strategies for generating epitope-tagged GLP-1R constructs

3.2.1 C-terminal epitope-tagged GLP-1R constructs

The recombinant DNA plasmid of a C-terminal HA-tagged GLP-1R (GLP-1R-HA) was generated by three-part-ligation using the method described in **Section 2.10**, in which GLP-1R (*Bgl*II-*Xho*I) encoding the full length GLP-1R, including a start codon but no stop codon, was generated by digesting a PCR product with *Bgl*II and *Xho*I (**Figure 3.2b**); a dsDNA fragment encoding HA-tag sequence with a stop codon and sticky ends (*Xho*I-*Xba*I) was prepared by annealing a complementary pair of oligonucleotides (**Section 2.11, Figure 3.2d**) and; the vector (pcDNA3.1(+)) was digested with *Bam*HI and *Xba*I (**Figure 3.2c**). Since the coding sequence of the GLP-1R contains a *Bam*HI site, this RE site was avoided in PCR cloning of the GLP-1R (**Figure 3.2a**). After ligation and transforming into competent DH5 α , 24 colonies were obtained, from which ten DNA clones were isolated using a QIAGEN plasmid mini kit (**Section 2.4**) and assessed for the insert of the GLP-1R by digesting each clone with *Nhe*I and *Xho*I (**Figure 3.3a**). The insert of the C-terminal HA-tag was only ~40bp, which was too small to be seen in an agarose gel. Therefore, the DNA clones containing the GLP-1R insert were assessed for function (generation of cAMP in response to GLP-1 7-36 amide). All clones were found to be positive (**Figure 3.3b**). Clone 9 was randomly chosen for a RE site analysis according to the plasmid map (**Figure 3.4a**), in

which three RE sites in the coding sequence of the GLP-1R including *Bam*HI, *Kas*I and *Kpn*I were confirmed (**Figure 3.4b**). This clone was then subjected to automated DNA sequencing (**Section 2.13**). The sequencing result showed that the coding sequence of both GLP-1R and HA-tag were 100% correct and in the same reading frame (**Figure 3.10ii**). This confirmed DNA clone was used as the GLP-1R-HA construct throughout the present study.

The C-terminal EGFP-tagged GLP-1R (GLP-1R-EGFP) construct was generated by simply inserting a fragment of the GLP-1R(*Nhe*I-*Xho*I) isolated from the GLP-1R-HA construct (**Figure 3.2**) into pEGFP-N1(*Nhe*I-*Xho*I). After a 'home-made' plasmid isolation (**Section 2.4**) and RE digest with *Nhe*I-*Xho*I (**Section 2.7**), one of the plasmids containing an insert of the expected size was prepared using a QIAGEN plasmid mini kit (**Section 2.4**) and identified by the RE site analysis (**Figure 3.5**). This strategy improved the efficiency for full DNA sequencing (**Figure 3.10iii**).

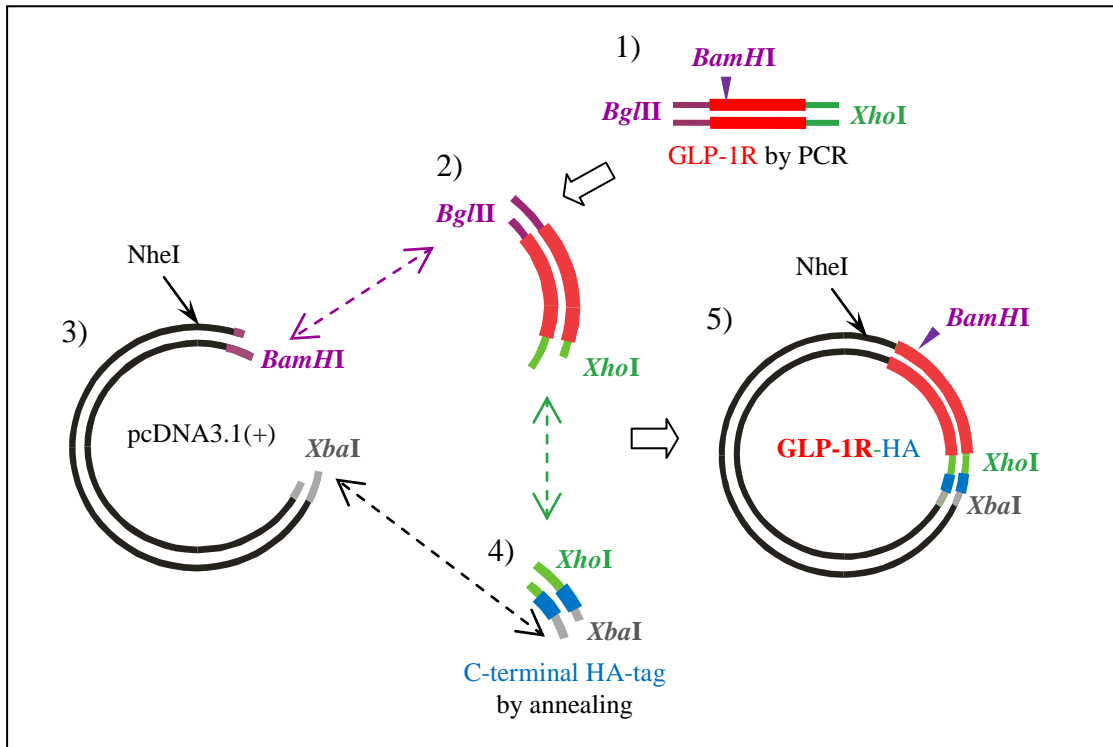


Figure 3.2. Diagram of the three-part-ligation strategy for generating the GLP-1R-HA construct. The GLP-1R DNA sequence in red was cloned by PCR (1) followed by a digest with *Bgl*III-*Xho*I (2). The C-terminal HA-tag in blue was prepared by annealing a complementary pair of oligonucleotides (4) and the vector was prepared by digesting pcDNA3.1(+) with *Bam*HI-*Xba*I (3). Joins between the DNA pieces are indicated by dashed double arrows. Compatible sticky-ends or the same RE sites are indicated in the same color (i.e., purple, green and grey). Although the sticky-ends generated by digesting with *Bam*HI and *Bgl*III were compatible and could be joined by ligation, neither *Bam*HI nor *Bgl*III sites were available in the resulting product. However, an upstream *Nhe*I in the vector was still available as indicated (5).

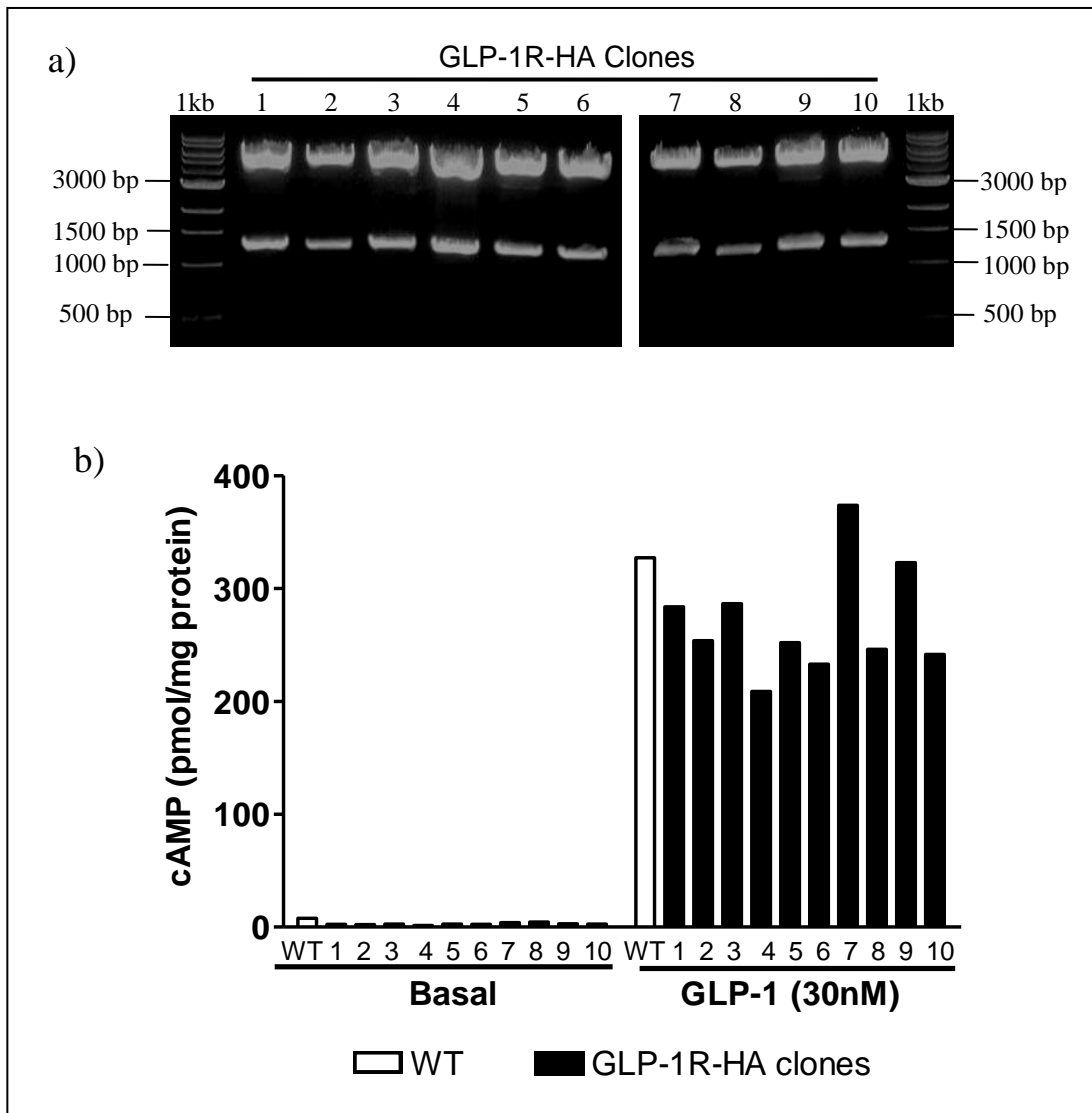


Figure 3.3. Preliminary confirmation of potential GLP-1R-HA clones. To confirm plasmids contained an insert of the expected size of the GLP-1R-HA construct, 10 plasmids (GLP-1R-HA clones) were subjected to a digest with *NheI-XhoI*. The lanes of the DNA size marker (1kb ladder) and the GLP-1R-HA clones are indicated on the agarose gel electrophoresis image (a). HEK293 cells were then transiently transfected with either the untagged WTGLP-1R or plasmid DNA clones which contained an insert of the expected size (GLP-1R-HA clones 1-10). After 48h, the cells were challenged with 30nM GLP-1 7-36 amide (GLP-1) for 10min, at 37°C and levels of intracellular cAMP were determined relative to the cellular protein content (b).

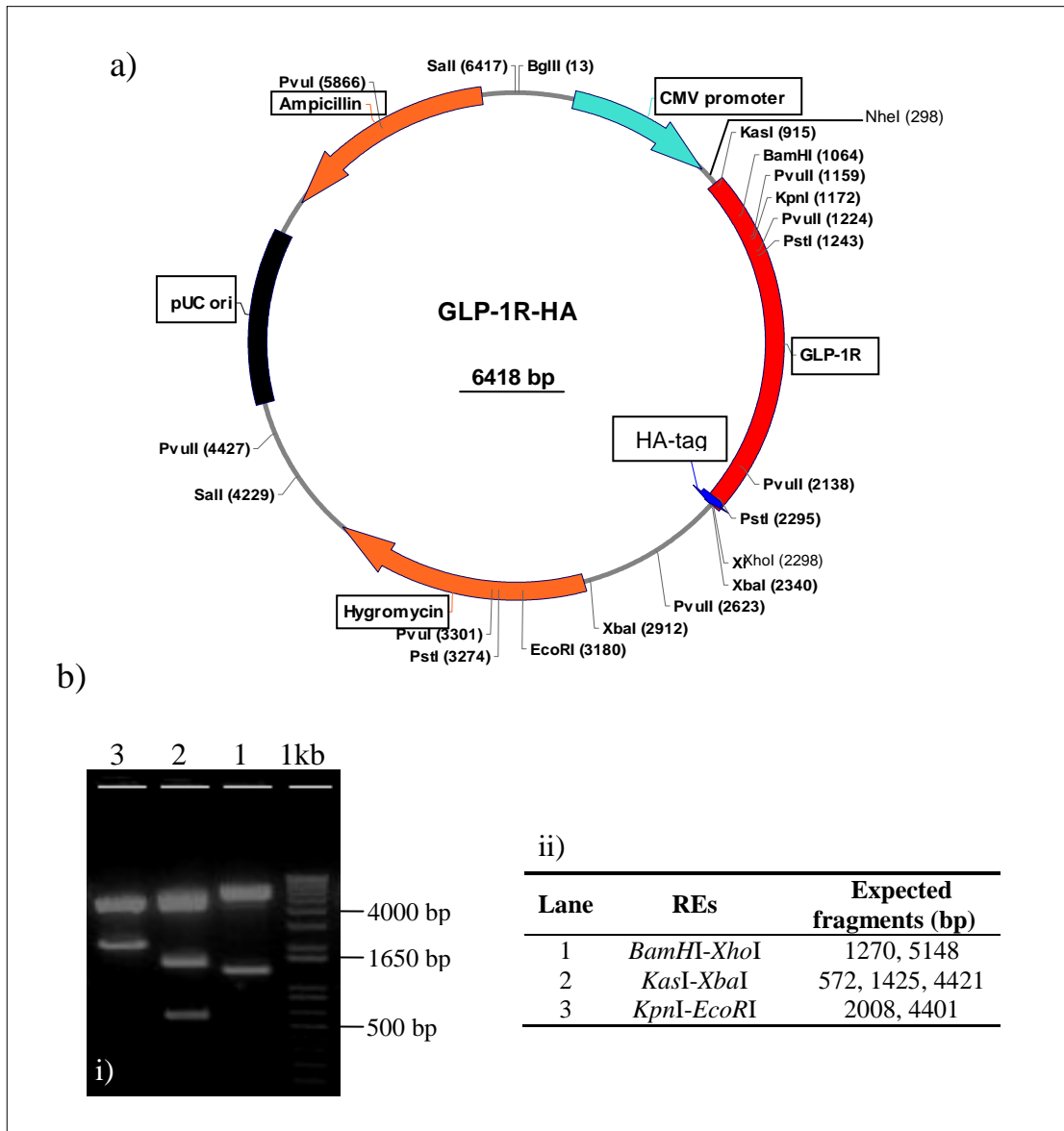


Figure 3.4. Plasmid map and RE digest of the GLP-1R-HA construct. The size, main RE sites and important regions (highlighted in boxes) of the expected construct are shown in the DNA plasmid map (a). The construct was identified by separate RE digestion with *BamHI-XhoI*, *KasI-XbaI* and *KpnI-EcoRI*. The DNA in each digest was separated by agarose gel electrophoresis (b, i). The expected sizes of the resulting bands following digestion are indicated (b, ii).

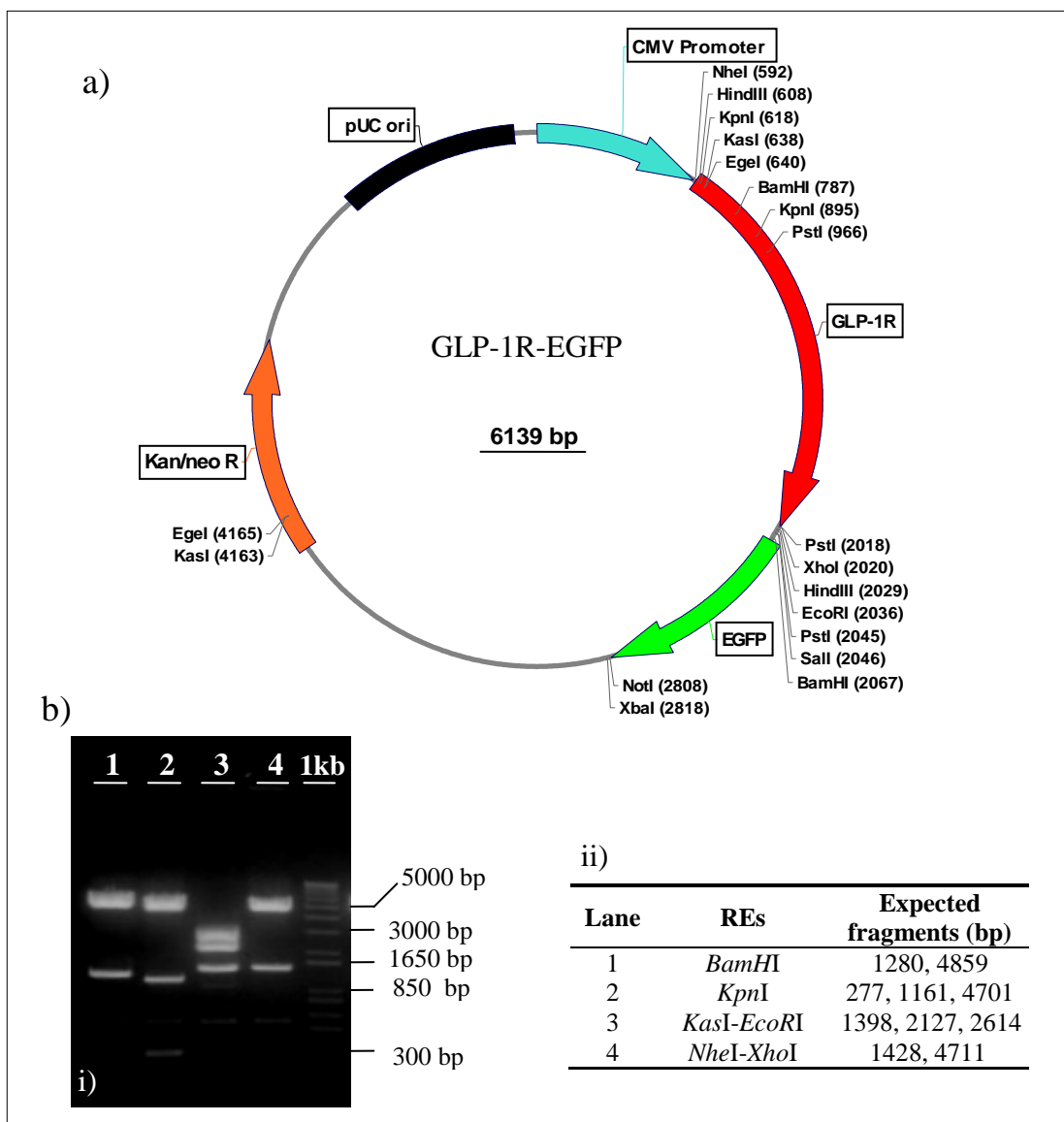


Figure 3.5. Plasmid map and RE digest of the GLP-1R-EGFP construct. The construct size, main RE sites and important regions (highlighted in boxes) of the expected construct are shown in the DNA plasmid map (a). The construct was identified by separate RE digest with *BamHI*, *KpnI*, *KasI-EcoRI* and *NheI-XhoI*. The DNA in each digest was then separated by agarose gel electrophoresis (b, i). The expected sizes of the resulting DNA bands following digestion are indicated in the table (b, ii).

3.2.2 *The GLP-1R constructs containing an N-terminal HA-tag*

A three-part-ligation was also used to generate the N-terminal HA-tagged (HA-GLP-1R) construct, in which: the HA-tag (*Bam*HI-*Spe*I) was generated by annealing a complementary pair of oligonucleotides and contained a start codon; the GLP-1R (*Nhe*I-*Xho*I) including a stop codon but no start codon was cloned by PCR and; the vector was prepared from pcDNA3.1 by digesting with *Bam*HI and *Xho*I. From all 6 colonies obtained from ligation, 5 DNA clones contained the insert of HA-GLP-1R (**Figure 3.6a**), in which 4 clones (of 4 clones assessed) were confirmed by GLP-1 7-36 amide-mediated cAMP production (**Figure 3.6b**). Surprisingly, a series of RE sites analyses performed in these clones implied that the functional insert in each clone was actually contamination by the initial template (data not shown) instead of the expected construct containing an HA-tag. This was a good example of the need for RE sites analysis before subjecting a candidate construct to full DNA sequencing. In addition, care must be taken in the interpretation of functional screens of individual DNA clones as these data indicate that positive results do not necessarily mean correct clones. These points were considered in future cloning experiments.

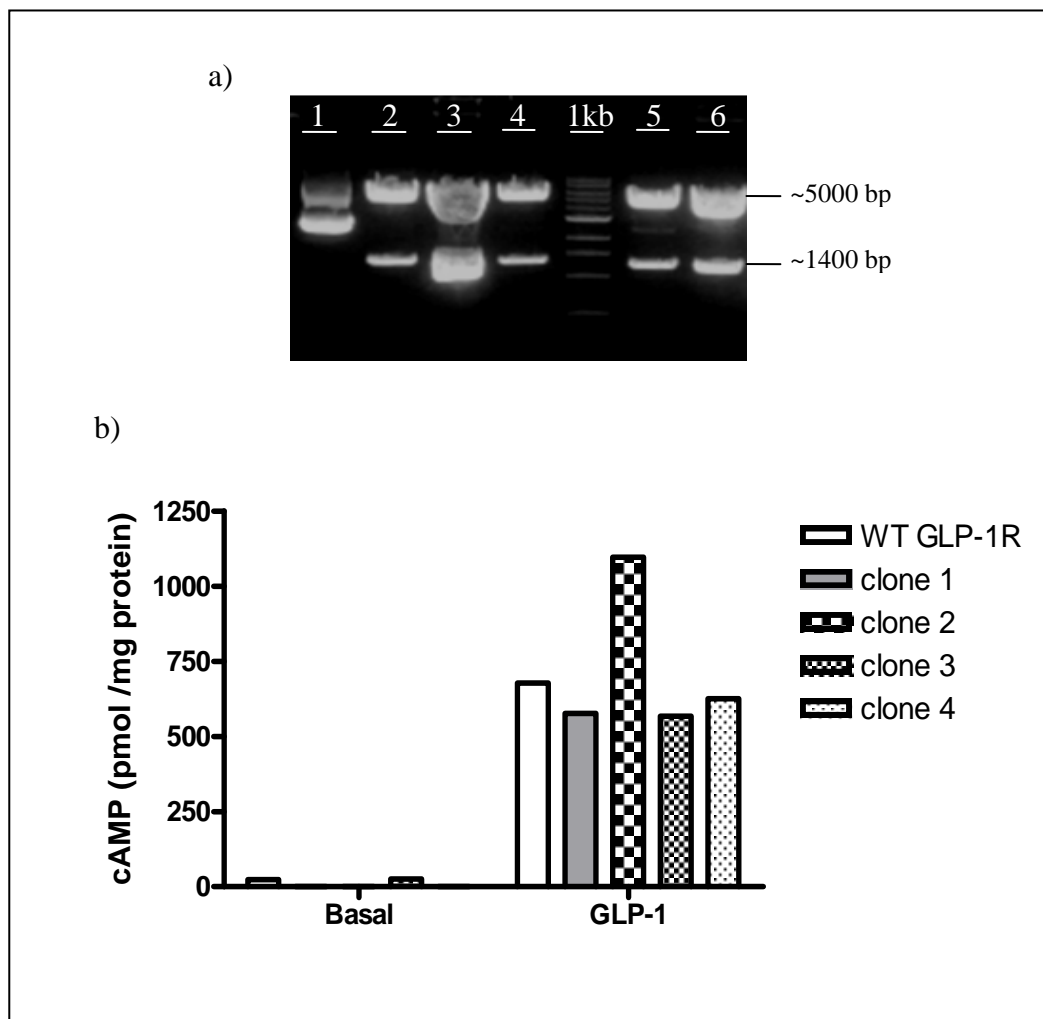


Figure 3.6. Preliminary confirmation of potential HA-GLP-1R clones. In order to identify potential HA-GLP-1R constructs, the presence of an insert of the expected size in six plasmid DNA clones was checked by a RE digestion with *NheI-XhoI*. The lanes of the DNA size marker (1kb ladder) and the HA-GLP-1R clones (1 to 6) are indicated on the agarose gel electrophoresis image (a). HEK293 cells were then transiently transfected with either WTGLP-1R or plasmid DNA clone 2, 4, 5 and 6 which contained an insert of the expected size. After 48h, the cells were challenged with 30nM GLP-1 7-36 amide (GLP-1) for 10min, at 37°C in the absence of IBMX and levels of intracellular cAMP were determined relative to the cellular protein content (b). A further RE sites analysis suggested that these DNA clones were actually incorrect constructs (see main text; data not shown).

Cloning of the HA-GLP-1R construct was attempted again while an N-terminal HA-tagged and C-terminal EGFP-tagged GLP-1R (HA-GLP-1R-EGFP) were generated using the two-stage-PCR strategy to introduce an HA-tag into the constructs. In stage 1, the first PCR was performed using the 5'~primer A (**Figure 2.2b**) and the 3'~primer in **Figure 2.1a** as described previously (**Section 2.6**) to generate the GLP-1R with a truncated N-terminal HA-tag (23bp). The PCR product was then separated and purified as described in **Section 2.8 & 2.9**. In stage 2, a second PCR was performed using the purified product (1 μ L) obtained from the first PCR as the template but using the 5'~primer B (**Figure 2.2b**) and either the 3'~primer in **Figure 2.1a** or the 3'~primer **Figure 2.1c** (that either contained (for HA-GLP-1R) or did not contain (for HA-GLP-1R-EGFP) a stop codon). The purified and *SpeI-XhoI* digested final PCR products from stage 2, referred to as HA-GLP-1R(*SpeI-XhoI*), containing the stop codon, was then ligated with the pcDNA3.1(+)(*NheI-XhoI*) to generate the HA-GLP-1R construct. The other HA-GLP-1R(*SpeI-XhoI*) without a stop codon was ligated with pEGFP-N1(*NheI-XhoI*) to generate the HA-GLP-1R-EGFP construct. In the preliminary insert confirmation as above, there were four clones for each construct showing the presence of the GLP-1R insert. Before sending for DNA sequencing, RE site analysis was performed on all clones of both constructs (**Figure 3.7 & Figure 3.8**). The sequencing results confirmed that both HA-GLP-1R and HA-GLP-1R-EGFP constructs were generated successfully (**Figure 3.10 iv & v**).

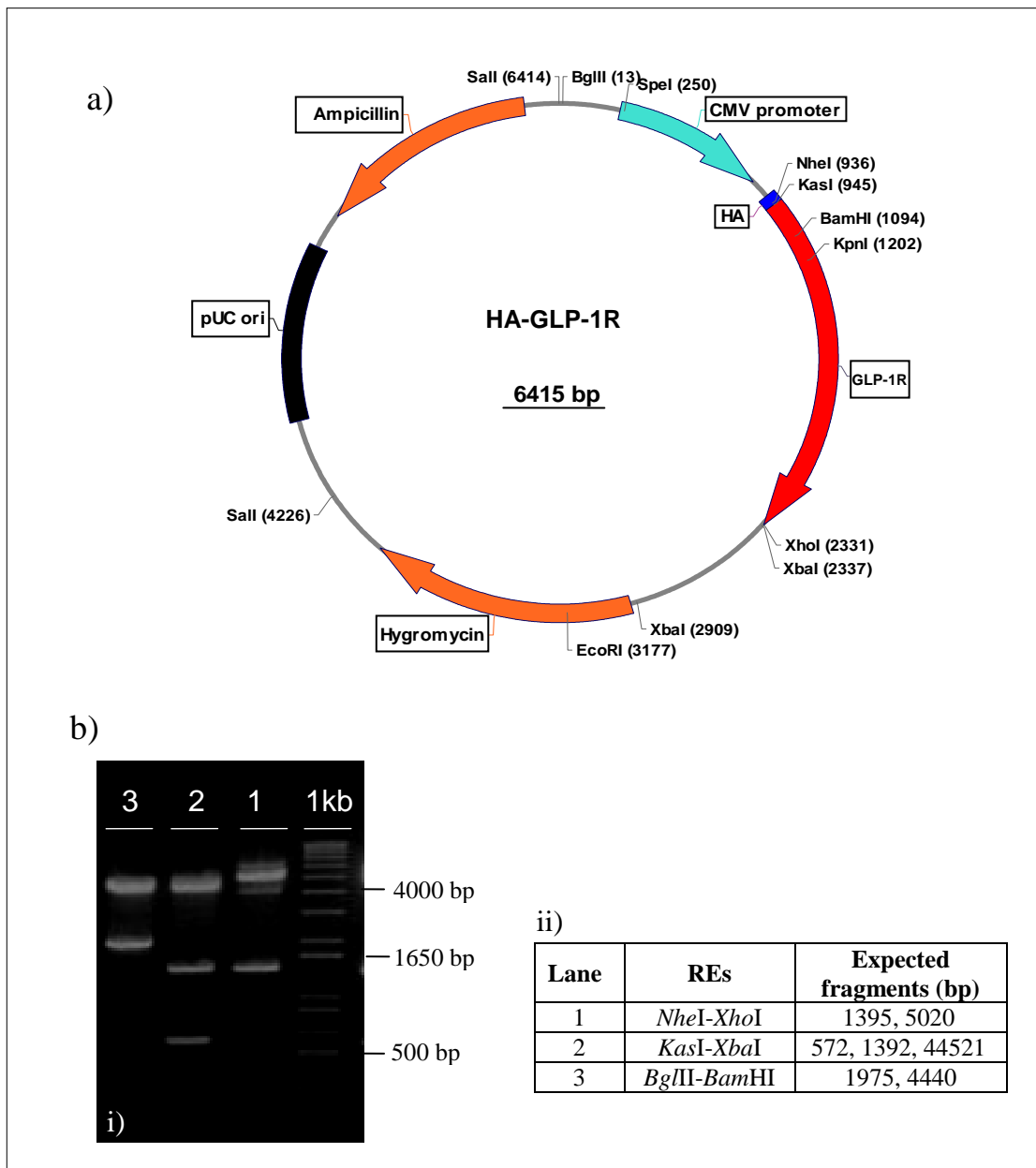


Figure 3.7. Plasmid map and RE digest of the HA-GLP-1R construct. The construct size, main RE sites and important regions (highlighted in boxes) of the expected construct are shown in the DNA plasmid map (a). The construct was identified by separate RE digestion with either *NheI-XhoI*, *KasI-XbaI* or *BglII-BamHI*. The DNA in each digestion was separated by agarose gel electrophoresis (b, i). The position of the wells and DNA size marker (1kb ladder) are noted. The expected sizes of the resulting DNA bands following digestion are indicated in the table (b, ii).

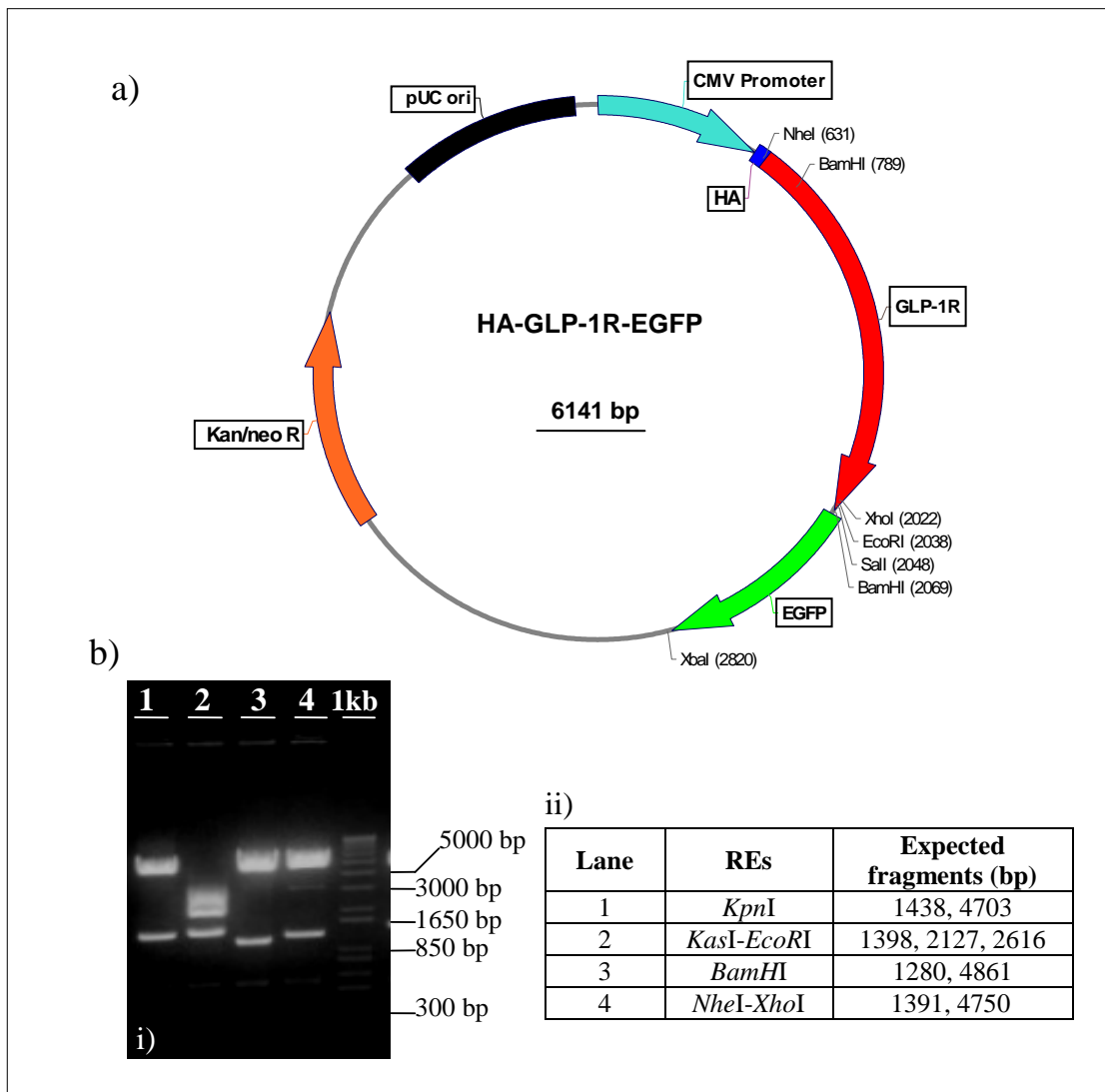


Figure 3.8. Plasmid map and RE digest of the HA-GLP-1R-EGFP construct.

The construct size, main RE sites and important regions (highlighted in boxes) of the construct are shown in the DNA plasmid map (a). The construct was identified by separate RE digest with *KpnI*, *KasI-EcoRI*, *BamHI* or *NheI-XhoI*. The DNA in each digest was separated by agarose gel electrophoresis. The DNA size marker (1kb ladder) and the position of the wells is noted on the gel image (b, i). The expected sizes of the resulting DNA bands following digest are indicated in the table (b, ii).

3.2.3 The N-terminal EGFP-tagged and C-terminal HA-tagged GLP-1R (EGFP-GLP-1R-HA) construct

The sequence of GLP-1R-HA(*Bgl*III-*Xho*I) without a start codon was cloned by PCR using the GLP-1R-HA construct as the template and the primers shown in **Figure 2.2b**. After performing a digest of the purified PCR product with *Bgl*III and *Xho*I, the resulting fragment, GLP-1R-HA(*Bgl*III-*Xho*I), was then ligated with pEGFP-C1 (*Bgl*III-*Sal*I) to obtain the EGFP-GLP-1R-HA (**Figure 3.9**). The sequencing result of this construct is shown in **Figure 3.10 vi**.

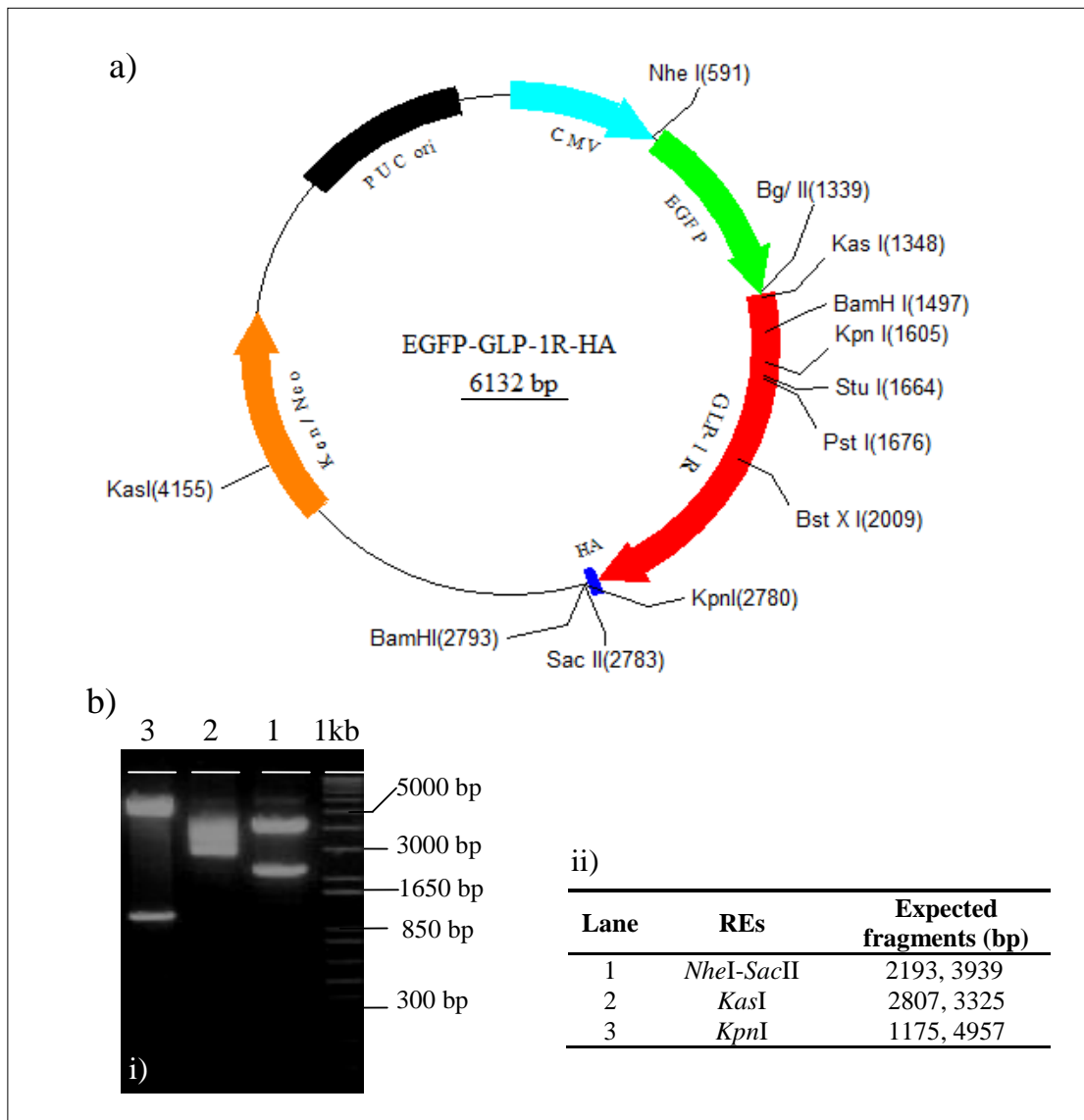


Figure 3.9. Plasmid map and RE digest of the EGFP-GLP-1R-HA construct.

The construct size, main RE sites and important regions of the expected construct are indicated in the DNA plasmid map (a). The construct was identified by separate RE digest with *NheI-SacII*, *KasI*, or *KpnI*. The DNA in each digest was separated by agarose gel electrophoresis. The DNA size marker (1kb ladder) and the position of the wells is noted on the gel image (b, i). The expected sizes of the resulting DNA bands following digest are indicated in the table (b, ii).

i.	WTGLP-1R:	<i>GCCACC</i> <u>ATG</u>	GLP-1R(4-1389)	<u>TGA</u>
ii.	GLP-1R-HA:	<i>GCCACC</i> <u>ATG</u>	GLP-1R(4-1389) HA ^C	<u>TGA</u>
iii.	GLP-1R-EGFP:	<i>GCCACC</i> <u>ATG</u>	GLP-1R(4-1389) EGFP ^C	<u>TGA</u>
iv.	HA-GLP-1R:	<i>GCCACC</i> <u>ATG</u>	HA ^N GLP-1R(4-1389)	<u>TGA</u>
v.	HA-GLP-1R-EGFP:	<i>GCCACC</i> <u>ATG</u>	HA ^N GLP-1R(4-1389) EGFP ^C	<u>TGA</u>
vi.	EGFP-GLP-1R-HA:	<i>GCCACC</i> <u>ATG</u>	EGFP ^N GLP-1R(4-1389) HA ^C	<u>TGA</u>
vii.	HA ^N :	...TAC CCA TAC GAT GTT CCA GAT TAC GCTAGC...		
viii.	HA ^C :	...TAC CCA TAC GAT GTT CCA GAT TAC GCT....		

EGFP^C: contained by pEGFP-N1; EGFP^N: contained by pEGFP-C1

Figure 3.10. DNA sequencing results of epitope-tagged GLP-1R constructs compared with the WTGLP-1R. Bases in italics represent the Kozak sequence. The start codon is identified by the single underline; the stop codon by a double underline and; the position and sequence of epitope tags by shaded boxes. The human GLP-1R cDNA sequence (1392 bases in total) without a start or stop codon (4-1389) is highlighted in bold font.

3.3 Results

3.3.1 Visualisation of EGFP-tagged GLP-1Rs in HEK293 cells

The EGFP-tagged GLP-1R constructs (GLP-1R-EGFP, HA-GLP-1R-EGFP and EGFP-GLP-1R-HA) generated in **Section 3.2** were transiently transfected into HEK293 cells using Lipofectamine 2000 as described in **Section 2.15**. In these constructs, a small HA-tag was present or absent at the opposite terminus of the receptor to the EGFP-tag (**Figure 3.10iii, v, vi**). At the same time, the WTGLP-1R and the EGFP-containing vectors pEGFP-N1 (used to generate GLP-1R-EGFP and HA-GLP-1R-EGFP) and pEGFP-C1 (used to generate EGFP-GLP-1R-HA) were also transiently expressed in HEK293 cells. Following transfection (30h), confocal imaging of cells with the constructs containing an EGFP-tag or EGFP alone (ie. EGFP-containing vectors) demonstrated clear EGFP-fluorescence, whereas cells transfected with the WTGLP-1R showed no fluorescence (**Figure 3.11a**). However, the fluorescence in the different transfectants demonstrated different subcellular distributions. The fluorescence of EGFP alone, expressed from either pEGFP-N1 or pEGFP-C1 were identical and showed a whole cell distribution including nuclear (**Figure 3.11, c & e**). The cells transiently expressing GLP-1R constructs containing a C-terminal EGFP-tag (GLP-1R-EGFP and HA-GLP-1R-EGFP) showed strong plasma membrane fluorescence and a relatively weak intracellular fluorescence (**Figure 3.11, b & d**). In contrast, confocal images of cells transfected with the EGFP-GLP-1R-HA showed intracellular EGFP-fluorescence, which lacked clear plasma membrane localization (**Figure 3.11f**).

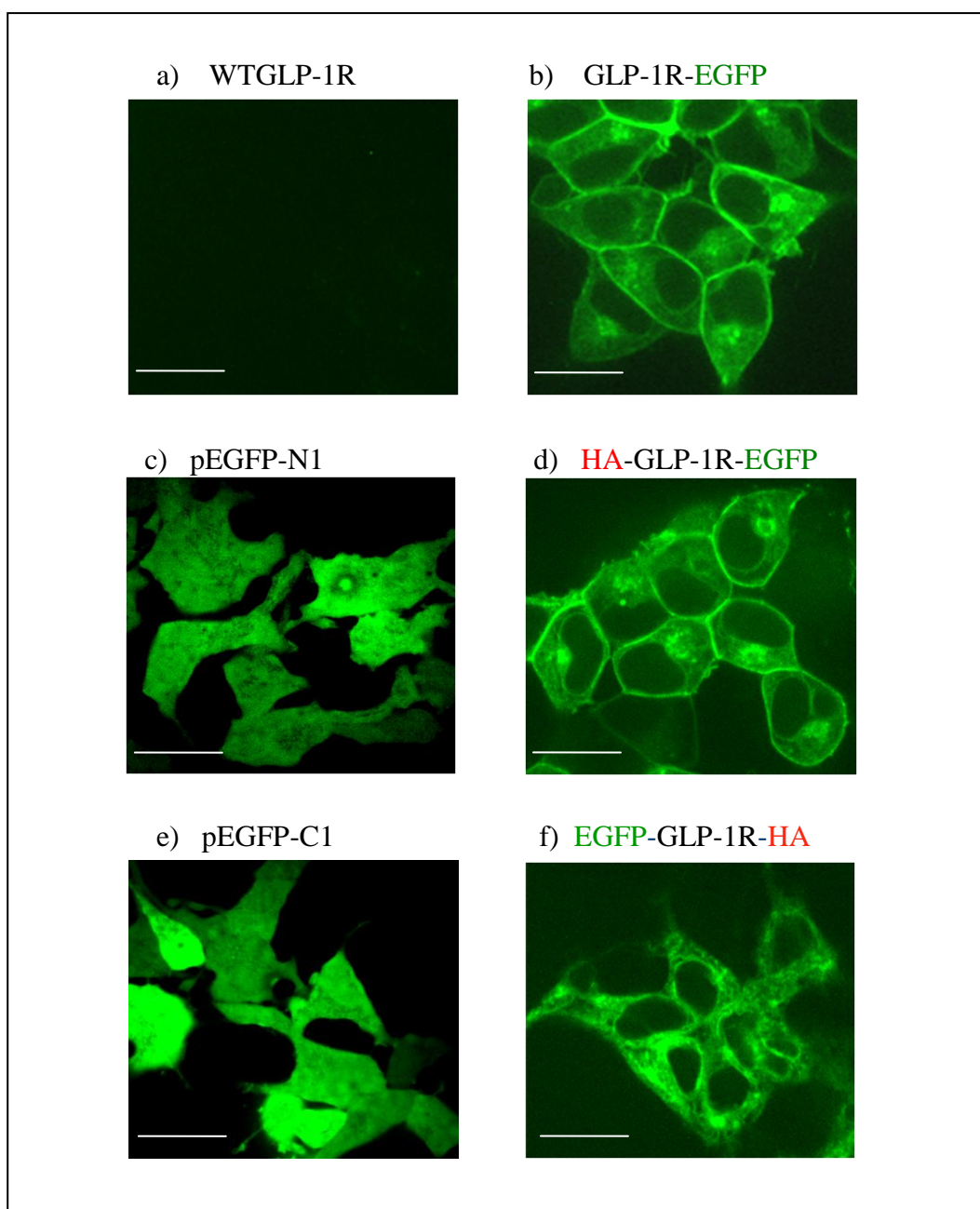


Figure 3.11. Confocal images of live cells with transient expression of GFP-tagged GLP-1Rs. HEK293 cells were transiently transfected with either WTGLP-1R (a), GFP-tagged GLP-1Rs (GLP-1R-GFP, b; HA-GLP-1R-GFP, d; and GFP-GLP-1R-HA, f) or GFP-containing vectors (pGFP-N1 and pGFP-C1). After 30h, live cells were imaged by confocal microscopy. Images are representative of cells observed in 5 independent experiments. Scale bar (in the bottom left of each image), 5 μ m.

3.3.2 Immunoreactivity of epitope-tagged GLP-1Rs

At 24-30h after transfection, whole-cell lysates were prepared from the HEK293 cells with transient expression of epitope-tagged GLP-1R constructs and subjected to immunoblotting using specific antibodies against the epitope-tags. In these constructs, either the HA-epitope or EGFP-epitope was attached to either the N- or C-terminus of the receptor sequence (**Figure 3.12a**). The pattern of immunoreactivity varied among the constructs and depended on the nature and localization of the epitope tag. All of the C-terminal tags were detected and showed two immunoreactive bands, except for the construct containing an N-terminal EGFP-tag (EGFP-GLP-1R-HA), which showed only one band. Thus, two bands at ~47kDa and ~64kDa were detected using an anti-HA antibody in lysates from cells transfected with the GLP-1R-HA construct (**Figure 3.12b, lane 2**). Both of these HA-immunoreactive bands were apparent as soon as the GLP-1R-HA became detectable by HA-immunoreactivity (6h after transfection) and were present until the last blot performed at 72h after transfection (data not shown). Thus, this two-band version was not a feature of a particular time following transient expression. Similarly, two bands at ~66kDa and ~93kDa were detected using an anti-GFP antibody in lysates from cells transfected with either the GLP-1R-EGFP (**Figure 3.12c, lane 3**) or HA-GLP-1R-EGFP (**Figure 3.12b, lane 5**) constructs. In contrast, no HA-immunoreactivity was observed in any construct containing an N-terminal HA-tag (HA-GLP-1R & HA-GLP-1R-EGFP; **Figure 3.12b, lane 4 & 5**) despite the presence of the receptor in the HA-GLP-1R-EGFP construct, which was demonstrated by the two bands of EGFP immunoreactivity and the EGFP-fluorescence in confocal imaging as described above (**Figure 3.12b, lane 5 & Figure 3.11d**). However, this was not the case when the EGFP-tag was at the N-terminus of the receptor (EGFP-GLP-1R-HA), in

which an HA-tag was also present at the C-terminus of the receptor (**Figure 3.12a**). In the lysates from cells transfected with this construct, only one immunoreactive band with a molecular size of ~66Da was detected by either anti-HA or anti-EGFP antibodies (**Figure 3.12b, lane 6 & c, land 6**). This band corresponded to the lower of the two bands (~66kDa and ~93kDa) observed in the construct containing both the HA-tag and EGFP-tag (HA-GLP-1R-EGFP, **Figure 3.12c, lane 5**). The same molecular size was predicted for these two constructs as the only difference between them was the location of the epitope tags. There was no evidence for the higher molecular size band in the EGFP-GLP-1R-HA construct using antibodies against either epitope-tag.

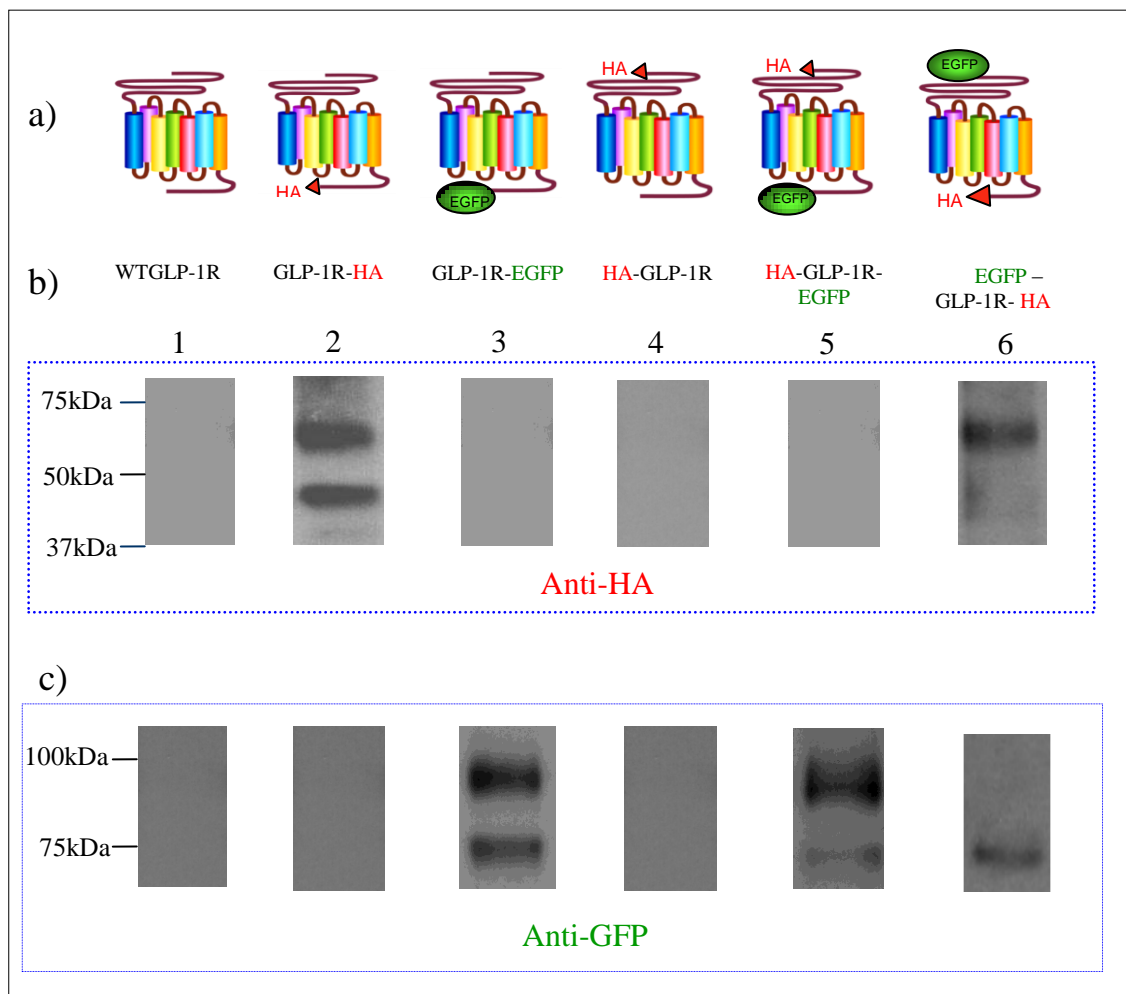


Figure 3.12. Immunoblotting of cell lysates following transfection of cells with GLP-1R constructs. HEK293 cells were transiently transfected with plasmids containing either the WTGLP-1R or various epitope-tagged constructs as indicated (a). After 24-30h, cell lysates were prepared and immunoblotted using either an anti-HA antibody (b) or an anti-GFP antibody (c). Data are representative of 3 independent experiments.

The predicted molecular size of the GLP-1R is ~53kDa, the HA-tag ~1kDa, and the EGFP-tag ~27kDa. The detection of two distinct immunoreactive bands when using antibodies against the C-terminal epitope tags in almost all GLP-1R constructs implied that these bands may represent different forms of the receptor, possibly differently glycosylated forms of the receptor. As described (**Section 3.1**), Endo H and PNGase F can remove *N*-glycans from glycoproteins differently. Endo H cleaves oligomannose or hybrid *N*-glycans (but not complex *N*-glycans) between the two core GlcNAc residues, whereas PNGase F cleaves all intact *N*-glycans between the innermost GlcNAc and asparagine residue (**Figure 3.1**). Consequently, whole-cell lysates from the cells with transient expression of the GLP-1R constructs containing either a C-terminal HA- or EGFP-tag, were treated with either Endo H or PNGase F (**Section 2.20**). These treatments altered the pattern of the immunoblots compared to that seen in untreated lysates. Thus, after treatment with Endo H, the molecular size of the lower band was reduced from ~47kDa to ~42Da (**Figure 3.13b, i, lane 2**) in GLP-1R-HA and from ~66kDa to ~52kDa in GLP-1R-EGFP, HA-GLP-1R-EGFP and EGFP-GLP-1R-HA (**Figure 3.13a i, lane 2 & ii, lane 2; Figure 3.13b, ii, lane 2**), whereas the position of the upper band (~64kDa in GLP-1R-HA and ~93kDa in both GLP-1R-EGFP and HA-GLP-1R-EGFP) was not affected. In contrast, treatment of cell lysates with PNGase F resulted in a loss of both bands in either HA- or EGFP-tagged receptors which were replaced by a single band (~42kDa in GLP-1R-HA and ~52kDa in GLP-1R-EGFP, HA-GLP-1R-EGFP and EGFP-GLP-1R-HA), (**Figure 3.13a, i, lane 3 & ii, lane 3; Figure 3.13b, i, lane 3 & ii, lane 3**).

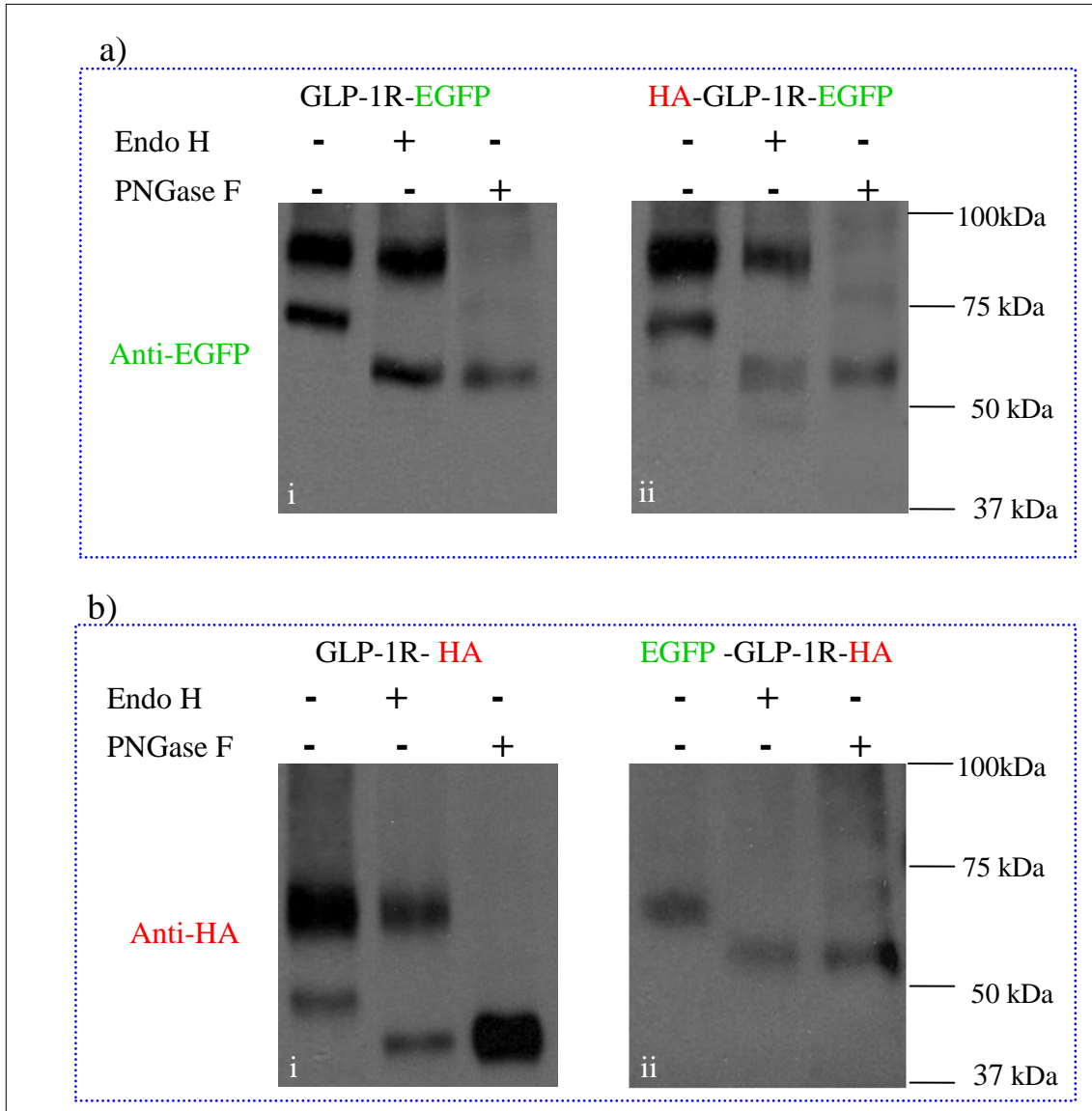


Figure 3.13. Glycosidase treatments of epitope-tagged GLP-1Rs. HEK293 cells were transiently transfected with plasmids containing epitope-tagged GLP-1Rs as indicated. After 30h, cell lysates were prepared and either untreated or treated with either Endo H or PNGase F. Immunoblotting was then carried out using either an anti-GFP (a) or anti-HA (b) antibody as indicated. Data are representative of 3 independent experiments.

3.3.3 Similar pharmacologic properties of epitope-tagged GLP-1Rs except EGFP-GLP-1R-HA in HEK293 cells

GLP-1-mediated cAMP generation was determined in HEK293 cells with transient expression of the GLP-1R constructs generated in **Section 3.2**. At 30h after transfection, the cells were challenged with GLP-1 7-36 amide at a range of concentrations from 100pM to 300nM and cAMP generation was assessed as described (**Section 2.24**). This revealed similar agonist effects at the WTGLP-1R and each construct containing an HA-tag at either terminus and/or an EGFP-tag at the C-terminus of the receptor. Thus, concentration-response curves and pEC_{50} values were similar for all of the constructs with the exception of EGFP-GLP-1R-HA (**Figure 3.14a, b, c, d & e; Table 3.1**). GLP-1 7-36 amide failed to elevate cAMP in the cells transiently transfected with this construct, (**Figure 3.14f**) even though the expression of a full-length receptor had been demonstrated by immunoblotting against its C-terminal HA-tag. It was interesting that the GLP-1 7-36 amide concentration-response curve obtained in cells transiently expressing HA-GLP-1R was similar to those seen in the other constructs despite the absence of HA-immunoreactivity in whole-cell lysates prepared from the same cells.

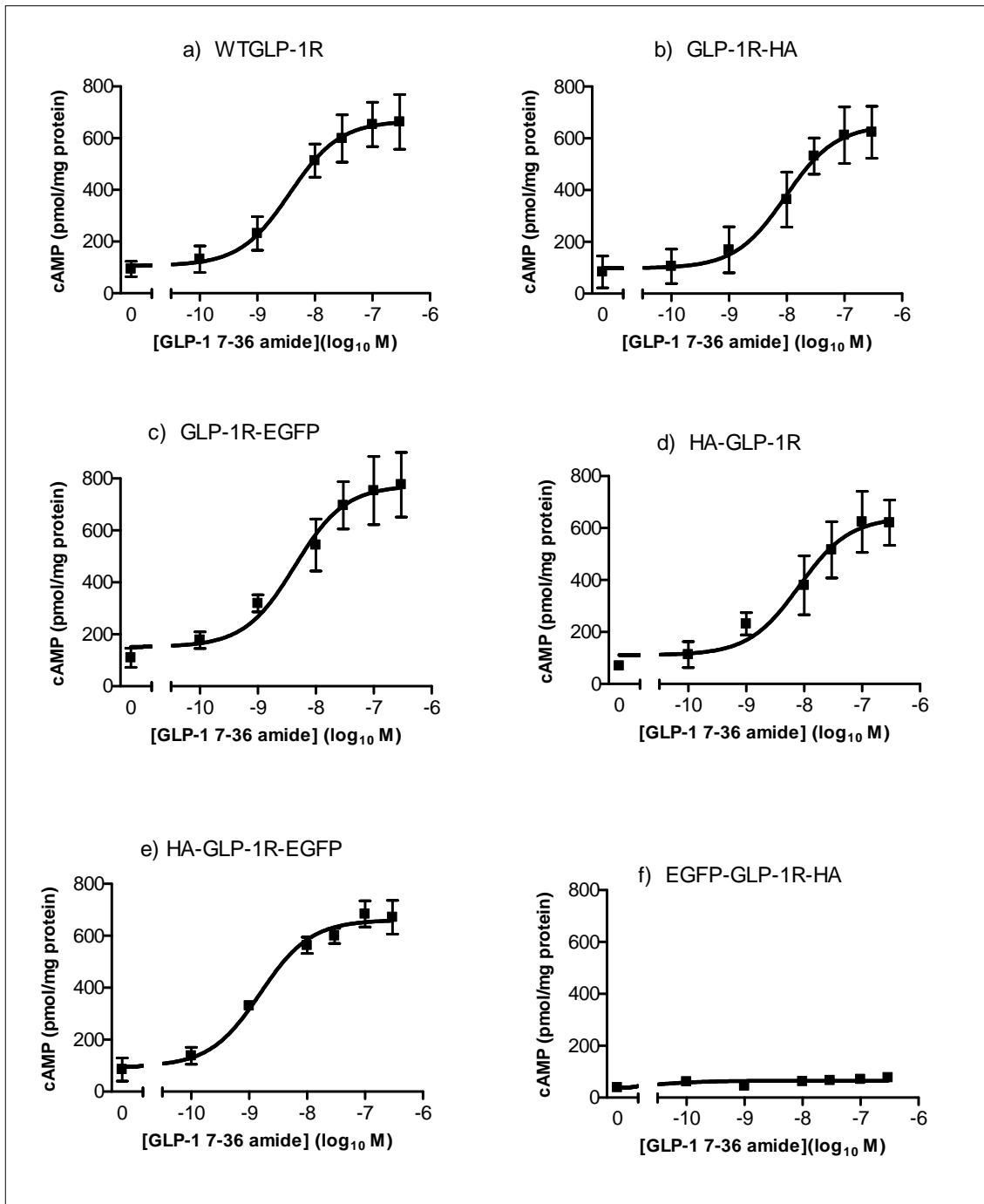


Figure 3.14. Functional coupling of GLP-1R constructs. HEK293 cells were transiently transfected with either WTGLP-1R or various epitope-tagged constructs as indicated. After 30h, cells were stimulated with GLP-1 7-36 amide for 10min at the concentrations indicated in the absence of IBMX and cAMP levels were determined. Data are mean±sem, n=3. pEC₅₀ values are indicated in **Table 3.1**.

Furthermore, ligand binding of the epitope-tagged GLP-1Rs were determined by performing homologous competition binding assays. These assays were kindly performed at AstraZeneca (Alderley Park, Macclesfield, U.K.) in membranes prepared from the cells at 30h after transfection. The binding affinity (K_D) of GLP-1 7-36 amide for each of all functional epitope-tagged GLP-1Rs was comparable to WTGLP-1R and in the low nM range (**Table 3.1**). In these cells with transient expression, the B_{max} value of the untagged GLP-1R (**Table 3.1**) was clearly higher than endogenous GLP-1Rs in pancreatic β -cells ($B_{max} = 180.3 \pm 38.7$ fmol/mg protein in rat; Sloop et al., 2004) or in cell lines with endogenously expressed GLP-1Rs (e.g. rat RINm5F insulinoma cells where the B_{max} has been reported as 65.4 ± 21.24 fmol/mg protein; Göke et al., 1992). Importantly, however, there were no significant differences in B_{max} values between the untagged and tagged receptors ($p > 0.05$, by Dunnett's test following one-way ANOVA), providing some evidence that this epitope tagging did not affect the ability of these cells to express the GLP-1R. Further, both the binding affinity and potency for cAMP generation were unaffected by tagging (**Table 3.1**), highlighting a lack of effect of the presence of the epitope tags on either ligand binding or receptor coupling. Not surprisingly, there was no detectable binding in the membranes prepared from the cells transfected with the EGFP-GLP-1R-HA construct. This was consistent with the lack of plasma membrane located EGFP-fluorescence, the lack of a fully glycosylated immunoreactive band and the absence of GLP-1 7-36 amide-mediated cAMP production.

Table 3.1. Agonist potency and affinity estimates of the GLP-1R constructs

	WTGLP-1R	GLP-1R-HA	GLP-1R-EGFP	HA-GLP-1R	HA-GLP-1R-EGFP
pEC ₅₀	8.46±0.12	8.03±0.07	8.34±0.05	8.13±0.18	8.69±0.16
pK _D	8.71±0.34	8.06±0.14	8.45±0.38	7.83±0.03	8.09±0.05
B _{max} (pmol/mg protein)	24.85±2.80	20.05±3.90	21.34±4.56	19.51±0.69	22.21±3.17

Potency estimates represented by pEC₅₀ values were derived for GLP-1 7-36 amide-mediated cAMP generation in intact cells transiently transfected with the indicated GLP-1R constructs. pK_D values represent affinity estimates of GLP-1 7-36 amide, which were determined in membranes prepared from cells using homologous competition binding assays. Data are mean±sem, n=3.

3.3.4 *Stable expression of GLP-1R-EGFP in HEK293 cells*

Evidence obtained from the experiments based on transient expression revealed that the presence of EGFP-tag at the C-terminus of the receptor (HA-GLP-EGFP and GLP-1R-EGFP) did not affect the *N*-linked glycosylation, plasma membrane localization, agonist affinity or functional coupling of the receptors. In addition, *N*-terminal HA-tags were not detectable in immunoblotting and their presence in the construct did not affect the properties of the receptors. Consequently, the GLP-1R-EGFP construct was used for developing a stable cell line. After transfection, twenty G418-resistant clones were obtained after 20 days of G418 (1 µg/mL) selection (**Section 2.16**), among which, there were 14 clones showing EGFP-fluorescence in living cells. However, one clone (clone 15) was distinct by showing EGFP-fluorescence in all viable cells. This clone was referred to as HEK293: GLP-1R-EGFP and grown and stored in a relative large scale. At the same time, stable transfected clones with the vector of pEGFP-N1 were selected by EGFP-fluorescence to generate the control cell line (clone 28) and referred to as HEK293:EGFP.

A labdane diterpene, FSK is commonly used to raise cAMP levels in both intact cells and membranes as it is able to activate adenylate cyclase (AC) in a G-protein-independent manner. Thus, in the functional assessment of cAMP production, FSK was used as a control in both parental (HEK293) and established (HEK293:GLP-1R-EGFP and HEK293:EGFP) cell lines. As expected, only HEK293:GLP-1R-EGFP cells generated cAMP production in response to GLP-1 7-36 amide (100nM) while FSK-induced cAMP was detectable in all cell lines (**Figure 3.15**).

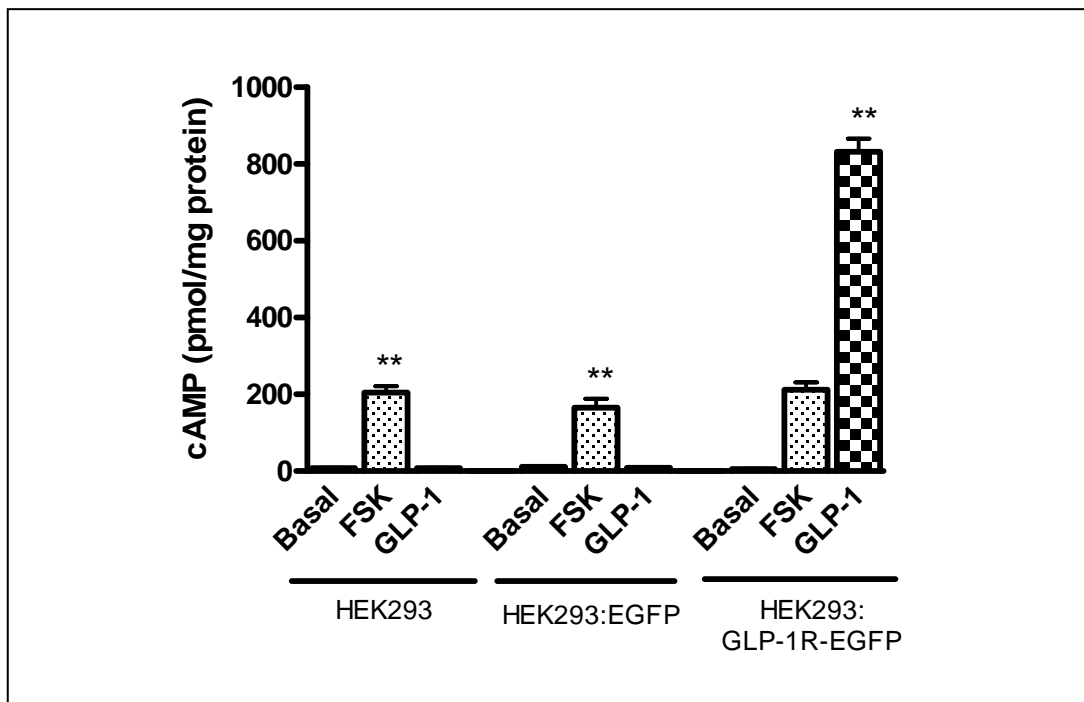


Figure 3.15. GLP-1 induced cAMP generation in HEK293:GLP-1R-EGFP cells but neither in wild-type HEK293 nor HEK293:EGFP cells. Intact cells with stable expression of GLP-1R-EGFP (HEK293:GLP-1R-EGFP) or EGFP (HEK293:EGFP) were challenged with either 10 μ M forskolin (FSK) or 100nM GLP-1 7-36 amide (GLP-1) in the presence of IBMX (500 μ M) for 10min at 37°C and levels of intracellular cAMP were determined relative to the cellular protein content. **, $p < 0.05$, by Dunnett's test following one-way ANOVA. Data are mean+sem, n=3.

Consistent with HEK293 cells transiently expressing GLP-1R-EGFP, confocal imaging of HEK-GLP-1R-EGFP cells demonstrated that the receptor was located predominantly at the plasma membrane, with intense, continuous EGFP-fluorescence while intracellular fluorescence was relatively weak (**Figure 3.16a, i, in green**). This was distinct from that in stable HEK293:EGFP cells, which showed a typical whole cell distribution of fluorescence (**Figure 3.16b, i, in green**). Trypan blue is excluded by viable cells and becomes fluorescent in the far-red region of the spectra (600–720nm) once bound to some (but not all) proteins. This fluorescence has minimal overlap with EGFP-fluorescence (Mosiman et al., 1997). Therefore, trypan blue was used as a plasma membrane marker in intact cells to identify the cell surface of the same cells visualized for EGFP-fluorescence (**Figure 3.16a, ii & b, ii in red**). Co-localization is demonstrated by yellow in stable HEK293:GLP-1R-EGFP cells (**Figure 3.16a, iii**) but by orange in HEK293:EGFP indicating a relatively low EGFP-fluorescence in the overlap region (**Figure 3.16b, iii**).

Ligand binding affinity at the receptor expressed in the HEK293:GLP-1R stable cell line was similar to that in the HEK293Flp-In cell line with stable expression of the WTGLP-1R (HEK293Flp-In:WTGLP-1R, generated by AstraZeneca, Alderley Park, U.K.). This was based on homologous competition binding assays performed in cell membranes prepared from these two cell lines, which resulted in comparable K_D and B_{max} values of the two cell lines (**Figure 3.17**). Parallel experiments to measure GLP-1 7-36 amide-mediated cAMP elevation revealed similar potencies of GLP-1 7-36 amide (**Figure 3.18**) although the E_{max} values were lower in the HEK293:GLP-1R-EGFP cell line (868 ± 20 pmol/mg protein, $53 \pm 1.2\%$ of those in the HEK293Flp-In:WTGLP-1R cell line).

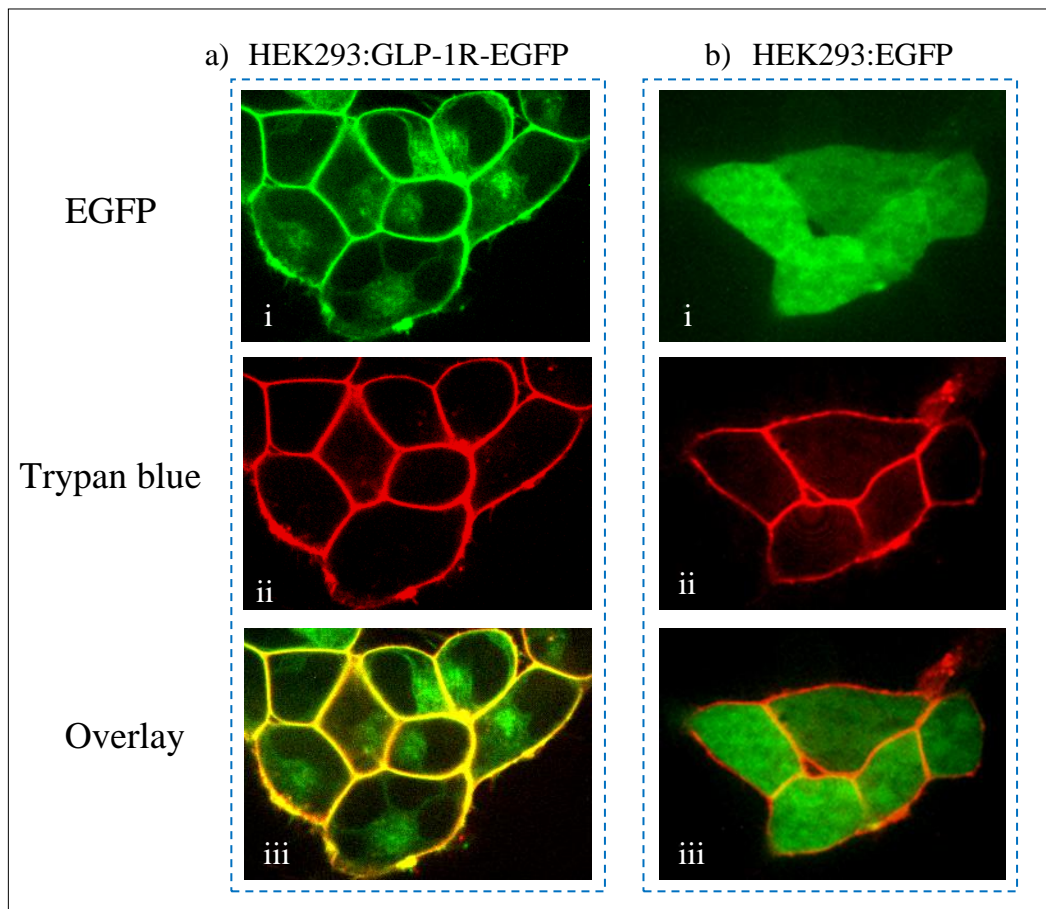


Figure 3.16. Confocal images of live cells with stable expression of the C-terminal EGFP-tagged GLP-1R or EGFP. GLP-1R-EGFP (a) or EGFP (b) were stably expressed in HEK293 cells. The EGFP fluorescence signals are shown in green (a, i & b, i); the cell membrane was stained with trypan blue and is shown in red (a, ii & b, ii) and; EGFP and trypan blue fluorescence signals were computer-overlaid (a, iii & b, iii). Images represent 3 independent experiments.

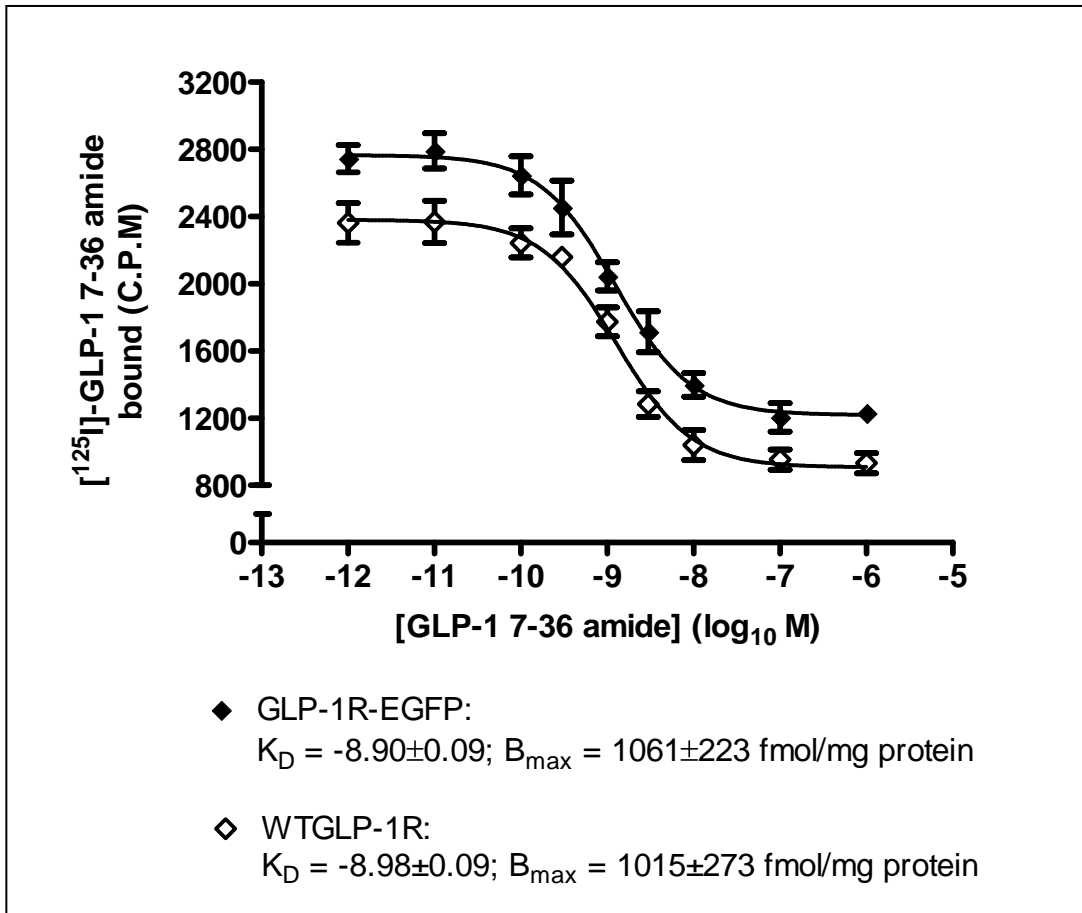


Figure 3.17. Homologous competition binding of GLP-1 7-36 amide to stably expressed WTGLP-1R and GLP-1R-EGFP. Cell membranes were prepared from HEK293Flp-In:WTGLP-1R and HEK293:GLP-1R-EGFP cells, in which WTGLP-1R or GLP-1R-EGFP were stably expressed respectively. After incubating the cell membranes with [¹²⁵I]-GLP1 7-36 amide (final concentration 0.1nM) and GLP-1 7-36 amide at a range of concentrations as indicated, at room temperature for 3h, the total level of bound [¹²⁵I]-GLP1 7-36 amide was determined by counting [¹²⁵I]-radioactivity (CPM) on a gamma counter. K_D and B_{max} values were then determined by homologous competition binding as described in **Section 2.25.1**. Data are mean±sem, n=3.

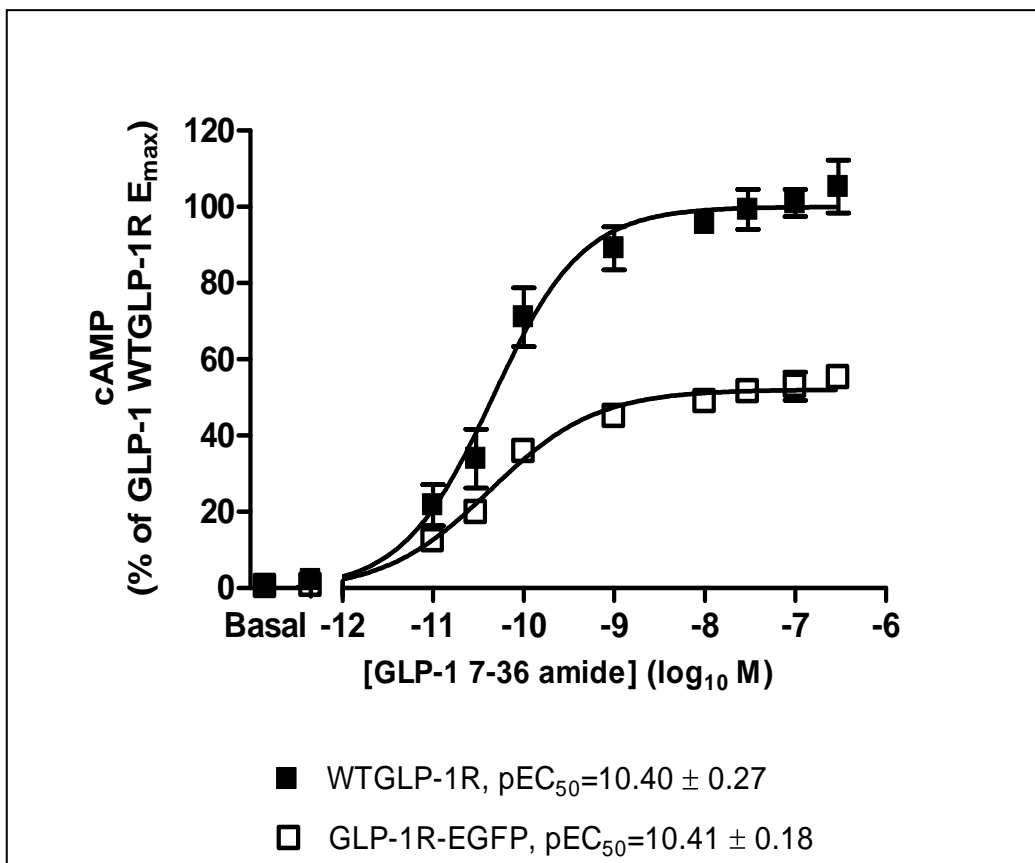


Figure 3.18. Functional coupling of stably expressed WTGLP-1R and GLP-1R-EGFP. HEK293Flp-In:WTGLP-1R or HEK293:GLP-1R-EGFP cells were challenged with GLP-1 7-36 amide at the concentrations indicated for 10min at 37°C in the presence of IBMX (500µM). Levels of intracellular cAMP were determined as a percentage relative to the E_{max} of the WTGLP-1R (1638±66 pmol/mg protein). pEC₅₀ values are indicated. Data are mean±sem. n=3.

3.3.5 *Cell surface expression of the GLP-1R-EGFP requires N-linked glycosylation*

Similarly to transient expression, immunoblotting performed on lysates prepared from cells with stable expression of the GLP-1R-EGFP construct gave the typical two-band pattern (~66kDa and ~93kDa; **Figure 3.19a, i, lane 2**). Furthermore, Endo-H or PNGase digestion altered this pattern (**Figure 3.13b, i, lane 2& 3 and Figure 3.19a, i, lane 3 & 4**). Cell surface proteins in intact HEK293:GLP-1R-EGFP cells were biotinylated. This was followed by preparation of the cell lysates and thus biotinylated cell surface proteins could be isolated from other cell fragments (**Section 2.18**). Immunoblotting with an anti-GFP antibody only detected one band (~93kDa) in the biotinylated cell surface proteins of the HEK293:GLP-1R-EGFP cell line (**Figure 3.19a, i, lane 1**). The size of this band was identical to the band with the high molecular size of the two bands observed in immunoblots of whole lysates prepared from the same cells (compare **Figure 3.19a, i, lane 1** with **lane 2**). Thus, the plasma membrane only contained the fully glycosylated mature form of the receptor (**Figure 3.19a, i, lane 3 & 4**).

Tunicamycin is often used as a glycosylation inhibitor (Varki et al., 2009). Thus, HEK293: GLP-1R-EGFP cells were treated with tunicamycin to block *N*-linked glycosylation. In these experiments, the concentration of tunicamycin was increased progressively (**Section 2.21**) to prevent cell death, which occurred on immediate exposure to higher concentrations (Data not shown). Following this treatment with progressively greater concentrations of tunicamycin, only one immunoreactive band of ~66kDa was detected, which was coincident with the lower of the two bands seen in

untreated HEK293: GLP-1R-EGFP cells (compare **Figure 3.19b, i, lane 1** with **Figure 3.19a, i, lane 2**). However, the molecular size of this band at ~66kDa was reduced to ~52kDa when whole cell lysates from tunicamycin-treated HEK293:GLP-1R-EGFP cells were treated with either Endo H or PNGase F (**Figure 3.19b, i, lanes 2 and 3**). Confocal imaging of tunicamycin-treated HEK293:GLP-1R-EGFP cells showed the intracellularly localised EGFP fluorescence with a lack of cell surface fluorescence observed in untreated HEK293:GLP-1R-EGFP cells (compare **Figure 3.19a, ii** with **b, ii**).

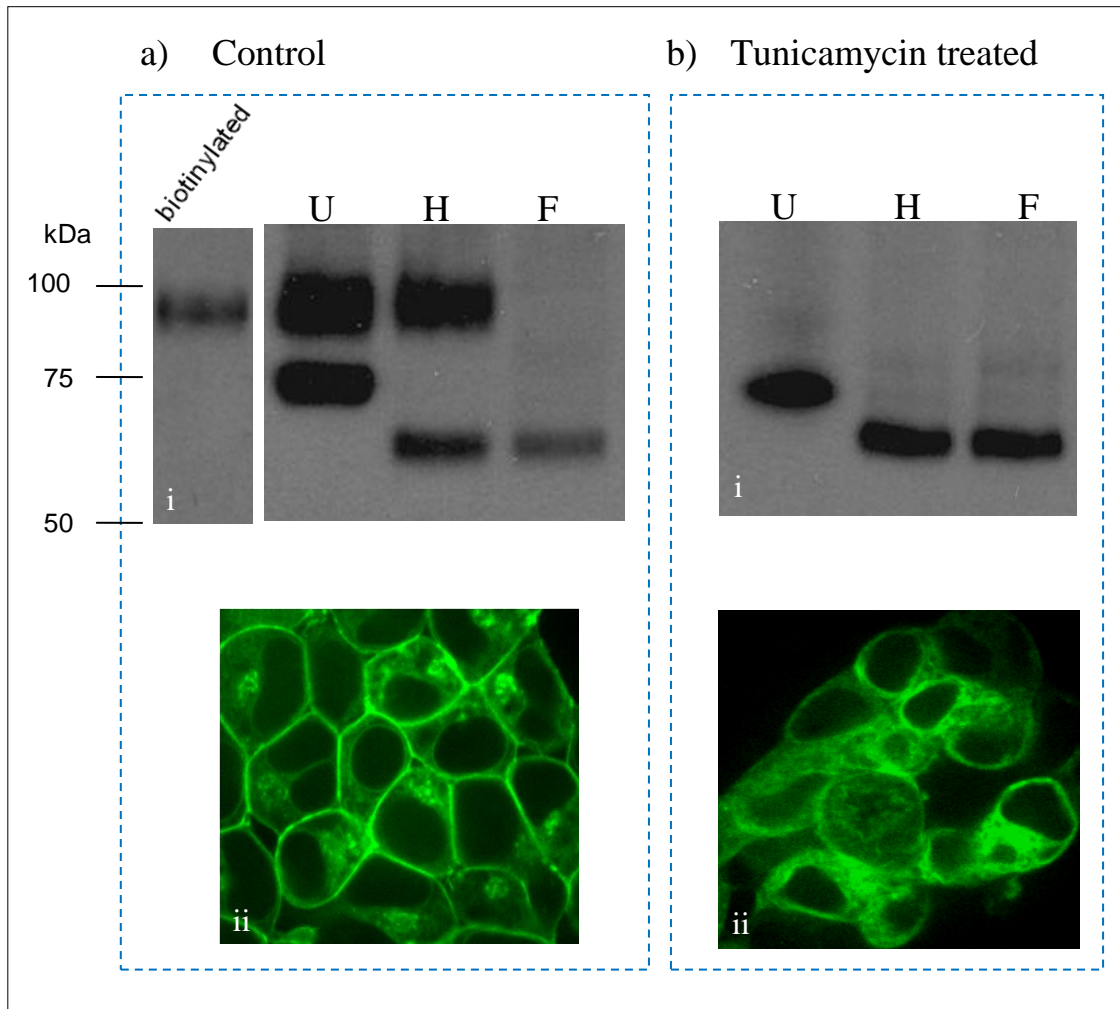


Figure 3.19. Influence of tunicamycin treatment on the immunoblotting pattern and subcellular distribution of the GLP-1R. HEK293:GLP-1R-EGFP cells were either untreated (Control, a) or treated with tunicamycin (0.1 μ g/mL for 80h, 0.2 μ g/mL for 60h and 0.4 μ g/mL for a further 40h) (b). Cells were then imaged by confocal microscopy (a, ii and b, ii). Cell lysates prepared from the same cells were subjected to treatment with either Endo H (H), PNGase F (F) or vehicle (U, lysate buffer). Immunoblotting was then performed using an anti-GFP antibody (a, i and b, i). Alternatively, proteins at the plasma membrane of intact HEK293:GLP-1R-EGFP cells without the treatment of tunicamycin were biotinylated, captured using streptavidin and subjected to immunoblotting using the anti-GFP antibody (a, i; “biotinylated”). Data are representative of 3 independent experiments.

3.4 Discussion

In this chapter, a range of different epitope-tagged GLP-1Rs were generated and transiently or stably expressed in HEK293 cells to examine the immunoblotting pattern and subcellular distribution of the GLP-1R and potential *N*-linked glycosylation. Evidence here demonstrates that recombinant over expression of the GLP-1R in HEK293 cells is predominantly located at the plasma membrane. The receptor shows a two-band pattern of immunoreactivity, which represent different *N*-linked glycosylation states. Furthermore, the plasma membrane only contains the fully glycosylated, mature form of the receptor, which is represented by the upper band of the two immunoreactive bands detected in immunoblots. In contrast, an immature form of the receptor resulted from N-terminal EGFP-tagging was detected in immunoblotting as a band consistent with the lower of the two bands seen with the C-terminally EGFP-tagged receptor. This immature form lacked the plasma membrane localization and was not detectable in assays of ligand binding and receptor function. In addition, blocking *N*-linked glycosylation abolishes receptor maturation and plasma membrane localization. Key findings presented here suggest that, after the initial *N*-linked glycosylation in the ER, the GLP-1R is fully glycosylated during trafficking through the Golgi complex. Only the fully glycosylated mature form of receptor is able to reach the functional destination, the plasma membrane.

3.4.1 Expression profile of the GLP-1R in HEK293 revealed by different epitope-tagged constructs

As presented in this chapter, the transient or stable expression of the different epitope-tagged GLP-1R constructs in HEK293 cells not only allowed detection of receptor expression by using antibodies against the different epitope tags but also enabled various comparisons between epitope-tagged receptors and the wild-type receptor. Immunoblotting of total cell lysates from fully functional C-terminal epitope-tagged GLP-1Rs revealed two distinct immunoreactive bands with molecular sizes of ~66kDa and ~93kDa by using an anti-GFP antibody (for GLP-1R-EGFP and HA-GLP-1R-EGFP) and bands of ~47kDa and ~64kDa using an anti-HA antibody (for GLP-1R-HA). This two-band immunoreactivity pattern from three different constructs detected by different specific antibodies suggests that they are not due to nonspecific binding. Furthermore, this two-band immunoreactivity pattern was altered by glycosidase treatments indicating these two bands represent the GLP-1R protein with different *N*-glycans. Endo H can remove oligomannose (formed by initial glycosylation in the ER) or hybrid *N*-glycans (formed in Golgi but based on those oligomannoses which cannot form complex *N*-glycans) but not complex *N*-glycans. However, PNGase F is able to deglycosylate all *N*-glycans including complex *N*-glycans formed in trans-Golgi cisternae. Thus the upper of the two bands represents the fully glycosylated mature form of the receptor as it was only deglycosylated by PNGase F but resistant to Endo H. In contrast, the lower of the two bands was reduced by either Endo H or PNGase F treatment and hence represents the initially glycosylated, immature form of the receptor. Although different from the one immunoreactive band version detected in previous studies (Widmann et al, 1995; Vahl et al, 2007, Shu et al., 2009), these data are consistent with that of the rat GLP-1R expressed recombinantly in CCL39 fibroblasts (Widmann et al., 1995) and insulinoma cells (Widmann et al., 1996). Interestingly, the

similar pattern of immunoreactivity observed in both of these previous studies relied on two specific antibodies prepared in rabbit against the N-terminal tail (corresponding to amino acids 19-145) or the C-terminal tail (corresponding to amino acids 407-463) of rat GLP-1R (Widmann et al., 1995). However, this two-band immunoreactivity pattern almost never appears again or has been ignored in studies using other specific antibodies against either a certain region of the GLP-1R protein or an epitope tag (Salapatek et al., 1999; Xiao et al., 2000; Vázquez et al., 2005b; Syme et al., 2006; Kumar et al., 2007; Vahl et al., 2007; Schlatter et al., 2007; Zhang et al., 2009; Shu et al., 2009). As immunodetection was only performed in a recombinant system in the present study, it is not possible to state definitively that the two-band pattern is not a consequence of receptor over-expression. However, many GPCRs are subject to post-translational glycosylation and the GLP-1R contains a number of asparagine residues in glycosylation sequons suggesting that glycosylation (and the two-band pattern of immunoreactivity) would not be a unique feature of recombinantly over-expressed GLP-1Rs. Further, the endogenously expressed GLP-1R in rat 1056A insulinoma cells and rat pancreatic β -cells also shows a two-band pattern of immunoreactivity (Widmann et al., 1995; 1996), although to date this has not been demonstrated for receptors from human β -cells.

Consistent with the C-terminally GFP-tagged GLP-1Rs made previously (Salapatek et al., 1999; Xiao et al., 2000; Syme et al., 2006), both GLP-1R-EGFP and HA-GLP-1R-EGFP revealed strong fluorescence at the cell surface and also some minor fluorescence in intracellular compartments when expressed in HEK293 cells. This localization pattern of the GLP-1R is similar to that displayed in human pancreatic β -cells (Tornehave et al., 2008). However, in the latter study, localization was detected by

a fluorescence microscopy and not confocal imaging, so identification of the subcellular distribution is more problematic. More importantly, all the epitope-tagged receptors that showed a two-band pattern of immunoreactivity in the present study demonstrated similar ligand affinity and agonist potency to the WTGLP-1R. Consequently, the data shown here suggest that: a) the GLP-1R can be detected as two forms, an immature form and the fully glycosylated mature form; b) N-terminal HA-tagged receptors are not detected by HA-immunoreactivity despite good functional expression and; c) both GLP-1R-HA and visible GLP-1R-EGFP are ideal tools for investigating receptor expression, trafficking and signalling of the GLP-1R because of their strong epitope tag-immunoreactivities and the generation of functional receptors. There was a lower E_{\max} for cAMP generation in cells with stable expression of the C-terminal EGFP-tagged GLP-1R compared to that seen in cells with stable expression of the untagged (wild-type) GLP-1R, which was not observed in the cells with the transient expression of the same construct. Whether this is a consequence of clonal differences or some other reason is unclear. Certainly the pK_D , B_{\max} and pEC_{50} values in the stable HEK293:GLP-1R were comparable to those in the cell line with stable expression of the untagged GLP-1R suggesting that the EGFP-tagging had not had a major impact on receptor expression, affinity and efficacy.

3.4.2 The role of N-linked glycosylation in the trafficking of GLP-1R

The export of GPCRs from the ER to the plasma membrane is critical for producing functional, membrane-bound receptors (Conn et al., 2010). The expression level of membrane-bound receptors dictates agonist sensitivity and potentially the magnitude of cellular responses. Compared with the extensive studies on mechanisms of ligand

binding, G-protein coupling, desensitization, and internalization, molecular mechanisms underlying the export processes of GPCRs from the ER to the cell surface and regulation of receptor signalling by these processes are relatively less well understood (Duvernay et al., 2005). The life of GPCRs begins at the ER where they are synthesised, folded and assembled. Properly folded receptors are recruited into ER-derived vesicles and start trafficking through the Golgi apparatus to the plasma membrane. Although it is well recognised that most GPCRs undergo co-translational glycosylation in the ER and are further post-translationally glycosylated during trafficking (Strader et al., 1994), the role of such glycosylation in exporting the receptor to the cell surface may vary considerably. In Family A GPCRs, *N*-linked glycosylation has been shown to play an important role in appropriate membrane trafficking of, for example, the β -adrenoceptor (Rands et al., 1990), AT1a angiotensin II receptor (Deslauriers et al., 1999; Lanctot et al., 2005; Shukla et al., 2006), thyrotropin receptor (Nagayama et al., 2000), follicle-stimulating hormone receptor (Davis et al., 1995; Guan et al., 2010) and the relaxin receptor (Kern et al., 2007). However, mutation of all putative *N*-linked glycosylation sites in the α_1 -adrenoceptor, H₂ histamine receptor, M₂-muscarinic receptor and the neuropeptide S receptor does not significantly influence cell surface expression (Fukushima et al., 1995; van Koppen and Nathanson, 1990; Sawutz et al., 1987; Clark et al., 2010). In addition, glycosylation of the neurokinin 1 receptor and bradykinin B₂ receptor stabilize them at the plasma membrane despite not being an absolute requirement for receptor exportation (Tansky et al., 2007; Michineau et al., 2006). In Family B GPCRs, the role of glycosylation seems more complicated. For example, several previous studies suggest that for the secretin receptor, the corticotropin-releasing factor receptor type 1, PTH/PTHrP receptor, the calcitonin receptor and the calcitonin

receptor-like receptor, *N*-linked glycosylation at one of the consensus sites is sufficient to ensure correct delivery of the receptor to the plasma membrane. Thus, single or even combined mutations at glycosylation sites does not alter either cell surface expression or function despite impaired glycosylation. In contrast, the non-glycosylated receptor, in which all *N*-linked glycosylation sites are blocked, is deficient in these functions (Pang et al., 1999; Assil and Abou-Samra, 2001; Zhou et al., 2000; Davidson et al., 1995; Ho et al., 1999; Buhlmann et al., 2000). In addition, for most of these receptors, deglycosylation decreases ligand binding or influences ligand specificity without decreasing cell surface expression, suggesting glycosylation is important for attaining an appropriate structure of the receptor rather than cell surface expression (Pang et al., 1999; Zhou et al., 2000; Ho et al., 1999; Buhlmann et al., 2000; Kamitani and Sakata, 2001).

In the present study, the biotinylated cell surface proteins from cells with stable expression of the C-terminally EGFP-tagged GLP-1R (HEK293:GLP-1R-EGFP) revealed a single immunoreactive band (~93kDa). This band corresponded to the upper of the two bands (~66kDa and ~93kDa) detected in total cell lysates from the same cells, suggesting that only the fully glycosylated mature form of the GLP-1R is able to traffic to the cell surface. This finding argues against a previous study, in which both bands were located at the plasma membrane despite the absence of the upper band in the cytosolic fraction (Widmann et al., 1995). The sucrose step gradients used to separate the plasma membrane and cytosolic fractions in that study may have caused the difference. It might, for example, be difficult to separate the plasma membrane fraction without contamination of the soluble cytosolic fraction. N-terminal EGFP-tagged GLP-1R (EGFP-GLP-1R-HA) also revealed a single immunoreactive band (~66kDa) but this

corresponded to the lower of the two EGFP-immunoreactive bands (~66kDa and ~93kDa) observed with HA-GLP-1R-EGFP. The single immunoreactive band was detected by an antibody against the C-terminal HA-tag and deglycosylated by either Endo H or PNGase F suggesting that this band represented a full-length but immature form of the receptor. In addition, this N-terminal EGFP-tagged GLP-1R was not functional, implying the functional receptor must be in a fully glycosylated mature form and represented by the higher band (~93kDa in EGFP-tagged GLP-1Rs and ~64kDa in the GLP-1R-HA). This finding agrees with a radioautographic demonstration showing the GLP-1R and GLP-1 binding complex at ~66kDa in mammalian expression systems (Widmann et al., 1995; Xiao et al., 2000; Vázquez et al., 2005a; Chen et al., 2009), in which the predicted molecular size of the GLP-1R is ~53kDa and GLP-1 represents 3.5kDa. Furthermore, there is no evidence showing this non-functional EGFP-GLP-1R-HA is located at the plasma membrane. Similarly, tunicamycin treatment of these stable HEK293:GLP-1R-EGFP cells to block *N*-linked glycosylation not only resulted in a lack of the upper immunoreactive band but also altered the subcellular pattern of fluorescence of the C-terminal EGFP-tagged GLP-1R, converting it into an intracellular distribution. Taken together, these data demonstrate that the GLP-1Rs expressed at the plasma membrane are fully glycosylated and functional; blocking the initially glycosylated GLP-1R from further glycoosylation results in intracellularly located receptors. Therefore, *N*-linked glycoosylation is essential for the cell surface expression of the GLP-1R. Compared with other members of Family B GPCRs, this finding is in line with the secretin receptors and the calcitonin receptor-like receptors, in which inhibition of *N*-linked glycoosylation by tunicamycin impaired their trafficking to the cell surface (Pang et al., 1999; Buhlmann et al., 2000) but opposite to the PTH/PTHrP

receptors and the calcitonin receptors, in which tunicamycin treatment had no effect on receptor expression at the cell surface (Bisello et al., 1996; Zhou et al., 2000; Ho et al., 1999).

In the present study, the initially glycosylated immature form of EGFP-GLP-1R-HA, represented by the lower of the two immunoreactive bands, was not expressed at the plasma membrane and was therefore not functional. This is supported by a recent study, in which the expression of an N-terminally EGFP-tagged GLP-1R in CHO cells is detected mainly at ~70kDa by an anti-GFP antibody and located intracellularly with a lack of cell surface fluorescence (Bavec and Ličar, 2009). Interestingly, in this recent study, the expression of GFP-GLP-1R in Rin m5F cells (naturally expressing the GLP-1R) dramatically increased insulin release in response to GLP-1 although this receptor showed both low ligand affinity and poor GLP-1-mediated cAMP production in CHO cells. Composing this with the findings of the present study, the implication is that the immature form of the receptor may either directly contribute to β -cell signalling or be processed quickly in certain cellular environment e.g. β -cells.

3.4.3 Tunicamycin treatment for inhibiting N-linked glycosylation

N-glycans are initially synthesized by sequentially adding fourteen sugars to a lipid-like molecule termed dolichol phosphate (Dol-P) and followed by ‘en-bloc’ transfer of the entire glycan to an Asn-X-Ser/Thr sequon in a protein. The first step in the formation of the core oligosaccharide is the addition of *N*-acetylglucosamine to Dol-P, which is catalyzed by *N*-acetylglucosaminyl phosphate transferase (GPT). Since GPT is sensitive to tunicamycin, the latter is widely used both *in vitro* and *in vivo* to block *N*-linked glycosylation at the first step (Elbein, 1987; Zhang et al., 2007; Nakagawa et al.,

2009; Roy et al., 2010). However, there are several caveats that have been considered in assessment of receptor glycosylation using tunicamycin treatment. Firstly, tunicamycin may inhibit protein synthesis in some cells (Reed et al., 1981; Nakajima et al., 2010). Secondly, the amount of tunicamycin required to prevent glycosylation varies depending on the cell type, media used for growth, the age or growth phase of the cells and length of exposure. Thus, the concentration of tunicamycin used to treat cultured eukaryotic cells or tissue slices is in a large range (0.1 to 10 μ g/mL) (Elbein, 1987). Thirdly, tunicamycin might be cytotoxic, especially in cells with transient transfection (Olden et al., 1979; Duksin et al., 1982; Seilberg and Duksin, 1983). Lastly, tunicamycin treatment of stable cell lines will prevent glycosylation of newly synthesised receptor without affecting the glycosylation of receptors that are already located at the plasma membrane (Zhou et al., 2000). Consequently, in the present study, a strategy of progressively increasing concentrations (0.1-2 μ g) of tunicamycin with a relative long exposure (160h) was explored for preventing glycosylation in cells with stable expression of the C-terminal EGFP-tagged GLP-1R (HEK293:GLP-1R-EGFP). Unexpectedly, this tunicamycin treatment allowed formation of the initially glycosylated GLP-1Rs since these receptors were sensitive to either Endo H or PNGase F as assessed by immunoblotting. One of the possible reasons might be that the concentration of tunicamycin used for treating the cells was not sufficient to inhibit GPTs, which catalyse the first step in the biosynthesis of glycosylation precursors; hence the glycan is added to newly synthesised proteins. However, the route from the initial glycosylation precursors to complex *N*-glycans involves a number of enzymes (Burda and Aebi, 1999) and hence this long exposure to tunicamycin may affect certain enzymes or substrates required for full glycosylation.

Glycosylation of proteins, including GPCRs, may be problematic for structural biology as they often require glycosylation in order to fold correctly but the presence of glycan generally inhibits crystallization (Davis et al., 1993; Kwong et al., 1999; Lee et al., 2009). Thus, a solution may be to generate glycosylated proteins and then remove the attached glycans by glycosidase. As mentioned above, PNGase F cleaves complex *N*-glycans completely without leaving any residue (**Figure 3.1**). However PNGase-treated proteins tend to aggregate (Davis et al., 1995). Unlike this, Endo H removes *N*-glycans but leaves a single GlcNAc residue at each glycosylation site. Thus, Endo H-sensitive, initially glycosylated proteins are required for crystallization (Davis et al., 1993; Kwong et al., 1999). Almost all strategies used to generate Endo H-sensitive glycoproteins require expression of a construct encoding the protein of interest in a certain expression system (Dukkipati et al., 2008; Lee et al., 2009). Hence, already established stable mammalian cell lines cannot readily implement this task (Chang et al., 2007). The approach of tunicamycin treatment used in the present study generated Endo-H-sensitive initially glycosylated GLP-1Rs from a stable cell line based on HEK293, which may provide a starting point to utilize already established stable mammalian cell lines for generating GPCR proteins suitable for crystallization.

CHAPTER 4 The Signal Peptide of the GLP-1R

4.1 Introduction

GPCRs account for almost one third of all human membrane proteins (attached to, or associated with the membrane of a cell or an organelle) and two thirds of receptors (Almén et al., 2009). Although all proteins are synthesized (or translated) by ribosomes using the information encoded in molecules of messenger RNA (mRNA), ribosomes perform this translation process by two main pathways: in the cytosol and; on the ER membrane (forming rough ER). The use of a certain translation pathway for a regular protein is dictated by the presence (or absence) of a signal sequence at the N-terminus of the growing polypeptide (Blobel, 2000; Mitra et al., 2006; Kramer et al., 2009). In the cytosol, once the translation process is initiated by the start codon contained in the mRNA (AUG typically used by eukaryotes), ribosomes synthesizing a protein without a signal sequence (e.g., the enzymes of glycolysis, tubulins for making microtubules and actin for making microfilaments) remain suspended in the cytosol and continue synthesis until the polypeptide is completed (Cross et al., 2009). In contrast, for proteins containing an N-terminal signal sequence (e.g. secretory proteins and membrane proteins) the translation ceases after this signal sequence has been synthesized. This is known as elongation arrest (Blobel, 2000; Ott and Lingappa, 2002; Berndt et al., 2009) and persists until ribosomes are attached to the membranes of the ER and a translocon complex is built (Robson and Collinson, 2006; Mitra et al., 2006). Thus, translation is restarted on the rough ER and the growing nascent protein crosses the ER membrane to the ER lumen through a translocon channel (Fulga et al., 2001; Hessa et al., 2005; Zhang et al., 2009). Membrane proteins remain anchored in the ER membrane with extracellular domains exposed to the ER lumen, transmembrane domains embedded in

the membrane in a number of different ways and, intracellular domains within the cytoplasm (Singer, 1990; van Geest and Lolkema, 2000; Sadka and Linial, 2005; Booth and Curnow, 2009). This differs to soluble secretory proteins, which co-translationally pass into the ER lumen and fold there without any other cellular membrane (Lippincott-Schwartz et al., 2000; Nickel and Seedorf, 2008). As membrane proteins with seven transmembrane domains, almost all GPCRs require a signal sequence for targeting to the ER lumen during synthesis, sharing a common membrane topology with Type III (containing multiple transmembrane domains) membrane proteins (Wallin and von Heijne, 1995; Bockaert and Pin, 1999; White and von Heijne, 2005; Davies et al., 2007; Almén et al., 2009).

In eukaryotes, a typical N-terminal signal sequence, with an average length of ~20-30 residues (Hiss and Schneider, 2009), consists of three distinct regions: an often positively charged n-region, a central hydrophobic core (h-core) and a polar c-region (von Heijne, 1990; Schneider and Fechner, 2004; Clérico et al., 2008). After a signal sequence has been synthesized and emerged from the ribosomal polypeptide exit tunnel, this ribosome-nascent-chain (RNC) complex (**Figure 4.1.1**) is immediately recognised by the signal recognition particle (SRP) (Egea et al., 2005), a conserved ribonucleoprotein particle in the cytosol (Ott and Lingappa, 2002; Halic and Beckmann, 2005; Berndt et al., 2009; **Figure 4.1.2**). In eukaryotes, binding of the SRP causes elongation arrest of the nascent chain (Halic and Beckmann, 2005; Zhang et al., 2009). Through its GTP-dependent interactions with the SRP receptor (SR) on the cytosolic surface of the ER membrane, the SRP targets the RNC to the ER (Walter and Lingappa, 1986; Fulga et al., 2001; Pitonzo et al., 2009; **Figure 4.1.3**). The docking of the RNC to the ER membrane releases the SRP from the RNC and allows translation to continue, while the growing protein crosses the ER membrane to the ER lumen through a translocon channel, which consists of the Sec61-complex (Crowley et al., 1994;

Jungnickel and Rapoport, 1995; Hatsuzawa et al., 1996; Sadlish et al., 2005; Jennifer et al., 2005; Hedge and Kang, 2008; Boy and Koch, 2009; Pitonzo et al., 2009; **Figure 4.1.4**). Following this, for some proteins the signal sequence, namely the signal peptide, is cleaved off by signal peptidases in the ER lumen. In contrast, signal anchor sequences are not cleaved and form a part of the mature protein (von Heijne, 1990; Nilsson et al., 1994; Blobel, 2000; Paetzel et al., 2002; Choo et al., 2009).

In addition to allowing recognition and binding of the SRP and thus leading the nascent chain to the ER, an N-terminal signal sequence may participate in a number of post-targeting events, e.g. protein folding and trafficking. This is highly dependent upon whether the signal sequence is a cleaved signal peptide or an un-cleaved signal anchor (Hegde and Bernstein, 2006; Hiss and Schneider, 2009; Pantazaka, 2009). Therefore, knowledge whether or not a signal sequence is cleaved is crucial to understanding the expression, folding and trafficking of a protein (Choo et al., 2005; 2009). Since the c-region immediately before the cleavage site has some conserved features with small, uncharged residues at the -1 and -3 positions relative to the cleavage site (von Heijne, 1990), there are a number of computational methods available for identifying the potential cleavage site of a signal sequence. One of the most popular and accessible is the SignalP World Wide Web server ([http:// www.cbs.dtu.dk/services/SignalP/](http://www.cbs.dtu.dk/services/SignalP/)), (Nielsen et al., 1997; Bendtsen et al., 2004; Leversen et al., 2009). However, almost all prediction methods are challenged by numerous exceptions (Choo and Ranganathan, 2008; Hiss and Schneider, 2009). For example, the accuracy of these predictive algorithms (in terms of whether or not the sequence is cleaved) was <80% in a set of 270 recombinant secreted proteins (not GPCRs) with experimentally verified cleavage sites (Zhang and Henzel, 2004). Although there has been considerable effort with predictive algorithms to improve their accuracy (Schneider and Fehner 2004; Bendtsen et al., 2004; Klee and Ellis, 2005; Plewczynski et al., 2008), in a recent report, SignalP

maintains consistency and achieves the best overall accuracy, ranging from 87% to 91% (Choo et al., 2009).

Since very few GPCRs have had their signal sequences investigated experimentally, whether a GPCR contains a cleaved signal peptide or a non-cleavable signal anchor sequence has largely relied on predictive algorithms. Over 90% of GPCRs (most Family A members) are predicted to use TM1 of the mature protein as a non-cleavable signal anchor sequence (Wallin and von Heijne, 1995; Rutz et al., 2006). In contrast, only a small group of GPCRs (most Family B and C members) are predicted to contain a cleaved signal peptide. Amongst Family B GPCRs there have been clear difficulties in predicting whether or not the signal sequence is cleaved. For example, the CRF receptor 1 (CRF-R₁) and the CRF-R_{2(a)} are both predicted to have an N-terminal cleavable signal peptide with >98% probability as assessed using SignalP 3.0 (Bendtsen et al., 2004). However, when assessed experimentally, the signal peptide of CRF-R₁ is cleaved (Alken et al., 2005), whereas the putative signal peptide of the CRF-R_{2(a)} is not and hence forms a part of the extracellular N-terminal domain of the mature receptor (Rutz et al., 2006). This pseudo-signal peptide of the CRF-R_{2(a)} is incapable of mediating ER targeting but contributes to receptor activation (Schulz et al., 2010). Similar to most Family A GPCRs, TM1 of the CRF-R_{2(a)} is thought to serve as a signal anchor sequence during translocation of the nascent protein across the ER membrane (Rutz et al., 2006). Like other members of Family B GPCRs, the human GLP-1R contains a potential N-terminal signal peptide sequence corresponding to the first 23 amino acids of the receptor (UniProtKB/Swiss-Prot, P43220). However, it is unclear whether this putative signal peptide is cleaved or not and what role it plays. To answer these questions, experimental investigation was conducted in the present study to assess the role of this small N-terminal sequence of the GLP-1R.

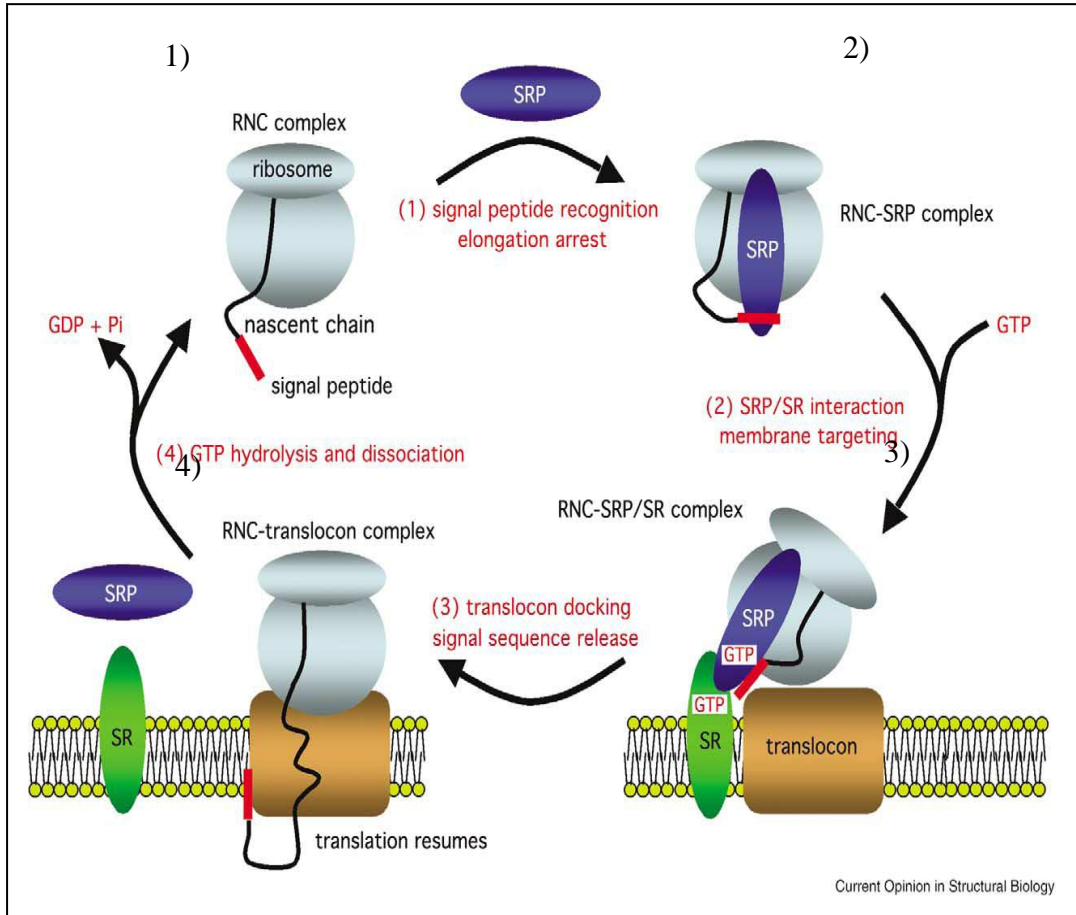


Figure 4.1. The SRP-mediated co-translational protein targeting cycle. A nascent polypeptide with a SP emerges from the ribosome and is recognized by the SRP (signal recognition particle), causing elongation arrest (1). The RNC (ribosome-nascent-chain) –SRP complex is then targeted to the membrane through GTP-dependent interactions between the SRP and its SR (SRP receptor) (2). At the ER membrane, after ribosome docking to the translocon, the SP is released from the SRP 3) and, following GTP hydrolysis, the SRP–SR targeting complex dissociates (4). From Egea et al., 2005.

4.2 Results

4.2.1 *Predicting cleavage of the signal peptide of GLP-1R constructs using the SignalP 3.0 server*

The SignalP 3.0 server predicts the presence and location of signal peptide cleavage sites in amino acid sequences from Gram-positive and Gram negative prokaryotes and eukaryotes (Nielsen et al., 1997; Bendtsen et al., 2004). This server is based on a combination of several artificial neural networks (SignalP-NN) and hidden Markov models (SignalP-HMM; Nielsen and Krogh, 1998). SignalP-NN reports three scores for each submitted sequence and their significantly high standards (cut-offs). The C-score is the 'cleavage site' score. The S-score predicts the probability of the presence of a signal peptide and thus an S-mean score is calculated for the length of the predicted signal peptide. Y-max is a derivative of the C-score, which, when combined with the S-score results in a better cleavage site prediction than the raw C-score alone. This is due to the fact that multiple high-peaking C-scores can be found in one sequence even when only one is the true cleavage site. The cleavage site is assigned from the Y-score where the slope of the S-score is steep and a significant C-score is found.

When the wild-type human GLP-1R amino acid sequence (Accession, NP_002053; Version, NP_002053.3; GI:166795283; Gene ID: 2740 GLP1R) was submitted, an N-terminal signal peptide sequence was predicted with the maximal cleavage site probability predicted between residues Pro²³ and Arg²⁴ with a Y-score at 0.62 (cutoff 0.33) which was combined with C-score (0.55) and the S-score (**Figure 4.2a**). Thus Met¹-Pro²³ is predicted as the signal peptide with an S-mean score at 0.819 (cut-off 0.48; **Figure 4.3**). On the other hand, SignalP-HMM reported that the same sequence of the GLP-1R contained a signal peptide with a probability of 0.999 but its maximal cleavage

site probability was between residues Ala²¹ and Gly²² (**Figure 4.3**). This sequence represents the first 23 residues of the GLP-1R and meets all of the characteristic features of a cleaved signal peptide in eukaryotic membrane proteins (Hiss and Scheneider, 2009). For example, the first 9 residues (Met¹-Arg⁹) are consistent with the polar n-region of a signal peptide with a net positive charge and residues Leu¹⁰ to Gly¹⁹ are consistent with a central h-core which is flanked at its C-terminus by a polar c-region corresponding to residues Arg²⁰ to Pro²³ (von Heijne, 1985; **Table 4.1a**). In addition, although the cleavage site was predicted differently at Pro²³-Arg²⁴ or Ala²¹-Gly²² by SignalP-NN and SignalP-HMM, respectively, both seemed to meet the “-1 and -3 ” rule (see above), in which residues at positions -3 and -1 of a cleavage site (Ala²¹ and Pro²³ ; and Gly¹⁹ and Ala²¹ respectively) were small and uncharged (von Heijne, 1990; **Table 4.1a**);). Consequently, mutation of Ala²¹ to Arg (A21R) was predicted by both algorithms to change the cleaved signal peptide into an uncleaved signal anchor sequence by replacing Ala²¹ with a large and positively charged arginine residue at either -3 or -1 (**Table 4.1b**). Surprisingly, when the N-terminal HA-tagged A21R mutated GLP-1R (HA-A21RGLP-1R; **Figure 4.2c**) was submitted to the same algorithm, no signal anchor sequence was predicted despite clearly reduced probabilities of both a signal peptide and cleavage compared with its control construct containing the wild-type receptor (HA-GLP-1R; **Figure 4.2b & Figure 4.3**). The signal anchor sequence can be predicted directly by SignalP-HMM and presumably by SignalP-NN by way of a high probability of the signal peptide but a low probability of cleavage. Interestingly, even the HA-GLP-1R was predicted to have no signal peptide sequence by SignalP-NN with an S-mean of 0.35 (lower than its cut-off, 0.48) and a relatively low probability of cleavage reported by both Y-max at 0.385 (cut-off 0.33) (**Figure 4.2b & Figure 4.3**) and SignalP-HMM (probability, 0.61; cleavage 0.35; **Figure 4.3**).

Similarly, the outcomes were conflicting when other epitope-tagged constructs were analysed, e.g. signal peptide-deleted GLP-1R either with or without an N-terminal HA-tag (HA- Δ SPGLP-1R; Δ SPGLP-1R; **Table 3.1**). In addition, for the constructs containing a relatively large N-terminal tag, e.g. EGFP-GLP-1R-HA, SignalP 3.0 server was not able to provide any clue as to whether the putative signal peptide of the GLP-1R would continue to behave as a signal peptide. These predictions concerning the epitope-tagged GLP-1R constructs indicated that experimental investigation was necessary to assess the putative signal peptide of the GLP-1R.

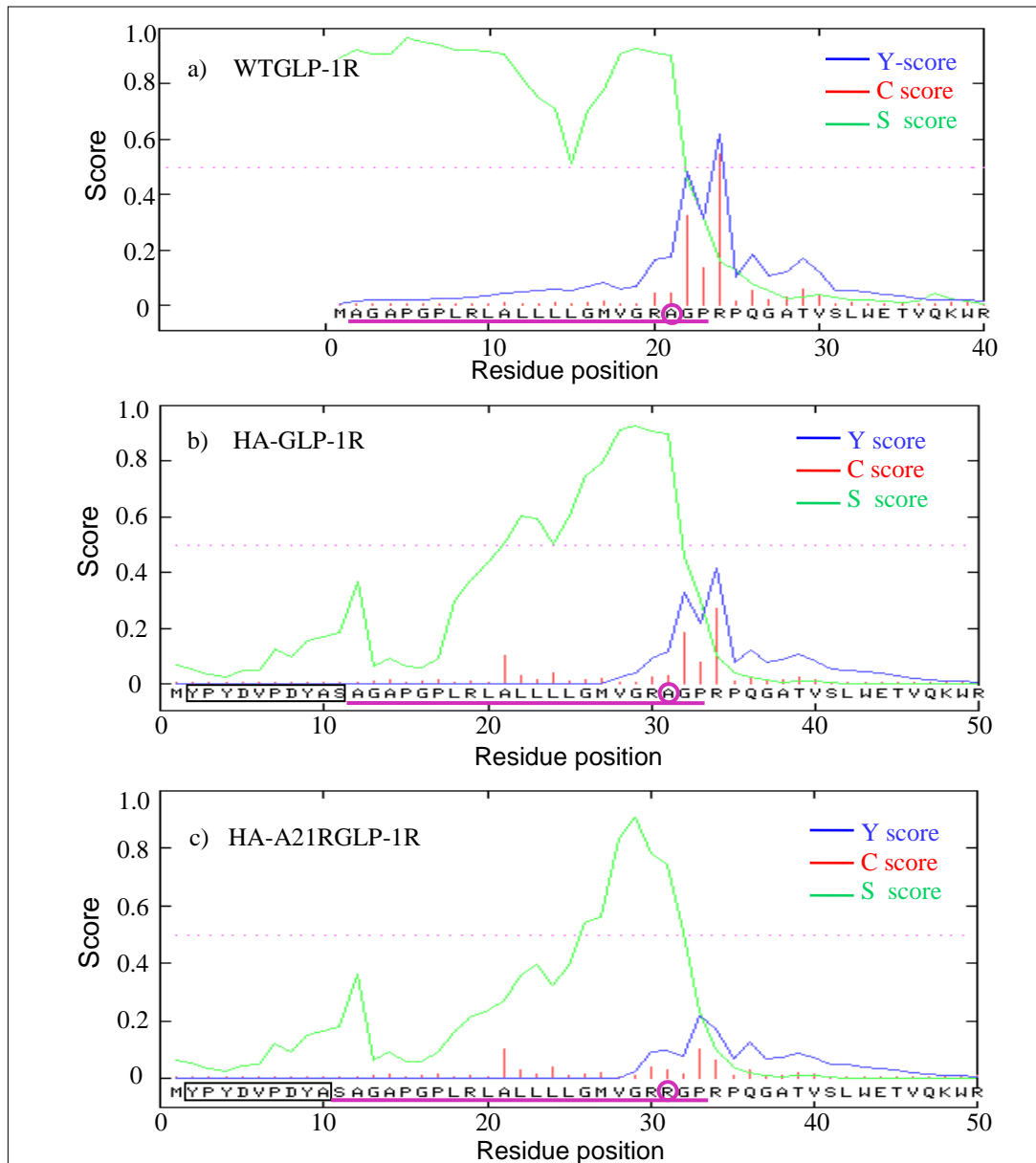


Figure 4.2. Predicted signal peptides and cleavage sites of the GLP-1R constructs (by SignalP-NN). Sequences of either the untagged WTGLP-1R (a), HA-GLP-1R (b) or the N-terminal HA-tagged A21R mutated construct (HA-A21RGLP-1R, c) were analysed by Signal P 3.0 server to predict the cleavage site of the signal peptide. The S-score in green is the probability of the presence of a signal peptide; the C-score in red is the cleavage site probability and the Y-score in blue is the cleavage site prediction derived from combining C-score with S-score; The residue Ala²¹, and predicted signal peptide of the WTGLP-1R (a) and their identical regions in either HA-GLP-1R or HA-A21RGLP-1R are labelled with a purple circle and underline, respectively. The HA-tag sequences are shown in boxes (b,c).

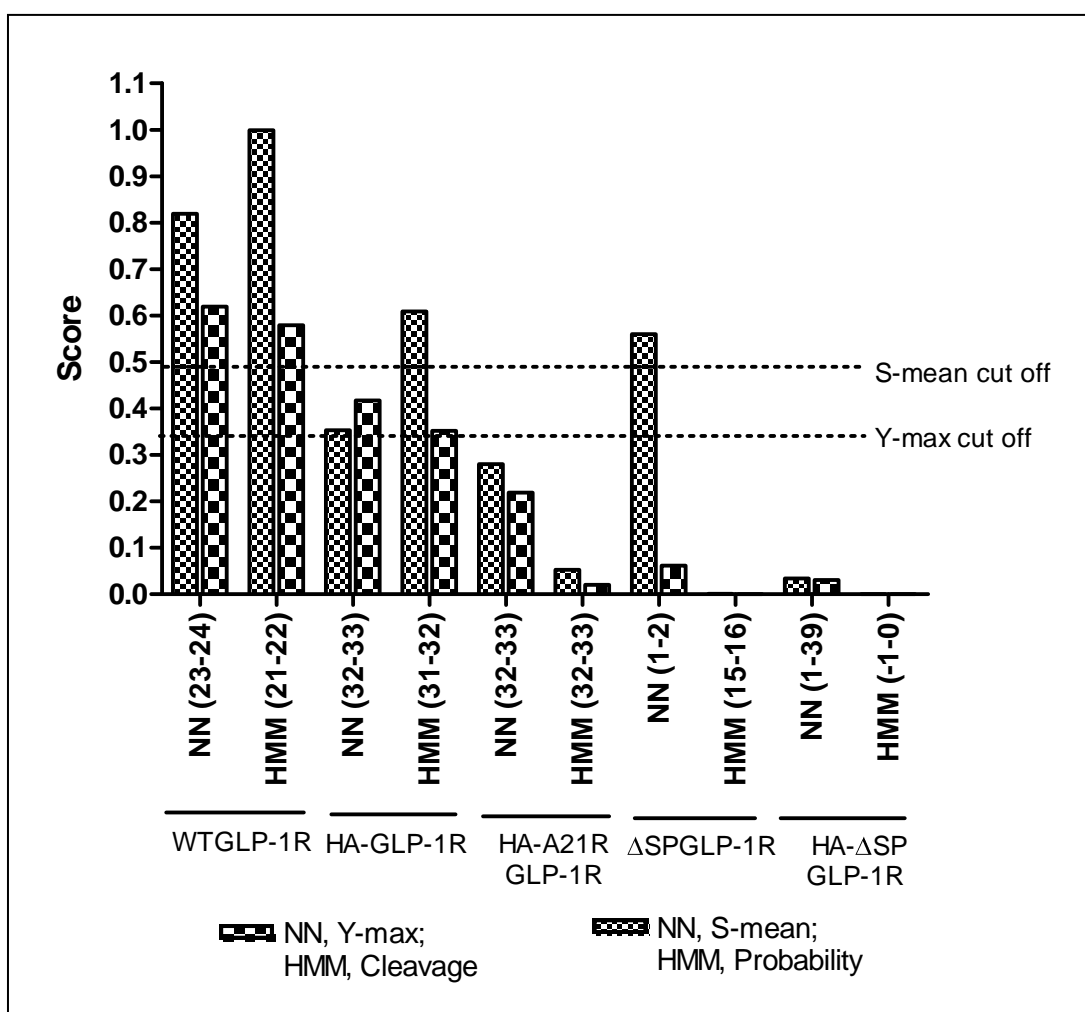


Figure 4.3. Comparison of signal peptides and cleavage sites of the GLP-1R constructs predicted by SignalP 3.0 server. Peptide sequences (in FASTA format) of the WTGLP-1R or mutated GLP-1Rs with or without the N-terminal HA-tag were submitted to Signal P 3.0 server to predict the probability and location of any cleaved signal peptide. The probability of a signal peptide was predicted by the S-mean score of SignalP-NN (NN) and SignalP-HMM score (HMM, Probability) respectively. Similarly, the cleavage site with the highest probability was predicted by the Y-max of NN and HMM, Cleavage. SignalP-NN gives the cut-off values and score above which is reported as ‘Yes’, which are represented by dashed lines as indicated. However, no cut off is given by SignalP-HMM.

Table 4.1. Characteristic features of the amino acids comprising residues 1-23 of the wild-type and mutated GLP-1R

a) WTGLP-1R

Sequence	1	2	3	4	5	6	7	8	9	10	11	12	13	14	15	16	17	18	19	20	21	22	23	
	M	A	G	A	P	G	P	L	R	L	A	L	L	L	L	G	M	V	G	R	A	G	P	
Hydrophobic	×	×	×	×		×		×		×	×	×	×	×	×	×	×	×	×			×	×	
Charged										+												+		
Small			×	×	×		×	×				×					×	×	×			×	×	×
Polar										×													×	

b) A21RGLP-1R

Sequence	1	2	3	4	5	6	7	8	9	10	11	12	13	14	15	16	17	18	19	20	21	22	23	
	M	A	G	A	P	G	P	L	R	L	A	L	L	L	L	G	M	V	G	R	R	G	P	
Hydrophobic	×	×	×	×		×		×		×	×	×	×	×	×	×	×	×	×				×	
Charged										+												+	+	
Small			×	×	×		×	×				×					×	×	×				×	×
Polar										×													×	×

The putative signal peptide sequence (residues 1-23) is represented in FASTA format, in which the potential hydrophobic core is highlighted in grey.

Residue 21 of the sequence is indicated by a circle. '×' represents 'Yes' in the listed features of the amino acids and '+' indicates positive charge.

4.2.2 Expression of full-length GLP-1Rs

As shown previously (**Section 3.3.2**), the N-terminal HA-tagged receptors were not detected by an anti-HA antibody although expression was confirmed by binding and function (**Figure 3.12b, Lane 4 & 5; Table 3.1**). This lack of detection was not a consequence of the inability of the antibody to recognise the protein as HA-immunoreactivity was clearly illustrated by using the constructs containing the same HA-tags located at the C-terminus of the receptor (GLP-1R-HA and EGFP-GLP-1R-HA; **Figure 3.12b, Lane 2 & 6**). When a key residue around the cleavage site was mutated, immunoreactivity of the epitope tags located at both the N- and C-termini were detected in the lysates of cells expressing the N-terminal HA-tagged and C-terminal EGFP-tagged A21RGLP-1R (HA-A21RGLP-1R-EGFP; **Figure 4.4a**). This indicates that the A21R mutant receptors were expressed as a full-length version and that the signal peptide was not cleaved (**Figure 4.4b, Lane 3 and c, Lane 3**). Immunoreactivity of both tags was also seen in the cells expressing the EGFP-GLP-1R-HA (**Figure 4.4a, b, Lane 4, c, Lane 4**). These full-length receptors (HA-A21RGLP-1R-EGFP and EGFP-GLP-1R-HA) revealed only one immunoreactive band in immunoblotting against either epitope tag (**Figure 4.4b, Lane 3 & 4; c, Lane 3 & 4**). The size of the band detected was similar to the lower (~66kDa) of the two bands representing the immature form of the receptor in cells expressing the HA-GLP-1R-EGFP (**Figure 4.4a**) in which the signal peptide was cleaved (**Figure 4.4b, Lane 1 & 2; c, Lane 1 & 2**).

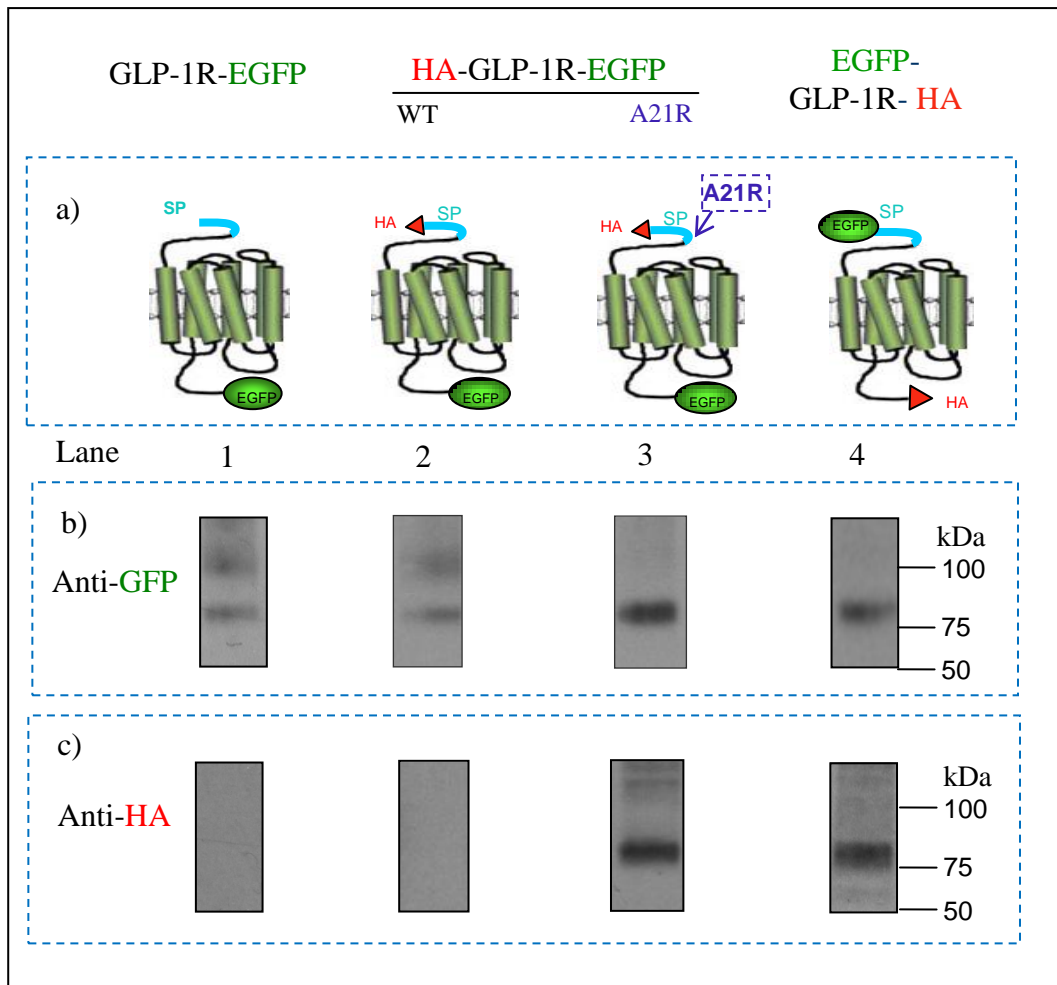


Figure 4.4. Immunoblotting of cell lysates following transfection of cells with either un-mutated or A21R mutated epitope-tagged GLP-1Rs. HEK293 cells were transiently transfected with plasmids containing either epitope-tagged un-mutated GLP-1Rs (GLP-1R-EGFP, HA-GLP-1R-EGFP and EGFP-GLP-1R-HA) or the HA-GLP-1R-EGFP containing the A21R mutation (HA-A21RGLP-1R-EGFP) as indicated (c). After 24-30h, cell lysates were prepared and immunoblotted using either an anti-GFP antibody (a) or an anti-HA antibody (b). Data are representative of at least 3 independent experiments.

4.2.3 Full-length EGFP-tagged GLP-1Rs lack cell surface fluorescence and function

Confocal imaging of cells transiently expressing HA-A21RGLP-1R-EGFP revealed intracellular EGFP-fluorescence, lacking any clear cell surface-located fluorescence (**Figure 4.5b**). This was distinct from cells with expression of C-terminal EGFP-tagged constructs containing the wild-type GLP-1R (GLP-1R-EGFP and HA-GLP-1R-EGFP). In both of these wild-type receptors, the EGFP-fluorescence was predominantly located at the cell surface (**Figure 4.5a & c**). However, the intracellular EGFP-fluorescence distribution of the C-terminally EGFP-tagged A21R mutant was similar to the wild-type receptor that had an EGFP-tag at the N-terminus (EGFP-GLP-1R-HA, **Figure 4.5d**). Furthermore, this corresponded to the functional coupling the receptor, in which challenge of cells expressing the A21R mutant showed little or no GLP-1 7-36 amide-mediated cAMP production in comparison with the response in cells expressing HA-GLP-1R-EGFP (**Figure 4.6**). Similarly, cells expressing the EGFP-GLP-1R-HA, as shown previously, also barely evoked cAMP generation in response to GLP-1 7-36 amide stimulation (**Figure 3.14f**). Therefore, the lack of signal peptide cleavage (in either EGFP-GLP-1R-HA or HA-A21RGLP-1R-EGFP) was associated with a lack of cell surface expression.

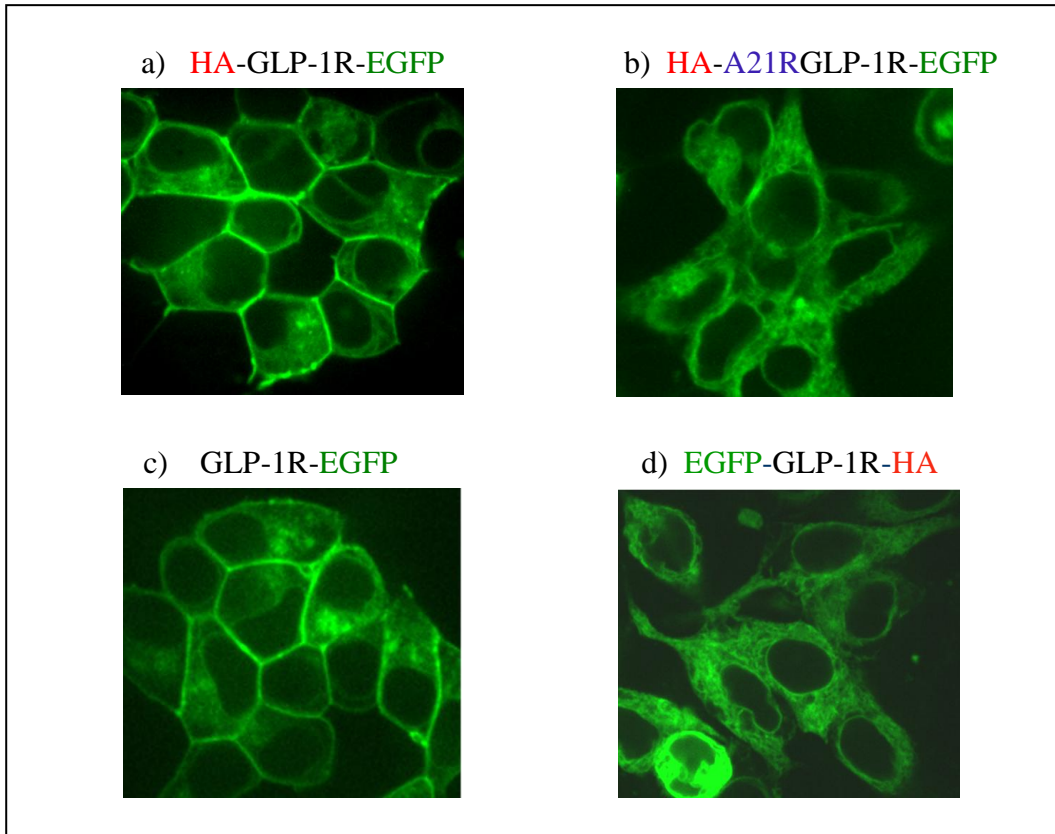


Figure 4.5. Confocal images of live cells with transient expression of either un-mutated or A21R mutated GLP-1Rs. HEK293 cells were transiently transfected with either N-terminal HA-tagged and C-terminal EGFP-tagged un-mutated GLP-1R (HA-GLP-1R-EGFP, a) or the A21R mutated equivalent (HA-A21RGLP-1R-EGFP, b). After 30h, live cells were imaged by confocal microscopy. The un-mutated GLP-1Rs with an EGFP-tag at either the C-terminus (GLP-1R-EGFP, c) or the N-terminus (EGFP-GLP-1R-HA, d) were used as controls. Images are representative of cells observed in 3 independent experiments.

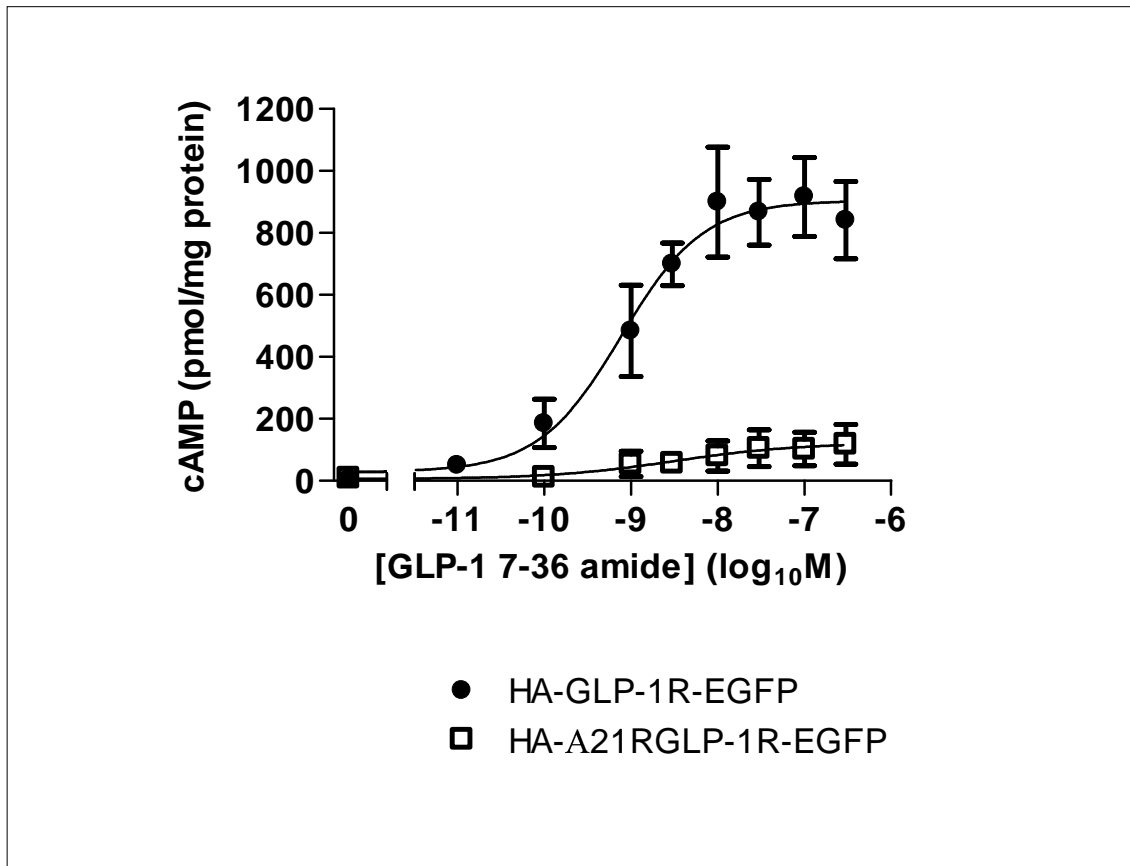


Figure 4.6. Functional coupling of epitope-tagged GLP-1Rs with or without a mutation near the predicted signal peptide cleavage site. HEK293 cells were transiently transfected with either HA-GLP-1R-EGFP or HA-A21RGLP-1R-EGFP. After 30h, the transfected cells were challenged with GLP-1 7-36 amide at the concentrations indicated in the presence of IBMX (500 μ M) and cAMP levels were determined after 10min stimulation at 37°C. pEC_{50} value for HA-GLP-1R-EGFP, 9.09 ± 0.22 . Data are mean \pm sem, n = 3.

4.2.4 Receptor expression requires the signal peptide sequence of the GLP-1R

In order to investigate the function of the signal peptide, the putative signal peptide sequence was removed from each of the GLP-1R-HA, GLP-1R-EGFP, HA-GLP-1R-EGFP and EGFP-GLP-1R-HA constructs, which had been detected by specific antibodies against their C-terminal epitope tags (**Figure 3.12b & c**). These signal peptide sequence-deleted (Δ SP) constructs were generated by PCR cloning as described previously (**Section 2.6**) and referred to as Δ SP-GLP-1R-HA, Δ SP-GLP-1R-EGFP, HA- Δ SP-GLP-1R-EGFP and EGFP- Δ SPGLP-1R-HA. In addition to full DNA sequencing (**Section 2.13**) of the inserts, the plasmid DNA of these constructs were confirmed by RE site analysis as described previously (**Section 2.7**), in which all of the resulting bands following different RE digest showed the expected sizes (**Figure 4.7 & Figure 4.8**). Following transient transfection in HEK293 cells, there was no immunoreactivity detected using the specific antibody to the C-terminal epitope tag in the whole cell lysates prepared from the cells expressing either the Δ SP-GLP-1R-EGFP or the Δ SP-GLP-1R-HA (**Figure 4.9a, Lane 4; b, Lane 2 respectively**). Similarly, in the cells transfected with the HA- Δ SPGLP-1R-EGFP, the expression of the receptor was not detected using either an anti-HA or anti-GFP antibody (**Figure 4.9a, Lane 6 & b, Lane 6**).

In order to assess whether deletion of the signal peptide sequence resulted in synthesis of the Δ SPGLP-1R followed by rapid degradation rather than a simple lack of expression, HEK293 cells transfected with either the GLP-1R-HA or Δ SP-GLP-1R-HA constructs were incubated in the presence of proteasome inhibitors. MG132 is a proteasome and cathepsin K ($K_i=4\text{nM}$) inhibitor and reported to block degradation of

short-lived proteins (Dorion et al., 1999). ALLN (MG101) is a proteasome and calpain I ($K_i=190\text{nM}$) /II ($K_i=220\text{nM}$) inhibitor. Thus, 24h after transient transfection, the cells were incubated for a further 6h with either MG132 ($10\mu\text{M}$) (Ruvolo et al., 2008) or ALLN ($261\mu\text{M}$, $100\mu\text{g/mL}$) (Willars et al., 2001). Although both inhibitors tended to increase the intensity of the upper ($\sim 64\text{kDa}$) band (and a lower ($\sim 42\text{kDa}$) band appeared following ALLN treatment) for the constructs containing the signal peptide sequence (**Figure 4.10, Lane 4 & 6**), neither of these inhibitors resulted in the appearance of HA immunoreactivity for the $\Delta\text{SP-GLP-1R-HA}$ (**Figure 4.10, Lane 4 & 6**). To eliminate the possibility of unstable mRNA caused by deletion of the signal peptide sequence, RT-PCR was performed in the total RNA isolated from the cells expressing either the GLP-1R-HA or the $\Delta\text{SP-GLP-1R-HA}$ at 12, 24 and 48h after transient transfection. In this RT-PCR, the mRNA was assessed for the sequence encoding full-length receptor immediately after the putative signal peptide (Arg^{24} -stop codon) as described (**Section 2.22**). Similar DNA bands at 1323bp representing the sequence encoding Arg^{24} to the end of the GLP-1R were observed in cells transfected with the constructs either with or without the signal peptide sequence at any of the times studied (**Figure 4.11**).

Interestingly, immunoblotting of the ΔSP version of the EGFP-GLP-1R-HA construct (EGFP- $\Delta\text{SP-GLP-1R-HA}$) transiently transfected into cells detected a low molecular size band of $\sim 30\text{kDa}$ by an antibody against its N-terminal EGFP-tag (**Figure 4.9a, Lane 8**), which was only slightly greater than the band of EGFP alone at $\sim 27\text{kDa}$ (**Figure 4.9a, Lane 9**). However, there was no evidence of HA immunoreactivity detected in the cells expressing this construct (**Figure 4.9b, Lane 8**).

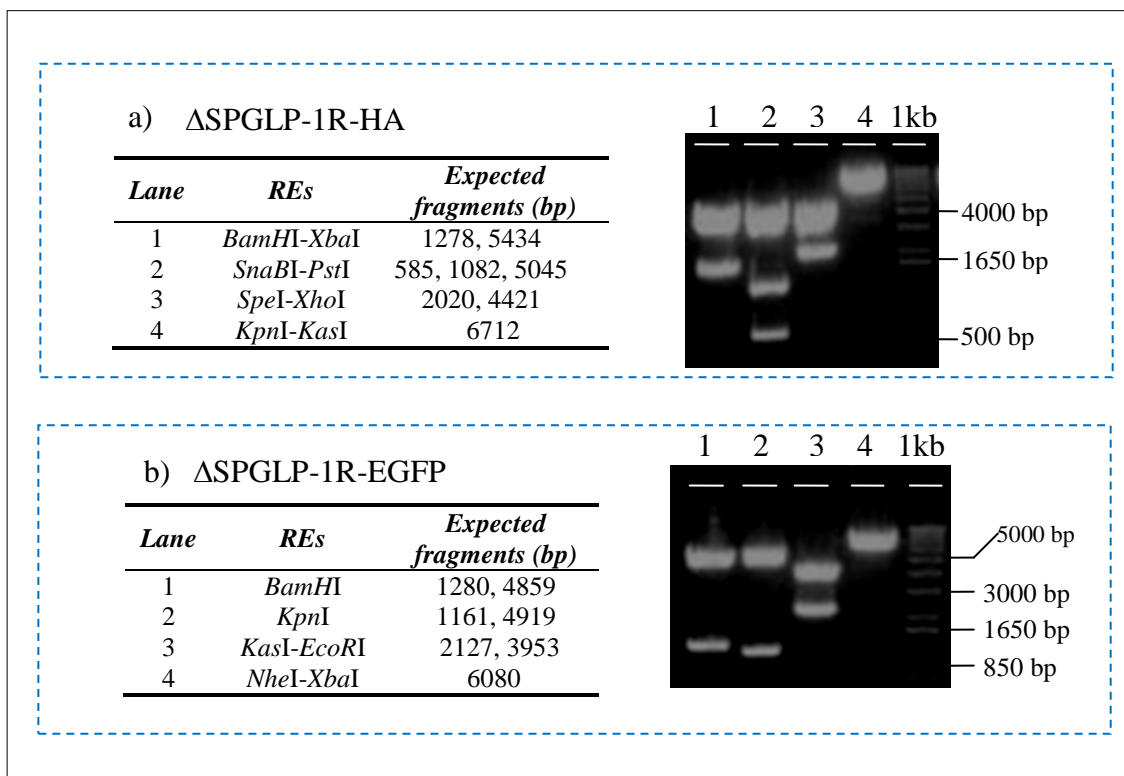


Figure 4.7. Identification of constructs of the C-terminal epitope-tagged GLP-1Rs without the signal peptide sequence. Based on the C-terminal epitope-tagged full-length GLP-1R constructs (GLP-1R-HA and GLP-1R-EGFP), signal peptide deleted versions of the constructs (Δ SPGLP-1R-HA and Δ SPGLP-1R-EGFP) were generated in which residues 2-23 were removed from the GLP-1R coding sequence. The potential constructs were identified by separate RE digestion with either *Bam*HI-*Xba*I, *Sna*BI-*Pst*I *Spe*I-*Xho*I or *Kpn*I-*Kas*I for Δ SPGLP-1R-HA (a) and, either *Bam*HI, *Kpn*I, *Kas*I-*Eco*RI or *Nhe*I-*Xba*I for Δ SPGLP-1R-EGFP (b). The positions of the wells and 1kb DNA ladder on the agarose gels are indicated. The sizes of the resulting bands following digestion were as expected (as listed in tables). After this confirmation, the plasmids were subjected to full DNA sequencing.

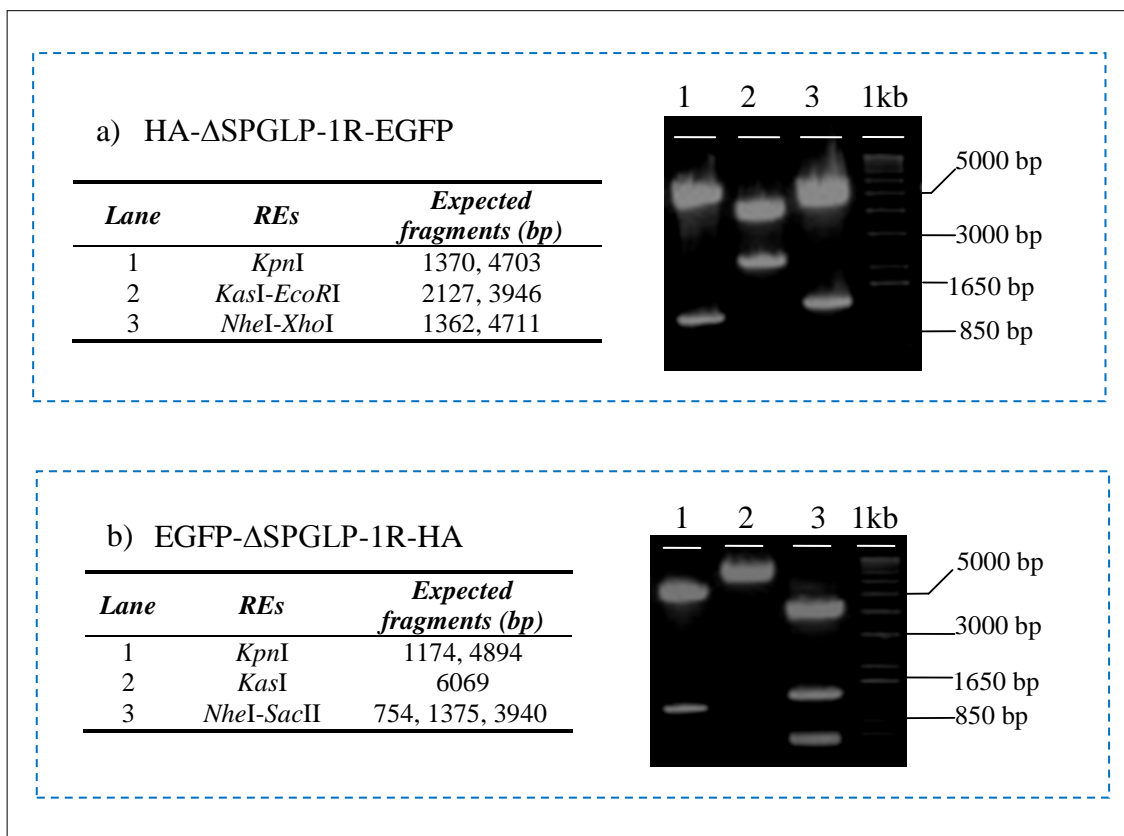


Figure 4.8. Identification of constructs of the Δ SPGLP-1Rs with an EGFP-tag and an HA-tag at either terminus. Based on the full-length GLP-1R constructs with an EGFP-tag and an HA-tag at either terminus (HA-GLP-1R-EGFP and EGFP-GLP-1R-HA), signal peptide-deleted versions of the constructs (HA- Δ SPGLP-1R-EGFP and EGFP- Δ SPGLP-1R-HA) were generated. The potential constructs were identified by separate RE digestion with either *KpnI*, *KasI-EcoRI* or *NheI-XhoI* for HA- Δ SPGLP-1R-EGFP (a) and, either *KpnI*, *KasI* or *NheI-SacII* for EGFP- Δ SPGLP-1R-HA (b). The positions of the wells and 1kb DNA ladder on the agarose gels are indicated. The sizes of the resulting bands following digestion were as expected (as listed in tables). After this confirmation, the plasmids were subjected to full DNA sequencing.

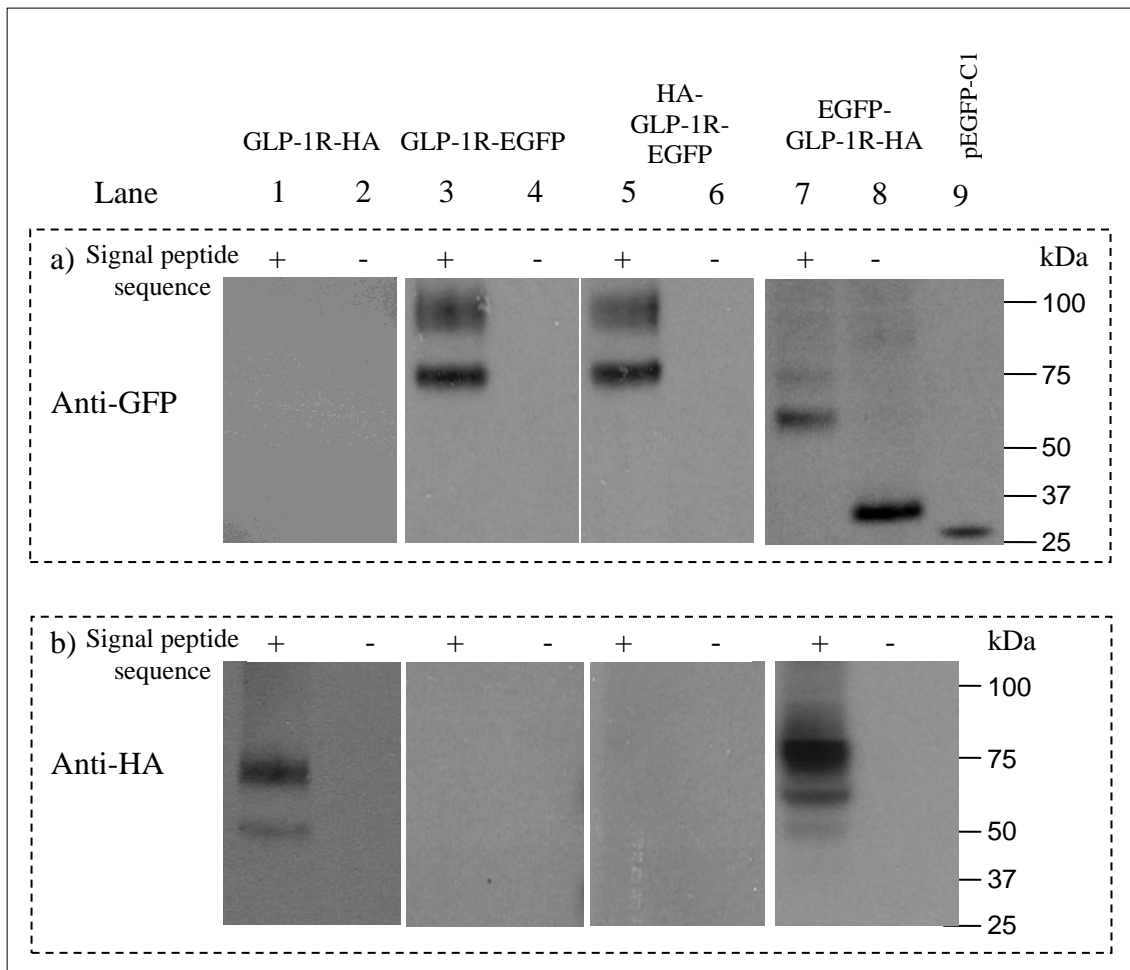


Figure 4.9. Immunoblotting of cell lysates following transfection of cells with epitope-tagged GLP-1Rs either with or without the signal peptide sequence. HEK293 cells were transiently transfected with constructs encoding fusion proteins consisting of HA- and/or EGFP-tagged GLP-1Rs with (+) or without (-) the signal peptide sequence. As a control the empty vector, pEGFP-C1, was also transfected to express EGFP alone. After 24-30h, immunoblotting on cell lysates was conducted using either an anti-GFP antibody (a) or an anti-HA antibody (b). Data are representative of 5 independent experiments.

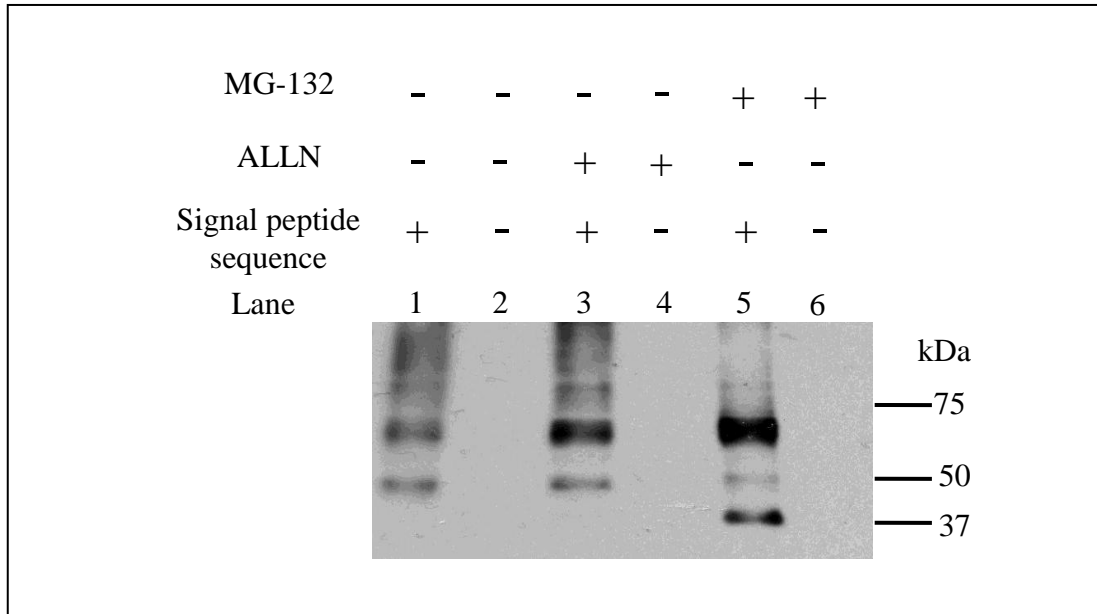


Figure 4.10. The effect of proteasome inhibitors on the expression of C-terminal HA-tagged GLP-1Rs either with or without the signal peptide sequence. HEK293 cells were transiently transfected with either GLP-1R-HA or the signal peptide-deleted equivalent, Δ SP-GLP-1R-HA. After 24h, the transfected cells were treated for a further 6h with either the proteasome and cathepsin K inhibitor, MG132 (10mM) or the proteasome and calpain 1 inhibitor, ALLN (MG101; 261mM). Immunoblotting was then conducted on the cell lysates using an anti-HA antibody. Data are representative of 3 independent experiments.

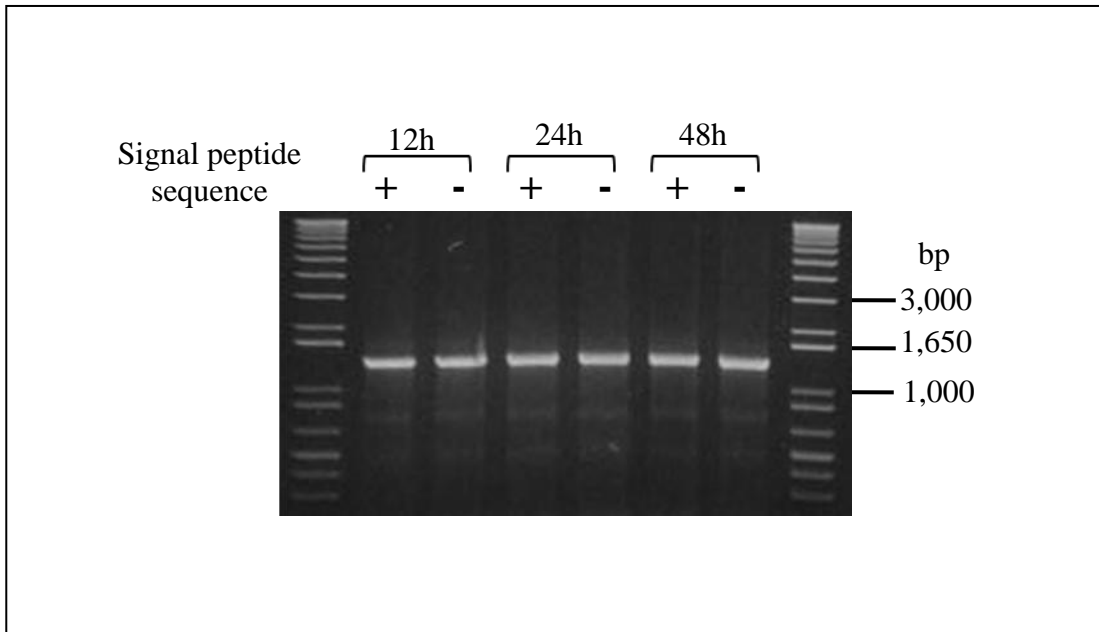


Figure 4.11. RT-PCR of the C-terminal HA-tagged GLP-1R either with or without the signal peptide sequence. HEK293 cells were transiently transfected with either the GLP-1R-HA or the signal peptide-deleted equivalent, Δ SP-GLP-1R-HA. Total RNA was isolated from the transfected cells at 12, 24 and 48h. After reverse transcription of mRNA to cDNA, RT-PCR was performed using the identical forward and reverse primers which were designed to amplify the sequence encoding the GLP-1R including the HA-tag but excluding the signal peptide sequence with a predicted size of 1323bp. Data are representative of 3 independent experiments.

Using confocal microscopy, cells transfected with Δ SP versions of EGFP-tagged GLP-1Rs were assessed. No fluorescence was observed in the cells transiently transfected with either the Δ SP-GLP-1R-EGFP (image not shown) or the Δ SP-GLP-1R-HA (**Figure 4.12b**) while the EGFP- Δ SP-GLP-1R-HA construct demonstrated a cytosolic and nuclear fluorescence (**Figure 4.12d**), consistent with the fluorescence pattern of EGFP alone (**Figure 4.12b**). Cells transfected with EGFP-tagged GLP-1R constructs with the signal peptide sequence removed (Δ SP-GLP-1R-EGFP, HA- Δ SP-GLP-1R-EGFP and EGFP- Δ SP-GLP-1R-HA) failed to evoke cAMP accumulation in response to GLP-1 7-36 amide while, under the same conditions, GLP-1 7-36 amide elevated cAMP generation in the cells expressing C-terminal EGFP-tagged constructs containing the signal peptide sequence (GLP-1R-EGFP and HA-GLP-1R-EGFP) with similar potency and E_{\max} to that of the untagged receptor (**Figure 4.13; Table 3.1**).

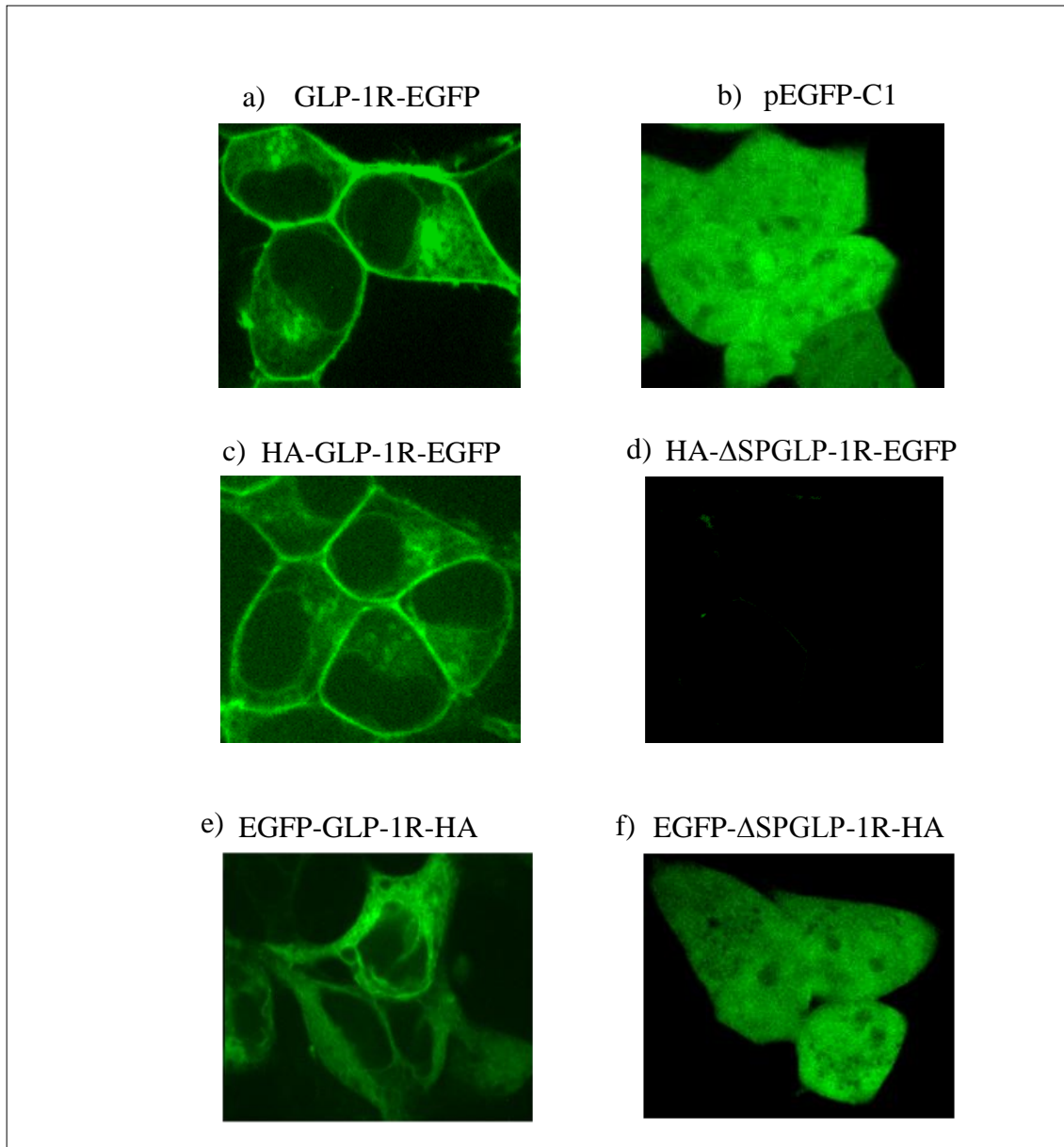


Figure 4.12 Confocal imaging of cells transfected with EGFP-tagged GLP-1Rs either with or without the signal peptide sequence. HEK293 cells were transiently transfected with fusion proteins consisting of HA- and/or EGFP-tagged GLP-1Rs either with (GLP-1R-EGFP, a; HA-GLP-1R-EGFP, c; and EGFP-GLP-1R-HA, e) or without (HA- Δ SPGLP-1R-EGFP, d; and EGFP- Δ SPGLP-1R-HA) the signal peptide sequence. As a control, the empty vector, pEGFP-C1, was also transfected to express EGFP alone. After 30-48h, live cells were imaged by confocal microscopy. Images are representative of cells observed in 5 independent experiments.

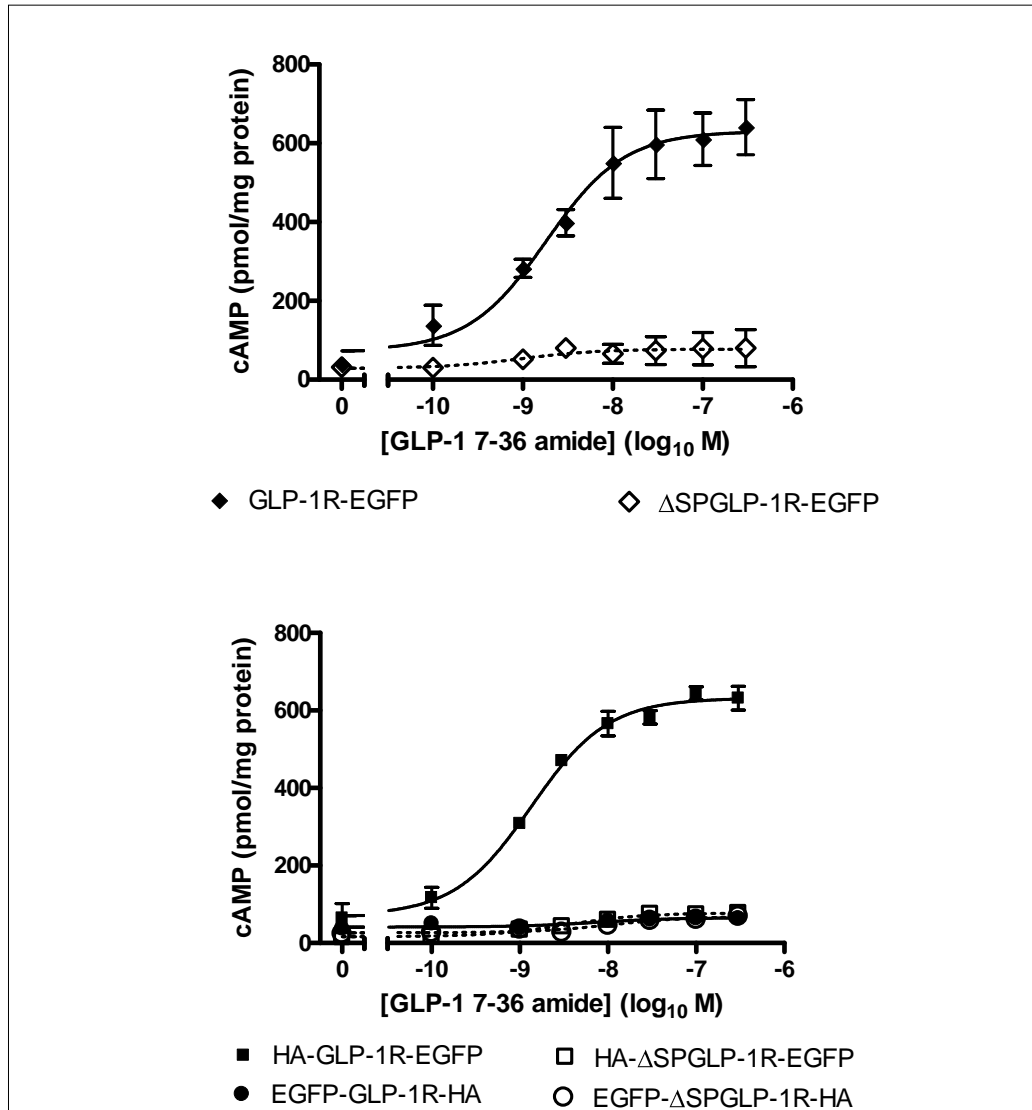


Figure 4.13. Functional coupling of the GLP-1R constructs either with or without the signal peptide sequence. HEK293 cells were transiently transfected with epitope-tagged GLP-1Rs either with (GLP-1R-EGFP, HA-GLP-1R-EGFP and EGFP-GLP-1R-HA) or without (Δ SPGLP-1R-EGFP, HA- Δ SPGLP-1R-EGFP and Δ SPEGFP-GLP-1R-HA) the signal peptide sequence. After 30h, the transfected cells were challenged with GLP-1 7-36 amide at the concentrations indicated in the absence of IBMX and cAMP levels were determined after 10min stimulation at 37°C. Data are mean \pm sem, n=3. pEC₅₀ values: GLP-1R-EGFP, 8.55 \pm 0.15; HA-GLP-1R-EGFP, 8.73 \pm 0.13

4.2.5 Increasing the positive charge within the N-terminus partially recovers the expression and function of the Δ SPGLP-1Rs

As shown above, the Δ SP receptor (corresponding to residues 24-463) was not expressed in the absence of an N-terminal signal peptide sequence. Replacing negatively charged Glu³⁴ with a positively charged, polar arginine residue (E34R) increased the net charge of the sequence immediately following the signal peptide. This resulted in the appearance of GFP-immunoreactivity in whole cell lysates prepared from cells expressing the E34R mutated HA- Δ SPGLP-1R-EGFP construct (HA- Δ SPE34RGLP-1R-EGFP) (**Figure 4.14aii & iv and bii & iv**), which was abolished by the removal of the signal peptide sequence from the HA-GLP-1R-EGFP construct (HA- Δ SPGLP-1R-EGFP), (**Figure 4.14ai & iii and bi & iii**). Thus, in the presence of the signal peptide sequence, the mutated (HA-E34R-GLP-1R-EGFP) and un-mutated (HA-GLP-1R-EGFP) receptors behaved identically in immunoblotting against the epitope tags, which revealed two bands using an anti-GFP antibody (**Figure 4.14ai & ii and bi & ii**) and no immunoreactivity using an anti-HA antibody (**Figure 4.14aiii & iv and biii & iv**). In contrast, in the absence of the signal peptide sequence, three bands were observed in the immunoblotting of HA- Δ SP-E34R-GLP-1R-EGFP using either anti-GFP antibody (**Figure 4.14aii & iv and bii & iv**) whereas no immunoreactivity was detected in the HA- Δ SPGLP-1R-EGFP construct by either antibody (**Figure 4.14ai & iii and bi & iii**). For the HA- Δ SP-E34R-GLP-1R-EGFP, although the immunoreactivity was relatively weak, the upper two bands were consistent with those seen for both the HA-GLP-1R-EGFP and the HA- Δ SP-E34R-GLP-1R-EGFP constructs. An additional lower molecular size unknown band was also observed (~52kDa) (**Figure 4.14bii**).

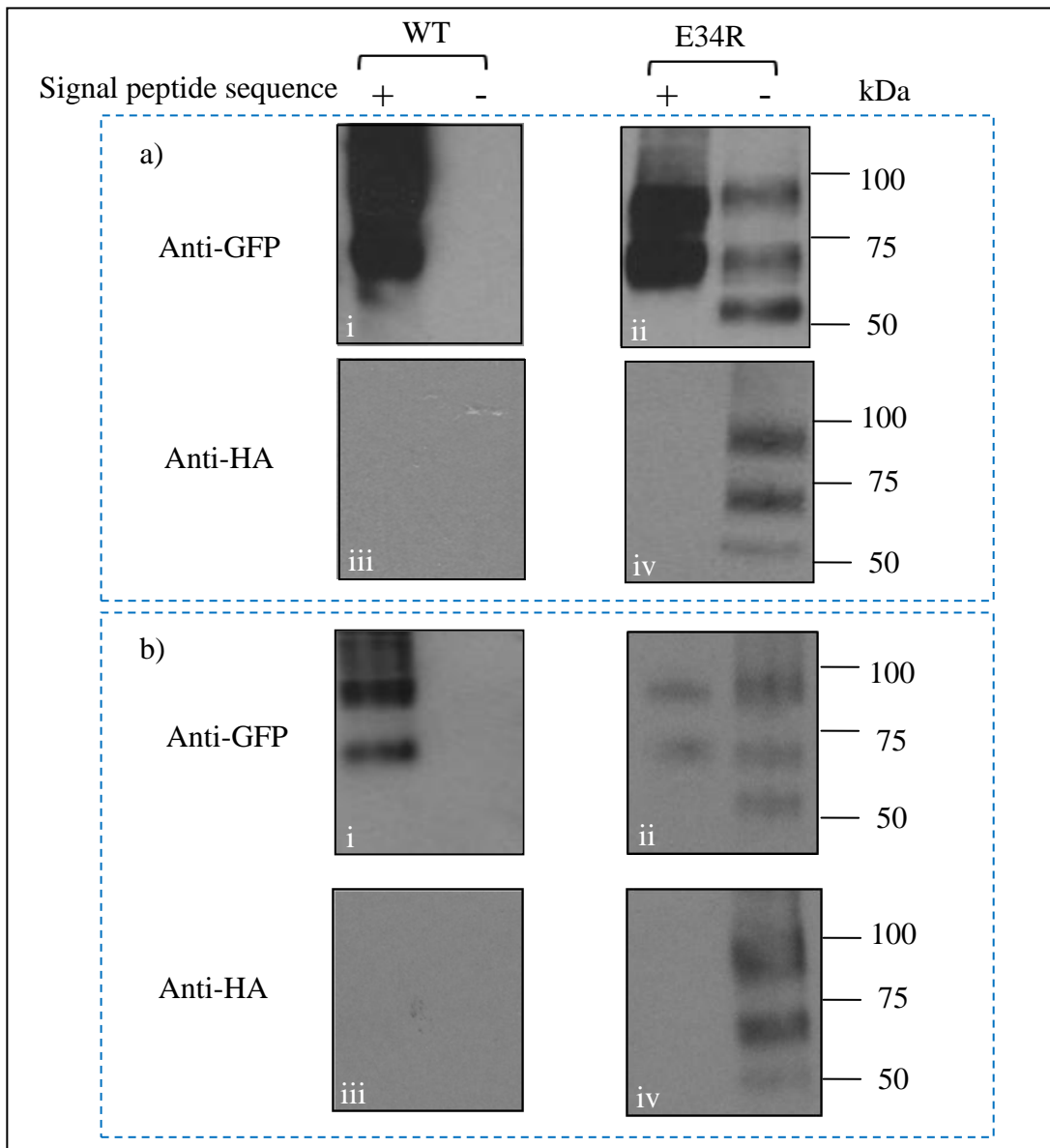


Figure 4.14. Immunoblotting of cell lysates following transfection of cells with either the un-mutated wild-type GLP-1R or the E34R mutants both either with or without the signal peptide sequence. HEK293 cells were transiently transfected with N-terminal HA-tagged and C-terminal EGFP-tagged wild-type GLP-1R (HA-GLP-1R-EGFP) or the E34R mutated equivalent (HA-E34RGLP-1R-EGFP) both with (+) or without (-) the signal peptide sequence. After 30h, immunoblotting was conducted on cell lysates using either an anti-GFP antibody or an anti-HA antibody (a). To more clearly show the relative patterns of immunoreactive bands, lanes for the constructs containing the signal peptide sequence (+) were loaded with five-fold less protein than lanes for the signal peptide-deleted constructs (-) (b). Data are representative of 3 independent experiments.

Similar to the HA-GLP-1R-EGFP construct shown above (**Figure 4.12c**), confocal imaging of live cells transiently expressing the E34R mutated receptor in the presence of the signal peptide sequence (HA-E34R-GLP-1R-EGFP) showed strong plasma membrane fluorescence and relatively weak intracellular fluorescence (**Figure 4.15a**). However, in the absence of the signal peptide (HA-E34R Δ SPGLP-1R-EGFP), the EGFP-fluorescence was predominantly cytosolic although there was potentially some overlap with trypan blue staining suggesting some localisation at the plasma membrane (**Figure 4.15b**). In the cells transfected with the mutated receptor containing the signal peptide sequence (HA-E34R-GLP-1R-EGFP), the concentration-dependence of GLP-1 7-36 amide-mediated cAMP elevation was comparable to that observed in cells expressing HA-GLP-1R-EGFP (**Figure 4.16**). When the signal peptide sequence was removed, GLP-1 7-36 amide stimulation of HEK293 cells transfected with the construct containing un-mutated receptor (HA- Δ SP-GLP-1R-EGFP) barely evoked cAMP generation, which was consistent with the lack of Δ SP-GLP-1R expression. Cells transfected with the construct in the absence of the signal peptide but in the presence of E34R mutation (HA- Δ SP-E34R-GLP-1R-EGFP) elevated cAMP production in response to GLP-1 7-36 amide with similar potency but a lower E_{max} than in cells expressing the construct in the presence of the signal peptide but either containing the un-mutated (HA-GLP-1R-EGFP) or mutated epitope-tagged receptor (HA-E34R-GLP-1R-EGFP) (**Figure 4.16**).

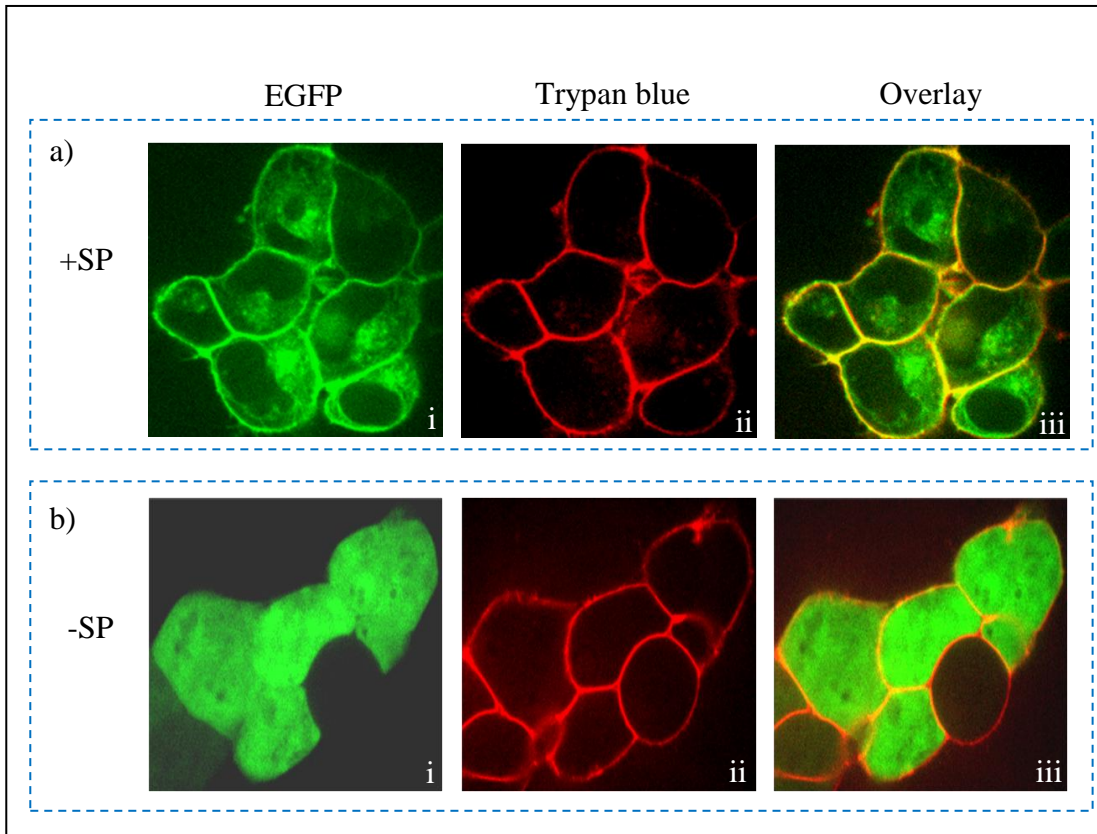


Figure 4.15. Confocal images of live cells with transient expression of the E34R mutated GLP-1Rs both either with or without the signal peptide sequence. HEK293 cells were transiently transfected with HA-E34RGLP-1R-EGFP either with (+SP) or without (-SP) the signal peptide sequence. The EGFP fluorescence is shown in green (a, i & b, i); the cell membrane was stained with trypan blue and is shown in red (a, ii & b, ii) and; EGFP and trypan blue fluorescence signals were computer-overlaid (a, iii & b, iii). Images represent 3 independent experiments.

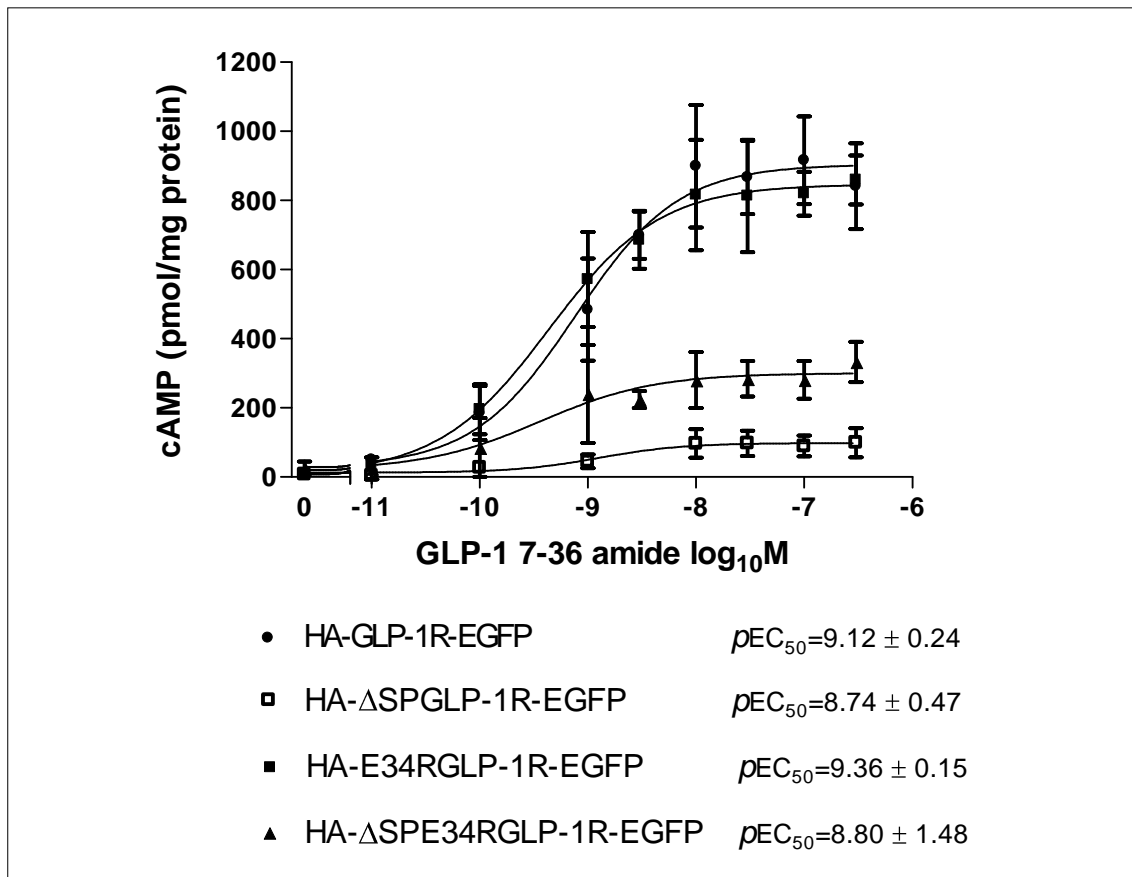


Figure 4.16. Functional coupling of the unmutated GLP-1R and E34RGLP-1R either with or without the signal peptide sequence. HEK293 cells were transiently transfected with the N-terminal HA-tagged and C-terminal EGFP-tagged receptor constructs. These were either the unmutated wild-type or E34 mutated GLP-1R that either containing (HA-GLP-1R-EGFP and HA-E34RGLP-1R-EGFP) or without (HA- Δ SPGLP-1R-EGFP and HA- Δ SPE34RGLP-1R-EGFP) the signal peptide sequence. The transfected cells were challenged with GLP-1 7-36 amide at the concentrations indicated in the absence of IBMX and cAMP levels determined after 10min stimulation. Data are mean \pm sem, n=3–6. pEC_{50} values are indicated

4.3 Discussion

In this chapter, a range of epitope-tagged mutated GLP-1Rs either with or without the putative signal peptide sequence were generated and transiently transfected in HEK293 cells to investigate whether or not the signal peptide sequence was cleaved from the protein and to explore potential roles of the signal peptide. The evidence shown here indicates that the GLP-1R indeed contains a cleaved signal peptide sequence, which is not contained either in the mature form (fully glycosylated) or in the immature form (partially glycosylated) of the receptor. The receptors cannot be expressed if the signal peptide sequence is removed, implying this sequence is essential for SRP-mediated ER targeting and therefore absolutely required for expression of the receptor. Blocking the cleavage of the signal peptide does not affect the synthesis of GLP-1R but results in an immature form, which is non-functional and lacks cell surface localization. This suggests that cleavage of the signal peptide is required for the processing and trafficking of the GLP-1R.

4.3.1 The signal peptide is required for biosynthesis of the GLP-1R

Once the biosynthesis of a GPCR is initiated by the start codon included in the mRNA sequence, at least four molecular steps are required for SRP-mediated ER targeting: 1) recognition and assembly of the SRP-RNC complex; 2) delivery of the RNC complex to the ER membrane *via* SRP-SR binding; 3) unloading and transfer of the RNC complex from the SRP to the translocon complex and; 4) releasing and recycling of the free SRP and SR (Pitonzo et al., 2009; Zhang et al., 2009). Although there are too many molecular interactions involved to fully understand the SRP-

mediated ER targeting, previous studies have demonstrated this is a rate-dependent process and affected by signal sequence variation (Mitra et al., 2006; Pitonzo et al., 2009; Kida et al., 2009; 2010). For example, higher affinity stable SRP-RNC complexes accelerate SRP-SR complex assembly over 100-fold (Zhang et al., 2009). Previous studies have shown that SRP binds to the RNC complex immediately after the hydrophobic core of a signal sequence is exposed and that elongation arrest occurs subsequently (Halic et al., 2004; Egea et al., 2005). Studies on a model secretory protein, proOmpF-Lpp, reveal that the maximal efficiency of elongation arrest is obtained with only 8-12 hydrophobic residues (Hatsuzawa et al., 1997). More recent studies show that the affinity of SRP for the RNC complex can be detected even before nascent chains have emerged from the tunnel and is thus related to the general translational status of the ribosome rather than to direct interaction between the SRP and the nascent chain (Bornemann et al., 2008; Lakkaraju et al., 2008; Grudnik et al., 2009). Thus, it appears that it is not difficult for a hydrophobic sequence to cause binding of the SRP but the targeting may not complete due to insufficient stability of the SRP-RNC complex (Janda et al., 2010). On the other hand, for the small group of GPCRs possessing a signal peptide sequence, this sequence is not a unique hydrophobic region as transmembrane domains are known to have a characteristically hydrophobic amino acid distribution (White et al., 2001; Sadka and Linial et al., 2005; Lavoie and Paiement, 2008). When the signal peptide sequence is removed, the first following hydrophobic region may be able to fully or partially take over the role and serve as a signal anchor.

The GLP-1R contains a relatively hydrophobic region in the N-terminal domain shortly after the signal peptide sequence (Gly²⁷-Try³⁹). In the N-terminal EGFP-tagged

GLP-1R containing the signal peptide sequence (EGFP-GLP-1R-HA), it is possible that the SRP recognizes and binds to the RNC containing the emerging h-core of the original signal peptide sequence (residues Ala²-Pro²³) with high affinity and that this is sufficient for all of the molecular steps of targeting so that receptor is expressed. Thus, the EGFP-GLP-1R-HA can be detected by either an anti-EGFP or anti-HA antibody and EGFP-fluorescence can be visualised. In contrast, when the signal peptide sequence is removed (Ala²-Pro²³), the first hydrophobic sequence, possibly TM1 emerging from the ribosome may also cause SRP binding to the RNC complex when it emerges from the ribosome. Recent evidence shows that the signal sequence variation affects interaction with the translocon (Hegde and Bernstein, 2006). Thus, the hydrophobic sequence following the signal peptide may be sufficient for elongation arrest but not for the remaining molecular steps required for ER targeting. Indeed, the expression of the EGFP-ΔSPGLP-1R-HA was only detected by an antibody to the N-terminal EGFP-tag (but not anti-HA antibody) with an immunoreactive band (~30kDa) slightly higher than EGFP alone (~27kDa). Further, the HA-ΔSPGLP-1R-HA could not be detected, indicating the synthesis of both constructs was stopped at a very early stage. This implies that the SRP-RNC complexes containing the small nascent polypeptide chain of the ΔSPGLP-1R remaining in the cytosol cannot target the ER membrane and thus synthesis cannot restart. This is also supported by the pattern of EGFP fluorescence in the cells transfected with the same construct (EGFP-ΔSP-GLP-1R-HA). Thus, fluorescence is located throughout the cytosol in a pattern consistent with that of a soluble, cytoplasmically located protein such as EGFP. There may be insufficient positive charge in the N-terminus of the construct for membrane integration (Kida et al., 2000; Bange et al., 2007; Zhang et al., 2009) following signal peptide removal thereby

preventing further synthesis and resulting in an apparently unrestricted sub-cellular distribution. This was confirmed by mutation of the negatively charged Glu³⁴ to the positively charged arginine (E34R). Thus, even in the absence of a signal peptide, this construct was synthesised and at least a proportion trafficked to the plasma membrane where it evoked cAMP production in response to GLP-1 7-36 amide. Interestingly EGFP-fluorescence of the HA-E34RΔSPGLP-1R-EGFP construct was also predominately cytosolic, indicating some proteins were located in the cytosol while others inserted into the ER membrane and were then processed in a similar way to the receptor containing the signal peptide. It is unclear whether the E34R mutation leads to a reduction in the affinity for the SRP despite an increased facility for gating the translocon complex. However, all findings here are consistent with recent studies, which revealed that the great variation in both overall length and amino acid composition of signal sequences influence both the selection of protein targeting pathways and the interactions with the translocon (Kida et al., 2000; Hegde and Dornstein, 2006; Kramer et al., 2009).

Although a signal peptide only exists transiently during the synthesis of the receptor, the sequence, length and even the flanking sequence ensure the signal peptide performs its important roles in modulating protein targeting, translocation, its own cleavage and even post-cleavage events (Hedge and Bernstein, 2006; Choo and Ranganathan, 2008; Kida et al., 2010). This is reflected in the variation of the results following the removal of the signal peptide sequence in GPCRs and other membrane proteins. The Family A endothelin B GPCR is still expressed following removal of its signal peptide sequence but this causes retention within the ER. This suggests that another region, possibly the first TM domain, provides good ER-gating but the N-

terminal domain of the receptor cannot be post-translationally translocated across the ER membrane (Köchler et al., 2002). Similarly, the Family B vasoactive intestinal polypeptide type-1 receptor is synthesized but not trafficked to the plasma membrane in the absence of its signal peptide (Couvineau et al., 2004). The mutated Family B CRF-R₁ lacking the signal peptide displays wild-type properties with respect to ligand binding and activation of AC. However, this mutant receptor is expressed at 10-fold lower levels than the wild-type receptor containing the signal peptide sequence due to decreased translation levels (Alken et al., 2005). The evidence shown in the present study reveals that the signal peptide of the GLP-1R is essential for receptor synthesis but cleavage is not.

4.3.2 Cleavage of the GLP-1R signal peptide

Most integral membrane proteins are synthesized by ribosomes bound to the ER membrane *via* SRP-mediated ER targeting, which is highly reliant on the signal sequence within proteins. Of the two types of signal sequences, the signal peptide sequence is cleaved by signal peptidases in the ER lumen after it is inserted into the ER membrane. In contrast, a signal anchor sequence is not cleaved and forms part of the mature protein (Hegde and Bernstein 2006; Schrul et al., 2010). The majority of GPCRs are predicted to contain a signal anchor sequence which forms a part of a transmembrane domain (usually TM1) of the mature receptor, while only ~5% of GPCRs contain a putative signal peptide sequence (Wallin and von Heijne, 1995). Although only a small group of GPCRs including most Family B members are predicted to have a cleaved signal peptide sequence, this cleavage does not always occur. For example, the signal peptide of the CRF-R₁, the vasoactive intestinal peptide-1 receptor,

endothelin B receptor and PTH/PTHrP receptor are cleaved whereas the putative signal peptide of the CRF-R_{2(a)} is not cleaved and forms part of the mature receptor (Shimada et al., 2002; Couvineau et al., 2004; Alken et al., 2005; Rutz et al., 2006). To predict whether a protein contains a cleaved signal peptide is difficult and there are different outcomes among the available algorithms. Amongst these algorithms, ~90% is the highest accuracy of prediction (SignalP 3.0; Choo et al., 2009). In addition, it seems more difficult to predict a relatively long signal peptide (>30 amino acids). For example, in a recent benchmark using a set of 136 eukaryotic proteins containing long signal peptides as reference, the best prediction tool only detected 63% (Hiss and Scheneider, 2009). Using the program SignalP 3.0, although a high probability is predicted for the wild-type GLP-1R to have a signal peptide by both SignalP-NN (0.819) and SignalP-HMM (0.999), the most probable cleavage site is predicted differently between Pro²³ and Arg²⁴ or Ala²¹ and Gly²², respectively. The addition of a small HA epitope tag at the N-terminus elongates the putative signal peptide from 23 to 32 amino acids and this resulted in conflicting predictions for epitope-tagged GLP-1R constructs. For example, SignalP-NN predicted that the HA-GLP-1R did not contain a signal peptide (S-mean lower its cut-off) but cleavage is still predicted (Y-max slightly higher than cut-off). By mutation of a critical residue at the predicted cleavage site, the HA-A21R-GLP-1R was predicted to not have a signal anchor sequence by either Signal-NN or SignalP-HMM. Furthermore SignalP 3.0 failed to predict a signal peptide sequence in the EGFP-GLP-1R-HA. In the present study, using the N-terminally HA-tagged GLP-1R constructs (HA-GLP-1R, HA-GLP-1R-EGFP), cleavage of the signal peptide was confirmed experimentally. In cells with expression of these constructs, HA immunoreactivity was not detected, although both binding and cAMP production were

consistent with that of the wild-type, untagged GLP-1R. In cells transfected with the construct containing both an N-terminal HA-tag and C-terminal EGFP-tag (HA-GLP-1R-EGFP), the pattern of EGFP immunoreactivity (~66kDa and 93kDa) and EGFP fluorescence at the plasma membrane were similar with those in cells transfected with the construct that contained only a C-terminal EGFP-tag (GLP-1R-EGFP). This indicates that the N-terminal HA-tag of HA-GLP-1R-EGFP is cleaved along with the signal peptide of the GLP-1R at a very early stage. These data provide the first experimental evidence for cleavage of the signal peptide of the GLP-1R. Thus, incorporation of the signal peptide structure within models of the extracellular, N-terminal domain of the GLP-1R (Lin and Wang, 2009) is not required when modelling the mature receptor.

In contrast to the HA-GLP-1R-EGFP construct, the EGFP-GLP-1R-HA construct was generated by fusing an EGFP-tag to the N-terminus of the GLP-1R and an HA-tag to the C-terminal. In this construct the EGFP-tag was directly next to the signal peptide sequence. This resulted in a lack of signal peptide cleavage, which was supported by both immunoreactivities of EGFP and HA being detected, indicating synthesis and retention of a full-length receptor. However, all experimental evidence including immunoblotting, agonist binding, receptor coupling and EGFP fluorescence distribution suggested this was a non-functional and immature form of the receptor (**see Chapter 3**). In order to distinguish the role of signal peptide cleavage from the presence of the N-terminal EGFP-tag on receptor trafficking, A21R mutated HA-GLP-1R-EGFP (HA-A21RGLP-1R-EGFP) was generated to block the cleavage site according to the -3 and -1 rule (von Heijne, 1990). For the constructs EGFP-GLP-1R-HA and HA-A21RGLP-1R-EGFP, only one immunoreactive band with molecular size at ~66kDa was detected

by either the anti-HA antibody or anti-GFP antibody. Further, there was intracellular EGFP-fluorescence and dramatically reduced GLP-1 7-36 amide-mediated cAMP elevation, suggesting that in the absence of cleavage of the signal peptide the receptor is expressed but not processed. These data suggest that the lack of cleavage may affect the co-translational folding of the GLP-1R and further block receptor trafficking to the Golgi and hence prevent full glycosylation.

Cleavage of signal peptide is a requirement for the processing and trafficking of for secretory proteins containing a cleaved signal peptide. The cleavage is crucial to process the preproteins to proteins and thus a block or delay of signal peptide cleavage may cause pathologic changes. For example, the cationic trypsinogen gene is expressed as pre-trypsinogen containing a cleaved signal peptide sequence (Chen et al., 2003), which is removed upon entry into the ER lumen. Trypsinogens are processed from pre-trypsinogen by the cleavage of the signal peptide and packaged into zymogen granules and eventually secreted into the pancreatic juice (Király et al., 2006). A cleavage site mutation in the cationic trypsinogen gene, which interferes with signal peptide cleavage, has been identified in chronic pancreatitis and in hereditary pancreatitis families (Witt et al., 1999; Patuzzo et al., 2003). In addition, the A24D mutation, associated with neonatal diabetes, is retained in the ER and not efficiently secreted as this mutation affects the efficiency of the signal peptide cleavage (Park et al., 2010). Similarly, as polytopic integral membrane proteins, the $\text{Na}^+/\text{Ca}^{2+}\text{-K}^+$ exchanger (NCKX) proteins contain a cleavable signal peptide. When expressed in HEK293 cells, both NCKX proteins with and without the signal peptide cleaved can be detected in whole cell lysates. However, consistent with the GLP-1R, only NCKX proteins in which the signal peptide is cleaved are present in the plasma membrane (Kang and Schnetka, 2003).

Similarly, the calcium-sensing receptor is a Family C GPCR and contains a cleaved signal peptide sequence (residues Met¹-Ala¹⁹). Two peptide missense mutations (L11S; L13P) within the h-core of the signal peptide sequence have been identified in patients with familial hypocalciuric hypercalcemia (Pidasheva et al., 2005). When expressed recombinantly *in vitro*, these two single mutations reduce both intracellular and plasma membrane expression. In contrast to the GLP-1R, the putative signal peptide of CRF-R_{2a} is not cleaved. Indeed, cleavage of this sequence results in an increase in the amount of immature and intracellularly retained receptor (Rutz et al., 2006). Along with the findings of the present study, this might suggest that the effect of the cleavage of a signal sequence in processing and trafficking of the protein may depend on whether it is naturally cleaved.

Although it is thought that cleaved signal peptides are degraded rapidly (Martoglio and Dobberstein, 1998), recent studies reveal that some liberated signal peptides are further processed by the intramembrane-cleaving aspartic protease signal peptide peptidases, suggesting post-cleavage roles of the signal peptide (Lemberg and Martoglio, 2002; Martoglio, 2003; Schröder et al., 2010). More recently, a study has shown that signal peptide peptidase assembles with the cleaved signal peptide and newly synthesized misfolded membrane proteins into distinct oligomeric complexes, implying that the liberated signal peptide or its fragments released upon intramembrane cleavage may promote the folding of membrane proteins (Schrul et al., 2010). All of these highlight the necessity to experimentally verify whether a GPCR possesses a cleaved signal peptide.

A recent study reveals that a sequence (residues Glu²⁸-Try⁵⁴) after the signal peptide sequence (residues Met¹-Gly²⁶) of the endothelin B receptor assists the signal peptide in ensuring efficient translocon gating at the ER membrane (Alken et al., 2009). Removal of this domain leads to a marked decrease of receptor expression but does not affect the function or sub-cellular localization of the receptor. Reinserting this sequence into the receptor but with a C-terminal shift (between Pro⁸¹ and Pro⁸²) results in a wild-type-like receptor, indicating that this sequence does not need to directly follow the signal sequence for its function. Taking these data and the findings here, it may be speculated that the cleavage of a signal peptide might be also required to allow the following sequence to perform its function. More recently, it was shown that one of the missense variants (C46S) in the sequence following the signal peptide (residues Met¹-Thr²⁵) of the other human incretin receptor, the GIP receptor, abolishes agonist affinity (Fortin et al., 2010). Missense mutations within or close to the signal peptide sequence of the GLP-1R including P7H, R20K and R44H previously reported (Fortin et al., 2010) along with the E34R mutation described in the present study do not affect the pharmacological properties of the receptor. There is evidence that the expression of GLP-1R is down-regulated in type 2 diabetes (Xu et al., 2007; Shu et al., 2009). However, it is not clear whether pathological cellular signals, for example ER stress in disease states such as diabetes could affect the expression, processing and trafficking the GLP-1R through a low rate of translocon gating or an inefficient cleavage of the signal peptide.

CHAPTER 5 A Small-molecule Agonist and a Potential Endogenous Agonist of the GLP-1R

5.1 Introduction

Both GLP-1 7–36 amide and GLP-1 7–37 bind to the GLP-1R with similar affinity and show similar potency (Orskov et al., 1993). Besides native GLP-1, the *Heloderma suspectum* (Gila monster) peptides, exendin-3 and exendin-4 also act as agonists for the GLP-1R (Göke et al., 1993; Thorens et al., 1993). Both exendin-3 and exendin-4 are composed of 39 amino acids with approximately 50% sequence identity to GLP-1 7–36 amide but with an additional C-terminal extension of 9 residues (Mann et al., 2007; **Figure 5.1**). Exendin-4 differs from exendin-3 by two amino acid substitutions near the N-terminus, Gly²-Glu³ in place of Ser²-Asp³, but otherwise is identical (Eng et al., 1992). In contrast to active forms of GLP-1 (GLP-1 7-36 amide and GLP-1 7-37), neither exendin-4 nor exendin-3 contain alanine at position 2 (**Figure 5.1**) with the result that both are resistant to DPP-IV-mediated inactivation. Hence, synthetic exendin-4 (Exenatide) has been used for the treatment of type 2 diabetes (see **Chapter 1**). A truncated version of exendin-4 (by 8 residues at its N-terminus), exendin 9-39 (**Figure 5.1**) binds to the GLP-1R (Runge et al., 2008) with similar affinity to the full-length exendins (López de Maturana and Donnelly, 2002), and functions as an antagonist or even an inverse agonist (Göke et al., 1993; Thorens et al., 1993; Serre et al., 1998). Based on the ligands mentioned above, labeled ligands such as fluorescein-Trp²⁵-exendin-4 (Chicch et al., 1997), [¹²⁵I]-GLP-1 and Tyr³⁹-exendin-4 have been

successfully utilized for *in vitro* (Thorens et al., 1993) and *in vivo* ligand binding studies (Kolligs et al., 1995).

Currently it is thought that regions in the N-terminus and the extracellular loops together with TM6 of Family B receptors are involved in the binding of endogenous peptide (orthosteric) ligands (Lagerström and Schiöth, 2010). In addition, the current two-domain binding model of Family B GPCRs describes that the C-terminus of orthosteric ligand binds to the N-terminal domain of the receptor (Hoare, 2005). Consistent with this, the recent crystal structure of the isolated N-terminal domain of GLP-1R has shown to bind with the C-terminus of GLP-1 7-37 (Underwood et al., 2010).

Although DPP-IV-resistant GLP-1 mimics (e.g. Exenatide and Liraglutide) have become available for the treatment of type 2 diabetes, the patients using them have to face some general disadvantages of peptide therapeutics. For example, these peptide drugs must be administered at least once-daily by subcutaneous injection. They can also be antigenic and they are certainly expensive. Problems such as proteolytic degradation, fast clearance in the body, low solubility in water and immunogenicity have to be overcome or minimised (Bellmann-Sickert and Beck-Sickinger, 2010). Recently, a series of 11-amino acid GLP-1R agonists with high potencies and excellent *in vivo* activities in an ob/ob mouse model of diabetes have been reported (Mapelli et al., 2009; Haque et al., 2010). These peptide compounds consist of a structurally optimized 9-mer, which is closely related to the N-terminal 9 residues of GLP-1, but substituted with several unnatural amino acids including a C-terminal biphenylalanine dipeptide. This opens a new opportunity for developing small peptidic GLP-1R agonists with an

increased stability against proteolytic degradation and decreased immunogenicity. However, small-molecule ligands are most favourable for therapeutic use as they often have activity following oral administration. Two substituted cyclobutane derivatives, Boc5 and S4P (**Figure 5.2a**) were found following screening of a library containing nearly 50,000 compounds using a cell line stably co-expressing GLP-1Rs and a cAMP-responsive reporter (Chen et al., 2007). These compounds bind to the GLP-1R and increase intracellular cAMP production. They are full agonists and their effects can be blocked by exendin 9–39, indicating an involvement of binding within the orthosteric site. Boc5 also amplifies glucose-stimulated insulin secretion in isolated rat islets, inhibits food intake and reduces HbA1c to non-diabetic values in db/db mice (Su et al., 2008). Thus Boc5 highlights the potential of orally available GLP-1R agonists in the treatment of diabetes and obesity.

Beyond orthosteric sites, many GPCRs have been shown to have allosteric binding sites that are spatially and often functionally distinct (Schwartz and Holst et al., 2007). Examples of such allosteric sites have been found in all families of GPCRs (Wang et al., 2009) and it could be speculated that all GPCRs are likely to have such sites. For small-molecule allosteric modulators, the compounds themselves do not have agonist activities but bind to allosteric sites of the receptor and increase or decrease the binding and/or efficacy of an orthosteric agonist. Such ligands are often termed either PAMs or NAMs dependent on their effects (De amici et al., 2010). In contrast, some small-molecules are able to bind to allosteric sites of the receptor and provide agonism (ago-allosteric agents). Such agents may or may not influence the binding or efficacy of compounds acting at the orthosteric site (**see Chapter 1**). Compounds with allosteric or ago-allosteric properties are considered good possibilities for improved and novel

therapeutics (Bridges and Lindsley, 2008). Cinacalcet is a first commercially available allosteric drug targeting GPCRs, which is sold by Amgen (Thousand Oaks, California) under the trade name Sensipar in North America and Australia and as Mimpara in Europe. Cinacalcet is a mimic of Ca^{2+} -ion binding to an allosteric site of the calcium-sensing receptor, a Family C GPCR (De Amici et al., 2010). Recently, a small-molecule “compound 1” (2-(2'-methyl)thiadiazolylsulfanyl-3-trifluoromethyl-6,7-dichloroquinoxaline) has been discovered to act as a low-affinity, low-potency, ago-allosteric compound at the GLP-1R (Knudsen et al., 2007). An effort to convert compound 1 to a more potent agonist resulted in the development of compound 2 (**Figure 5.2b**), which stimulates cAMP production in membranes generated from baby hamster kidney cells expressing recombinant hGLP-1R and shows a bell-shaped concentration-response curve (Knudsen et al., 2007). Compound 2, is an ago-allosteric agent at the GLP-1R, not only increasing the affinity of the GLP-1R for GLP-1 but itself acting as an agonist without being inhibited by the orthosteric antagonist, exendin 9-39 (Knudsen et al., 2007). Compound 2 has recently been assessed *in vivo* in comparison to native GLP-1 and the mimics, Exenatide and Liraglutide. In that study, compound 2 effectively stimulated insulin secretion but with lower potency than GLP-1 or the mimetics (Irwin et al., 2010). Although combined injection of compound 2 with either Liraglutide or Exenatide did not substantially improve glucose-lowering or insulin-releasing responses in mice (Irwin et al., 2010), this still indicates a useful starting point for the identification or design of orally active allosteric GLP-1R compounds.

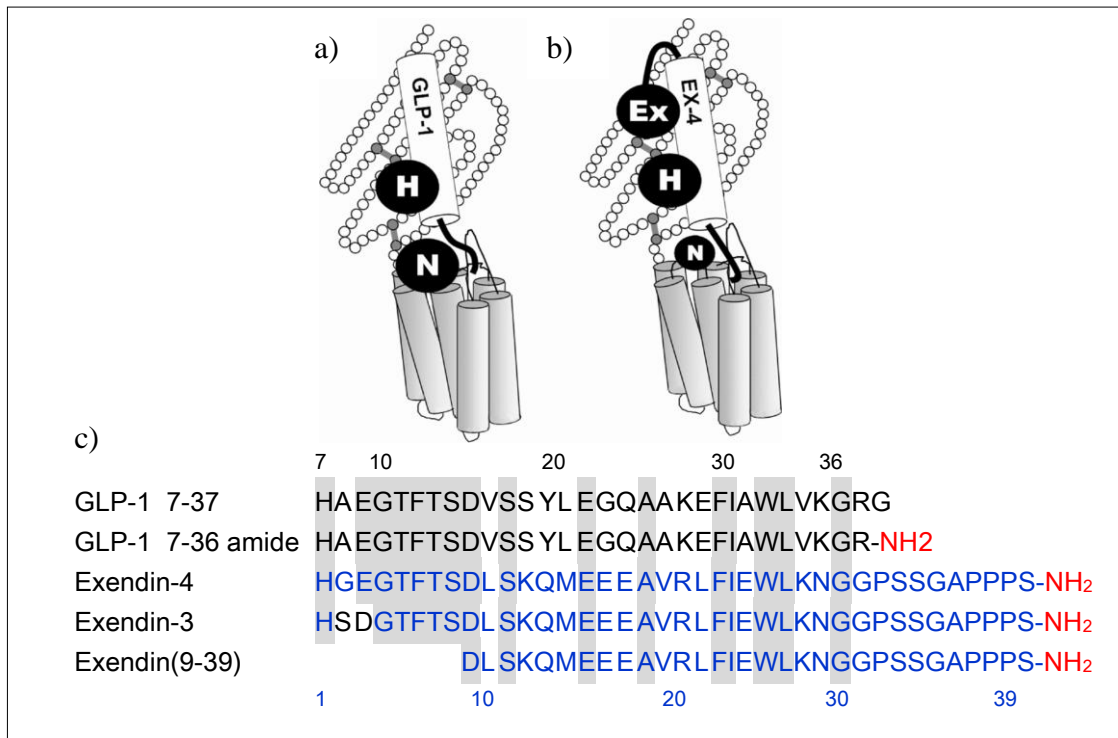


Figure 5.1. Models of GLP-1 (a) and exendin-4 (b) binding to the GLP-1R. The interactions N, H and Ex are depicted. N describes an interaction between the N-terminal region of the peptide and the core domain of the GLP-1R; this interaction is stronger for GLP-1 than for exendin-4. H describes the interaction between the helical region of the peptides and the N-domain of the receptor; this accounts for approximate 80% of the binding energy for both peptides. Ex describes an interaction absent from GLP-1 that accounts for exendin-4's C-terminal affinity and its ability to bind with high affinity to the isolated N-terminal domain of the GLP-1R (Runge et al., 2007). It is dependent, either directly or indirectly, upon the nine-residue C-terminal extension which forms the Trp-cage. EX-4 represents exendin-4. (c) **Amino acid sequence of GLP-1 and exendin peptides.** The amino acid residues highlighted in gray are conserved with GLP-1 7-36 amide. The sequences in blue are conserved with exendin-4. Picture adapted from Mann et al., 2007.

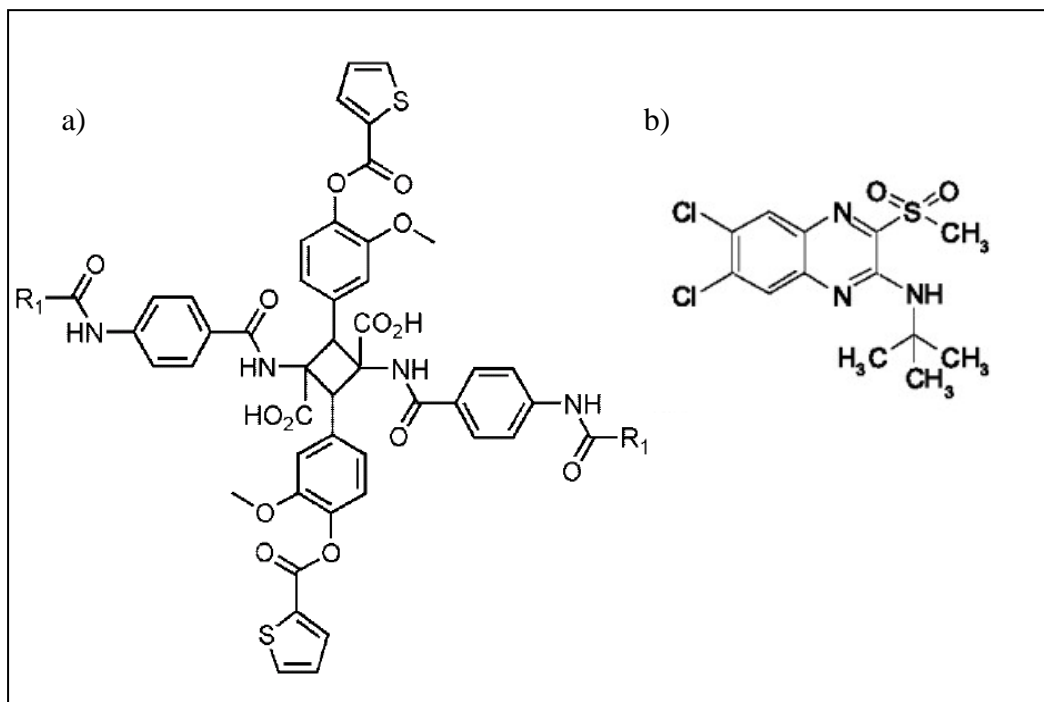


Figure 5.2. Non-peptide ligands of the GLP-1R. Compound 2 (a), Boc5 and S4P (b) are the examples of novel small molecular non-peptide ligands of the GLP-1R. R_1 represents cyclopentyl and $\text{OC}(\text{CH}_3)_3$ in Boc5 and S4P, respectively. Picture from De amichi et al., 2010

Recently an alternative ligand-induced activation for Family B GPCRs has been proposed, in which binding of orthosteric agonists allows a segment (acting as the endogenous agonist) at the N-terminal domain of their receptors to interact with another part of the receptor and cause the agonism (Beinborn, 2006). This hypothesis initially arose from observations on a Family B GPCR, the secretin receptor, in which secretin peptides with minor N-terminal modifications that no longer directly interacted with the main body of the receptor, still acted as full agonists (Dong et al., 2005). The argument was that this could not be explained by the current ligand binding model of Family B GPCRs. Thus, several synthetic peptides were then investigated and it was found that WDN, corresponding to the sequence of Trp⁷⁰-Asn⁷² in the N-terminus of the secretin receptor acts as a full agonist of the receptor (Dong et al., 2006). More recently, during the course of the present study, NRTFD, corresponding to Asn⁶³-Asp⁶⁷ of the GLP-1R has been described as an endogenous agonist of the GLP-1R (Dong et al., 2008). These studies have suggested that an endogenous agonist is a common structural feature of Family B GPCRs, since such synthetic peptides also activate other receptors in this family, e.g. the vasoactive intestinal polypeptide receptor 1.

Interestingly, both WDN and NRTFD are active at the secretin receptor and the GLP-1R and work with similar potency and efficacy even though the secretin receptor has no primary sequence of NRTFD and WDN does not occur within the GLP-1R (**Figure 5.3**). In contrast, the calcitonin receptor contains NRTWD and WDG in which only one residue is replaced compared with NRTFD and WDN, respectively (**Figure 5.3**). However, neither NRTFD nor WDN are active at the calcitonin receptor. In addition, the asparagine residue in either NRTFD, NRTWD or WDN of the Family B GPCRs is located in a sequon (Asn-X-Ser/Try) and represents a potential *N*-linked

glycoylation site (**Figure 5.3**). Furthermore, Asp⁶⁷ (the 'D' of NRTFD) has a critical role in forming intramolecular interactions with other residues within the N-terminal domain as shown in the recent crystal structure of the GLP-1-bound GLP-1R extracellular domain (Underwood et al., 2010). In this model, the side chain of Asp⁶⁷ directly interacts with Arg¹⁰² and with Arg¹²¹ through a water molecule. Both Arg¹⁰² and Arg¹²¹ further interact with many other residues within the N-terminal domain of the GLP-1R. Therefore, it seems difficult for Asp⁶⁷ to be exposed during ligand binding while playing a critical role in stabilising the structure of the hydrophobic binding cavity of the GLP-1R for the C-terminal of the ligand. Consequently, despite extensive pharmacology around the endogenous peptide ligand of the GLP-1R (Dong et al., 2008), the concept of an endogenous agonist of the GLP-1R needs further investigation.

In this chapter, allosteric agonism of compound 2 was examined and compared to that of the orthosteric agonist, GLP-1 7-36 amide, at both wild-type and N-terminal truncated GLP-1Rs. Real-time receptor internalization mediated by allosteric or orthosteric ligands were also observed and determined in HEK293 cells with stable expression of the GLP-1R-EGFP. In addition, the potential endogenous agonist on the GLP-1R was assessed by generating synthetic peptides (representing endogenous sequences) and receptor mutants based on the key residue of the endogenous agonist.

GL-R	54	TELVC	NRTFD	DKYSCW	PDTPAN	TTANIS	CPWYLP
GLP-1R	58	TDLFC	NRTFD	DEYACW	PDGEPG	SFVNVS	CPWYLP
GLP-2R	97	SGIFC	NGTFD	QYVCW	PHSSPG	NVS	-VPCPSYLP
SCTR	62	PVPGC	EGMWD	NI	SCWPS	SVPGRMVE	VECP RFLR
VIPR1	59	ETIGC	SKMWD	NI	TCWPA	TPRGQVVV	LACPLIFK
VIPR2	48	KHKAC	SGVWD	NI	TCWRP	ANVGETVT	VPCPKVFS
PACAP	50	SSPGC	PGMWD	NI	TCWKP	AHVGE	MVLVSCPELFR
CALCR	68	EGPYC	NRTWD	GWLCW	DDTPAG	VL	SYQFCPDYFP
CALCRL	61	EGVYC	NRTWD	GWLCW	NDVAAG	TE	SMQLCPDYFQ

Figure 5.3. Alignment of a putative endogenous agonist regions in the extracellular domain of Family B GPCRs. The conserved residues in Family B are highlighted in blue. The analogues endogenous agonist sequences are marked: NRTFD in red boxes and WDN in the green box. The sequons (Asn-X-Ser/Trp) are in red. Nine Family B GPCRs listed here include the glucagon receptor (GL-R); the glucagon-like peptide 1 and 2 receptor (GLP-1R, GLP-2R); the secretin receptor (SCTR); the vasoactive intestinal polypeptide receptor 1 and 2 (VIPR1, VIPR2); pituitary adenylate cyclase-activating polypeptide type I receptor (PACAP); the calcitonin receptor (CALCR) and the calcitonin receptor-like receptor (CALCRL).

5.2 Results

5.2.1 Signalling mediated by compound 2

In parallel experiments using the HEK293Flp-In:WTGLP-1R and HEK293:GLP-1R-EGFP cell lines, challenge of the cells with compound 2 for 10min resulted in a concentration-dependent increase in cAMP levels (**Figure 5.4**) with pEC_{50} values of 5.99 ± 0.18 and 5.78 ± 0.23 , respectively, although the E_{max} values were lower in the HEK293:GLP-1R-EGFP cell line (E_{max} values, 1771 ± 109 and 801 ± 65 pmol/mg protein, respectively). However, the concentration-response curve was slightly bell-shaped, with the response reaching a maximum at $10 \mu\text{M}$ and declining thereafter. This is consistent with a previous study, in which compound 2-mediated cAMP responses showed a bell-shaped relationship, most likely due to adverse effects of compound 2 (Knudsen et al., 2007). Since adverse effects of compound 2 on intact cells increase with exposure time (Coopman et al., 2010), a short time-course of cAMP production in the absence of IBMX was carried out in HEK293:GLP-1R-EGFP cells to optimize the time point at which to compare cAMP levels mediated by compound 2 and GLP-1 7-36 amide. The response to a high ($100 \mu\text{M}$) concentration of compound 2 was time-dependent but slower and lower than that to a maximal (100nM) concentration of GLP-1 (**Figure 5.5**). Compound 2-evoked cAMP generation increased up to approximately 5min but then showed a slight decline by 10min (**Figure 5.5b**). The response of the same cells to a maximal (100nM) concentration of GLP-1 was evident at earlier time-points and was still increasing at 10min (**Figure 5.5a**). In addition, cAMP production mediated by GLP-1 (100nM) was significantly greater than that in response to compound 2 ($100 \mu\text{M}$) at all the time points after 30s (**Figure 5.5c**). As a consequence of the reduction in cAMP levels between 5 and 10min during stimulation with compound 2, 5min was

chosen as an appropriate time point for measuring compound 2-mediated cAMP production and used for the following experiments unless otherwise stated.

GLP-1 7-36 amide-mediated cAMP generation was inhibited by the orthosteric competitive antagonist, exendin 9-39 (see **Section 5.1**) in the HEK293:GLP-1R-EGFP cells. A maximal (100nM) concentration of GLP-1 7-36 amide evoked lower levels of cAMP in the presence of exendin 9-39 (100nM) than that caused by the same concentration of GLP-1 7-36 amide alone (**Figure 5.6**). In contrast, parallel experiments showed that the cAMP response to a maximal (100 μ M) concentration of compound 2 in the presence of exendin 9-39 (100nM) was greater than that in the absence of exendin 9-39. The enhanced compound 2-mediated cAMP generation by exendin 9-39 was then investigated using concentrations of compound 2 ranging from 100nM to 100 μ M in a 5min assay in HEK293:GLP-1R-EGFP cells. Exendin 9-39 had little effect on the potency of compound 2 but increased the E_{max} value from 84 \pm 5% to 100 \pm 6% ($p < 0.05$) of the GLP-1 7-36 amide response (E_{max} of GLP-1, 573 \pm 18 pmol/mg protein, $n=3$) (**Figure 5.7**). These data mimic the effect observed in HEK293Flp-In:WTGLP-1R cells carried out parallel in our laboratory (Coopman et al., 2010). In our parallel experiments, exendin 9-39 decreased the potency of GLP-1 7-36 amide from $pEC_{50}=10.15\pm 0.07$ to $pEC_{50}=9.65\pm 0.07$ ($p < 0.001$; **Figure 5.7**).

The activation of G-proteins by GPCRs requires GTP in the system to initiate the reaction. However, a high concentration of GTP may generate relatively high levels of basal (or background) cAMP in assay system using cell membranes (Dimitriadis et al., 1991). In the present study, conditions were optimised (particularly GTP and GDP concentrations, time and membrane concentration; data not shown) such that GTP

(10 μ M) did not generate significant cAMP production in the absence of GLP-1R agonist in the membranes prepared from HEK293Flp-In:WTGLP-1R cells. In these membranes, a concentration of GLP-1 7-36 amide (10nM) that was sub-maximal for cAMP generation in intact cells ($pEC_{50}=10.15\pm 0.07$) evoked significant cAMP generation in the presence of GTP. This was inhibited by a high concentration of exendin 9-39 (1 μ M) but was not significantly inhibited by the lower concentration (100nM) (**Figure 5.8**). In contrast, either concentration of exendin 9-39 (100nM or 1 μ M) enhanced compound 2-mediated cAMP-responses in these membranes (**Figure 5.8**). Consistent with its ability to generate cAMP in a G-protein-independent way through the activation of AC, FSK (10 μ M) evoked robust cAMP production in the same membranes, which was not affected by the presence of exendin 9-39 (**Figure 5.8**).

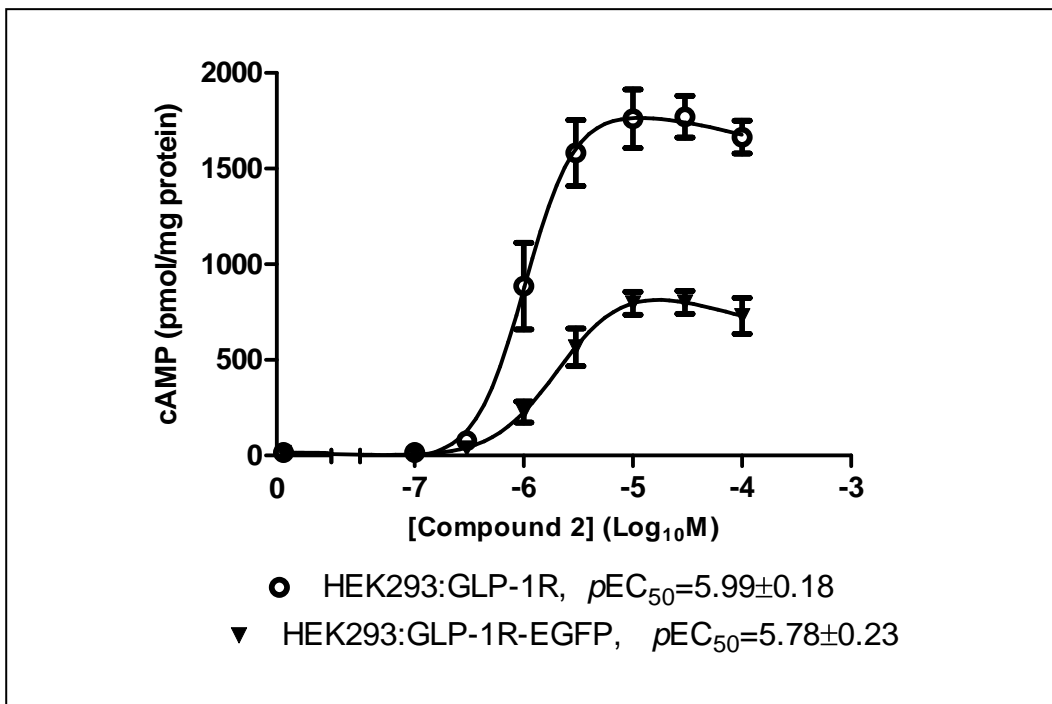


Figure 5.4. Compound 2-induced cAMP generation in cells stably expressing either WTGLP-1R or GLP-1R-EGFP. HEK293Flp-In:WTGLP-1R or HEK293:GLP-1R-EGFP cells were challenged with compound 2 at the concentrations indicated or Basal (0, KHB) for 10min, 37°C, in the presence of IBMX (500µM). The final concentration of DMSO was 5% v:v. Levels of intracellular cAMP were determined and are expressed relative to the cellular protein content. Data are mean±sem, n=6.

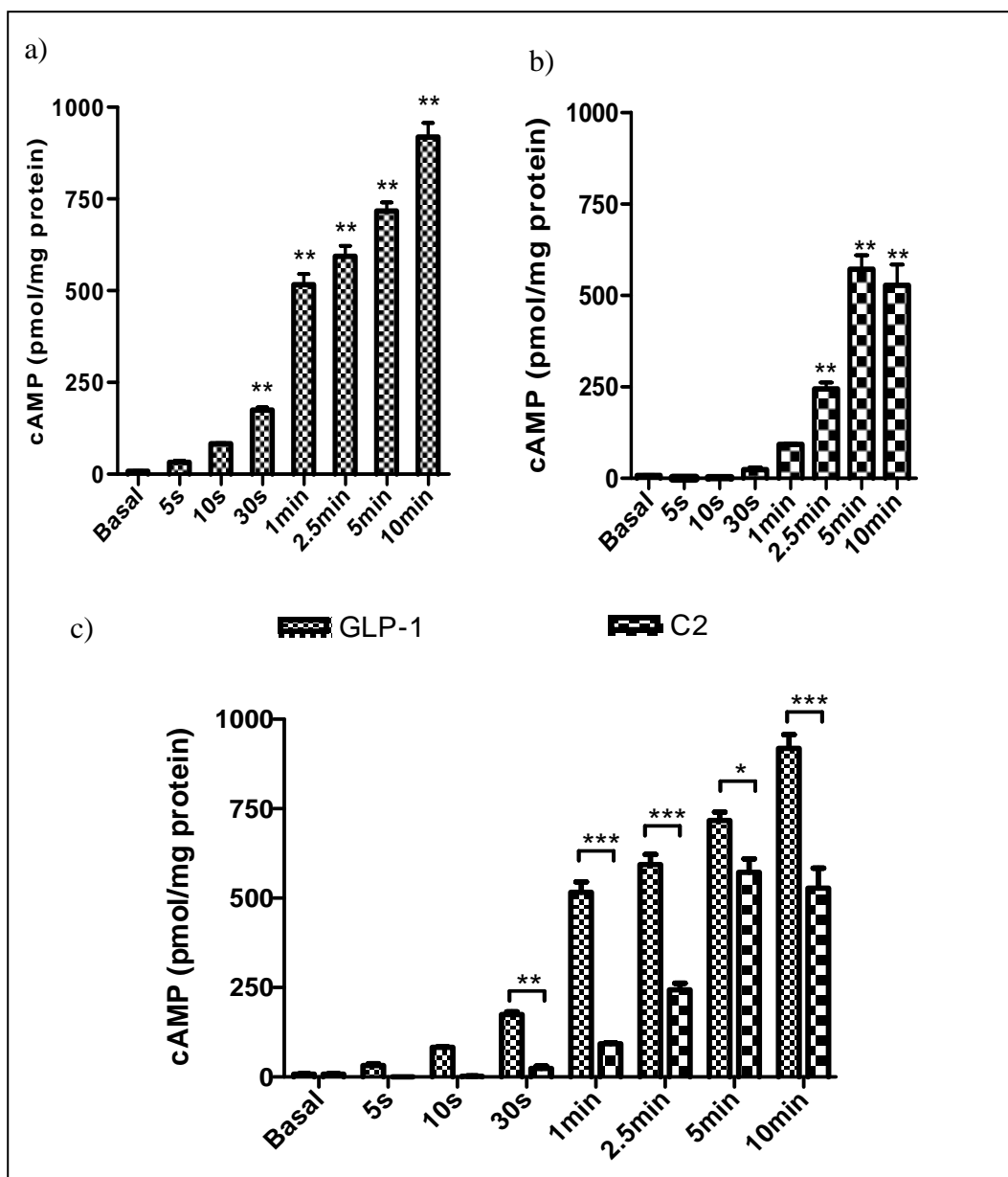


Figure 5.5. Short time-course of compound 2-induced cAMP generation in cells stably expressing GLP-1R-EGFP. HEK293:GLP-1R-EGFP cells were treated with vehicle (Basal, KHB with or without final concentration of DMSO at 10%, v:v) for 10min or challenged with compound 2 (C2) at 100 μ M (containing 10% DMSO) or GLP-1 (100nM) for the times indicated, at 37°C in the absence of IBMX. Levels of intracellular cAMP were determined relative to the cellular protein content. *, p<0.05, **, p<0.01, ***, p<0.001 compared with Basal by Dunnett's test following one-way ANOVA (a & b) or Student's t-test (GLP-1 vs. C2) (c). Data are mean+sem, n=3.

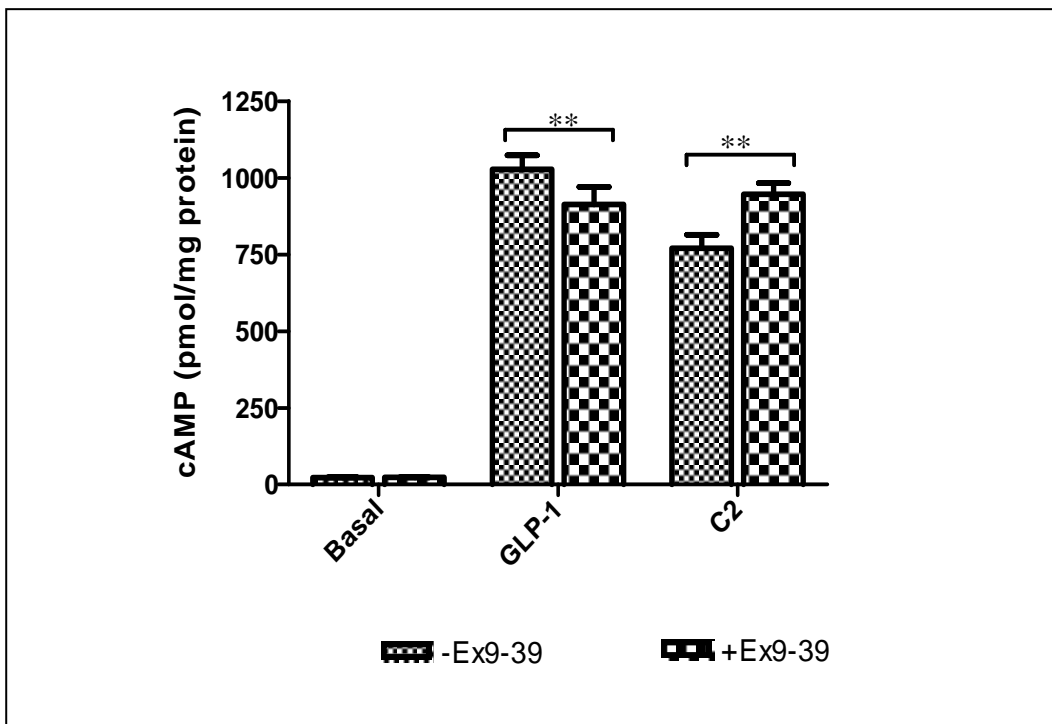


Figure 5.6. Functional interaction of compound 2 with exendin 9-39 and GLP-1 7-36 amide in HEK293 cells with stable expression of GLP-1R-EGFP. HEK293:GLP-1R-EGFP cells were treated with KHB (Basal), GLP-1 7-36 amide (GLP-1, 100nM) or compound 2 (C2, 100 μ M, containing final concentration of 5% DMSO, *v:v*) for 5min in the presence of IBMX (500 μ M). For each condition, exendin 9-39 (100nM) was either absent (-Ex9-39) or present (+Ex9-39). Levels of intracellular cAMP were determined relative to the cellular protein content. **, $p < 0.01$ by paired Student's *t*-test. Data are mean+sem, $n=3$.

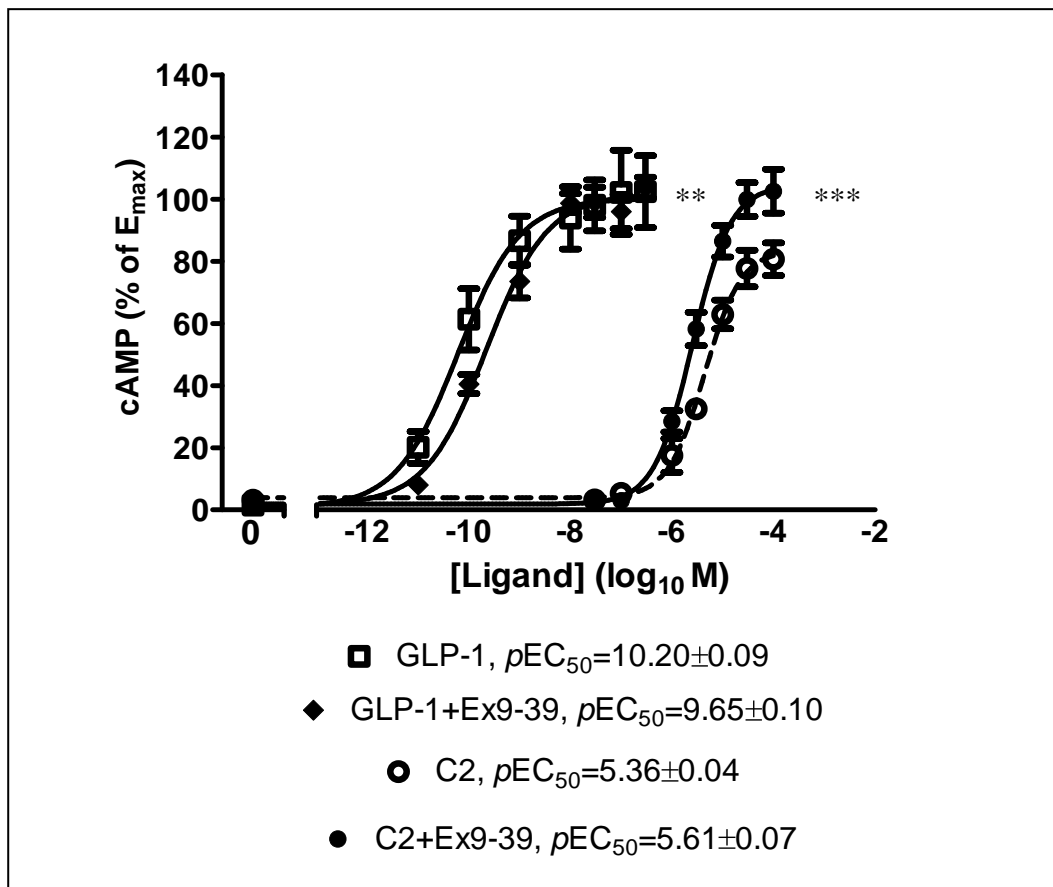


Figure 5.7. Exendin 9-39 enhances compound 2-mediated cAMP generation in HEK293 cells with stable expression of GLP-1R-EGFP. Intact HEK293:GLP-1R-EGFP cells were pre-treated for 10 min with either exendin 9-39 (+Ex9-39, 100nM) or vehicle in the presence of IBMX (500 μ M) before challenge for 5min with the indicated concentrations of GLP-1 7-36 amide (GLP-1) or compound 2 (C2) in the continued absence or presence of exendin 9-39 as indicated. When compound 2 was used, the final concentration of DMSO (vehicle) was 5% v:v. Levels of intracellular cAMP were determined relative to the cellular protein content and expressed as a percentage of the E_{max} of GLP-1 (573 \pm 18 pmol/mg protein). **, $p < 0.01$, ***, $p < 0.001$ by two way ANOVA between +Ex9-39 and -Ex9-39 for each agonist. Data are mean \pm sem, n=6.

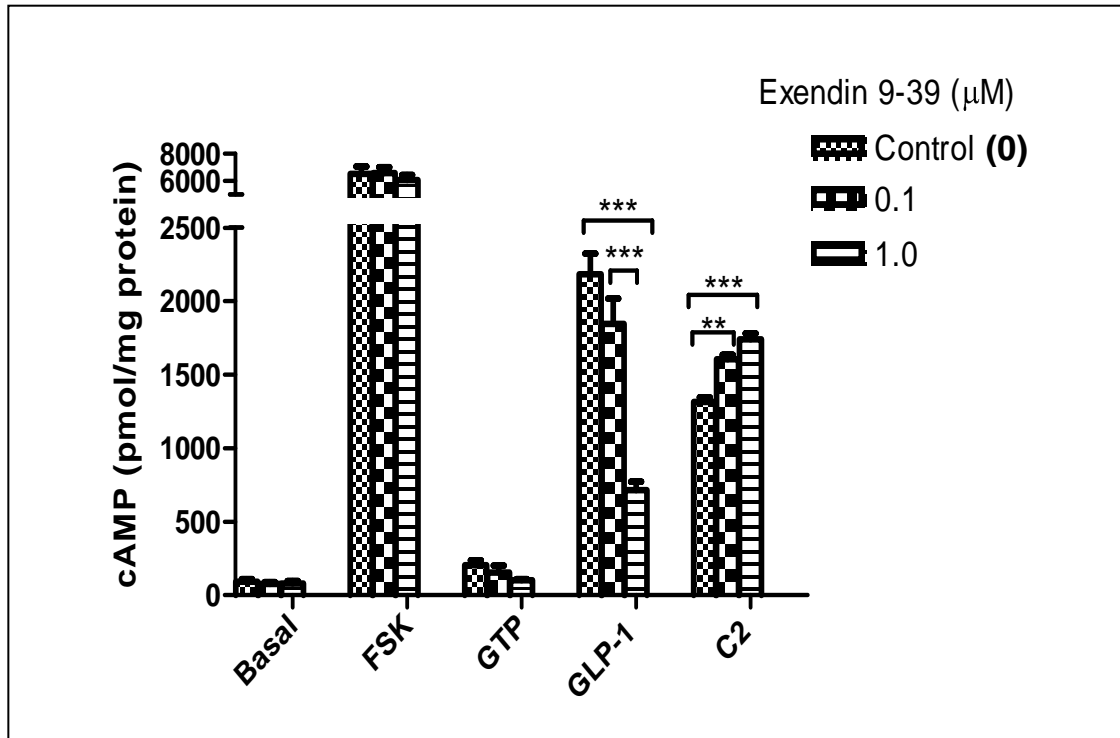


Figure 5.8. Functional interaction of exendin 9-39 with GLP-1 7-36 amide or compound 2 in membranes from HEK293:GLP-1R-EGFP cells. Membranes were prepared from HEK293:GLP-1R-EGFP cells and unchallenged (Basal) or challenged with either forskolin (FSK, 10μM) or GTP (10μM). Alternatively, membranes were challenged with either GLP-1 7-36 amide (10nM) or compound 2 (C2, 100μM) in the presence of 10μM GTP. For each of the conditions, membranes were also co-incubated with exendin 9-39 (0.1 or 1μM), which was then present throughout the assay. Reactions were conducted in the presence of IBMX (1.2mM) at 30°C for 5min and cAMP levels determined and expressed relative to membrane protein. The concentration of GLP-1 7-36 amide used (10nM) was sub-maximal; 100nM GLP-1 7-36 amide generated 8742±133 pmol/mg protein cAMP. All data are mean±sem, n=4. **, $p < 0.01$ and ***, $p < 0.001$ by Bonferoni's test following one-way ANOVA.

5.2.2 *Candidate sequences in the GLP-1R as an endogenous agonist*

The sequence of WDN, corresponding to Trp⁷⁰-Asn⁷² of the secretin receptor has been described as an endogenous agonist (Dong et al., 2006). Thus, synthetic peptides containing this WDN motif, and critically the aspartic acid residue, are able to act as agonists of the secretin receptor (Dong et al., 2006). At the start of this study there was no information relating to the GLP-1R and so, to determine whether the GLP-1R also contains an endogenous agonist, sequences analogous to the WDN motif of the secretin receptor were searched for in the GLP-1R. The N-terminal domain of the GLP-1R contains seven tryptophan residues including Trp³³, Trp³⁹, Trp⁷², Trp⁹¹, Trp¹¹⁰, Trp¹²⁰ and Trp¹²⁰ (see **Chapter 1**). However, only the tryptophan in WET (corresponding to Trp³³-Thr³⁵) is followed by a negatively charged residue (E) and then a polar one (T), which are similar to the aspartic acid and asparagine residues respectively, in the WDN motif. In addition, according to the residues conserved in Family B GPCRs, FDE (corresponding to Phe⁶⁶-Glu⁶⁸ in the GLP-1R) analogous to WDN in the secretin receptor (**Figure 5.3**) and also contains an aspartic acid residue in the middle of the tripeptide. Therefore, these two regions in the GLP-1R were nominated as the endogenous agonist candidates. Two strategies were used to determine whether any of them may act as an endogenous agonist of the GLP-1R. Firstly, short synthetic sequences, WET and FDE, corresponding to Trp³³-Thr³⁵ and Phe⁶⁶-Glu⁶⁸ respectively of the GLP-1R, were synthesized by Cambridge Peptides (CP) (Birmingham, UK). During this study a report emerged that NRTFD, corresponding to Asn⁶³-Asp⁶⁷ of the GLP-1R, formed the endogenous agonist of this receptor, with the aspartic acid residue being critical. NRTFD is slightly N-terminally shifted from the sequence FDE of the GLP-1R but still includes the aspartic acid residue and a sequon (Asn-X-Ser/Trp), “N-X-T” (see

Chapter 3), which is conserved in several Family B GPCRs (**Figure 5.3**). Thus, NRTFD was also synthesized by Cambridge Peptides (CP). As a second approach to the issue of the endogenous agonist, mutations were generated in the receptor at the potentially critical residue in both of these endogenous agonist candidates, which was Glu³⁴ in the WET sequence and Asp⁶⁷ in the FDE sequence.

5.2.3 Activation of the WTGLP-1R by synthetic peptides representing potential endogenous agonist sequences

In cells with stable expression of GLP-1Rs including HEK293Flp-In:WTGLP-1R, HEK293:GLP-1R-EGFP and CHOFlp-In:WTGLP-1R, there was surprisingly no cAMP response to any of the synthetic peptides (100µM) WET (CP), FDE (CP) or NRTFD (CP) (**Figure 5.9**). These data were inconsistent with the publication that appeared at this time highlighting NRTFD as a full agonist of the GLP-1R and suggesting that this was the endogenous agonist of the GLP-1R (Dong et al., 2008). Therefore, the conditions used for measuring cAMP levels in the present study were compared with those in the published study. One of the differences was that NRTFD-mediated cAMP production was detected in the presence of bacitracin in the published study (Dong et al., 2008). Interestingly, in the present study, bacitracin reduced cAMP generation in response to either GLP-1 7-36 amide (100nM; p<0.01) or forskolin (10µM; p<0.05) but had no effect on the lack of cAMP generation in response to the synthetic peptides (**Figure 5.10**). Thus, future cAMP measurements were made in the absence of bacitracin. In case the kinetics of any NRTFD (CP)-mediated response differed radically from that of GLP-1 7-36 amide, the time-course of cAMP generation in intact HEK293Flp-In:WTGLP-1R cells was investigated. There was no cAMP production detected in response to the synthetic peptides over a 90min period although GLP-1 7-36

amide stimulated a time-dependent, robust increase in cAMP production in the same cells, which reached a maximum after approximately 20min (**Figure 5.11**). Furthermore, cAMP assays were carried out on samples generated in Leicester at AstraZeneca (Alderley Park, Macclesfield, U.K.) using a similar method (HTRF cAMP femto kit, Cisbio Bioassays, Bedford, MA, U.S.A.) to that in the previous study (Dong et al., 2008). Once again there was no evidence of any agonism by NRTFD (CP) in the HEK293Flp-In:WTGLP-1R cells (data not shown).

The synthetic NRTFD (CP) was thus submitted to the Protein Nucleic Acid Chemistry Laboratory (PNAACL, University of Leicester, U.K.) for mass spectrum analysis. The analysis showed peaks representing the peptide NRTFD at ~652.3Da for $[M+H]^+$ and ~326.8Da for $[M+2H]^{2+}$ (**Figure 5.12a**). However, the analysis clearly indicated the presence of other (unknown) species, although the relative proportions of each of the components could not be assessed (**Figure 5.12a**). It was of some concern that some of the unknown species within the sample could act as antagonists or inhibitors of the GLP-1R itself or GLP-1R-mediated responses. Therefore, the ability of NRTFD (CP) to influence either forskolin- or GLP-1-mediated cAMP generation was assessed in cells either with or without stable expression of the GLP-1R. NRTFD (CP) (100 μ M) had no effect on these in any of the cells (**Figure 5.13**). However, at a higher concentration, NRTFD (CP) (1mM) abolished the cAMP response in HEK293Flp-In:WTGLP-1R cells evoked by an EC_{50} concentration (0.1nM) of GLP-1 7-36 amide, despite only partial inhibition by exendin 9-39 (100nM) (**Figure 5.14**).

NRTFD, along with a C-terminally extended NRTFD, NRTFDEYA were supplied by AstraZeneca (AZ), (Alderley Park, Macclesfield, U.K.) having been synthesised by

Pepscan Presto B.V. (Lelystad, The Netherlands). In contrast to NRTFD (CP), NRTFD (AZ) showed a relative high purity in the mass spectrum analysis (**compare Figure 5.12b with a**). NRTFDEYA (AZ) was not analyzed. According to the analysis by LC/Charged aerosol detector (CAD) systems, the actual concentrations of both NRTFD (AZ) and NRTFDEYA (AZ) were ~3mM and not 10mM as expected/calculated (information provided by AstraZeneca). This information was provided after some of the experiments had been performed and thus a concentration of 333 μ M rather than the expected 1mM had been used. In subsequent experiments 333 μ M was therefore used. NRTFD (AZ) (333 μ M) evoked a relatively weak cAMP response in the cells with stable expression of the GLP-1R but not in cells without expression of the receptor (**Figure 5.15**). Although the longer synthetic peptide, NRTFDTFDEYA (AZ) (333 μ M), did not provoke cAMP generation, the peptide did enhance forskolin-stimulated cAMP generation (**Figure 5.15**). Unfortunately due to the limited amount of material available, higher concentrations of either NRTFD (AZ) or NRTFDEYA (AZ) could not be tested.

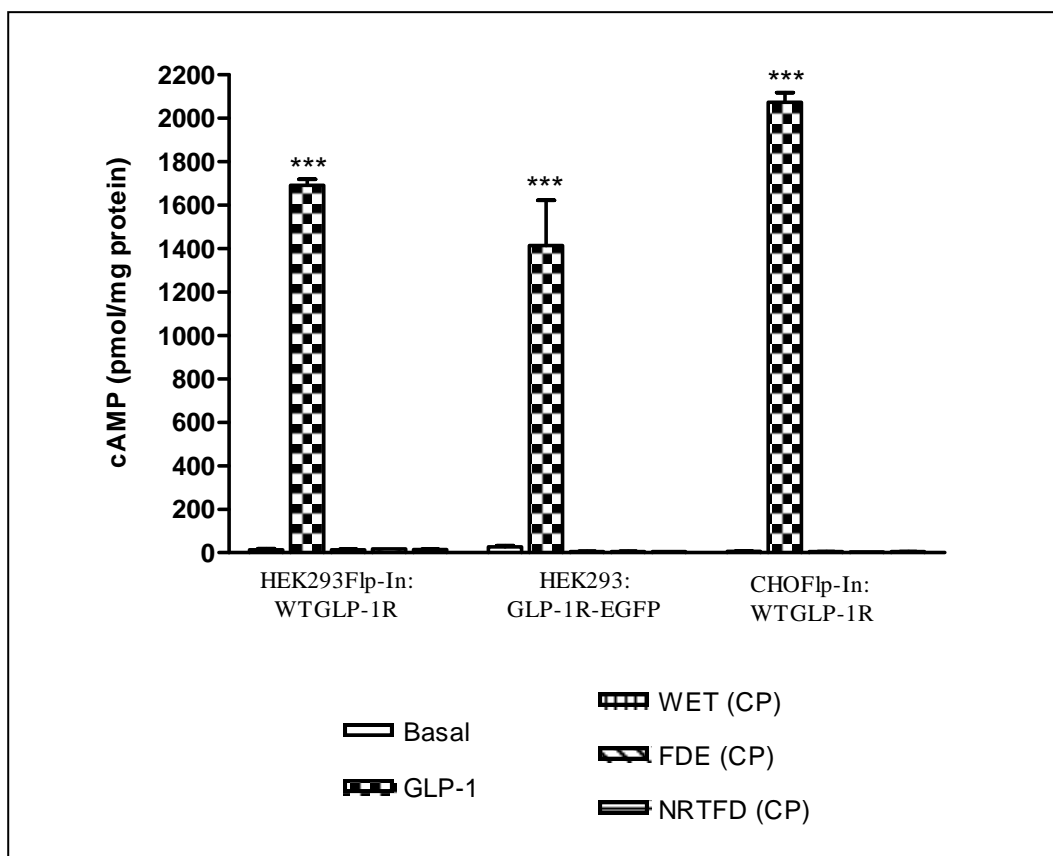


Figure 5.9. Small peptides corresponding to sequences of the GLP-1R do not evoke cAMP generation in cells with stable expression of GLP-1Rs. HEK293Flp-In:WTGLP-1R, HEK293:GLP-1R-EGFP or CHOFlp-In:WTGLP-1R cells were treated with KHB (Basal), GLP-1 7-36 amide (GLP-1, 100nM) or the synthesized small peptides WET (CP) (100 μ M), FDE (CP) (100 μ M) or NRTFD (CP) (100 μ M) at 37°C for 10min, in the presence of IBMX (500 μ M). Levels of intracellular cAMP were determined relative to the cellular protein content. ***, $p < 0.001$, compared with Basal by Dunnett's test following one-way ANOVA. Data are mean+sem, n=3.

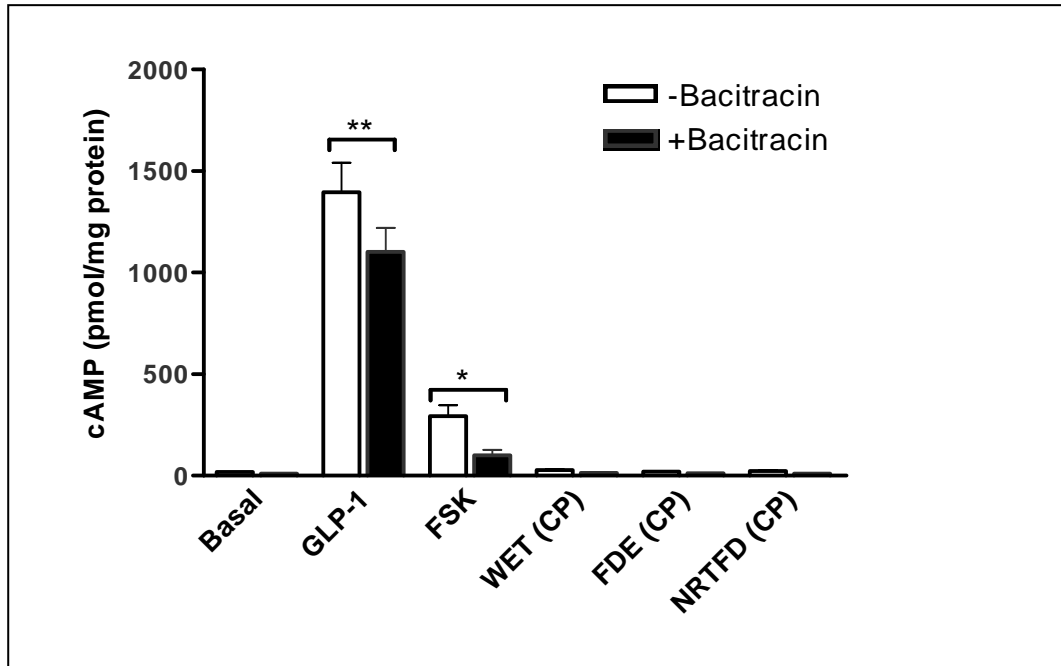


Figure 5.10. Effect of bacitracin on cellular cAMP production. HEK293Flp-In:WTGLP-1R cells were challenged with KHB (Basal), forskolin (FSK, 10 μ M) GLP-1 7-36 amide (GLP-1, 100nM) or the synthesized small peptides WET (CP) (100 μ M), FDE (CP) (100 μ M) or NRTFD (CP) (100 μ M) at 37°C for 10min, in the presence of IBMX (500 μ M). For each of the conditions, 0.1% (w:v) bacitracin was either absent (-Bacitracin) or present (+Bacitracin). Levels of intracellular cAMP were determined relative to the cellular protein content. *, $p < 0.05$, **, $p < 0.01$ by Student's t-test for each condition. Data are mean+sem. n=3.

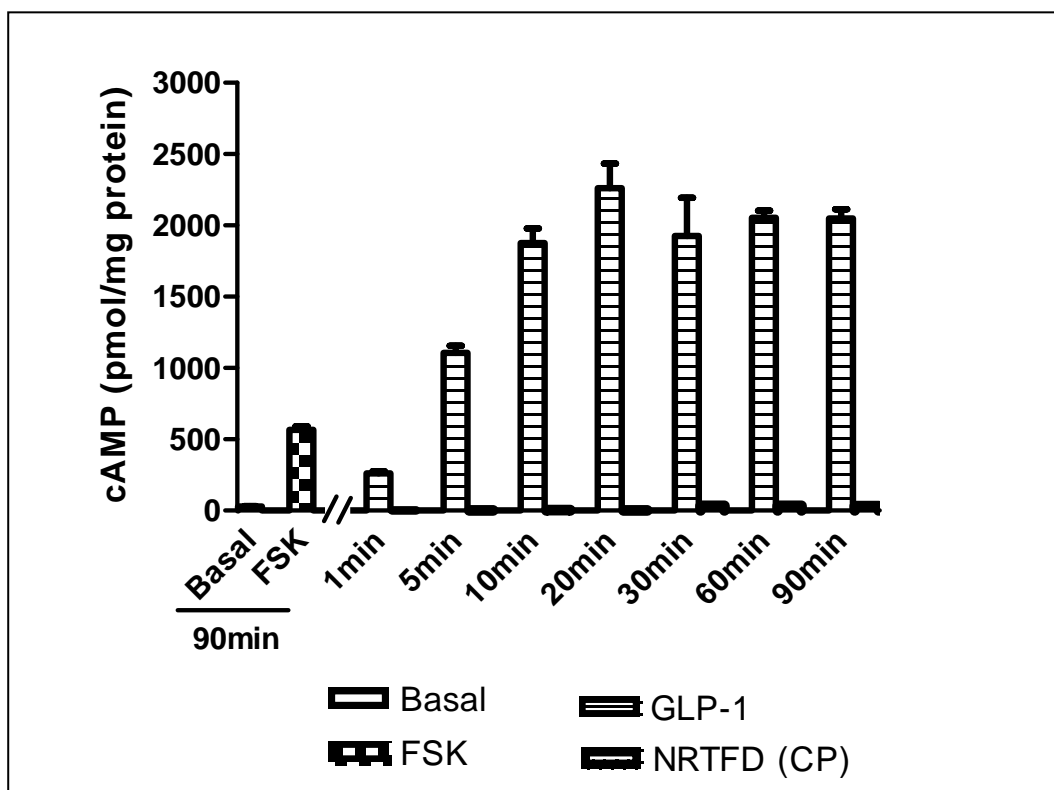


Figure 5.11. Time course of cAMP generation in HEK293Flp-In:WTGLP-1R cells challenged with either NRTFD (CP) or GLP-1 7-36 amide. HEK293Flp-In cells were challenged with GLP-1 7-36 amide (GLP-1, 100nM) or NRTFD (CP) (100 μ M) at 37°C, for the times indicated in the presence of IBMX (500 μ M). As controls, the cells were also treated with KHB (Basal) or forskolin (FSK, 10 μ M) for 90min. For each condition, levels of intracellular cAMP were determined relative to the cellular protein content. Data are mean+sem. n=3.

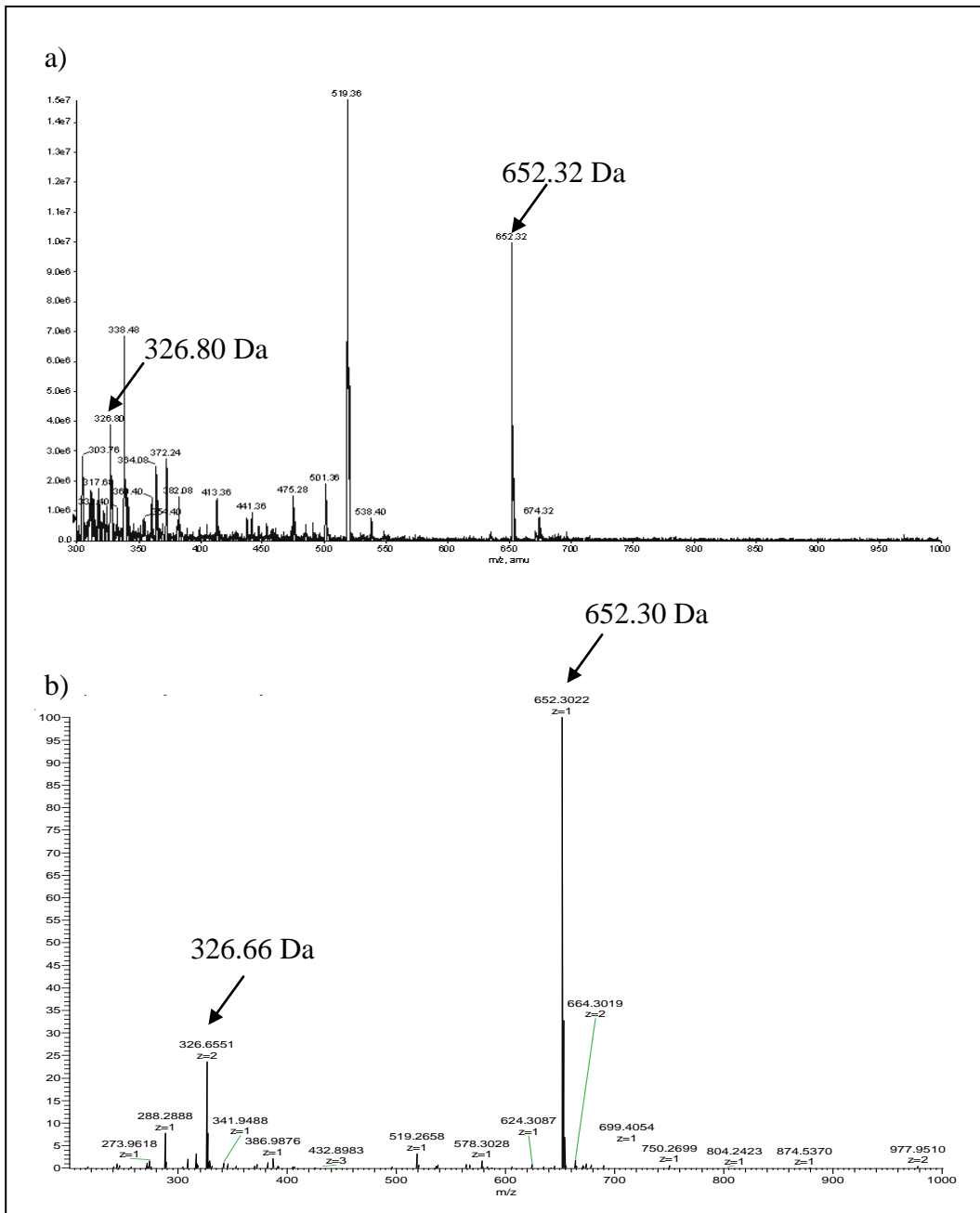


Figure 5.12. Sequence confirmation of NRTFD by full MS-spectrum. Either NRTFD (CP) (a) or NRTFD (AZ) (b) were subjected to full mass-spectrum analysis over the range $m/z=300-1000$. Calculated masses of NRTFD: $[M+H]^+ = 652.304$ Da; $[M+2H]^{2+} = 326.657$ Da. The peaks at ~ 652.3 Da and ~ 326.7 Da indicated by arrows represent the peptide of NRTFD. Analysis was performed by PNAACL (University of Leicester, U.K.).

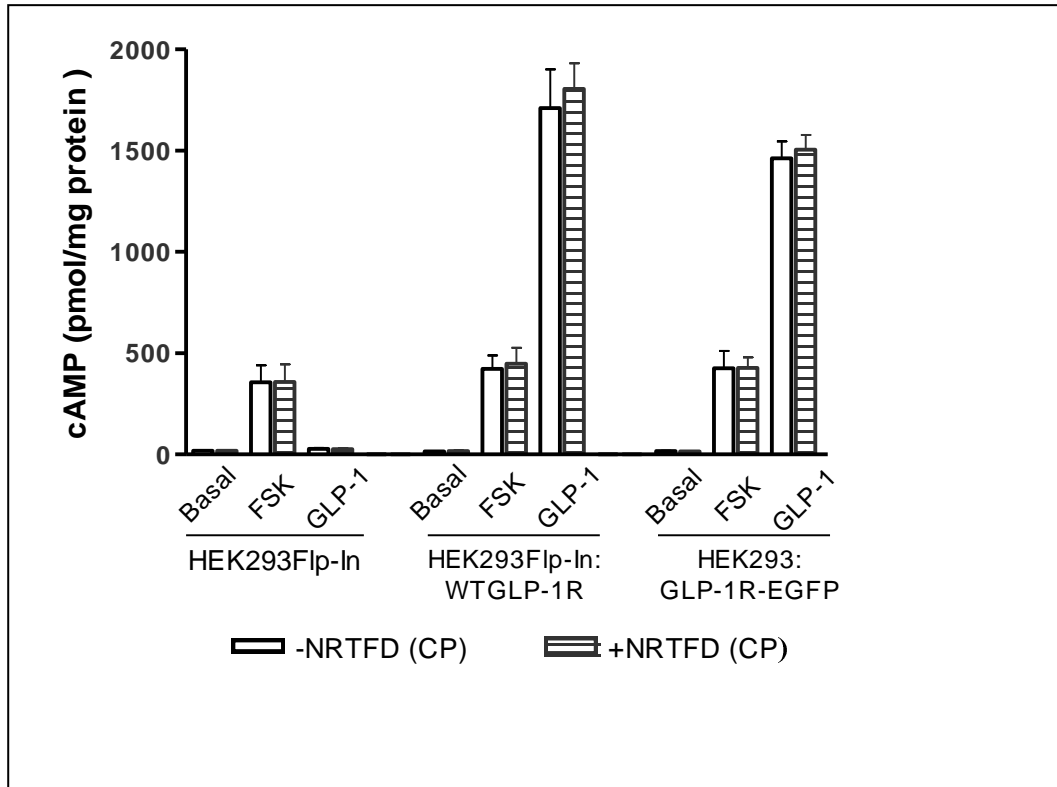


Figure 5.13. An examination of potential interaction of NRTFD (CP) with GLP-1 7-36 amide and forskolin in cells with or without stable expression of GLP-1Rs. HEK293Flp-In, HEK293Flp-In:GLP-1R or HEK293:GLP-1R-EGFP cells were treated with KHB (Basal), forskolin (FSK, 10 μ M) or GLP-1 7-36 amide (GLP-1, 100nM) at 37°C for 60min in the presence of IBMX (500 μ M). For each condition, NRTFD (CP) (100 μ M) was either present (+NRTFD (CP)) or absent (-NRTFD (CP)) and levels of intracellular cAMP were determined relative to the cellular protein content. Data are mean+sem, n=3.

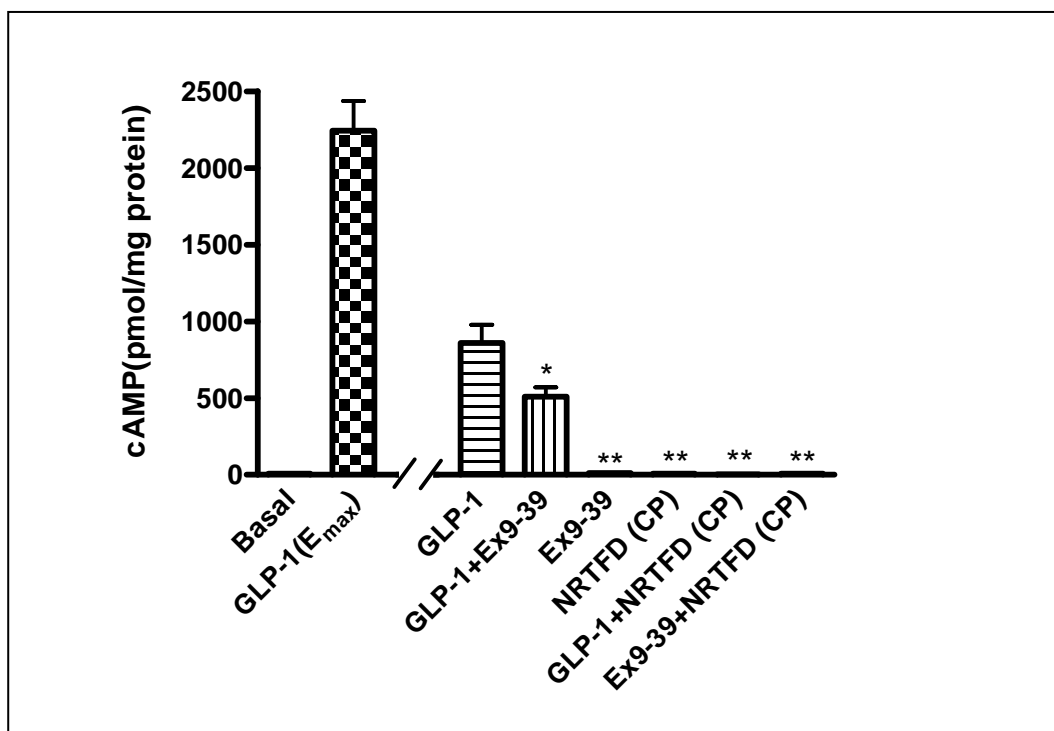


Figure 5.14. An examination of potential interaction of a high concentration of NRTFD (CP) with exendin 9-39 and GLP-1 7-36 amide in cells with stable expression of the GLP-1R. HEK293F_{1p}-In:WTGLP-1R cells were treated with GLP-1 7-36 amide (GLP-1, 0.1nM; approximate EC₅₀), exendin 9-39 (Ex9-39, 100nM), NRTFD (CP) (NRTFD (CP), 1mM) or a combination of the two ligands (GLP-1+Ex9-39, Ex9-39+NRTFD (CP) and NRTFD (CP)+GLP-1). The cells were also treated with KHB (Basal) or GLP-1(E_{max}, 100nM). For each condition, the treatment was carried out at 37°C for 60min in the presence of IBMX (500μM) and levels of intracellular cAMP were determined relative to the cellular protein content. *, $p < 0.05$, **, $p < 0.01$ compared with control (GLP-1, 0.1nM) by Dunnett's test following one-way ANOVA. Data are mean+sem. n=3.

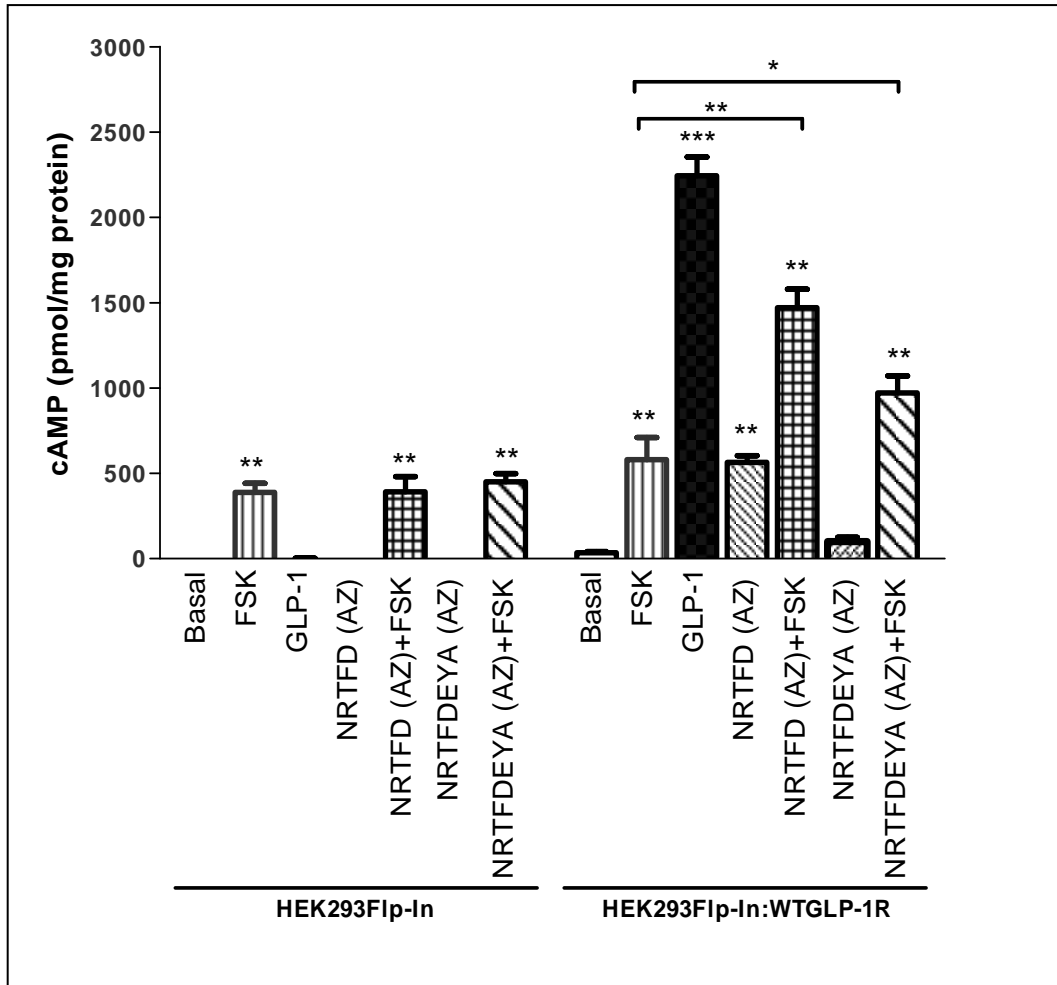


Figure 5.15. NRTFD (AZ) evokes cAMP production in cells with stable expression of GLP-1R but not in the parental cells lacking expression of the GLP-1R. HEK293Flp-In and HEK293Flp-In:WTGLP-1R cells were treated with KHB (Basal), forskolin (FSK, 10 μ M), GLP-1 7-36 amide (GLP-1, 100nM) NRTFD (AZ) (333 μ M) or NRTFDEYA (AZ) (333 μ M) either alone (NRTFD (AZ), NRTFDEYA (AZ)) or combined with 10 μ M forskolin (NRTFD (AZ)+FSK and NRTFDEYA (AZ)+FSK). For each of the conditions, the treatment was carried out at 37 $^{\circ}$ C for 60min in the presence of IBMX (500 μ M) and levels of intracellular cAMP were determined relative to the cellular protein content. *, $p < 0.05$, **, $p < 0.01$, ***, $p < 0.001$ compared with the appropriate Basal or as indicated by Bonferoni's test following one-way ANOVA. Data are mean+sem, n=3.

5.2.4 Signalling and regulation of mutated GLP-1Rs.

In order to examine the role of the potential endogenous agonist, several mutants were generated based on the two sequences of the GLP-1R (WET and FDE) with analogy to the WDN motif of the secretin receptor. As D is the critical residue in the endogenous agonist sequence (WDN) of the secretin receptor (Dong et al., 2006), the GLP-1R mutants were generated based on Glu³⁴ and Asp⁶⁷, which are equivalent to the E in WET and D in FDE. Subsequent work also confirmed D as the critical residue in both the NRTFD and NRTFDEYA sequences (Dong et al., 2008), which is equivalent to Asp⁶⁷ in the receptor. Thus E34A, D67A, D67E and D67R were generated based on the WTGLP-1R-HA construct to give E34AGLP-1R-HA, D67AGLP-1R-HA, D67EGLP-1R-HA and D67RGLP-1R-HA, respectively. In these mutations, alanine (A) provides a non-charged residue, glutamic acid (E) is negatively charged and arginine (R) is positively charged. In addition, as Asp⁶⁷ is thought to interact with a number of residues including Arg¹⁰², a D67R/R102D (D D67R/R102DGLP-1R-HA) double-mutant was generated in an attempt to allow this interaction but to remove Asp⁶⁷ from the FDE motif.

When transiently expressed in HEK293 cells, the E34AGLP-1R-HA was detected in a two-band version in immunoblots by an anti-HA antibody, which is identical to the WTGLP-1R-HA (**Figure 5.16a**). With the exception of this construct, the other mutants were detected by an anti-HA antibody as one immunoreactive band which was equivalent to the lower band in that of the WTGLP-1R-HA (**Figure 5.16a**).

The D67A, D67E and E34A mutants were also generated based on the HA-WTGLP-1R-EGFP construct to generate HA-D67AGLP-1R-EGFP, HA-D67EGLP-1R-

EGFP and HA-E34AGLP-1R-EGFP respectively. When transiently expressed in HEK293 cells, these constructs presented similar patterns of immunoreactivity in immunoblots using an anti-GFP antibody to these seen with their C-terminal HA-tagged versions using an anti-HA antibody (**Figure 5.17b**). The mutants containing an N-terminal HA-tag and C-terminal EGFP-tag were not, however, detected using an anti-HA antibody (data not shown). The previous data (**see Chapter 3**) showed that cell surface-located receptors were detected as the higher immunoreactive band in immunoblots (**Figure 3.19**). Consistent with this, the confocal images of HEK293 cells with transient expression of HA-D67AGLP-1R-EGFP or HA-D67EGLP-1R-EGFP revealed intracellularly located EGFP-fluorescence (**Figure 5.17a, ii & iv, respectively**), whereas HA-E34AGLP-1R-EGFP showed clear plasma membrane located fluorescence (**Figure 5.17a, iii**).

With the exception of E34A, none of the mutants evoked cAMP production in response to GLP-1 7-36 amide (100nM) (**Figure 5.16b**). In the cells with transient expression of the E34AGLP-1R-HA, GLP-1 7-36 amide evoked a similar cAMP response to that in cells transiently expressing the WTGLP-1R-HA with pEC_{50} values of 8.31 ± 0.2 and 8.45 ± 0.12 , respectively ($p > 0.05$) and E_{max} values of 636 ± 58 and 681 ± 113 pmol/mg protein, respectively ($p > 0.05$) (**Figure 5.18**). The synthetic peptide, WET (CP) (100 μ M or 1mM) was inactive on the E34AGLP-1R-HA (data not shown).

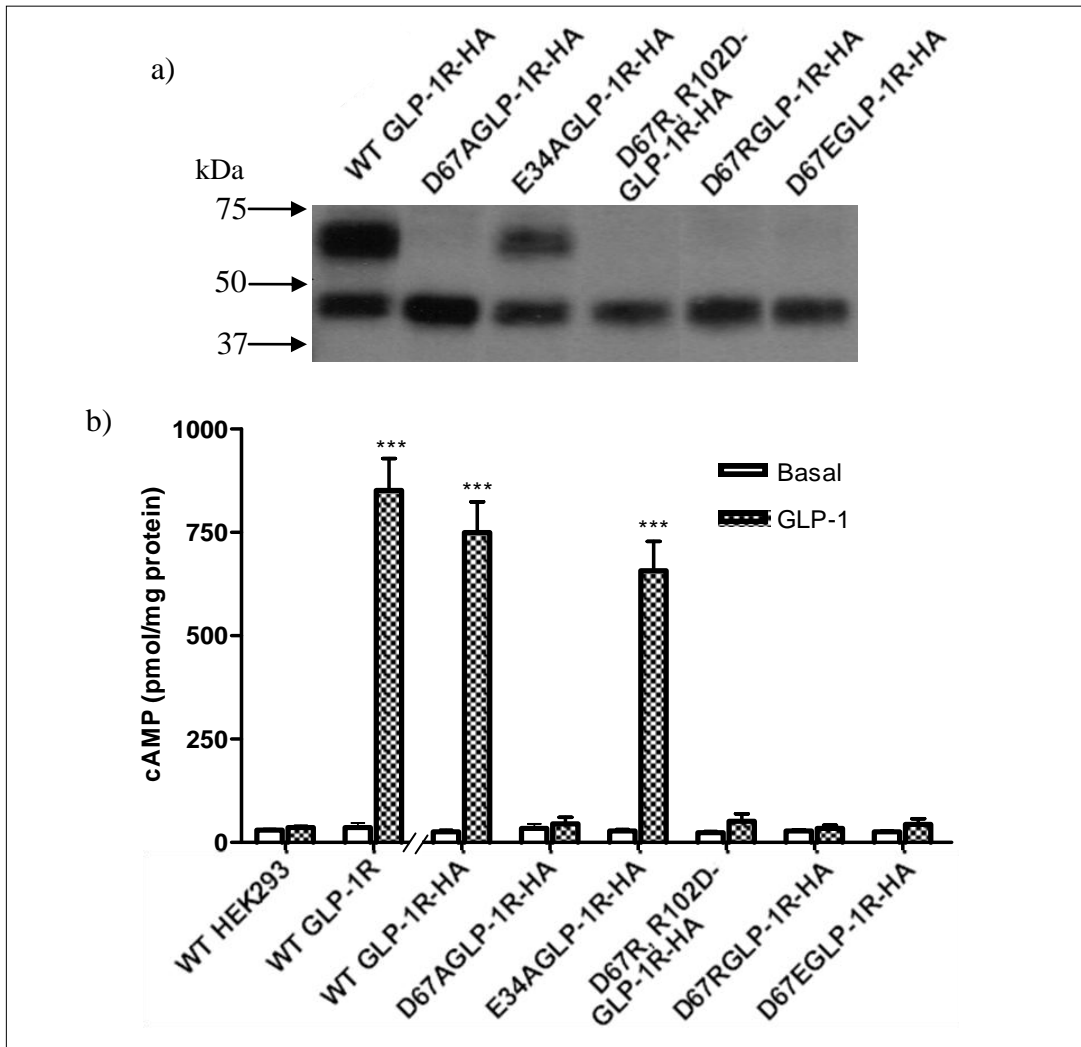


Figure 5.16. Immunoblotting and functional coupling of mutated GLP-1Rs. HEK293 cells were transiently transfected with HA-tagged constructs of either the wild-type GLP-1R (WTGLP-1R-HA) or mutated GLP-1Rs as indicated. After 30h, cell lysates were prepared and immunoblotted using an anti-HA antibody (a) or intact cells were challenged with GLP-1 7-36 amide at 100nM (GLP-1) or KHB (Basal) at 37°C for 10min in the presence of 500µM IBMX (b). The same challenge was also performed in untransfected HEK293 cells (WT HEK293) and the cells with transient expression of the untagged GLP-1R (WTGLP-1R). For each of the conditions, levels of intracellular cAMP were determined relative to the cellular protein content. ***, $p < 0.001$ by Student's paired t-test. Data are mean+sem, $n=3$. The immunoblotting data are representative of 3 independent experiments.

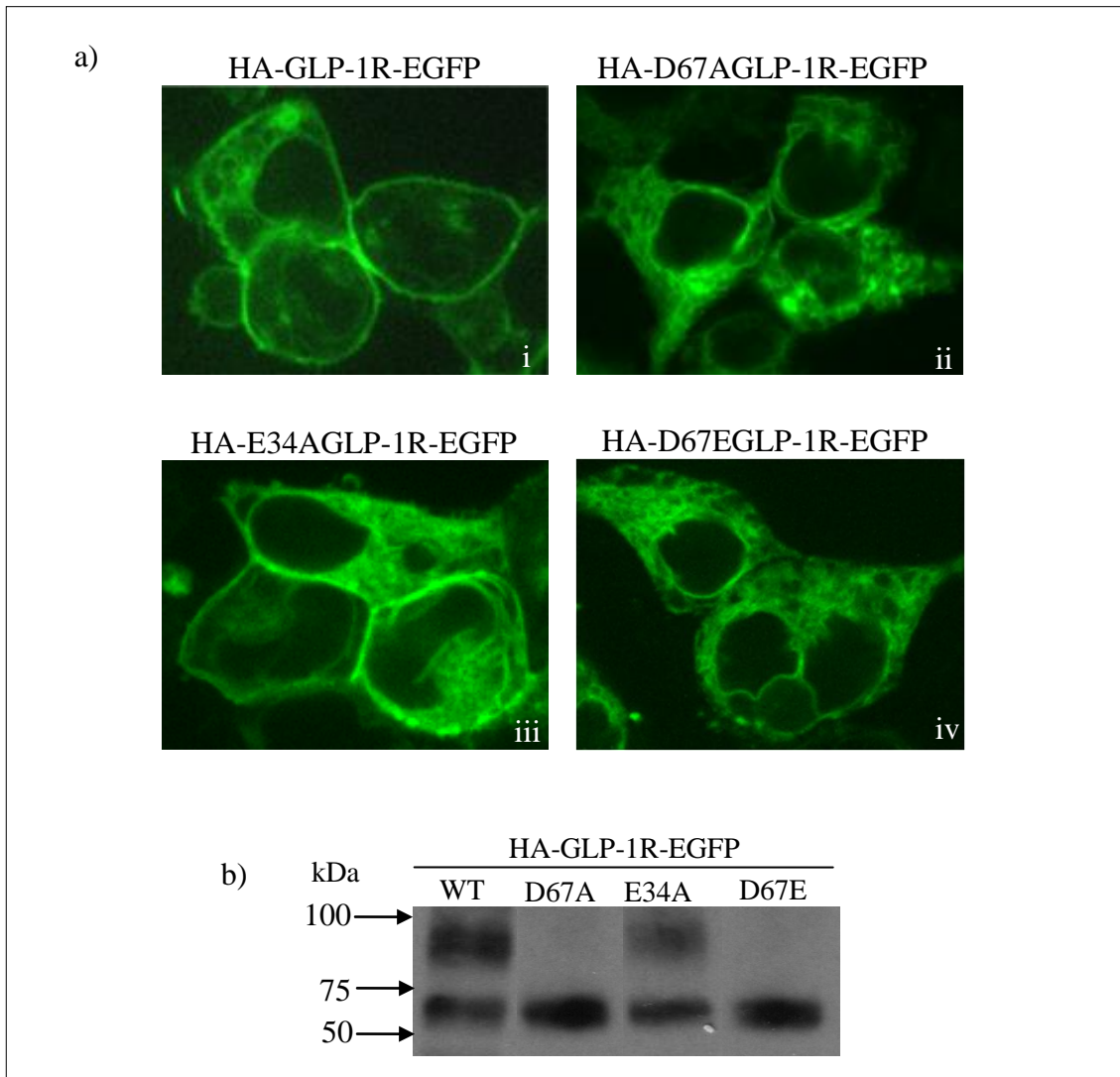


Figure 5.17. Cellular localisation and immunoblotting of the epitope-tagged GLP-1Rs with or without mutations when expressed in HEK293 cells. HEK293 cells were transiently transfected with N-terminal HA-tagged and C-terminal EGFP-tagged constructs of either the wild type GLP-1R (WT) or mutated GLP-1Rs (D67A, E34A or D67E) as indicated. After 30h, live cells were imaged by confocal microscopy (a i-iv). Cell lysates were also prepared and immunoblotted using an anti-GFP antibody (b). Data are representative of 3 independent experiments.

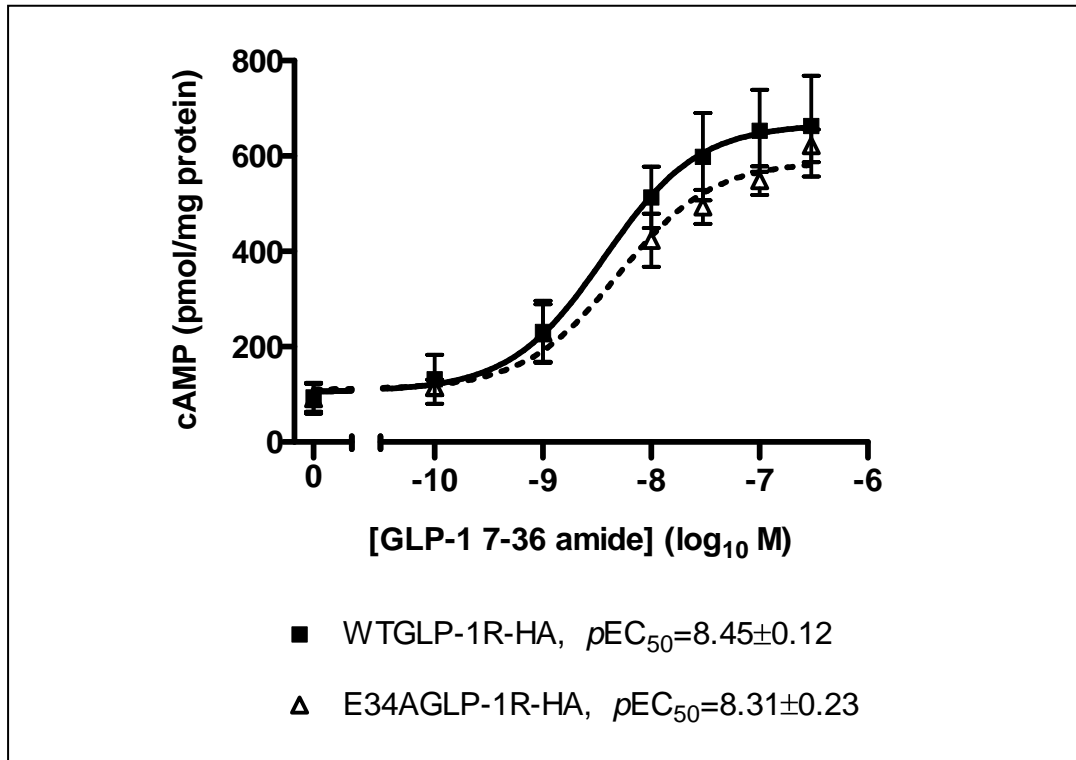


Figure 5.18. GLP-1 7-36 amide-induced cAMP generation in HEK293 cells with transient expression of E34AGLP-1R-HA. HEK293 cells with transient expression of E34AGLP-1R-HA or WTGLP-1R-HA were challenged with GLP-1 7-36 amide at the concentrations indicated for 10min, 37°C, in the presence of IBMX (500µM). Levels of intracellular cAMP were determined relative to the cellular protein content. Data are mean±sem, n=3

The pattern of immunoreactivity in immunoblots and the pattern of fluorescence in confocal microscopy observed for the epitope-tagged receptor constructs containing the D67 mutants (D67A, D67R, D67E and D67R/R102D) suggested that the lack of functional responses may be a consequence of a lack of cell-surface expression. Recently, it has been reported that the surface expression, ligand binding, and biological activity of other ER-retained mutants of the GLP-1R are improved significantly when biosynthesis is slowed using low temperature (30°C) (Chen et al., 2010). The present study also observed an enhanced upper immunoreactive band, representing mature protein, in the cells with expression of WTGLP-1R-HA after treatment with the proteasome inhibitor, MG132 (**See Chapter 4**). Consequently, attempts were made to increase cell surface expression by either culturing cells at a lower temperature or MG132 treatment. In addition, compound 2 did not evoke cAMP generation in cells with transient expression of the D67 mutants (data not shown) further suggesting that these constructs were not expressed at the cell surface. Given the proposed allosteric mechanism of action of compound 2 and its likely independence from the N-terminal domain of the receptor (which is mutated in these constructs), compound 2-mediated cAMP levels were measured simultaneously with that of GLP-1 7-36 amide to provide an indication of cell surface expression. At 6h after transfection, cells were treated with MG132 (10µM) for 10h or cultured at a lower temperature (30°C) for 20h. Both treatments resulted in compound 2-mediated cAMP response in all D67-based mutants although the low temperature treatment was less effective than MG132 (**Figure 5.19**). Although only the lower of the two immunoreactive bands seen with the WTGLP-1R-HA were seen in cells transiently transfected with the D67-based mutants (**Figure 5.16a**), treatment of these cells with MG132 led to the appearance of the higher

molecular weight immunoreactive band (~64kDa) and an additional lower molecular weight band of unknown composition (~37kDa) (but clearly containing the HA-tag) (**Figure 5.20**) which was not present in the same constructs without MG132 treatment (**Figure 5.16a**).

Treatment with MG132 resulted in modest cAMP response to GLP-1 7-36 amide for the D67E mutant although it was lower (~50%) than that mediated by compound 2 (**Figure 5.19; Figure 5.21**). There was no significant GLP-1 7-36 amide-mediated cAMP production detected in the D67R, D67R/R102D or D67A mutants (**Figure 5.19; Figure 5.21**). NRTFD (AZ) (333 μ M) did not evoke cAMP generation in cells with transient expression of any of the D67 mutants even when the cells were treated with MG132 (**Figure 5.21**, data not shown for D67R and D102R/R102D), although unfortunately due to a limited supply of the synthetic peptide, these experiments were only performed once.

An N-terminal truncated GLP-1R (Myc- Δ NTGLP-1R) and its wild-type version (Myc-WTGLP-1R) were a kind gift from Dr D. Donnelly's laboratory (University of Leeds, Leeds, U.K.) at the last stage of the present study and were used for preliminary assessment of compound 2- and NRTFD (AZ)-mediated agonism. Both of these constructs contained a signal peptide derived from HA at the N-terminus of the receptor, which was immediately followed by a Myc-tag and then the N-terminal domain-deleted mutant or the WTGLP-1R (**see Chapter 2**). In cells with transient expression of Myc-WTGLP-1R, GLP-1 7-36 amide (100nM) stimulated cAMP production (589 \pm 46 pmol/mg protein) but this was not seen with the Myc- Δ NTGLP-1R construct (**Figure 5.22**). Similarly, NRTFD (AZ) was inactive at the Myc- Δ NTGLP-1R although it

evoked relatively weak cAMP response in cells expressing the Myc-WTGLP-1R ($54\pm 4\%$ of that of GLP-1 7-36 amide in the same cells) (**Figure 5.22**). In contrast, compound 2 evoked robust cAMP responses by either the Myc-WTGLP-1R or the Myc- Δ NTGLP-1R ($108\pm 5\%$ and $82\pm 4\%$ of the response to GLP-1 7-36 amide in cells expressing the Myc-WTGLP-1R) (**Figure 5.22**).

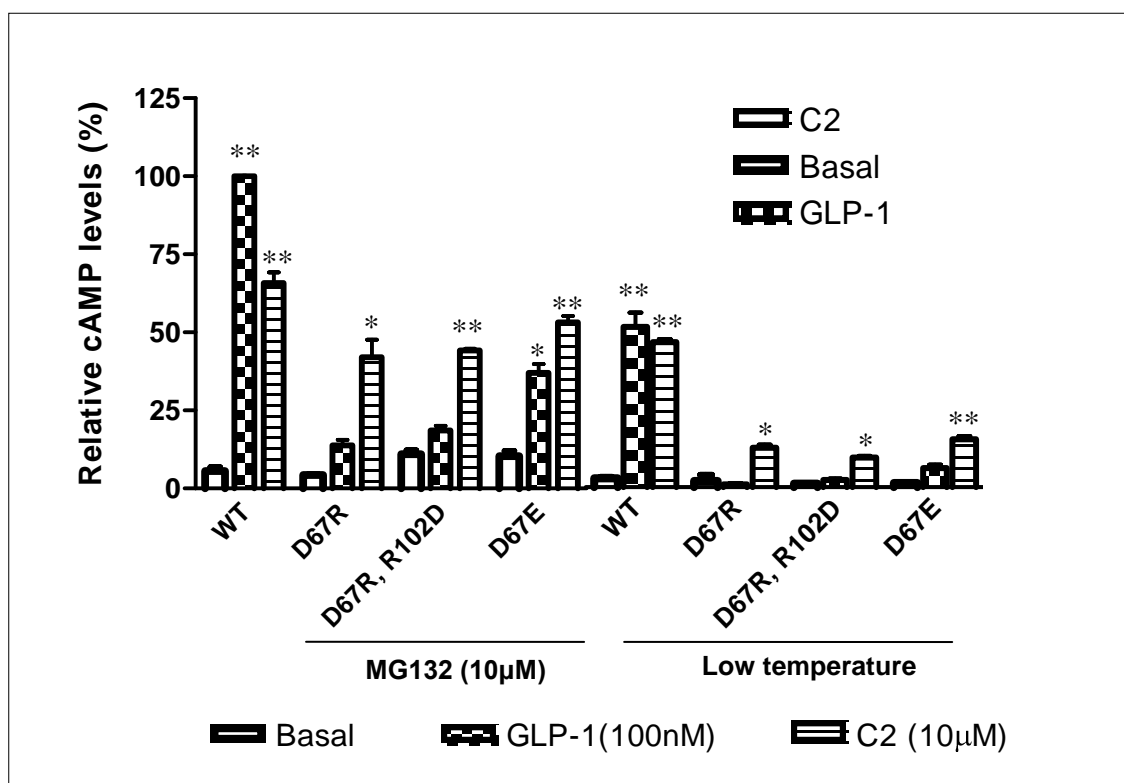


Figure 5.19. Effect of MG132- or low temperature-treatment of cells transiently transfected with wild-type or mutated GLP-1Rs on agonist-mediated cAMP generation. HEK293 cells were transiently transfected with C-terminal HA-tagged constructs either of the wild-type (WT) or mutated (D67R, R102D and D67E) GLP-1Rs as indicated. After 6h the cells were cultured at 30°C for a further 20h (Low temperature). Alternatively, at 16h after transfection, the cells were treated with MG132 (10µM) for a further 10h. At 26h after transfection, all cells were challenged with either GLP-1 7-36 amide (GLP-1, 100nM), compound 2 (C2, 10µM) or KHB (Basal) at 37°C for 10min in the presence of IBMX (500µM) and cAMP levels were determined relative to the GLP-1 (100nM) response of untreated cells expressing the wild-type GLP-1R and cultured at 37°C in the absence of MG132 (492±26pmol/mg protein). *, $p<0.05$, **, $p<0.01$, compared with the appropriate Basal by Dunnett's test following one-way ANOVA on the raw data (pmol/mg protein). Data are mean±sem, n=3.

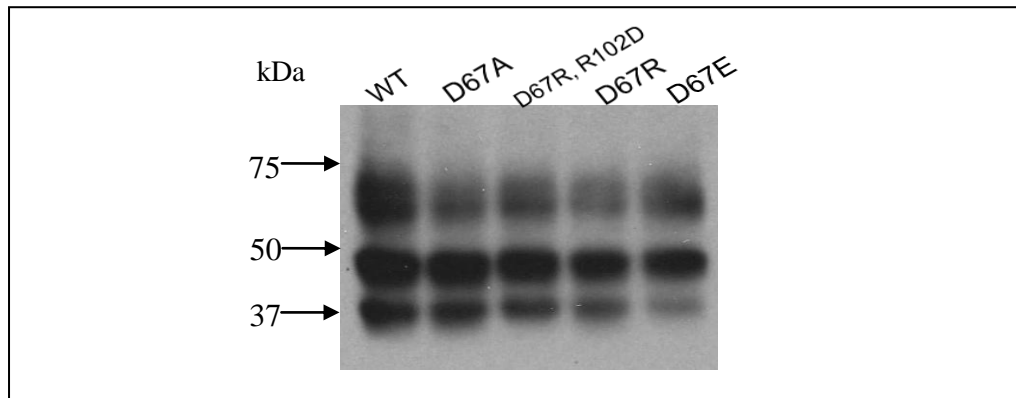


Figure 5.20. Immunoblotting of wild-type or mutated GLP-1Rs in cells treated with MG132. HEK293 cells were transiently transfected with C-terminal HA-tagged constructs either of the wild-type (WT) or mutated (D67A, D67R, R102D and D67E) GLP-1Rs as indicated. At 16h after transfection, the cells were treated with MG132 (10 μ M) for a further 10h. Cell lysates were prepared from the MG132-treated cells and immunoblotted using an anti-HA antibody. Data are representative of 3 independent experiments.

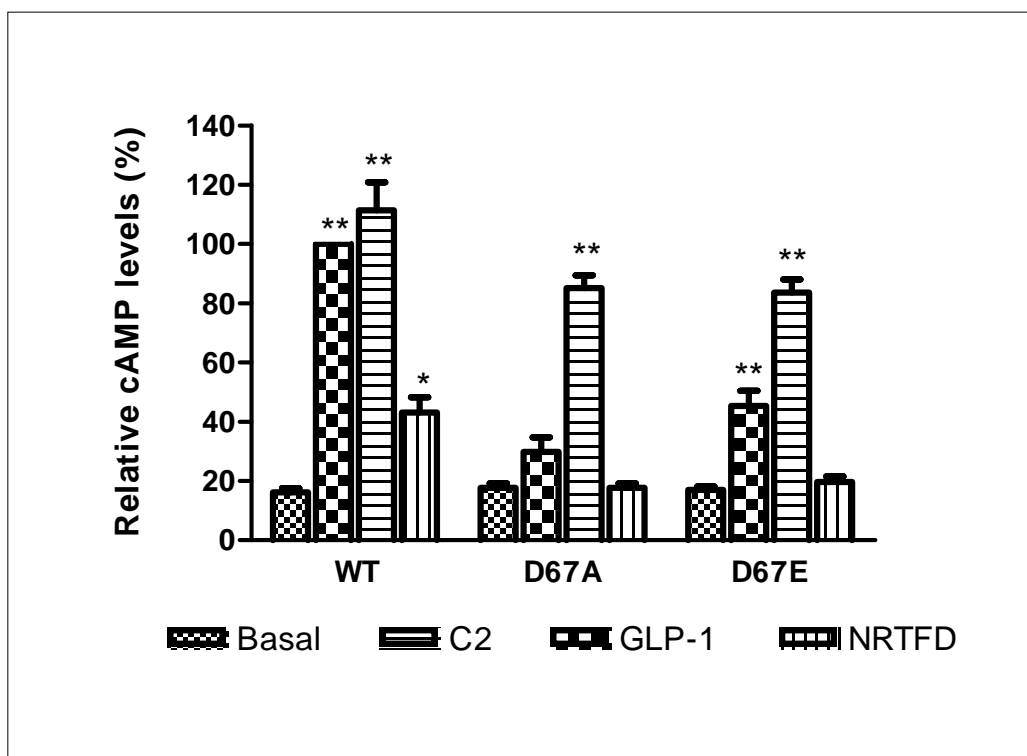


Figure 5.21. Assessment of potential functional coupling of mutated GLP-1Rs mediated by compound 2 and NRTFD (AZ). HEK293 cells were transiently transfected with epitope-tagged constructs of either wild-type or mutated GLP-1Rs as indicated. After 16h, the cells were treated with MG132 (10 μ M) for a further 10h. Cells were challenged with GLP-1 7-36 amide (GLP-1, 100nM), NRTFD (AZ) (333 μ M) or KHB (Basal) for 60min, or compound 2 (C2, 10 μ M) for 10min at 37°C in the presence of IBMX (500 μ M); and cAMP levels determined relative to that of the WTGLP-1R-HA in response to GLP-1 7-36 amide (573 \pm 47 pmol/mg protein). *, $p < 0.05$, **, $p < 0.01$ by Dunnett's test following one-way ANOVA on the raw data (pmol/mg protein). Data are mean \pm sem, n = 4.

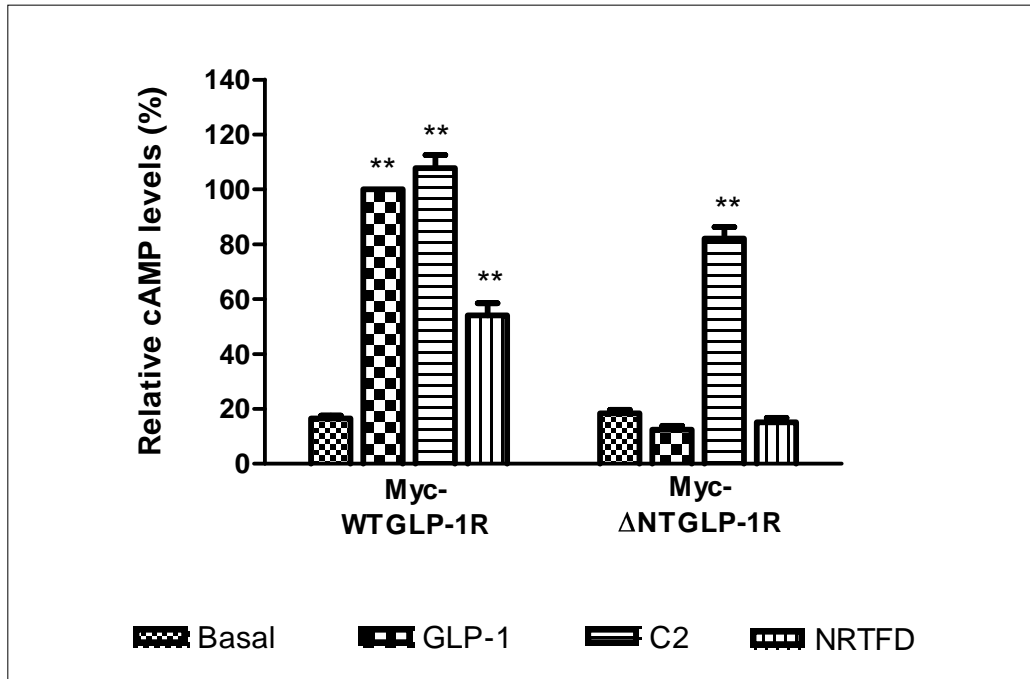


Figure 5.22. Assessment of potential functional coupling of the N-terminal domain deleted GLP-1R. HEK293 cells were transiently transfected with either Myc-WTGLP-1R or Myc-ΔNTGLP-1R as indicated. After 16h, the cells were treated with MG132 (10μM) for a further 10h. Cells were challenged with GLP-1 7-36 amide (GLP-1, 100nM), NRTFD (AZ) (333μM) or KHB (Basal) for 60min, or compound 2 (C2, 10μM) for 10min at 37°C in the presence of IBMX (500μM); and cAMP levels determined relative to that of the WTGLP-1R in response to GLP-1 (589±46 pmol/mg protein). *, $p < 0.05$, **, $p < 0.01$ by Dunnett's test following one-way ANOVA on the raw data (pmol/mg protein). Data are mean±sem, n = 4.

It was shown previously in this study that only the fully glycosylated, mature form of the GLP-1R is expressed at the plasma membrane. This form of the receptor is represented by the upper of the two immunoreactive bands in immunoblots. The D67A mutant was only detected as a single immunoreactive band, which was equivalent to that representing immature protein in blots of the wild-type receptor. In order to assess whether this immature form of the GLP-1R could be trafficked to the cell membrane by a fully mature GLP-1R, the D67A mutant containing a C-terminal EGFP-tag was co-expressed with the WTGLP-1R containing a C-terminal HA-tag. The typical two immunoreactive bands (molecular weights ~47kDa and ~64kDa) were detected by anti-HA antibody in lysates from the co-transfected cells but not in lysates from the cells transfected with HA-D67GLP-1R-EGFP alone (**Figure 5.23b, Lane 0**). When using an anti-GFP antibody, the typical two bands were detected at ~66kDa and ~93kDa for the cells co-transfected with HA-WTGLP-1R-EGFP, but only the lower immunoactive band at ~66kDa was detected for the HA-D67AGLP-1R-EGFP (**Figure 5.23a, Lanes 0**). It is known that ligand may alter receptor cell surface-localisation. For example, agonists can cause receptor internalization while antagonists (or inverse agonists) may stabilise receptors at the cell surface (Smit et al., 1996). Thus, treatment with either exendin 9-39 (100nM) or GLP-1 7-36 amide (100nM) for 10h was carried out in the cells either with co-expression or with expression of D67A mutant alone. Interestingly, exendin 9-39 partially restored the upper EGFP-immunoreactive band at ~93kDa in the cells with co-expression of the HA-D67AGLP-1R-EGFP and WTGLP-1R-HA but not in the cells with the expression of the HA-D67AGLP-1R-EGFP alone (**Figure 5.23a, Lanes E**). This effect was not seen in the cells treated with GLP-1 7-36 amide (100nM) (**Figure 5.23a, Lanes G**).

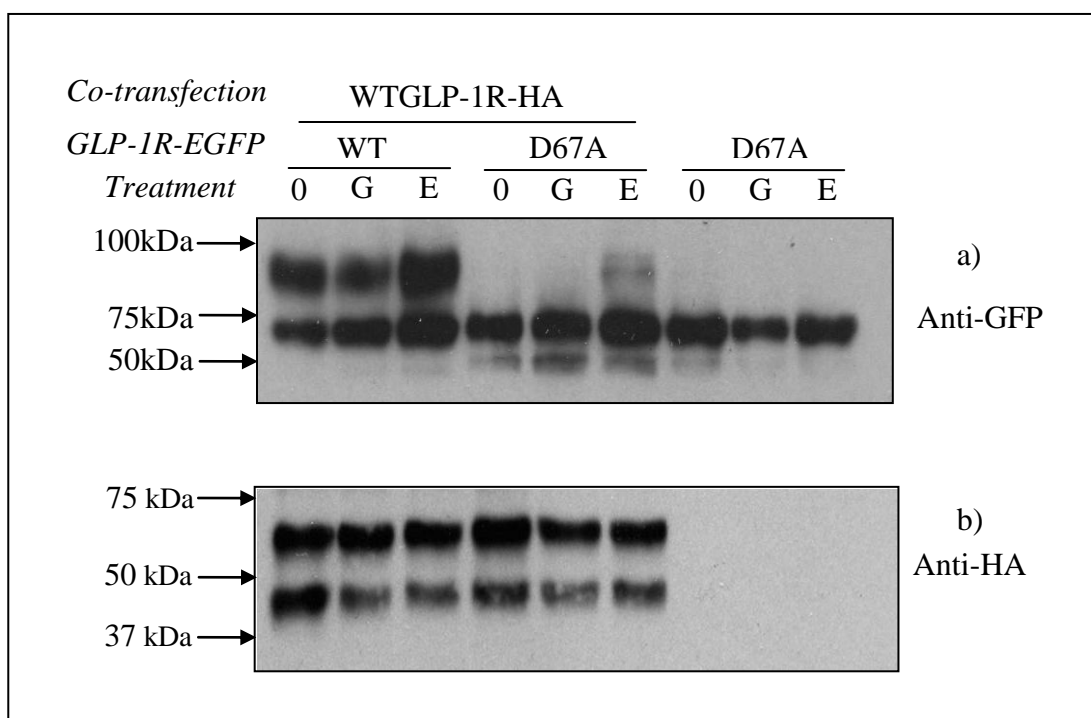


Figure 5.23. Effect of the orthosteric-antagonist, exendin 9-39, on the pattern of immunoblotting of wild-type and mutated GLP-1Rs. HEK293 cells were co-transfected with WTGLP-1R-HA and EGFP-tagged constructs of either wild-type (WT) or mutated (D67A) GLP-1R, or transfected with D67AGLP-1R-EGFP (D67A) alone. After 16h, the cells were either treated with GLP-1 7-36 amide (G, 100nM) or exendin 9-39 (E, 100nM), or cultured without any treatment (0) for a further 10h. Whole cell lysates were then prepared from all cells and immunoblotted using either anti-GFP (a) or anti-HA (b) antibodies. Data are representative of 3 independent experiments.

5.2.5 Receptor internalization mediated by different ligands in HEK293 cells with stable expression of the GLP-1Rs

Intact HEK293:GLP-1R-EGFP cells allow the observation of the real-time movement of receptor stimulated by different ligands. Real-time confocal imaging of live HEK293-GLP-1R-EGFP cells revealed intense, continuous plasma membrane fluorescence (**Figure 5.24a**). Treatment of cells for 40min with 100nM GLP-1 7-36 amide caused a marked loss of this plasma membrane fluorescence and the appearance of intense intracellular fluorescence in discrete puncta or in larger patches (**Figure 5.24b**). In the first 10min of treatment with GLP-1 7-36 amide (100nM), fluorescence aggregated in small discrete patches at the plasma membrane, and this was followed by movement of these puncta into the interior of the cell where they coalesced in discrete regions (**Figure 5.25a**). Quantification of changes in plasma membrane and cytosolic fluorescence (see **Methods 2.23.2**) indicated that internalization was at a maximum by approximately 30min (**Figure 5.25a**) and that relatively little fluorescence remained at the cell membrane (**Figure 5.25a & Figure 5.26**). Over a 60min period, a very minor amount of internalization occurred in the presence of DMSO (**Figure 5.25f & Figure 5.26**) but this was not different from cells in buffer alone (data not shown). Neither exendin 9-39 (100nM) nor NRTFD (AZ) (333 μ M, data not shown) had any impact on the distribution of fluorescence over and above that seen in vehicle-treated cells (**Figure 5.25f, Figure 5.26**). However, pre-incubation of cells with exendin 9-39 (100nM) for 10min or with NRTFD (AZ) (333 μ M) for 60min reduced the rate and extent of internalization mediated by GLP-1 7-36 amide (100nM) (**Figure 5.25b & e, Figure 5.26; Figure 5.27b, c & d**). After addition of compound 2 (10 μ M), there was a delay of approximately 10min before the initiation of detectable internalization, which then

progressed at a slower rate and was less extensive than that mediated by GLP-1 7-36 amide ($E_{\max}=70\pm 7\%$, $n=36$ cells in 3 independent experiments) (**Figure 5.25c**, **Figure 5.26** & **Figure 5.27**). Pre-incubation of cells with exendin 9-39 (100nM) for 10min reduced the rate and extent of internalization mediated by compound 2 (10 μ M) to essentially basal levels (**Figure 5.25d**, **Figure 5.26** & **Figure 5.27c & d**). Co-application of GLP-1 7-36 amide (100nM) and compound 2 (10 μ M) resulted in an initial internalization that was faster than that seen in cells treated with either GLP-1 7-36 amide or compound 2 alone (**Figure 5.26** & **Figure 5.27a**). However, between 20 and 60min the extent of internalization was less pronounced than that with GLP-1 7-36 amide alone but still greater than that with compound 2 alone (**Figure 5.26** & **Figure 5.27c & d**).

The extent of GLP-1R expression at the plasma membrane in HEK293-Flp-In:GLP-1R cells and the extent of any ligand-induced receptor internalization was also determined by radioligand binding (see **Method 2.26**). Less receptors remained at the cell surface after the cells were treated with GLP-1 7-36 amide (100nM) than following treatment with exendin 9-39 (100nM), (**Figure 5.28**). Co-application of compound 2 (10 μ M) and GLP-1 7-36 amide (100nM) resulted in much less GLP-1R remaining at the cell surface. The amount of cell surface-located receptor was slightly lower (although $p>0.05$) following treatment with compound 2 (10 μ M) than GLP-1 7-36 amide (100nM) (**Figure 5.28**).

The ability of compound 2 (10 μ M) to cause a greater reduction in cell-surface receptor (as assessed by ligand binding) than GLP-1 7-36 amide (100nM) was contradictory to confocal imaging experiments carried out in HEK293:GLP-1R-EGFP

cells (**Figure 5.27d**). However, compound 2 clearly has adverse effects (Coopman, et al., 2010) and therefore a similar binding assay was performed on cells with stable expression of muscarinic M₃ receptors (Tovey and Willars, 2004) to assess any general adverse effects on other receptors. Compound 2 but not GLP-1 7-36 amide (100nM) or exendin 9-39 (100nM) reduced binding of the muscarinic antagonist, [³H-NMS] to the M₃ receptor in a concentration-dependent manner (**Figure 5.29**).

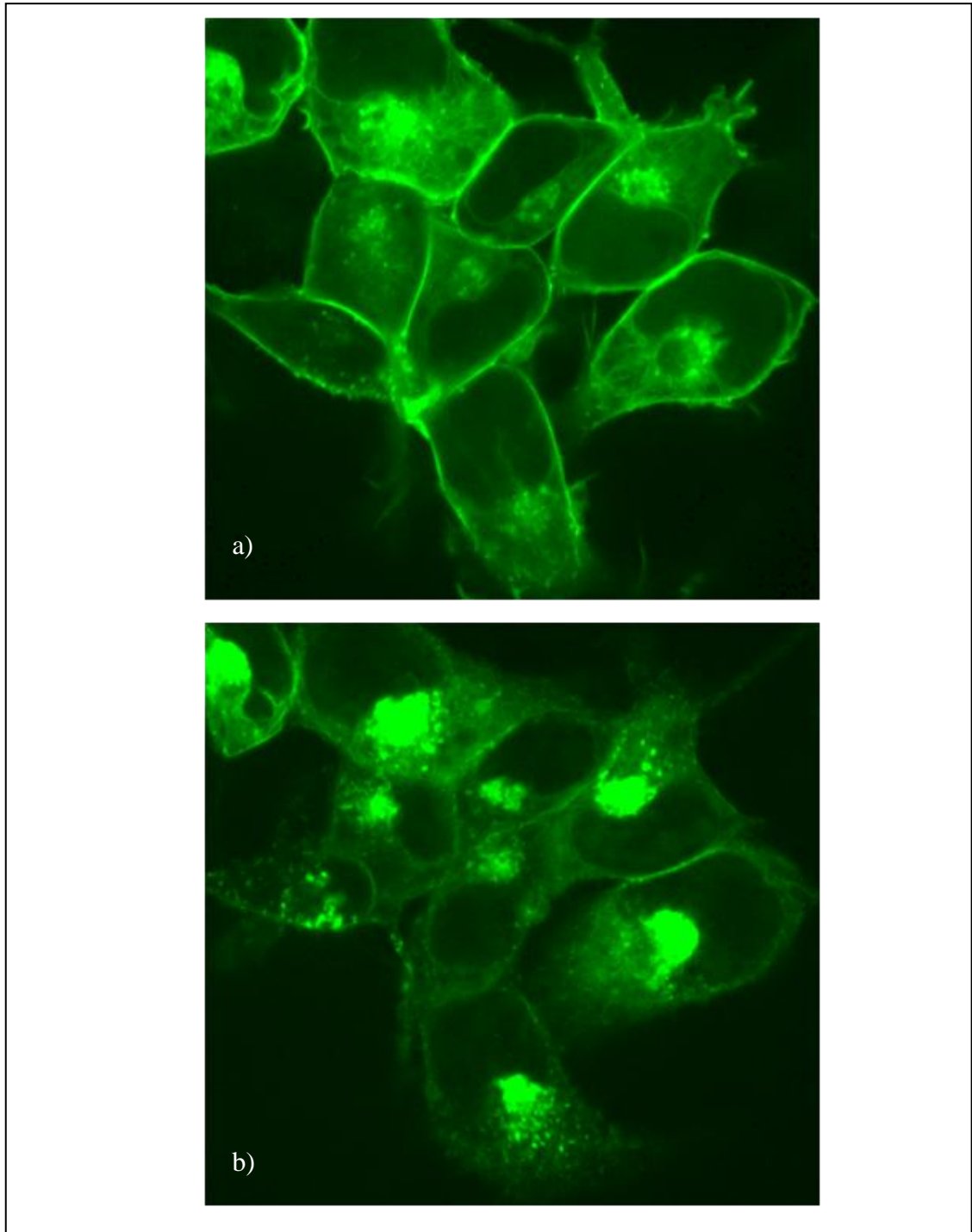


Figure 5.24. Confocal images of intact cells with stable expression of GLP-1R-EGFP before and after a challenge with GLP-1 7-36 amide. Confocal images were taken of intact HEK293 cells with stable expression of a C-terminal EGFP-tagged GLP-1R before (a) and 40min after (b) stimulation with GLP-1 7-36 amide (100nM) 37°C. Data are representative of 12 independent experiments.

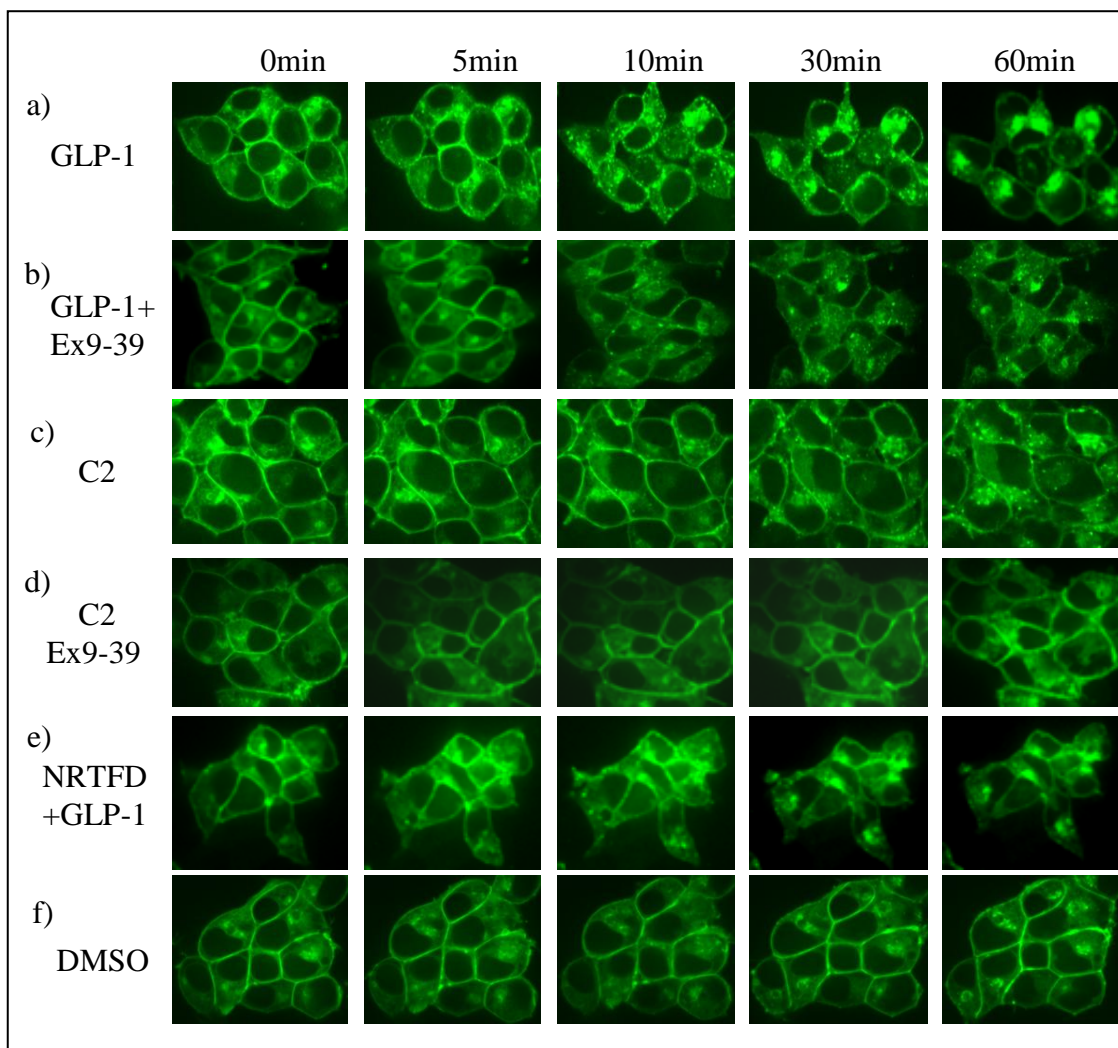


Figure 5.25. Confocal imaging of agonist-mediated internalisation of the GLP-1R. HEK 293 cells with stable expression of the GLP-1R-EGFP were imaged by confocal microscopy over a 60min period during which time the cells were challenged with: GLP-1 7-36 amide (GLP-1, 100nM) in the absence or presence of exendin 9-39 (Ex 9-39, 100nM); compound 2 (C2, 10 μ M) in the absence or presence of exendin 9-39 (100nM) or; DMSO (0.1% v/v) as indicated. Alternatively, the cells were treated with NRTFD (AZ) (333 μ M) at 37 $^{\circ}$ C for 1h before performing confocal imaging over a further 60min period during which the cells were challenged with GLP-1 7-36 amide (GLP-1, 100nM) in the presence of NRTFD (AZ) (333 μ M). Addition of NRTFD alone did not influence the distribution of fluorescence. Images were taken periodically over the 60min period and shown here are images representative of 3 experiments showing the distribution of EGFP fluorescence at 0, 5, 10, 30 and 60 min.

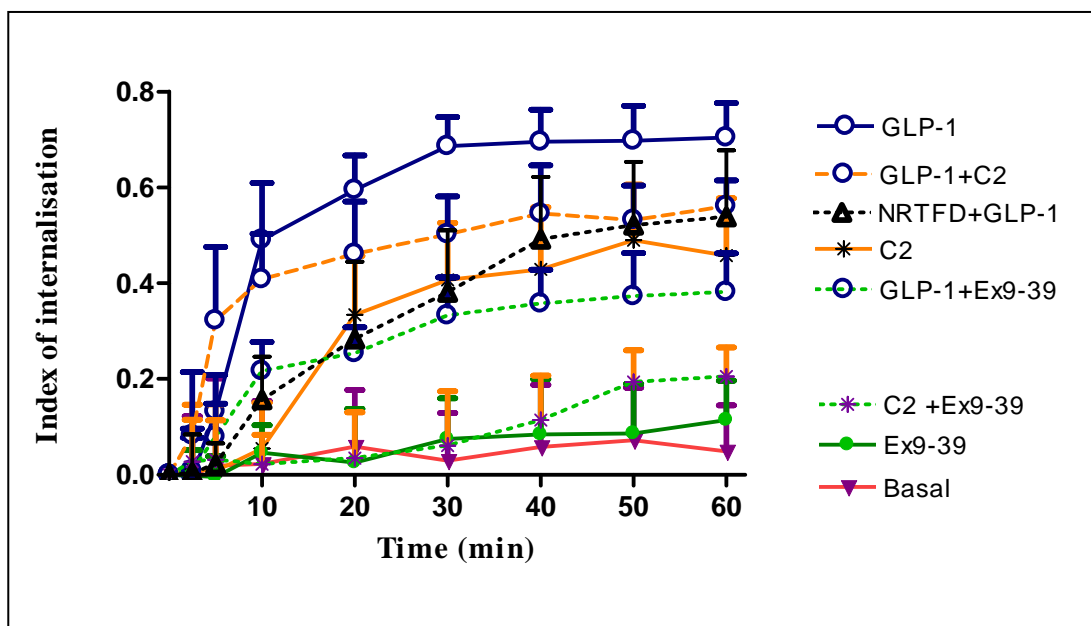


Figure 5.26. Quantification of agonist-mediated internalisation of the GLP-1R. Confocal images were taken of HEK293 cells with stable expression of the GLP-1R-EGFP during exposure to: GLP-1 7-36 amide (GLP-1, 100nM) in the absence or presence of exendin 9-39 (Ex 9-39, 100nM); compound 2 (C2, 10 μ M) in the absence or presence of exendin 9-39 (100nM); GLP-1 7-36 amide (100nM) and compound 2 (10 μ M); exendin 9-39 (100nM) or; DMSO (0.1% v/v) as indicated at 37°C for 60min. Alternatively, the cells were treated with NRTFD (AZ) (333 μ M) at 37°C for 60min, then subjected to confocal imaging over a further 60min period, during which, the cells were challenged with GLP-1 7-36 amide (GLP-1, 100nM) in the presence of NRTFD (AZ) (333 μ M). For each condition, an index of internalisation was derived from 6 randomly chosen cells in each of three independent experiments, using the procedure described in the Methods. An increase in the ‘Index of internalisation’ indicates an increase in receptor internalisation. Data are mean+sd, n=18 cells in 3 independent experiments.

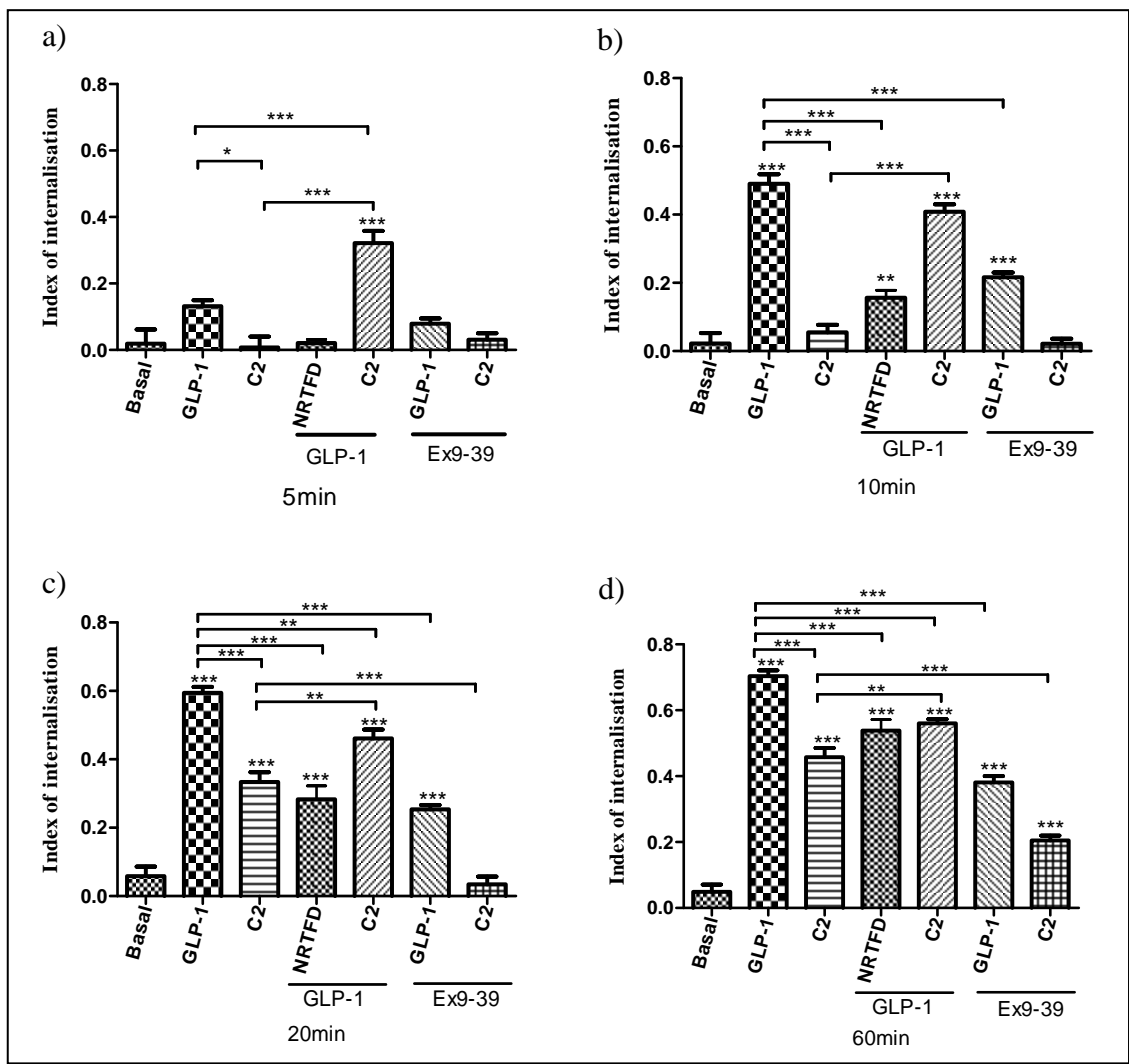


Figure 5.27. Comparison of GLP-1R internalisation mediated by different agonists. Quantification of agonist-mediated internalisation of the GLP-1R from **Figure 5.25** at 5min (a), 10min (b), 20min (c) and 60min (d). *, $p < 0.05$, **, $p < 0.01$, ***, $p < 0.001$ by Bonferroni's test following one-way ANOVA. For clarity, only comparison versus Basal, GLP-1 or C2 are shown. Data are mean+sd, n=18 cells in 3 independent experiments.

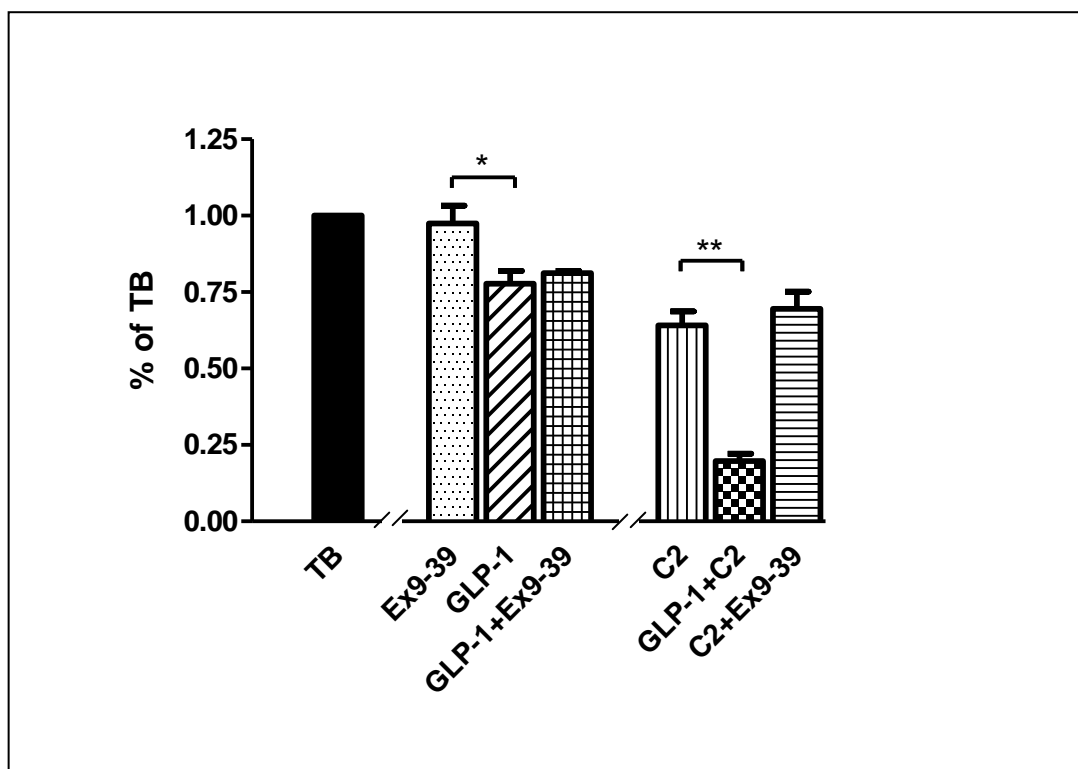


Figure 5.28. Binding of [¹²⁵I]-GLP 1 7-36 amide to intact cells with stable expression of the WTGLP-1R. HEK293Flp-In:WTGLP-1R cells were treated with either KHB, GLP-1 7-36 amide (GLP-1, 100nM), compound 2 (C2, 10 μ M) or both. Alternatively the cells were treated with either GLP-1 or C2 in the presence of exendin 9-39 (Ex9-39, 100nM). For each of the conditions, the treatment was carried out at 37°C for 20min. After appropriate washing as described in the Methods, the cells were further incubated with [¹²⁵I]-GLP1 7-36 amide (final concentration 0.054nM) either in the absence (total binding, TB, 100%) or presence of GLP-1 7-36 amide (1 μ M) to determine non-specific binding, at 4°C overnight. The levels of specifically-bound [¹²⁵I]-GLP1 7-36 amide (TB-NSB) were then determined for each condition relative to the cellular protein content. Data are expressed as a percentage of the specific binding following treatment with KHB. *, $p < 0.05$ and **, $p < 0.01$ compared with either GLP-1 or C2 as indicated by Dunnett's test following one-way ANOVA on the raw data (c.p.m.). Data are mean+sem, n=3.

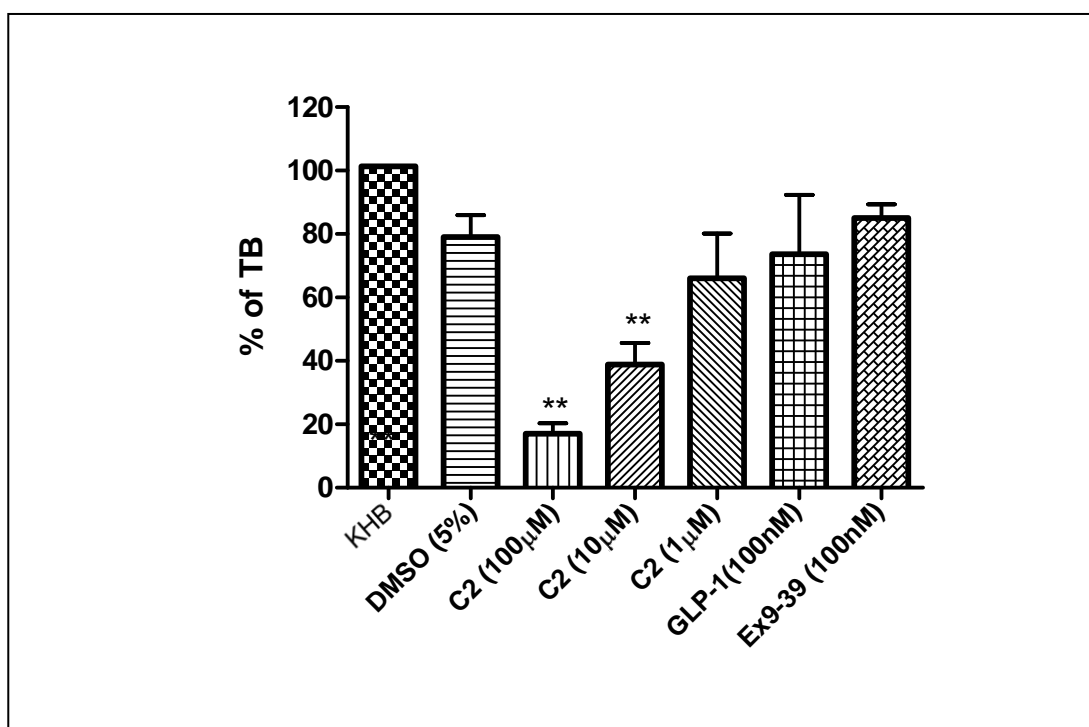


Figure 5.29. Compound 2 affects the binding of the muscarinic receptor antagonist 1-[N-methyl-³H] scopolamine methyl chloride to intact cells with stable expression of muscarinic M₃ receptors. HEK293:M3 cells were treated with either KHB, DMSO, compound 2 (C2), GLP-1 7-36 amide (GLP-1), or exendin 9-39 (Ex9-39) at 37°C for 60min, at the concentrations indicated. After washing as described in methods with KHB, the cells were further incubated with 1-[N-methyl-³H] scopolamine methyl chloride (³H]-NMS, 0.2nM), either in the presence (non-specific binding, NSB) or the absence (total binding, KHB) of atropine (2μM) at 37°C for 1h. The levels of specifically-bound [³H]-NMS (KHB-NSB) were then determined for each condition relative to the cellular protein content. Data are expressed as a percentage of the specific binding following treatment with KHB. For **, *p*<0.01 compared with KHB based on raw data (d.p.m.) by Dunnett's test following on-way ANOVA. Data are mean+sem. n=3.

5.3 Discussion

5.1.1 Summary

In this chapter, the agonism of compound 2 for important GLP-1R events (cAMP generation, receptor internalization) was examined and compared with the primary endogenous orthosteric agonist, GLP-1 7-36 amide. Further, the interaction of compound 2 with the orthosteric antagonist was examined along with its activity on receptor mutants.

Compound 2 evoked slower cAMP responses by the WTGLP-1R with much lower potency than GLP-1 7-36 amide. Exendin 9-39, an orthosteric antagonist increased compound 2-mediated responses by the WTGLP-1R in both cellular and membrane-based assays. Compound 2 but not GLP-1 7-37 amide showed a significant activity on the N-terminal truncated GLP-1R. Compound 2 also displayed time-dependent but receptor activation-independent adverse effects, demonstrated here by its ability to reduce ligand binding to receptors, including those unrelated to the GLP-1R. Using a stable cell line expressing a C-terminal EGFP-tagged GLP-1R, potential receptor internalization mediated by orthosteric and allosteric ligands was observed in real-time and determined quantitatively. Under basal conditions, confocal imaging of these cells showed clear plasma membrane and slight intracellular fluorescence. Compound 2 induced less pronounced receptor internalization than GLP-1 7-36 amide and with slower kinetics. Both GLP-1 7-36 amide- and compound 2-mediated receptor internalization were inhibited by exendin 9-39.

The recently described endogenous agonist of the GLP-1R, was examined in this chapter using synthetic small peptides and receptor mutants based on the two candidate regions, namely to Trp³³-Thr³⁵ and Phe⁶⁶-Glu⁶⁸. Synthetic NRTFD (AZ) displayed partial agonism on cAMP generation by the WTGLP-1R, but was not effective in cells with expression the N-terminal-truncated GLP-1R or Asp⁶⁷-based mutants (D67A, D67E, D67R and D67R/R102D). However, there were clear difficulties in the trafficking of these receptor mutants to the plasma membrane. NRTFD (AZ) was not able to induce receptor internalization and slightly inhibited that caused by GLP-1 7-36 amide. GLP-1 7-36 amide but not WET (CP) evoked cAMP-responses by the E34A mutant identical to the WTGLP-1R. When analyzed by mass spectrum, NRTFD (AZ) showed a relatively high purity but NRTFD (CP) displayed obvious impurities. A high concentration of NRTFD (CP) abolished cAMP-response mediated by an EC₅₀ concentration of GLP-1 7-36 amide. Mass spectrum analysis was not performed on WET (CP), FDE (CP) or NRTFDEYA (AZ).

In this chapter, Asp⁶⁷ of the GLP-1R (equivalent to D in NRTFD) was found to play a critical role in the processing and trafficking of the receptor. Mutants based on this residue, including D67A, D67E, D67R and D67R/R102D revealed one immunoreactive band in immunoblotting representing an immature form of the receptor. Confocal imaging of these mutants showed a lack of plasma membrane localised fluorescence. Treatment with MG132, a proteasome inhibitor, partially restored cell surface expression of these mutants as assessed by immunoblotting and the ability of the allosteric agent, compound 2 to mediate a response. Interestingly, treatment with exendin 9-39 increased cell surface located D67A mutant in cells with co-expression of the WTGLP-1R.

5.1.2 Allosteric agonism of compound 2 at the GLP-1R

The antidiabetogenic effects mediated by GLP-1 at the GLP-1R make this receptor a good target for the treatment for type 2 diabetes. Indeed this target is well-validated and there are currently two classes of drugs currently available that are designed to enhance the activity of the GLP-1R, specifically agonists of the GLP-1R and inhibitors of DPP-IV, which enhance the levels of endogenous GLP-1 by inhibiting its degradation. The peptide GLP-1 mimics that have been engineered to be DPP-IV-resistant must be administered at least once-daily by subcutaneous injection (Montanya and Sesti, 2009) while oral small molecule DPP-IV inhibitors have the potential risks of side effects (Stulc and Sedo, 2010). The need for improved therapeutics that target GLP1R function is clear. Allosteric small-molecule drugs not only have oral bioactivity but also have the potential benefit of binding to a site on the receptor that is distinct from that used by the orthosteric agonists. Thus, allosteric ligands can act at the receptor at the same time as the endogenous orthosteric agonist and increase affinity and/or efficacy of the latter, potentially providing more ‘physiological’ regulation (Bridges and Lindsley, 2008). Recently compound 2 has been described as an ago-allosteric agonist (Knudsen et al., 2007), not only increasing the affinity of the GLP-1R for GLP-1 as a positive allosteric modulator but itself also acting as an agonist (Knudsen et al., 2007). This provides hope for the development of high affinity, orally active compounds and clinical applicability for the treatment of type 2 diabetes.

The GLP-1R, similar to other GPCRs belonging Family B, couples to $G\alpha_s$, AC and enhances cAMP generation (Coopman et al., 2010) although some recombinant GLP-1Rs have been reported to couple to $G\alpha_{q/11}$ and $G\alpha_i$ (Bavec et al., 2003; Hällbrink et al., 2001; Montrose-Rafizadeh et al., 1999). Compound 2 has also been found to activate

$G\alpha_s$ in membranes and generate cAMP in both membranes (Knudsen et al., 2007) and intact cells with concentration-dependence (Coopman et al., 2010). Consistent with this, in the present study, compound 2 evoked cAMP generation in cell lines with stable expression of either the untagged GLP-1R or the GLP-1R with a C-terminal EGFP epitope-tag despite a lower potency than that of the GLP-1 7-36 amide. Concentration-response curves were slightly biphasic, similar to that in membranes (Knudsen et al., 2007), likely due to adverse effects of compound 2 (Coopman et al., 2010). As a consequence of these time-dependent effects, the efficacy of compound 2 was time-dependent, but it always displayed partial-agonism. Thus, typical sigmoidal curves of compound 2 were obtained by shortening the assay.

In the initial report on compound 2, it increased GLP-1 affinity (Knudsen et al., 2007). However, in the present study, pre-incubation with compound 2 reduced binding of [125 I]-GLP-1 in intact cells with stable expression of the GLP-1R. A similar decline was also observed in the binding of muscarinic receptor antagonist [3 H]-NMS to muscarinic M_3 receptors that were stably expressed in HEK293 cells, suggesting general adverse effects of compound 2. Consistent with this, compound 2 decreases the viability of HEK293 cells either with or without expression of the GLP-1R (Coopman et al., 2010). Therefore, it seems that the adverse effects of compound 2 are independent on the receptor but derives from its chemical nature. Indeed, chemical modification of compound 2 can generate compounds with typical sigmoidal rather than bell-shaped concentration-response curves (Knudsen et al., 2007).

It is thought that compound 2 interacts with an allosteric site as exendin 9-39, an orthosteric antagonist of the GLP-1R, did not inhibit compound 2-mediated cAMP generation (Knudsen et al., 2007; Coopman et al., 2010). A recent 3D-model of the

GLP-1R predicts that this allosteric site of the receptor might be a cavity near TM5 and TM6 (Lin and Wang, 2009). The lack of dependence of compound 2 on the N-terminal domain was examined in the present study using a mutant absolutely lacking the N-terminal domain of the GLP-1R. Challenge of the cells expressing this N-terminal truncated GLP-1R with compound 2 resulted in a significant cAMP response, which was not seen in the same cells challenged with GLP-1 7-36 amide. This provides the first direct evidence for compound 2 binding at a site distinct from the N-terminal domain and therefore distinct from a major portion of the orthosteric binding site.

Compared to GLP-1 7-36 amide, compound 2 mediated slower and less pronounced receptor internalization. The mechanisms underlying internalization or the consequences of this were not explored here and it is unclear if they are identical following activation by allosteric and orthosteric agonists. For most mammalian GPCRs, the mechanisms of internalization are predominantly based on GRK-dependent receptor phosphorylation and arrestin regulation of receptors through a clathrin-dependent pathway (see **Chapter 1**) although these mechanisms vary between receptors (Jovic et al., 2010). For the GLP-1R, a clathrin-dependent pathway for internalization has been implicated in several types of cells (Widmann et al., 1995; Vázquez et al., 2005; Jorgensen et al., 2005) although a caveolin-mediated pathway has also been reported in HEK293 and MIN6 cells (Syme et al., 2006). The differences in internalization mediated by compound 2 and GLP-1 7-36 amide could result from partial agonism of compound 2 or differences in receptor occupancy. However, cytotoxicity of compound 2 prevented the use of higher concentrations to explore if these would enhance internalization. Interestingly, combination of GLP-1 7-36 amide with compound 2 initiated internalization faster than GLP-1 7-36 amide alone but turned to slower and

less pronounced. It is possible that the adverse effects of compound 2 influence internalization, particularly at later time points.

Although internalization of ligand-bound GPCRs is thought to be important for ligand dissociation and is generally associated with receptor desensitisation and re-sensitisation, it has been proposed that internalised GPCRs in endosomes can continue to activate G-protein-independent signalling, e.g., MAPK signalling (DeWire et al., 2007; Ritter and Hall, 2009). However, very recently, internalised thyrotropin receptor (Calebiro et al., 2009) and parathyroid hormone receptor (Ferrandon et al., 2009) were found to stimulate cAMP production in a sustained manner in endosomes by remaining associated with their cognate G-protein subunit and AC. In addition, emerging evidence shows that once internalised, the GPCRs produce an persistent cellular cAMP-responses distinct from that elicited at the cell surface (Jalink and Moolenaar, 2010; Calebiro et al., 2010). It is unclear if the internalised GLP-1Rs continue to mediate any signalling. There is also no clue if such signalling is identical following receptor internalization mediated by allosteric and orthosteric agonists.

Interestingly, exendin 9-39 inhibited compound 2-mediated receptor internalization and also enhanced compound 2 efficacy in the present study. It is possible that exendin 9-39 generates a receptor conformation unable to internalise, even in the presence of an allosteric agonist. However, the exendin 9-39-enhanced compound 2 efficacy persisted in a membrane cAMP assay and was not therefore a consequence of altered receptor trafficking. Exendin 9-39 may facilitate the stabilisation of a more active receptor conformation by compound 2 or protect the GLP-1R against the adverse effects of compound 2. Alternatively, in the presence of compound 2 binding to the allosteric site, exendin 9-39 may induce a receptor conformational change, which blocks receptor

phosphorylation and thus reduces arrestin-dependent internalization. This conformational change of the receptor could also facilitate G-protein coupling. Therefore, it is possible that exendin 9-39-enhanced compound 2 efficacy may be independent on its effects on compound 2-mediated receptor internalization.

5.1.3 The endogenous agonist of the GLP-1R

The idea of an endogenous agonist in Family B GPCRs suggests that with the binding of the orthosteric agonist, conformational changes allow a sequence within the N-terminal domain of the receptor (the endogenous agonist) to interact with another part of the receptor and it is this which activates the receptor (Dong et al., 2006 and 2008). Thus, synthetic peptides that include the endogenous agonist sequence should act as full agonists at the receptor. Within the present study, the potential of an endogenous agonist of the GLP-1R was investigated based on the endogenous agonist (WDN) of the secretin receptor (Family B GPCR). Thus, WET (corresponding to Trp³³-Thr³⁵ of the GLP-1R) and FDE (corresponding to Phe⁶⁶-Glu⁶⁸ and analogous to WDN of the secretin receptor) were selected. Further, the sequence of NRTFD corresponding to Asn⁶³-Asp⁶⁷ of the GLP-1R was investigated as this was proposed as the endogenous agonist in a meeting and subsequently published as a full paper (Dong et al., 2008). In that study, synthetic NRTFD and NRTFDEYA acted as full agonists of the GLP-1R with a potency of 1.2 μ M and 8.5 μ M, respectively, (Dong et al., 2008). This was assessed in the present study using NRTFD (CP) synthesized by Cambridge Peptides and NRTFD (AZ) and NRTFDEYA (AZ) synthesized by Pepscan Presto B.V. and supplied by AstraZeneca. No activity of NRTFD (CP) was detected using a range of concentrations (generally up to 100 μ M) in at least three cell lines (HEK293, HEK293Flp-In, CHO) with stable expression of functional GLP-1Rs. Neither the use of bacitracin nor longer treatments

(up to 1h) provided any evidence of agonism by NRTFD (CP). Mass-spectrum analysis confirmed the presence of NRTFD in NRTFD (CP), although other species were also clearly present. An exposure to a high concentration of NRTFD (CP) (1mM) abolished the cAMP-response mediated by an EC₅₀ concentration of GLP-1-7-36 amide. Given the reported low potency of NRTFD (Dong et al., 2008), it is difficult to say with any certainty whether the presence of such inhibitors within the preparation would be sufficient to prevent agonism by NRTFD. NRTFD (AZ) was a purer preparation and this clearly acted as a relatively weak partial agonist at the WTGLP-1R albeit at a fairly high concentration (333μM). It was possible that the intrinsic activity of NRTFD (AZ) could be higher if higher concentrations were used, but this would mean that the potency must be at least 277-fold less than previously reported (Dong et al., 2008), despite a very similar *p*EC₅₀ (10.34) of GLP-1 7-36 amide in that study compared to that in the present study (10.40). NRTFDEYA (AZ) was inactive at the same receptors. It is of course possible that this preparation also contained impurities that were able to act as antagonists but a limited quantity meant that this could not be assessed. However, further investigations were limited by the availability of NRTFD. In addition, NRTFD (AZ) did not cause any detectable receptor internalization and also inhibited GLP-1-mediated receptor internalization. This suggests partial agonism of NRTFD (AZ). Thus, for example, buprenorphine, a weak partial agonist inhibits μ-opioid receptor (a Family A GPCR) desensitization and internalization induced by more potent agonist, met-enkephalin (Virk et al., 2009).

The idea of an endogenous agonist suggests that synthetic peptides representing that sequence within the receptor should bind to the receptor at a site distinct from the orthosteric agonist. The previous study of the GLP-1R endogenous agonist (Dong et al.,

2008) demonstrated at least two pieces of evidence for synthetic NRTFD binding to the GLP-1R at a site distinct from GLP-1 7-36 amide: a) synthetic NRTFD acted as a full agonist at a D67E mutant (D67 equivalents to D in NRTFD and is reported as the key residue in the endogenous agonist) while GLP-1 7-36 amide mediates an impaired response at the same mutant and; b) the orthosteric antagonist exendin 9-39 inhibited the cAMP-response mediated by an EC₅₀ concentration of GLP-1 7-36 amide (0.1nM) but did not affect that caused by synthetic NRTFD (1μM). Because of the big difference in the EC₅₀ values and limited availability of NRTFD (AZ), antagonism by exendin 9-39 of synthetic NRTFD at the GLP-1R was not examined in the present study. However, several Asp⁶⁷-based mutants including D67A, D67E, D67R and D67R/R102D were generated here to assess the role of this endogenous sequence in GLP-1 agonism. Surprisingly, when expressed in HEK293 cells, these mutants were not appropriately processed (i.e. not trafficked to the cell surface), indicating that Asp⁶⁷ is critical for proper assembly and folding of the receptor protein (see below). This is consistent with the recently available crystal structures of the GLP-1R (Runge et al., 2008; Underwood et al., 2010). Treatment with the proteasome inhibitor, MG132, partially restored the cell surface-expression of these mutants (demonstrated by the altered pattern of immunoblotting and the restoration of cAMP responses mediated by the allosteric agonist, compound 2). However, there was still no detectable cAMP production evoked by NRTFD (AZ) in the cells expressing these Asp⁶⁷-based mutants or the N-terminal truncated GLP-1R although GLP-1 7-36 amide mediated a response (~50% of compound 2) at the D67E mutant. It was difficult to accurately assess the level of cell surface-located receptor mutants and compound 2 only provided an indicator of expression. Further, it was unclear if compound 2 was able to enter the cell and cause

some component of the cAMP response by acting on intracellular receptors. Therefore, it was possible that the inability of NRTFD (AZ) to evoke cAMP generation by mutated GLP-1Rs may be caused by both relatively low levels of cell surface-located receptors and the low potency of NRTFD (AZ). However, the relative intrinsic activities of compound 2 and NRTFD (AZ) in the wild-type receptor suggests that the assay would have had the sensitivity to detect NRTFD (AZ)-mediated responses in the mutants had the intrinsic activity of NRTFD (AZ) been similar in comparison to compound 2 across all of the constructs. The inability of NRTFD (AZ) to evoke cAMP responses in the N-terminally truncated GLP-1R was also confusing and taken at face value with the absence of effect on the mutated receptors would suggest that the presence of a properly folded N-terminus of the GLP-1R is required for NRTFD-mediated receptor activation.

Besides the sequences around the FDE motif (FDE, NRTFD and NRTFDEYA), the WET motif was also assessed for its potential as an endogenous agonist of the GLP-1R. This was eliminated as GLP-1 7-36 amide acted at both E34A and E34R mutants similarly to the wild-type receptor and synthetic WET (CP) was inactive at either the mutant or the wild-type receptor. Although it is not possible to independently test for potential efficacy of WET (CP) (i.e. it may simply not work in the way that NRTFD (CP) did not), evidence in the present study is not fully in agreement with the idea of an endogenous agonist within the GLP-1R. This is supported to some extent by the recent crystal structures of the N-terminal domain of the GLP-1R in complex with orthosteric ligands (Runge et al., 2008; Underwood et al., 2010). The critical role of Asp⁶⁷ in stabilizing the structure of the N-terminal domain of the GLP-1R has been confirmed in both of these crystal structures. Thus, when bound with exendin 9-39, Asp⁶⁷ interacts directly with Try⁶⁹ and Ala⁷⁰, Trp⁷² and Arg¹²¹ and with Arg¹⁰² through a water

molecule (Runge et al., 2008). Similarly, in the complex bound with GLP-1, Asp⁶⁷ interacts directly with Arg¹⁰² and with Arg¹²¹ *via* a water molecule (Underwood et al., 2010). In both of these complexes, Arg¹²¹ also interacts with Val³³ and Lys²⁷ of exendin and GLP-1, respectively, and with a number of other residues within the N-terminal domain of the receptor (Runge et al., 2008; Underwood et al., 2010). Consequently, if NRTFD (corresponding to Asn⁶³-Asp⁶⁷ of the GLP-1R) is the endogenous agonist and interacts with another part of the receptor, such conformational rearrangement around Asp⁶⁷ is difficult to reconcile with the present structural data.

5.1.4 Asp⁶⁷ in the processing and trafficking of the GLP-1R

In the present study, all of the mutated GLP-1Rs based on Asp⁶⁷ including D67A, D67E, D67R and D67R/R102D were detected as only one immunoreactive band in immunoblotting, which was equivalent to the lower one of the two immunoreactive bands detected in the WTGLP-1R. This lower band represents the immature form of the receptor that has not trafficked to the cell surface (see **Chapter 3**). Consistent with this, confocal images revealed that the fluorescence of D67A and D67E mutants containing a C-terminal EGFP-tag were intracellular. This suggests that Asp⁶⁷ is critical for the processing and trafficking of the GLP-1R. It is well known that the ER has an essential function in protein folding and maturation (Naidoo, 2009). Newly produced GPCRs are not functional until they fold into their appropriate 3D structures and are packaged in the ER and trafficked to the plasma membrane (Conn et al., 2007). Misfolded receptor proteins are retained in the ER and targeted for degradation (Conn and Ulloa-Aguirre, 2010). Several diseases associated with GPCRs have been traced to proteins that are misfolded and further result in impaired plasma membrane expression (Conn et al., 2007). For example, defects involving the ER-retained arginine vasopressin receptor 2,

a family A GPCR, are associated with nephrogenic diabetes insipidus (Hermosilla et al., 2004; Robben et al., 2009). Similarly, loss-of-function mutations of the thyrotropin receptor, another Family A GPCR, can cause destabilisation of the receptor, preventing its cell surface expression and leading to congenital hypothyroidism (Sequeira et al., 2002).

Existing evidence has suggested that mutations of GPCRs that cause ER-retention are generally located at residues that are critical for stabilising the structure; and frequently show a change in residue charge or a breakage in interactions with other residues (Conn and Ulloa-Auirre, 2009). For example, mutagenesis studies have identified a G90K mutant of the gonadotropin-releasing hormone receptor (GnRH-R), a Family A GPCR, which leads to a misfolded protein with impaired plasma membrane expression and is associated with hypogonadotropic hypogonadism (HH) (Janovick et al., 2005). The N-terminal domain of Family B receptors have a common structure (known as the secretin recognition fold), which is stabilized by three conserved disulfide bonds and five conserved residues including Asp⁶⁷ in the GLP-1R (see **Chapter 1**). Indeed, in the models based on the same structure mentioned above (Underwood et al., 2010; code: 3IOL) removing the ligand and all solvent molecules still resulted in the wild-type receptor with interactions between Asp⁶⁷ and Arg¹⁰² and between Asp⁶⁷ and Arg¹²¹. The D67A mutant would lose interactions with Arg¹⁰² or Arg¹²¹ while the D67R/R102D mutant may maintain the interaction between Arg⁶⁷ and Asp¹⁰² but not with Arg¹²¹. Further, the D67E mutant should have the right functionality to both Arg¹⁰² and Arg¹²¹ but the extra length of the residue would make it too difficult to accommodate meaningful interactions (personal communication, Dr G. Robb, AstraZeneca, Alderley Park, Macclesfield, U.K.). This strongly suggests that mutations at Asp⁶⁷ may result in misfolded ER-retained proteins.

It has been suggested that co-expression with binding partners or chaperones may enhance the cell surface expression of GPCRs exhibiting poor surface trafficking in heterologous cells through promoting proper folding of the receptor (Dunham and Hall, 2009). Evidence also suggests that misfolded receptor proteins may affect the folding and processing of wild-type receptors (Conn et al., 2007). The co-expression of D67A mutant with WTGLP-1R did not alter the one-immunoreactive band of D67A in immunoblotting. Interestingly, incubating these co-transfected cells with the orthosteric antagonist, exendin 9-39 resulted in a slight restoration of the upper immunoreactive band, which represents the mature protein of the D67A mutant. This was not seen in the same (co-transfected) cells but treated with GLP-1 7-36 amide or in the cells expressing D67A alone and treated with either exendin 9-39 or GLP-1 7-36 amide. The mechanism underlying this is unclear. Perhaps co-expression with the wild-type receptor increased cell surface expression of D67A mutant, which was further enhanced by the treatment with exendin 9-39. Indeed, antagonists have been shown previously to stabilize GPCRs at the cell surface into conformations that are more resistant to down-regulation. For example, treatment of cells expressing the histamine-H₂ receptor with the antagonists cimetidine and ranitidine, leads to an increase in receptor number (Smit et al., 1996). Furthermore, HH associated with GnRH-R mutants with impaired receptor trafficking can be treated with pharmacological chaperones, non-peptide GnRH-R antagonists that facilitate appropriate receptor folding and increase cell surface expression (Finch et al., 2010). It is unclear if pharmacological chaperones can rescue ER-retained GLP-1R proteins, e.g. Asp⁶⁷-based mutants and further increase their signalling. This remains to be explored.

CHAPTER 6 Final Discussion

6.1 Summary of results

The findings here demonstrate that C-terminal epitope-tagged GLP-1Rs behave similarly to the untagged receptor in HEK293 cells. Thus, these epitope-tagged receptors bound GLP-1 7-36 amide with similar affinities and coupled to cAMP generation with similarly potencies to the untagged GLP-1R. Consequently, C-terminal epitope tags provide the probes to investigate the expression of the GLP-1R by immunoblotting and imaging. These recombinantly expressed GLP-1Rs have been used to show that only the mature, fully glycosylated receptor is expressed at the plasma membrane. Particularly, the C-terminal EGFP-tagged construct has been used to establish a HEK293 cell line with the stable expression of a visible GLP-1R and this has provided a good cellular model for observation and determination of real time ligand-mediated receptor internalization.

The N-terminal HA-tag in the GLP-1R constructs generated by the present study has been used to investigate the cleavage of the N-terminal signal peptide sequence. These data reveal that the putative signal peptide sequence, most likely corresponding to the first 23 residues of the GLP-1R, is indeed cleaved and does not form part of the mature protein. Cleavage of the signal peptide is essential for processing and trafficking of the GLP-1R to the plasma membrane. Blocking this cleavage by either inserting an EGFP-tag at the N-terminus of the WTGLP-1R or generating an A21R mutant resulted in full-length and intracellularly located, immature (i.e. not fully glycosylated) proteins. This information has been used in conjunction with information from a mutagenesis

strategy to develop a 3D model of the GLP-1R (Coopman et al., in preparation). However, the signal peptide sequence plays a critical role for synthesis of the GLP-1R. Removal of this sequence abolished the expression of the receptor.

The putative ago-allosteric agent of the GLP-1R, compound 2, mediated cAMP-responses with lower potency compared with GLP-1 7-36 amide in cells with stable expression of the GLP-1Rs. Compound 2 caused GLP-1R internalization although it was slower and less than that caused by GLP-1 7-36 amide. Interestingly, exendin 9-39 enhanced the cAMP production but blocked receptor internalization mediated by compound 2. However, compound 2 has adverse effects, highlighted here by a reduction in ligand binding to an unrelated GPCR (the muscarinic M₃ receptor). Most importantly, compound 2 is able to activate an N-terminally-deleted GLP-1R providing direct evidence for action of compound 2 at an allosteric site.

The recently described endogenous agonist of the GLP-1R, NRTFD (corresponding to residues Asn⁶³-Asp⁶⁷ of the GLP-1R and where D is the critical residue) acted as a weak partial agonist on the wild-type GLP-1R but was inactive on the N-terminal-truncated GLP-1R. NRTFD did not cause receptor internalization and blocked that mediated by GLP-1 7-36 amide. Findings here suggest that Asp⁶⁷ in the N-terminal domain of the GLP-1R is critical for the processing and trafficking of the receptor. Thus, Asp⁶⁷-based mutants (D67A, D67E, D67R or D67R/R102D) were expressed as immature receptor proteins detected by immunoblotting and showed intracellular localization in confocal imaging. Treatment with the proteasome inhibitor, MG132, partially restored cell surface expression of Asp⁶⁷-based mutants. This was based on both compound 2-mediated cAMP response and appearance of the higher

immunoreactive band representing mature form of the receptor. Despite this expression, NRTFD still failed to evoke cAMP generation in cells transiently expressing the constructs. Co-expression of the wild-type GLP-1R did not help the D67A mutant process to a mature form of the protein. However, exendin 9-39 treatment of cells co-transfected with this mutant and the wild-type GLP-1R resulted in the appearance of a higher molecular weight immunoreactive band, consistent with the mature form of the D67A mutant receptor.

6.2 Discussion and implications for further research

Data in the present study have provided clear experimental evidence for that the N-terminal putative signal peptide of the GLP-1R is cleaved and this cleavage is essential for the trafficking and processing of the GLP-1R, which argues against a recent model of the GLP-1R containing a signal peptide sequence (Lin and Wang, 2009). Despite the crystal structure of the extracellular domain of the GLP-1R in complex with GLP-1 or exendin 9-39 being available (Runge et al., 2008; Underwood et al., 2010), the crystal structure of the whole receptor has not been determined. Indeed, crystal structures of Family B GPCRs with a large N-terminal domain are likely to be extremely difficult to determine. However, these findings have contributed useful information for modelling the GLP-1R.

The addition of epitope tags to GPCRs has facilitated a wide variety of studies on their structure and function. Epitope-tagging requires careful consideration about the nature of the epitope tag and its location within the receptor. A number of constructs containing an HA- and/or an EGFP-tag at either terminus of the GLP-1R have been generated and assessed in the present study to provide useful information for epitope-

tagging the GLP-1R. For example, evidence here shows that C-terminal tagging is most likely to retain the native properties of the GLP-1R including receptor expression, processing, trafficking and function. In contrast, to insert an epitope tag at the N-terminus of the GLP-1R just before the signal peptide needs to be considered carefully. A small tag e.g. HA-tag at the N-terminus is cleaved with the signal peptide and thus not detectable. Inconsistent with a recent study suggesting that an N-terminal EGFP-tag does not alter expression or function of the GLP-1R (Bavec and Licar, 2009), the presence of an N-terminal EGFP-tag resulted in an intracellularly located immature protein in the present study. These data reveal that Ala²¹ is critical for the cleavage of the signal peptide and that mutation of A21R is sufficient to alter the trafficking of the GLP-1R by blocking cleavage, highlighting a potential problem of inserting an epitope tag in this region. In addition, the highly structured N-terminal domain of the GLP-1R has been demonstrated in the recent crystal structure of this region (Runge et al., 2008; Underwood et al., 2010). These structures of the GLP-1R show several interactions between Asp⁶⁷ and other residues e.g. Arg¹⁰² and Arg¹²¹ (Runge et al., 2008; Underwood et al., 2010). Consistent with this, the Asp⁶⁷-based mutants generated in the present study resulted in immature intracellularly located receptor proteins, which are likely to be a consequence of impaired interactions and the loss of structure within this region.

Recent imaging studies of intact cells show that some GPCRs, e.g. the GnRHR, are normally inefficiently exported from the ER, such that only a fraction of the synthesised protein is transferred to the plasma membrane and the remainder is retained in the ER and targeted for degradation (Armstrong et al., 2010; Conn and Ulloa-Aguirre, 2010). This provides a therapeutic opportunity by using pharmacoperone drugs to enhance

receptor function by increasing the concentration of the receptor at the plasma membrane (Zhao et al., 2007; Conn and Ulloa-Aguirre, 2010). The evidence here has clearly shown that in HEK293 cells, recombinantly expressed GLP-1R is located predominately at the plasma membrane but also with some intracellular retention. Although this is clearly in a recombinant expression system, in which levels may be very high, it is unclear in pancreatic β -cells whether the GLP-1R is fully or partially expressed at the cell surface. Although it is thought that the GLP-1R are most strongly expressed on the surface of the β -cells facing the endothelium (Tornehave et al., 2008), the sub-cellular distribution of receptors was not very clear (Tornehave et al., 2008; Shu et al., 2009). In addition, there is evidence showing down-regulation of the GLP-1R in β -cells in type 2 diabetes (Xu et al., 2007; Shu et al., 2009). This is consistent with mildly reduced (~30%) responses to GLP-1 in type 2 diabetes (Fritsche et al., 2000; Kjems et al., 2003) although the reduced insulinotropic activity of GLP-1 in patients with type 2 diabetes may be compensated for higher plasma concentrations of GLP-1 (Meier and Nauck, 2010). There is clearly a need to investigate the expression and subcellular distribution of the GLP-1R in β -cells throughout the different stages of type 2 diabetes. It is currently unclear whether pharmacoperone drugs represent a sensible approach to enhance GLP-1-based treatments for type 2 diabetes *via* rescue of misrouted or ER-accumulated GLP-1R in β -cells. Obviously, to assess this would require suitable *in vitro* models of human β -cells, access to human β -cells and high quality human GLP-1R antibodies.

The inability of the orthosteric antagonist, exendin 9-39 to inhibit compound 2-mediated cAMP generation shown previously (Knudsen et al., 2007; Coopman et al., 2010) and in the present study provides good evidence for an allosteric action of

compound 2. The observation of compound 2 coupling the N-terminal domain-deleted GLP-1R to cAMP production in the present study is the first direct evidence for compound 2 binding to a site distinct from the N-terminal domain where GLP-1 binds initially. The precise location of the allosteric binding site of compound 2 has, however, not been explored in the present study. Such information may help in the development the therapeutically useful small-molecule GLP-1R agonists.

Emerging evidence has shown that GLP-1 and mimics mediate anti-apoptotic signalling by both G-protein-dependent and -independent pathways (Bernal-Mizrachi, 2009). For example, PKB is an essential mediator linking GLP-1 signalling to the intracellular machinery that modulates β -cell growth and survival (Wang et al., 2004). Although the role of any anti-apoptotic and proliferative effects of GLP-1 mimics on β -cells in type 2 diabetic patients remain to be defined, it is important to understand the role of any allosteric agonist of the GLP-1R in such events. This of course relies on the availability of high potency compounds (that may or may not be analogues of compound 2). Our studies (here and recently published) have demonstrated compound 2-mediated cAMP and intracellular Ca^{2+} responses (Coopman et al., 2010). However, compound 2-mediated effects in other potentially important signalling pathways remain to be further investigated along with potential differences in the trafficking and regulation of the GLP1-R mediated by orthosteric and allosteric compounds.

It has been shown here that the orthosteric antagonist, exendin 9-39 enhances compound 2-mediated cAMP production and inhibits internalisation of the GLP-1R. Physiologically, the metabolic products of GLP-1 degradation by DPP-IV, GLP-1 9-36 amide and GLP-1 9-37, represent ~85% of circulating postprandial GLP-1. Although these compounds can act as GLP-1R antagonists (Knudsen and Pridal, 1996), it is

unclear what roles these metabolites play physiologically or indeed if they could interact with allosteric agonists to influence their pharmacology. This remains to be further explored.

Consistent with a recent study (Dong et al., 2008), which shows that the binding of GLP-1 allows the NRTFD sequence in the N-terminal domain of the GLP-1R to interact with another part of the receptor and cause agonism, the synthetic peptide NRTFD (AZ) clearly showed activity on the WTGLP-1R in the present study although it was a fairly weak and partial agonist. Data suggested that the lack of agonism by NRTFD (CP) may have been a consequence of the presence of inhibitors or antagonists present within the preparation. It cannot be ruled out that the low efficacy of NRTFD (AZ) was caused by other species within the preparation. NRTFD (AZ) failed to activate the N-terminal truncated GLP-1R and the current data provide no evidence that the endogenous NRTFD sequence acts as endogenous agonist, certainly independently of the N-terminal domain. It was hoped that this would be addressed directly by the D67A mutant, where the D represents that in the NRTFD. However this residue was shown to be essential for stabilising the structure of the N-terminal domain, which is critical for receptor trafficking. All of the mutants based on this residue including D67A, D67E, D67R and D67R/R102D resulted in little or no cell surface expression that severely limited the assessment of the role of this residue as a critical component of the endogenous agonist. Partial rescue of the D67A and D67E mutant receptors by proteasome inhibition, although partially restoring responses to the allosteric (but not orthosteric) agonist did not restore responses to NRTFD (AZ). Thus, although the present study supports the concept of agonism by NRTFD, the data provide no direct support that the endogenous sequence plays the role of endogenous agonist. This needs to be further addressed by,

for example, restoring expression of D67 mutated receptors and the identification of the potential region(s) in the GLP-1R that NRTFD interacts with.

In summary, the present study has demonstrated novel features that add to the growing interest in the function, structure and regulation of the GLP-1R. This has opened up possibilities for studies that will further extend our understanding of agonism at the GLP-1R and the trafficking and processing required for the regulation of cell-surface expression.

References

- Abu-Hamdah R, Rabiee A, Meneilly GS, Shannon RP, Andersen DK and Elahi D (2009) Clinical review: The extrapancreatic effects of glucagon-like peptide-1 and related peptides. *J Clin Endocrinol Metab.* **94**:1843-1852.
- Achour L, Labbé-Jullié C, Scott MG and Marullo S (2008) An escort for GPCRs: implications for regulation of receptor density at the cell surface. *Trends Pharmacol Sci.* **29**:528-535.
- Alken M, Rutz C, Köchl R, Donalies U, Oueslati M, Furkert J, Wietfeld D, Hermosilla R, Scholz A, Beyermann M, Rosenthal W and Schülein R (2005) The signal peptide of the rat corticotropin-releasing factor receptor 1 promotes receptor expression but is not essential for establishing a functional receptor. *Biochem. J.* **390**:455-464.
- Alken M, Schmidt A, Rutz C, Furkert J, Kleinau G, Rosenthal W and Schülein R (2009) The sequence after the signal peptide of the G protein-coupled endothelin B receptor is required for efficient translocon gating at the endoplasmic reticulum membrane. *Mol Pharmacol.* **75**:801-811.
- Almén MS, Nordström KJ, Fredriksson R and Schiöth HB (2009) Mapping the human membrane proteome: a majority of the human membrane proteins can be classified according to function and evolutionary origin. *BMC Biol.* **7**:50.
- Al-Sabah S and Donnelly D (2003) The positive charge at Lys-288 of the glucagon-like peptide-1 (GLP-1) receptor is important for binding the N-terminus of peptide agonists. *FEBS Lett.* **553**:342-346.
- American Council on Exercise BMI Calculator at Ace Fitness: <http://www.acefitness.org/calculators/bmi-calculator.aspx>, accessed 07 August, 2010.
- An HJ, Froehlich J and Lebrilla CB (2009) Determination of glycosylation sites and site-specific heterogeneity in glycoproteins. *Curr Opin Chem Biol.* **13**:421-426.
- Anderson JW, Kendall CWC and Jenkins DJA (2003) Importance of weight management in type 2 diabetes: review with meta-analysis of clinical studies. *J Am Coll Nutr* **22**:331-339
- Apweiler R, Hermjakob H and Sharon N (1999). On the frequency of protein glycosylation as deduced from analysis of the SWISS-PROT database. *Biochimica et Biophysica Acta.* **1473**:4-8.
- Armstrong SP, Caunt CJ, Finch AR and McArdle CA (2010) Using automated imaging to interrogate gonadotrophin-releasing hormone receptor trafficking and function. *Mol Cell Endocrinol.* 2010 Aug 3. [Epub ahead of print]
- Ashby MC, Ibaraki K and Henley JM (2004) It's green outside: tracking cell surface proteins with pH-sensitive GFP. *Trends Neurosci.* **27**:257-261.

- Assil IQ and Abou-Samra AB (2001) N-glycosylation of CRF receptor type 1 is important for its ligand-specific interaction. *Am. J. Physiol. Endocrinol. Metab.* **281**:E1015-1021.
- Balzarini J (2007) Targeting the glycans of glycoproteins: a novel paradigm for antiviral therapy *Nat Rev Microbiol.* **5**:583-597.
- Bange G, Wild K and Sinning I (2007) Protein translocation: checkpoint role for SRP GTPase activation. *Curr Biol.* **17**:R980-982.
- Barnard ND, Katcher HI, Jenkins DJ, Cohen J and Turner-McGrievy G (2009) Vegetarian and vegan diets in type 2 diabetes management. *Nutr Rev.* **67**:255-263.
- Bavec A and Licar A (2009) Functional characterization of N-terminally GFP-tagged GLP-1 receptor. *J Biomed Biotechnol.* **2009**:498149.
- Bavec A, Hallbrink M, Langel U and Zorko M (2003) Different role of intracellular loops of glucagon-like peptide-1 receptor in G-protein coupling. *Regul Peptides* **111**:137-144.
- Bazarsuren A, Grauschopf U, Wozny M, Reusch D, Hoffmann E, Schaefer W, Panzner S and Rudolph R (2002) In vitro folding, functional characterization, and disulfide pattern of the extracellular domain of human GLP-1 receptor. *Biophys Chem.* **96**:305-318.
- Bazzano LA, Serdula M and Liu S (2005) Prevention of type 2 diabetes by diet and lifestyle modification. *J. Am. Coll. Nutr.* **24**:310-319.
- Beinborn M (2006) Class B GPCRs: a hidden agonist within? *Mol Pharmacol.* **70**:1-4.
- Beinborn M, Worrall CI, McBride EW and Kopin AS (2005) A human glucagon-like peptide-1 receptor polymorphism results in reduced agonist responsiveness. *Regul Pept.* **130**:1-6.
- Bellmann-Sickert K and Beck-Sickinger AG (2010) Peptide drugs to target G protein-coupled receptors. *Trends Pharmacol Sci.* **31**:434-441
- Bendtsen JD, Nielsen H, von Heijne G and Brunak S.J (2004) Improved prediction of signal peptides: SignalP 3.0. *Mol Biol.* **340**:783-795.
- Benedict C, Hallschmid M, Hatke A, Schultes B, Fehm HL, Born J and Kern W (2004) Intranasal insulin improves memory in humans. *Psychoneuroendocrinology* **29**:1326–1334.
- Benovic JL, Pike LJ, Cerione RA, Staniszewski C, Yoshimasa T, Codina J, Caron MG and Lefkowitz RJ (1985) Phosphorylation of the mammalian beta-adrenergic receptor by cyclic AMP-dependent protein kinase. Regulation of the rate of receptor phosphorylation and dephosphorylation by agonist occupancy and effects on coupling of the receptor to the stimulatory guanine nucleotide regulatory protein. *J Biol Chem.* **260**:7094–7101.
- Benya RV, Kusui T, Katsuno T, Tsuda T, Mantey SA, Battey JF, and Jensen RT (2001) Glycosylation of the Gastrin-Releasing Peptide Receptor and Its Effect on Expression, G Protein Coupling, and Receptor Modulatory Processes *Mol. Pharmacol.* **58**:1490-1501.

- Berndt U, Oellerer S, Zhang Y, Johnson AE and Rospert S (2009) A signal-anchor sequence stimulates signal recognition particle binding to ribosomes from inside the exit tunnel. *Proc Natl Acad Sci U S A*. **106**:1398-403.
- Bisello A, Greenberg Z, Behar V, Rosenblatt M, Suva LJ and Chorer M (1996) Role of glycosylation in expression and function of the human parathyroid hormone/parathyroid hormone-related protein receptor. *Biochemistry* **35**:15890-15895
- Blobel G (2000) Protein targeting. *Chembiochem*. **1**:86-102.
- Blonde L (2009) Current antihyperglycemic treatment strategies for patients with type 2 diabetes mellitus. *Cleve Clin J Med*. **76**:S4-11.
- Bockaert J and Pin JP (1999) Molecular tinkering of G protein-coupled receptors: an evolutionary success. *EMBO J*. **18**:1723–1729.
- Böhme I and Beck-Sickinger AG (2009) Illuminating the life of GPCRs. *Cell Commun Signal*. **7**:16.
- Bonner TI. Class B Orphans. Last modified on 2010-07-07. Accessed on 2010-09-01. IUPHAR database (IUPHAR-DB), <http://www.iuphar-db.org/DATABASE/FamilyMenuForward?familyId=17>.
- Bookchin RM and Gallop PM (1968) Structure of hemoglobin A1c: nature of the N-terminal beta chain blocking group. *Biochem. Biophys. Res. Commun*. **32**:86–93.
- Booth PJ and Curnow P (2009) Folding scene investigation: membrane proteins. *Curr Opin Struct Biol*. **19**:8-13.
- Bornemann T, Jöckel J, Rodnina MV and Wintermeyer W (2008) Signal sequence-independent membrane targeting of ribosomes containing short nascent peptides within the exit tunnel. *Nat Struct Mol Biol*. **15**:494-499.
- Bos JL (2003) Epac: a new cAMP target and new avenues in cAMP research. *Nat Rev Mol Cell Biol*. **4**:733-738.
- Boy D and Koch HG (2009) Visualization of distinct entities of the SecYEG translocon during translocation and integration of bacterial proteins. *Mol Biol Cell*. **20**:1804-1815.
- Bräuner-Osborne H, Wellendorph P and Jensen AA (2007) Structure, pharmacology and therapeutic prospects of family C G-protein coupled receptors. *Curr Drug Targets*. **8**:169-184.
- Bridges TM and Lindsley CW (2008) G-protein-coupled receptors: from classical modes of modulation to allosteric mechanisms. *ACS Chem Biol*. **3**:530-341.
- Brooks SA. (2009) Strategies for analysis of the glycosylation of proteins: current status and future perspectives. *Mol Biotechnol*. **13**:421-426.
- Brown BL, Albano JDM, Ekins RP, Sgherzi AM and Tampion W (1971) A simple and sensitive saturation assay method for the measurement of adenosine 3959-cyclic monophosphate. *Biochem J* **121**:561–562.

- Brubaker PL and Drucker DJ (2002) Structure-function of the glucagon receptor family of G-protein-coupled receptors: the glucagon, GIP, GLP-1, and GLP-2 receptors. *Receptors Channels* **8**:179–188.
- Buhlmann N, Aldecoa A, Leuthauser K, Gujer R, Muff R, Fischer JA and Born W (2000) Glycosylation of the calcitonin receptor-like receptor at Asn60 or Asn112 is important for cell surface expression. *FEBS Lett* **486**:320-324.
- Bullock BP, Heller RS and Habener JF (1996) Tissue distribution of messenger ribonucleic acid encoding the rat glucagon-like peptide 1 receptor. *Endocrinology* **137**:2968-2978.
- Bullock WO, Fernandez JM and Short JM (1987) XL1-Blue: a high efficiency plasmid transforming recA Escherichia coli strain with beta-galactosidase selection. *BioTechniques* **5**:376-378.
- Burcelin R, Serino M and Cabou C (2009) A role for the gut-to-brain GLP-1-dependent axis in the control of metabolism. *Curr Opin Pharmacol.* **9**:744-752.
- Burda P and Aebi M (1999) The dolichol pathway of N-linked glycosylation. *Biochim Biophys Acta.* **1426**:239-257.
- Buse JB, Rosenstock J, Sesti G, Schmidt WE, Montanya E, Brett JH, Zychma M and Blonde L; LEAD-6 Study Group (2009) Liraglutide once a day versus exenatide twice a day for type 2 diabetes: a 26-week randomised, parallel-group, multinational, open-label trial (LEAD-6). *Lancet.* **374**:39-47.
- Buteau J, El-Assaad W, Rhodes CJ, Rosenberg L, Joly E and Prentki M (2004) Glucagon-like peptide-1 prevents β -cell glucolipotoxicity. *Diabetologia* **47**:806–815.
- Bylund DB, Deupree JD and Tews ML (2004) Radioligand-Binding methods for Membrane Preparations and Intact Cells. Willars GB and John Challiss RA, editor. Receptor Signal Transduction Protocols. Second edition. Human Press, Totowa, New Jersey
- Cabrera-Vera TM, Vanhauwe J, Thomas TO, Medkova M, Preininger A, Mazzoni MR and Hamm, HE (2003) Insights into G-protein structure, function, and regulation. *Endocr. Rev.* **24**:765–781.
- Calebiro D, Nikolaev VO, Gagliani MC, de Filippis T, Dees C, Tacchetti C, Persani L and Lohse MJ (2009) Persistent cAMP-signals triggered by internalized G-protein-coupled receptors. *PLoS Biol.* **7**:e1000172.
- Calebiro D, Nikolaev VO, Persani L and Lohse MJ (2010) Signaling by internalized G-protein-coupled receptors. *Trends Pharmacol Sci.* **31**:221-228.
- Campbell RK (2009) Fate of the beta-cell in the pathophysiology of type 2 diabetes. *J Am Pharm Assoc* (2003). **49**:S10-15.
- Cassano PA, Rosner B, Vokonas PS and Weiss ST (1992) Obesity and body fat distribution in relation to the incidence of non-insulin-dependent diabetes mellitus. A prospective cohort study of men in the normative aging study. *Am J Epidemiol.* **136**:1474-1486.

- Chang VT, Crispin M, Aricescu AR, Harvey DJ, Nettleship JE, Fennelly JA, Yu C, Boles KS, Evans EJ, Stuart DI, Dwek RA, Jones EY, Owens RJ and Davis SJ (2007) Glycoprotein Structural Genomics: Solving the Glycosylation Problem. *Structure* **15**:267-273.
- Charbonnel B, Karasik A, Liu J, Wu M, Meininger G (2006) Efficacy and safety of the dipeptidyl peptidase-4 inhibitor sitagliptin added to ongoing metformin therapy in patients with type 2 diabetes inadequately controlled with metformin alone. *Diabetes Care* **29**:2638–2643.
- Chen D, Liao J, Li N, Zhou C, Liu Q, Wang G, Zhang R, Zhang S, Lin L, Chen K, Xie X, Nan F, Young AA and Wang MW (2007) *Proc Natl Acad Sci USA* **104**: 943–948.
- Chen JM., Kukor Z, Le Maréchal C, Tóth M, Tsakiris L, Raguénès O, Férec C and Sahin-Tóth M (2003) Evolution of Trypsinogen Activation Peptides. *Mol. Biol. Evol.* **20**:1767–1777.
- Chen Q, Miller LJ and Dong M (2010) Role of N-linked glycosylation in biosynthesis, trafficking, and function of the human glucagon-like peptide 1 receptor. *Am J Physiol Endocrinol Metab.* **299**:E62-68.
- Chen Q, Pinon DI, Miller LJ and Dong M (2009) Molecular basis of glucagon-like peptide 1 docking to its intact receptor studied with carboxyl-terminal photolabile probes. *J Biol Chem.* **284**:34135-34144.
- Chiasson JL (2009) Early insulin treatment in type 2 diabetes: what are the cons? *Diabetes Care.* **32**:S270-274.
- Chicchi GG, Cascieri MA, Graziano MP, Calahan T and Tota MR (1997) Fluorescein-Trp25-exendin-4, a biologically active fluorescent probe for the human GLP-1 receptor. *Peptides* **18**:319-321.
- Choo KH, Ranganathan S. (2008) Flanking signal and mature peptide residues influence signal peptide cleavage. *BMC Bioinformatics.* **9**:S15.
- Choo KH, Tan TW and Ranganathan S (2009) A comprehensive assessment of N-terminal signal peptides prediction methods. *BMC Bioinformatics.* **10**:S2.
- Clark SD, Tran HT, Zeng J and Reinscheid RK (2010) Importance of extracellular loop one of the neuropeptide S receptor for biogenesis and function. *Peptides.* **31**:130-138.
- Class C Orphans. Last modified on 2010-07-01. Accessed on 2010-09-01. IUPHAR database (IUPHAR-DB), <http://www.iuphar-db.org/DATABASE/FamilyMenuForward?familyId=18>.
- Clérico EM, Maki JL and Gierasch LM (2008) Use of synthetic signal sequences to explore the protein export machinery. *Biopolymers.* **90**:307-319.
- Combettes MM (2006) GLP-1 and type 2 diabetes: physiology and new clinical advances. *Curr Opin Pharmacol.* **6**:598-605.
- Conn PM and Janovick JA (2009) Trafficking and quality control of the gonadotropin releasing hormone receptor in health and disease. *Mol Cell Endocrinol.* **299**:137-145.

- Conn PM and Ulloa-Aguirre A (2010) Trafficking of G-protein-coupled receptors to the plasma membrane: insights for pharmacoperone drugs. *Trends Endocrinol Metab.* **21**:190-197.
- Conn PM, Ulloa-Aguirre A, Ito J and Janovick JA (2007) G protein-coupled receptor trafficking in health and disease: lessons learned to prepare for therapeutic mutant rescue in vivo. *Pharmacol Rev.* **59**:225-250.
- Convineau A, Rouyer-Fessard C, Darmoul D, Maoret JJ, Carrero I, Ogier-Denis E and Laburthe M (1994) Human intestinal VIP receptor: cloning and functional expression of two cDNA encoding proteins with different N-terminal domains. *Biochem Biophys Res Commun.* **200**:769-776.
- Cooke DW and Plotnick L (2008) Type 1 diabetes mellitus in pediatrics. *Pediatr Rev.* **29**(11)374-384; quiz 385.
- Coopman K, Huang Y, Johnston N, Bradley SJ, Wilkinson GF and Willars GB (2010) Comparative Effects of the Endogenous Agonist GLP-1 7-36 Amide and a Small Molecule Ago-allosteric Agent 'Compound 2' at the GLP-1 Receptor. *J Pharmacol Exp Ther.* **334**:795-808.
- Cordeaux Y and Hill SJ (2002) Mechanisms of cross-talk between G-protein-coupled receptors. *Neurosignals.* **11**:45-57.
- Creutzfeldt W and Ebert R (1985) New developments in the incretin concept. *Diabetologia* **28**: 565-573.
- Cross BC, Sinning I, Luirink J and High S (2009) Delivering proteins for export from the cytosol. *Nat Rev Mol Cell Biol.* **10**:255-264.
- Cunha DA, Ladrière L, Ortis F, Igoillo-Esteve M, Gurzov EN, Lupi R, Marchetti P, Eizirik DL and Cnop M (2009) Glucagon-like peptide-1 agonists protect pancreatic beta-cells from lipotoxic endoplasmic reticulum stress through upregulation of BiP and JunB. *Diabetes.* **58**:2851-2862.
- Davidson JS, Flanagan CA, Zhou W, Becker II, Elario R, Emeran W, Sealfon SC, and Millar RP (1995) Identification of N-glycosylation sites in the gonadotropin-releasing hormone receptor: role in receptor expression but not ligand binding. *Mol Cell Endocrinol* **107**:241-245.
- Davies MN, Gloriam DE, Secker A, Freitas AA, Mendao M, Timmis J and Flower DR (2007) Proteomic applications of automated GPCR classification. *Proteomics.* **7**:2800-2814.
- Davis D, Liu X and Segaloff DL (1995) Identification of the sites of N-linked glycosylation on the follicle-stimulating hormone (FSH) receptor and assessment of their role in FSH receptor function. *Mol Endocrinol* **9**:159-170
- Davis N, Forges B and Wylie-Rosett J (2009) Role of obesity and lifestyle interventions in the prevention and management of type 2 diabetes. *Minerva Med.* **100**:221-228.
- Davis SJ, Puklavec MJ, Ashford DA, Harlos K, Jones EY, Stuart DI and Williams AF (1993) Expression of soluble recombinant glycoproteins with predefined glycosylation: application to the crystallization of the T-cell glycoprotein CD2. *Protein Eng.* **6**:229-232.

- De Amici M, Dallanoce C, Holzgrabe U, Tränkle C and Mohr K (2010) Allosteric ligands for G-protein-coupled receptors: a novel strategy with attractive therapeutic opportunities. *Med Res Rev.* **30**:463-549.
- De Leon DD, Crutchlow MF, Ham JY and Stoffers DA (2006) Role of glucagon-like peptide-1 in the pathogenesis and treatment of diabetes mellitus. *Int J Biochem Cell Biol* **38**:845–859.
- De Marinis YZ, Salehi A, Ward CE, Zhang Q, Abdulkader F, Bengtsson M, Braha O, Braun M, Ramracheya R, Amisten S, Habib AM, Moritoh Y, Zhang E, Reimann F, Rosengren AH, Shibasaki T, Gribble F, Renström E, Seino S, Eliasson L and Rorsman P (2010) GLP-1 inhibits and adrenaline stimulates glucagon release by differential modulation of N- and L-type Ca²⁺ channel-dependent exocytosis. *Cell Metab.* **11**:543-553.
- Deacon CF and Holst JJ (2006) Dipeptidyl peptidase IV inhibitors: a promising new therapeutic approach for the management of type 2 diabetes. *Int J Biochem Cell Biol.* **38**:831–844.
- Deacon CF, Knudsen LB, Madsen K, Wiberg FC, Jacobsen O and Holst JJ (1998) Dipeptidyl peptidase IV resistant analogues of glucagon-like peptide-1 which have extended metabolic stability and improved biological activity. *Diabetologia* **41**:271–278.
- Deslauriers B, Ponce C, Lombard C, Larguier R, Bonnafous JC and Marie J (1999) N-glycosylation requirements for the AT1a angiotensin II receptor delivery to the plasma membrane. *Biochem. J.* **339**:397–405.
- DeWire SM, Ahn S, Lefkowitz RJ and Shenoy SK (2007) Beta-arrestins and cell signaling. *Annu Rev Physiol.* **69**:483-510.
- Diabetes UK. What is diabetes? Available at <http://www.diabetes.org.uk/Guide-to-diabetes/Introduction-to-diabetes> (accessed on 18 June, 2010).
- Dimitriadis GD, Richards SJ, Parry-Billings M, Leighton B, Newsholme EA and Challiss RA (1991) Beta-adrenoceptor-agonist and insulin actions on glucose metabolism in rat skeletal muscle in different thyroid states. *Biochem J.* **278**:587-593.
- Doherty GJ and McMahon HT (2009) Mechanisms of endocytosis. *Annu Rev Biochem* **78**: 857-902.
- Dong M, Gao F, Pinon DI and Miller LJ (2008) Insights into the structural basis of endogenous agonist activation of family B G protein-coupled receptors. *Mol Endocrinol.* **22**:1489-1499.
- Dong M, Pinon DI, and Miller LJ (2005) Insights into the structure and molecular basis of ligand docking to the g protein-coupled secretin receptor using charge-modified amino-terminal agonist probes. *Mol Endocrinol* **19**:1821–1836.
- Dong M, Pinon DI, Asmann YW and Miller LJ (2006) Possible endogenous agonist mechanism for the activation of secretin family G protein- coupled receptors. *Mol Pharmacol.* **70**:206-213.

- Dorion S, Berube J, Huot J and Landry J (1999) A Short Lived Protein Involved in the Heat Shock Sensing Mechanism Responsible for Stress-activated Protein Kinase 2 (SAPK2/p38) Activation. *J. Biol. Chem.* **274**:37591–37597.
- Drucker DJ, Dritselis A and Kirkpatrick P (2010) Liraglutide. *Nat Rev Drug Discov.* **9**:267-268.
- Drucker DJ, Sherman SI, Gorelick FS, Bergenstal RM, Sherwin RS and Buse JB (2010) Incretin-based therapies for the treatment of type 2 diabetes: evaluation of the risks and benefits. *Diabetes Care.* **33**:428-433.
- Dukkipati A, Park HH, Waghray D, Fischer S, Garcia KC (2008) BacMam system for high-level expression of recombinant soluble and membrane glycoproteins for structural studies. *Protein Expr Purif.* **62**:160-170.
- Dunham JH and Hall RA (2009) Enhancement of the surface expression of G protein-coupled receptors. *Trends Biotechnol.* **27**:541-545.
- Duvernay MT, Filipeanu CM and Wu G (2005) The regulatory mechanisms of export trafficking of G protein-coupled receptors. *Cell Signal.* **17**:1457-1465.
- Edavalath M and Stephens JW (2010) Liraglutide in the treatment of type 2 diabetes mellitus: clinical utility and patient perspectives. *Patient Prefer Adherence.* **24**:61-68.
- Egea PF, Stroud RM and Walter P (2005) Targeting proteins to membranes: structure of the signal recognition particle. *Curr Opin Struct Biol.* **15**: 213-220.
- Eknoyan G (2008). Adolphe Quetelet (1796-1874)—the average man and indices of obesity. *Nephrol. Dial. Transplant.* **23**:47–51.
- Elbein (1987) Inhibitors of the biosynthesis and processing of N-linked ligosaccharide chains. *Annu Rev Biochem.* **56**:497-534.
- Elghazi L and Bernal-Mizrachi E (2009) Akt and PTEN: beta-cell mass and pancreas plasticity. *Trends Endocrinol Metab.* **20**:243-251.
- Eng J, Kleinman WA, Singh L, Singh G and Raufman JP (1992) Isolation and characterization of exendin-4, an exendin-3 analogue, from *Heloderma suspectum* venom. Further evidence for an exendin receptor on dispersed acini from guinea pig pancreas, *J. Biol. Chem.* **267**:7402–7405.
- Ferguson SS (2001) Evolving concepts in G-protein-coupled receptor endocytosis: the role in receptor desensitization and signaling. *Pharmacol Rev.* **53**:1-24.
- Ferrandon S, Feinstein TN, Castro M, Wang B, Bouley R, Potts JT, Gardella TJ and Vilaradaga JP (2009) Sustained cyclic AMP production by parathyroid hormone receptor endocytosis. *Nat Chem Biol.* **5**:734-742.
- Finch AR, Sedgley KR, Armstrong SP, Caunt CJ, McArdle CA (2010) Trafficking and signalling of gonadotrophin-releasing hormone receptors: an automated imaging approach. *Br J Pharmacol.* **159**: 751-760.
- Fortin JP, Schroeder JC, Zhu Y, Beinborn M and Kopin AS (2010) Pharmacological characterization of human incretin receptor *J Pharmacol Exp Ther.* **332**:274-280.

- Fritsche A, Stefan N, Hardt E, Häring H and Stumvoll M (2000) Characterisation of beta-cell dysfunction of impaired glucose tolerance: evidence for impairment of incretin-induced insulin secretion. *Diabetologia*. **43**:852-858.
- Fukushima Y, Oka Y, Saitoh T, Katagiri H, Asano T, Matsuhashi N, Takata K, van Breda E, Yazaki Y and Sugano K (1995) Structural and functional analysis of the canine histamine H2 receptor by site-directed mutagenesis: N-glycosylation is not vital for its action. *Biochem J*. **310**:553–558.
- Gallwitz B (2010) The evolving place of incretin-based therapies in type 2 diabetes. *Pediatr Nephrol* **25**:1207-1217.
- Ge X, Loh HH and Law PY (2009) mu-Opioid receptor cell surface expression is regulated by its direct interaction with Ribophorin I. *Mol Pharmacol*. **75**:1307-1316.
- Genuth S (2006) Insights from the diabetes control and complications trial/epidemiology of diabetes interventions and complications study on the use of intensive glycemic treatment to reduce the risk of complications of type 1 diabetes. *Endocr Pract* **12**: S34–S41.
- Gilbert MP and Pratley RE (2009) Efficacy and safety of incretin-based therapies in patients with type 2 diabetes mellitus. *Am J Med*. **122**:S11-24.
- Göke R, Fehmann HC, Linn T, Schmidt H, Krause M, Eng J and Göke B (1993) Exendin-4 is a high potency agonist and truncated exendin-(9-39)-amide an antagonist at the glucagon-like peptide 1-(7-36)-amide receptor of insulin-secreting beta-cells. *J. Biol. Chem*. **268**:19650-19655.
- Göke R, Just R, Lankat-Buttgereit B and Göke B (1994) Glycosylation of the GLP-1 receptor is a prerequisite for regular receptor function. *Peptides* **15**:675–681.
- Göke R, Oltmer B, Sheikh SP, Göke B (1992) Solubilization of active GLP-1 (7-36) amide receptors from RINm5F plasma membranes. *FEBS Lett*. **300**:232-236.
- Golde TE, Wolfe MS and Greenbaum DC (2009) Signal peptide peptidases: a family of intramembrane-cleaving proteases that cleave type 2 transmembrane proteins. *Semin Cell Dev Biol*. **20**:225-230.
- Goodge KA and Hutton JC (2000) Translational regulation of proinsulin biosynthesis and proinsulin conversion in the pancreatic beta-cell. *Semin Cell Dev Biol*. **11**:235-242.
- Grallath S, Schwarz JP, Böttcher UM, Bracher A, Hartl FU and Siegers K (2006) L25 functions as a conserved ribosomal docking site shared by nascent chain-associated complex *EMBO Rep*. **7**:78-84.
- Gray JA and Roth BL (2002) Cell biology. A last GASP for GPCRs? *Science*. **297**:529-531.
- Grieve DJ, Cassidy RS and Green BD (2009) Emerging cardiovascular actions of the incretin hormone glucagon-like peptide-1: potential therapeutic benefits beyond glycaemic control? *Br J Pharmacol*. **157**:1340-1351.
- Grudnik P, Bange G and Sinning I. (2009) Protein targeting by the signal recognition particle. *Biol Chem*. **390**:775-782.

- Guan R, Wu X, Feng X, Zhang M, Hébert TE and Segaloff DL (2010) Structural determinants underlying constitutive dimerization of unoccupied human follitropin receptors. *Cell Signal*. **22**:247-256.
- Gupta NA, Mells J, Dunham RM, Grakoui A, Handy J, Saxena NK and Anania FA (2010) Glucagon-like peptide-1 receptor is present on human hepatocytes and has a direct role in decreasing hepatic steatosis in vitro by modulating elements of the insulin signaling pathway. *Hepatology*. **51**:1584-1592.
- Halic M and Beckmann R (2005) The signal recognition particle and its interactions during protein targeting. *Curr Opin Struct Biol*. **15**:116-125.
- Halic M, Becker T, Pool MR, Spahn CM, Grassucci RA, Frank J and Beckmann R (2004) Structure of the signal recognition particle interacting with the elongation-arrested ribosome. *Nature*. **427**:808–814.
- Hallbrink M, Holmqvist T, Olsson M, Ostenson CG, Efendic S, and Langel U (2001) Different domains in the third intracellular loop of the GLP-1 receptor are responsible for $G\alpha_s$ and $G\alpha_i/G\alpha_o$ activation. *Biochim Biophys Acta Protein Struct Mol Enzymol* **1546**:79-86.
- Hamnvik OP and McMahan GT (2009) Balancing risk and benefit with oral hypoglycemic drugs. *Mt Sinai J Med*. **76**:234-243.
- Hanson MA and Stevens RC (2009) Discovery of new GPCR biology: one receptor structure at a time. *Structure*. **17**:8-14.
- Haque TS, Lee VG, Riexinger D, Lei M, Malmstrom S, Xin L, Han S, Mapelli C, Cooper CB, Zhang G, Ewing WR and Krupinski J (2010) Identification of potent 11mer glucagon-like peptide-1 receptor agonist peptides with novel C-terminal amino acids: Homohomophenylalanine analogs. *Peptides*. **31**:950-955.
- Harmar AJ (2001) Family-B G-protein-coupled receptors. *Genome Biol*. **2**:REVIEWS3013.
- Hatsuzawa K, Tagaya M and Mizushima S (1997) The hydrophobic region of signal peptides is a determinant for SRP recognition and protein translocation across the ER membrane. *J Biochem*. **121**:270-277.
- Hayes MR, Bradley L and Grill HJ (2009) Endogenous hindbrain glucagon-like peptide-1 receptor activation contributes to the control of food intake by mediating gastric satiation signaling. *Endocrinology*. **150**:2654-2659.
- Heasman SJ and Ridley AJ (2008) Mammalian Rho GTPases: new insights into their functions from in vivo studies. *Nat Rev Mol Cell Biol*. **9**:690-701.
- Hegde RS and Bernstein HD (2006) The surprising complexity of signal sequences. *Trends Biochem Sci*. **31**:563-571.
- Hegde RS and Kang SW (2008) The concept of translocational regulation. *J Cell Biol*. **182**:225–232.
- Heilker R, Wolff M, Tautermann CS and Bieler M (2009) G-protein-coupled receptor-focused drug discovery using a target class platform approach. *Drug Discov Today*. **14**:231-240.

- Helenius A and Aebi M (2001) Intracellular functions of N-linked glycans. *Science* **291**:2364–2369.
- Heller RS, Kieffer TJ and Habener JF (1996) Point mutation in the first and third intracellular loops of the glucagon-like peptide-1 receptor alter intracellular signaling. *Biochem. Biophys. Res. Commun* **223**:624–632.
- Hendriks G, Koudijs M, van Balkom BW, Oorschot V, Klumperman J, Deen PM and van der Sluijs P (2004) Glycosylation is important for cell surface expression of the water channel aquaporin-2 but is not essential for tetramerization in the endoplasmic reticulum. *J Biol Chem.* **279**:2975-2983.
- Henrik Nielsen and Anders Krogh (1998) Prediction of signal peptides and signal anchors by a hidden Markov model. Proceedings of the Sixth International Conference on Intelligent Systems for Molecular Biology (ISMB 6), AAAI Press, Menlo Park, California, pp. 122-130.
- Hessa T, Kim H, Bihlmaier K, Lundin C, Boekel J, Andersson H, Nilsson I, White SH and von Heijne G (2005) Recognition of transmembrane helices by the endoplasmic reticulum translocon. *Nature.***433**:377-381.
- Hiss JA and Schneider G (2009) Architecture, function and prediction of long signal peptides. *Brief Bioinform.* **10**:569-578.
- Ho HH, Gilbert MT, Nussenzveig DR and Gershengorn MC (1999) Glycosylation is important for binding to human calcitonin receptors. *Biochemistry* **38**:1866-1872.
- Hoare SRJ (2005) Mechanisms of peptide and nonpeptide ligand binding to Class B G-protein-coupled receptors. *Drug Discov. Today* **10**:417–427.
- Hollander P (2007) Anti-diabetes and anti-obesity medications: effects on weight in people with diabetes. *Diabetes Spectr.* **20**:159-165.
- Holst JJ (2007) The physiology of glucagon-like peptide 1, *Physiol Rev* **87**: 1409–1439.
- Holst JJ (2010) Glucagon and glucagon-like peptides 1 and 2. *Results Probl Cell Differ.* **50**:121-35.
- Holst JJ and Gromada J (2004) Role of incretin hormones in the regulation of insulin secretion in diabetic and nondiabetic humans. *Am J Physiol Endocrinol Metab* **287**:E199–E206.
- Holst JJ, Vilsbøll T, Deacon CF (2009) The incretin system and its role in type 2 diabetes mellitus. *Mol Cell Endocrinol.* **297**:127-136.
- Holz GG (2004) Epac: A new cAMP-binding-protein in support of glucagon-like peptide-1 receptor-mediated signal transduction in the pancreatic beta-cell. *Diabetes* **53**:5–13.
- Horton ES, Silberman C, Davis KL and Berria R (2010) Weight loss, glycemic control, and changes in cardiovascular biomarkers in patients with type 2 diabetes receiving incretin therapies or insulin in a large cohort database. *Diabetes Care.* **33**:1759-1765.
- Host JJ (2007) The Physiology of Glucagon-like Peptide 1. *Physiol Rev* **87**:1409-1439

- Hou JC and Min L (2009) Insulin granule biogenesis, trafficking and exocytosis. *Pessin JE Vitam Horm.* **80**:473-506.
- Hui H, Nourparvar A, Zhao X and Perfetti R (2003) Glucagon like peptide-1 inhibits apoptosis of insulin-secreting cells via a cyclic 5'AMP dependent protein kinase A- and a PI3K-dependent pathway, *Endocrinology* **144**:1444–1445.
- Irwin N, Flatt PR, Patterson S and Green BD (2010) Insulin-releasing and metabolic effects of small molecule GLP-1 receptor agonist 6,7-dichloro-2-methylsulfonyl-3-N-tert-butylaminoquinoxaline. *Eur J Pharmacol.* **628**:268-273.
- Ivic L, Zhang C, Zhang X, Yoon SO and Firestein S (2002) Intracellular trafficking of a tagged and functional mammalian olfactory receptor. *J. Neurobiol.* **50**:56-68.
- Jacoby E, Bouhelal R, Gerspacher M, Seuwen K (2006) The 7 TM G-protein-coupled receptor target family. *ChemMedChem.* **1**:761-782.
- Jalink K and Moolenaar WH (2010) G protein-coupled receptors: the inside story. *Bioessays.* **32**:13-16.
- Janda CY, Li J, Oubridge C, Hernández H, Robinson CV and Nagai K (2010) Recognition of a signal peptide by the signal recognition particle. *Nature* **465**:507-510.
- Janovick JA, Patny A, Mosley R, Goulet MT, Altman MD, Rush TS 3rd, Cornea A and Conn PM (2009) Molecular mechanism of action of pharmacoperone rescue of misrouted GPCR mutants: the GnRH receptor. *Mol Endocrinol.* **23**:157-168.
- Jennifer L. Garrison, Eric J. Kunkel, Ramanujan S. Hegde and Jack Taunton (2005) A substrate-specific inhibitor of protein translocation into the endoplasmic reticulum *Nature* **436**, 285-289
- Jensen PH, Kolarich D and Packer NH (2010) Mucin-type O-glycosylation--putting the pieces together. *FEBS J.* **277**:81-94.
- Jhala US, Canettieri G, Sreaton RA, Kulkarni RN, Krajewski S and Reed J (2003) cAMP promotes pancreatic β -cell survival via CREB-mediated induction of IRS2. *Genes* **17**:1575–1580.
- Jorgensen R, Kubale V, Vrecl M, Schwartz TW and Elling CE (2007) Oxyntomodulin differentially affects glucagon-like peptide-1 receptor beta-arrestin recruitment and signaling through Galpha(s). *J Pharmacol Exp Ther.* **322**:148–154.
- Jovic M, Sharma M, Rahajeng J and Caplan S (2010) The early endosome: a busy sorting station for proteins at the crossroads. *Histol Histopathol.* **25**:99-112.
- Kallal L and Benovic JL (2000) Using green fluorescent proteins to study G-protein-coupled receptor localization and trafficking. *Trends Pharmacol. Sci.* **21**:175–180.
- Kamitani S, Sakata T (2001) Glycosylation of human CRLR at Asn123 is required for ligand binding and signalling. *Biochim Biophys Acta* **1539**:131-139.
- Kang K and Schnetkamp PP (2003) Signal sequence cleavage and plasma membrane targeting of the retinal rod NCKX1 and cone NCKX2 Na⁺/Ca²⁺ - K⁺ exchangers. *Biochemistry.* **42**:9438-9445.

- Kashima Y, Miki T, Shibasaki T, Ozaki N, Miyazaki M, Yano H and Seino S (2001) Critical role of cAMP-GEFII–Rim2 complex in incretin potentiated insulin secretion. *J Biol Chem* **276**: 46046–46053.
- Kenakin T (2004) Efficacy as a vector: the relative prevalence and paucity of inverse agonism. *Mol Pharmacol.* **65**:2-11.
- Kenakin T and Miller LJ (2010) Seven transmembrane receptors as shapeshifting G-proteins: the impact of allosteric modulation and functional selectivity on new drug discovery. *Pharmacol Rev.* **62**:265-304.
- Kenakin TP (2009) 7TM receptor allostery: putting numbers to shapeshifting G-proteins. *Trends Pharmacol Sci.* **30**:460-469.
- Kern A, Agoulnik AI, and Bryant-Greenwood GD (2007) The Low-Density Lipoprotein Class A Module of the Relaxin Receptor (Leucine-Rich Repeat Containing G-Protein Coupled Receptor 7): Its Role in Signaling and Trafficking to the Cell Membrane *Endocrinology* **148**:1181-1194.
- Khunti K and Davies M (2010) Glycaemic goals in patients with type 2 diabetes: current status, challenges and recent advances. *Diabetes Obes Metab.* **12**:474-484.
- Kida Y, Kume C, Hirano M and Sakaguchi M. (2010) Environmental transition of signal-anchor sequences during membrane insertion via the endoplasmic reticulum translocon. *Mol Biol Cell.* **21**:418-429.
- Kida Y, Morimoto F and Sakaguchi M. (2009) Signal anchor sequence provides motive force for polypeptide chain translocation through the endoplasmic reticulum membrane. *Biol Chem.* **284**:2861-2866.
- Kim DH, D'Alessio DA, Woods SC and Seeley RJ (2009) The effects of GLP-1 infusion in the hepatic portal region on food intake. *Regul Pept.* **155**:110-114.
- Király O, Guan L, Szepessy E, Tóth M, Kukor Z and Sahin-Tóth M (2006) Expression of human cationic trypsinogen with an authentic N terminus using intein-mediated splicing in aminopeptidase P deficient Escherichia coli. *Protein Expr Purif.* **48**:104-111.
- Kitabchi AE and Nyenwe EA (2006) Hyperglycemic crises in diabetes mellitus: diabetic ketoacidosis and hyperglycemic hyperosmolar state. *Endocrinol Metab Clin North Am.* **35**:725-751.
- Kjems LL, Holst JJ, Vølund A and Madsbad S (2003) The influence of GLP-1 on glucose-stimulated insulin secretion: effects on beta-cell sensitivity in type 2 and nondiabetic subjects. *Diabetes.* **52**:380-386.
- Klee EW and Ellis (2005) Evaluating eukaryotic secreted protein prediction. *LB.BMC Bioinformatics.* **6**:256.
- Knop F.K., K. Aaboe, T. Vilsboll, S. Madsbad, J.J. Holst and T. Krarup (2008) Reduced incretin effect in obese subject with normal glucose tolerance as compared to lean control subjects, *Diabetes* **57**(Suppl. 1)
- Knop FK, Vilsboll T, Hojberg PV, Larsen S, Madsbad S, Volund A, Holst JJ and Krarup T (2007) Reduced incretin effect in T2DM: cause or consequence of the diabetic state? *Diabetes* **56**:1951–1959.

- Knudsen LB and Pridal L (1996) Glucagon-like peptide-1-(9-36) amide is a major metabolite of glucagon-like peptide-1-(7-36) amide after in vivo administration to dogs, and it acts as an antagonist on the pancreatic receptor. *Eur J Pharmacol.* **318**:429-435.
- Knudsen LB, Kiel D, Teng M, Behrens C, Bhumralkar D, Kodra JT, Holst JJ, Jeppesen CB, Johnson MD, de Jong JC, Jorgensen AS, Kercher T, Kostrowicki J, Madsen P, Olesen PH, Petersen JS, Poulsen F, Sidelmann UG, Sturis J, Truesdale L, May J, and Lau J (2007) Small-molecule agonists for the glucagon-like peptide 1 receptor. *Proc Nat Acad Sci U.S.A.* **104**:937-942.
- Koenig RJ, Peterson CM, Jones RL, Saudek C, Lehrman M and Cerami A (1976). Correlation of glucose regulation and hemoglobin A1c in diabetes mellitus. *N. Engl. J. Med.* **295**:417-420.
- Kolligs F, Fehmann HC, Goke R and Goke B (1995) Reduction of the incretin effect in rats by the glucagon-like peptide 1 receptor antagonist exendin (9-39) amide. *Diabetes.* **44**:16-19.
- Kozak M (1987) An analysis of 59-noncoding sequences from 699 vertebrate messenger RNAs. *Nucleic Acids Res.* **15**:8125-8148.
- Kramer G, Boehringer D, Ban N and Bukau B (2009) The ribosome as a platform for co-translational processing, folding and targeting of newly synthesized proteins. *Nat Struct Mol Biol.* **16**:589-597.
- Kreymann B, Williams G, Ghatei MA and Bloom SR (1987) Glucagon-like peptide-1 7-36: a physiological incretin in man. *Lancet.* **2**:1300-1304.
- Kristiansen K (2004) Molecular mechanisms of ligand binding, signaling, and regulation within the superfamily of G-protein-coupled receptors: molecular modeling and mutagenesis approaches to receptor structure and function. *Pharmacol Ther.* **103**:21-80.
- Kumar KG, Poole AC, York B, Volaufova J, Zuberi A and Richards BK (2007) Quantitative trait loci for carbohydrate and total energy intake on mouse chromosome 17: congenic strain confirmation and candidate gene analyses (Glo1, Glp1r). *Am J Physiol Regul Integr Comp Physiol.* **292**:R207-216.
- Kuzuya T and Matsuda A (1997). Classification of diabetes on the basis of etiologies versus degree of insulin deficiency. *Diabetes Care* **20**:219-220.
- Kwong PD, Wyatt R, Desjardins E, Robinson J, Culp JS, Hellmig BD, Sweet RW, Sodroski J and Hendrickson WA (1999) Probability analysis of variational crystallization and its application to gp120, the exterior envelope glycoprotein of type 1 human immunodeficiency virus (HIV-1). *J. Biol. Chem.* **274** 4115-4123
- Lakkaraju AK, Mary C, Scherrer A, Johnson AE and Strub K (2008) SRP keeps polypeptides translocation-competent by slowing translation to match limiting ER-targeting sites. *Cell.* **133**:440-451.
- Lanctot PM, Leclerc PC, Clément M, Auger-Messier M, Escher E, Leduc R and Guillemette G (2005) Importance of N-glycosylation positioning for cell-surface expression, targeting, affinity and quality control of the human AT1 receptor. *Biochem J.* **390**:367-376.

- Lavoie C and Paiement J (2008) Topology of molecular machines of the endoplasmic reticulum: a compilation of proteomics and cytological data. *Histochem Cell Biol.* **129**:117-128.
- Leahy JL (2005) Pathogenesis of type 2 diabetes mellitus. *Arch Med Res.* **36**:197-209.
- Lee JE, Fusco ML and Ollmann Saphire E. (2009) An efficient platform for screening expression and crystallization of glycoproteins produced in human cells. *Nat Protoc.* **4**:592-604.
- Lemberg MK and Martoglio B. (2002) Requirements for signal peptide peptidase-catalyzed intramembrane proteolysis. *Mol Cell.* **10**:735-744.
- Leversen NA, de Souza GA, Målen H, Prasad S, Jonassen I and Wiker HG (2009) Evaluation of signal peptide prediction algorithms for identification of mycobacterial signal peptides using sequence data from proteomic methods. *Microbiology* **155**:2375-83.
- Li L, El-Kholy W, Rhodes CJ and Brubaker PL (2005) Glucagon-like peptide-1 protects β -cells from cytokine-induced apoptosis and necrosis: role of protein kinase B. *Diabetologia.* **48**:1339-1349.
- Limon A, Reyes-Ruiz JM, Eusebi F and Miledi R (2007) Properties of GluR3 receptors tagged with GFP at the amino or carboxyl terminus. *PNAS* **104**:15526–15530.
- Lin F and Wang R (2009) Molecular modeling of the three-dimensional structure of GLP-1R and its interactions with several agonists. *J Mol Model.* **15**:53-65.
- Lippincott-Schwartz J, Roberts TH and Hirschberg K (2000) Secretory protein trafficking and organelle dynamics in living cells. *Annu Rev Cell Dev Biol.* **16**:557-589.
- Lipps G (editor) (2008). *Plasmids: Current Research and Future Trends*. Caister Academic Press.
- López de Maturana R and Donnelly D. The glucagon-like peptide-1 receptor binding site for the N-terminus of GLP-1 requires polarity at Asp198 rather than negative charge. *FEBS Lett.* **530**:244-248.
- López de Maturana R, Treece-Birch J, Abidi FH, Findlay JBC and Donnelly D (2004) Met-204 and Tyr-205 are together important for binding GLP-1 receptor agonists but not their N-terminally truncated analogues. *Protein and Peptide Letters* **11**:15-22.
- Mandel M and Higa A (1970) Calcium-dependent bacteriophage DNA infection. *J Mol Biol.* **53**:159-162.
- Mann R, Nasr N, Hadden D, Sinfield J, Abidi F, Al-Sabah S, de Maturana RL, Treece-Birch J, Willshaw A and Donnelly D (2007) Peptide binding at the GLP-1 receptor. *Biochem Soc Trans.* **35**:713-716.
- Mapelli C, Natarajan SI, Meyer JP, Bastos MM, Bernatowicz MS, Lee VG, Pluscec J, Riexinger DJ, Sieber-McMaster ES, Constantine KL, Smith-Monroy CA, Golla R, Ma Z, Longhi DA, Shi D, Xin L, Taylor JR, Koplowitz B, Chi CL, Khanna A, Robinson GW, Seethala R, Antal-Zimanyi IA, Stoffel RH, Han S, Whaley JM,

- Huang CS, Krupinski J and Ewing WR (2009) Eleven amino acid glucagon-like peptide-1 receptor agonists with antidiabetic activity. *Med Chem.* **52**:7788-7799.
- Marchese A, Paing MM, Temple BR and Trejo J (2008) G-protein-coupled receptor sorting to endosomes and lysosomes. *Annu Rev Pharmacol Toxicol.* **48**:601-629.
- Marshall RD (1974) The nature and metabolism of the carbohydrate-peptide linkages of glycoproteins. *Biochem. Soc. Symp.* **40**:17-26.
- Mathi SK, Chan Y, Li X and Wheeler MB (1997) Scanning of the glucagon-like peptide-1 receptor localizes G-protein-activating determinants primarily to the N terminus of the third intracellular loop. *Mol. Endocrinol.* **11**:424-432.
- Matuszek B, Lenart-Lipińska M and Nowakowski A (2007) Incretin hormones in the treatment of type 2 diabetes. Part I: influence of insulinotropic gut-derived hormones (incretins) on glucose metabolism. *Endokrynol Pol.* **58**: 522-528.
- May LT and Christopoulos A (2003). Allosteric modulators of G-protein-coupled receptors. *Curr Opin Pharmacol.* **3**:551-556.
- Mayor S and Pagano RE (2007) Pathways of clathrin-independent endocytosis, *Nat Rev Mol Cell Biol.* **8**:603-612.
- McDonald NA, Henstridge CM, Connolly CN and Irving AJ (2007) Generation and functional characterization of fluorescent, N-terminally tagged CB1 receptor chimeras for live-cell imaging. *Mol Cell Neurosci.* **35**:237-248.
- McIlhinney RAJ (2004) Generation and Use of Epitope-Tagged Receptors. Willars GB and John Challiss RA, editor. Receptor Signal Transduction Protocols. Second edition. Human Press, Totowa, New Jersey
- Meier JJ and Nauck MA (2010) Is the diminished incretin effect in type 2 diabetes just an epi-phenomenon of impaired beta-cell function? *Diabetes.* **59**:1117-1125.
- Meneghini LF (2009) Early insulin treatment in type 2 diabetes: what are the pros? *Diabetes Care.* **32**:S266-269.
- Mentlein R. (2009) Mechanisms underlying the rapid degradation and elimination of the incretin hormones GLP-1 and GIP. *Best Pract Res Clin Endocrinol Metab.* **23**:443-452.
- Meyuhas O (2008) Physiological roles of ribosomal protein S6: one of its kind. *Int Rev Cell Mol Biol.* **268**:1-37.
- Michineau S, Alhenc-Gelas F and Rajerison RM (2006) Human bradykinin B2 receptor sialylation and N-glycosylation participate with disulfide bonding in surface receptor dimerization. *Biochemistry.* **45**:2699-2707.
- Mikhail N (2008) Incretin mimetics and dipeptidyl peptidase 4 inhibitors in clinical trials for the treatment of type 2 diabetes. *Expert Opin Investig Drugs.* **17**:845-853.
- Millar RP and Newton CL (2010) The year in G-protein-coupled receptor research. *Mol Endocrinol.* **24**:261-274.
- Mitra K, Frank J and Driessen A (2006) Co- and post-translational translocation through the protein conducting channel. *Nat Struct Mol Biol.* **13**:957-964.

- Mojsov S, Heinrich G, Wilson IB, Ravazzola M, Orci L and Habener JF (1986) Preproglucagon gene expression in pancreas and intestine diversifies at the level of post-translational processing. *J Biol Chem* **261**:1180–1189.
- Montanya E and Sesti G (2009) A review of efficacy and safety data regarding the use of liraglutide, a once-daily human glucagon-like peptide 1 analogue, in the treatment of type 2 diabetes mellitus. *Clin Ther.* **31**:2472-2488.
- Montrose-Rafizadeh C, Avdonin P, Garant MJ, Rodgers BD, Kole S, Yang H, Levine MA, Schwindinger W, and Bernier M (1999) Pancreatic glucagon-like peptide-1 receptor couples to multiple G proteins and activates mitogen-activated protein kinase pathways in Chinese hamster ovary cells. *Endocrinology* **140**:1132-1140.
- Moore CA, Milano SK and Benovic JL (2007) Regulation of receptor trafficking by GRKs and arrestins. *Annu Rev Physiol.* **69**:451-482.
- Moore CE, Xie J, Gomez E and Herbert TP (2009) Identification of cAMP-dependent kinase as a third in vivo ribosomal protein S6 kinase in pancreatic beta-cells. *J Mol Biol.* **389**:480-494.
- Mosiman VL, Patterson BK, Canterero L and Goolsby CL (1997) Reducing cellular autofluorescence in flow cytometry: an in situ method. *Cytometry.* **30**:151-156.
- Muoio DM and Newgard CB (2008). Mechanisms of disease: molecular and metabolic mechanisms of insulin resistance and beta-cell failure in type 2 diabetes. *Nat Rev Mol Cell Biol.* **9**:193-205.
- Nagayama Y, Nishihara E, Namba H, Yamashita S, and Niwa M (2000) Identification of the sites of asparagine-linked glycosylation on the human thyrotropin receptor and studies on their role in receptor function and expression. *J Pharmacol Exp Ther* **295**:404-409.
- Naidoo N (2009) ER and aging-Protein folding and the ER stress response. *Ageing Res Rev.* **8**:150-159.
- Nakagawa H, Wakabayashi-Nakao K, Tamura A, Toyoda Y, Koshihara S, Ishikawa T (2009) Disruption of N-linked glycosylation enhances ubiquitin-mediated proteasomal degradation of the human ATP-binding cassette transporter ABCG2. *FEBS J.* **276**:7237-7252.
- Nakajima M, Koga T, Sakai H, Yamanaka H, Fujiwara R and Yokoi T (2010) Biochem N-Glycosylation plays a role in protein folding of human UGT1A9. *Pharmacol.* **79**:1165-1172.
- Nathan DM, Buse JB, Davidson MB, Ferrannini E, Holman RR, Sherwin R and Zinman B (2008) Management of hyperglycemia in type 2 diabetes: a consensus algorithm for the initiation and adjustment of therapy: update regarding thiazolidinediones: a consensus statement from the American Diabetes Association and the European Association for the Study of Diabetes. *Diabetes Care.* **31**:173-175.
- Nauck M, Schmidt WE, Ebert R, Strietzel J, Cantor P, Hoffmann G and Creutzfeldt W (1989) Insulinotropic properties of synthetic human gastric inhibitory polypeptide in man: interactions with glucose, phenylalanine, and cholecystokinin-8. *J.Clin.Endocrinol.Metab.* **69**:654-662.

- Nauck MA, El-Ouaghlidi A, Gabrys B, Huckling K, Holst JJ, Deacon CF, Gallwitz B, Schmidt W, Meier JJ (2004) Secretion of incretin hormones (GIP and GLP-1) and incretin effect after oral glucose in first-degree relatives of patients with type 2 diabetes. *Regul. Pept.* **122**:209–217.
- Nauck MA, Heimesaat MM, Orskov C, Holst JJ, Ebert R and Creutzfeldt WJ (1993) Preserved incretin activity of glucagon-like peptide 1 [7-36 amide] but not of synthetic human gastric inhibitory polypeptide in patients with type-2 diabetes mellitus. *Clin Invest* **91**:301-307.
- Nauck MA, Homberger E, Siegel EG, Allen RC, Eaton RP, Ebert R and Creutzfeldt W (1986) Incretin effects of increasing glucose loads in man calculated from venous insulin and C-peptide responses. *J Clin Endocrinol Metab* **63**:492-498.
- Nauck MA, Kleine N, Orskov C, Holst JJ, Willms B, Creutzfeldt W (1993) Normalization of fasting hyperglycaemia by exogenous glucagon-like peptide 1 (7-36 amide) in type 2 (non-insulin-dependent) diabetic patients. *Diabetologia* **36**:741-744.
- Nauck MA, Ratner RE, Kapitza C, Berria R, Boldrin M and Balena R (2009) Treatment with the human once-weekly glucagon-like peptide-1 analog taspoglutide in combination with metformin improves glycemic control and lowers body weight in patients with type 2 diabetes inadequately controlled with metformin alone: a double-blind placebo-controlled study. *Diabetes Care.* **32**:1237-1243.
- Nickel W and Seedorf M (2008). Unconventional mechanisms of protein transport to the cell surface of eukaryotic cells. *Annu Rev Cell Dev Biol.* **24**:287-308.
- Nielsen H, Engelbrecht J, Brunak S and von Heijne G (1997) Identification of prokaryotic and eukaryotic signal peptides and prediction of their cleavage sites. *Protein Engineering,* **10**:1-6.
- Nielsen H, Engelbrecht J, Brunak S, von Heijne G (1997) A neural network method for identification of prokaryotic and eukaryotic signal peptides and prediction of their cleavage sites. *Int J Neural Syst.* **8**:581-599.
- Niswender K (2010) Diabetes and obesity: therapeutic targeting and risk reduction - a complex interplay. *Diabetes Obes Metab.* **12**:267-287.
- Nyholm B, Walker M, Grauholt CH, Alberti KGMM, Holst JJ and Schmitz O (1999). Twenty-four hour profiles of insulin, substrates and gut incretin hormones: early defects in glucose tolerant offspring of type II (non-insulin dependent) diabetic patients. *Diabetologia* **42**:1314–1323.
- Okamoto T, Schlegel A, Scherer PE and Lisanti MP (1998) Caveolins, a family of scaffolding proteins for organizing "preassembled signaling complexes" at the plasma membrane. *J Biol Chem.* **273**:5419-5422.
- Olden K, Pratt RM and Yamada KM (1979) Selective cytotoxicity of tunicamycin for transformed cells. *Int J Cancer* **24**:60-66.
- Orskov C, Bersani M, Johnsen AH, Hojrup P and Holst JJ (1989) Complete sequences of glucagon-like peptide-1 from human and pig small intestine. *J.Biol.Chem.* **264**:12826-12829.

- Orskov C, Holst JJ, Knuhtsen S, Baldissera FG, Poulsen SS and Nielsen OV (1986) Glucagon-like peptides GLP-1 and GLP-2, predicted products of the glucagon gene, are secreted separately from pig small intestine but not pancreas. *Endocrinology* **119**:1467-1475.
- Orskov C, Holst JJ, Poulsen SS and Kirkegaard P (1987) Pancreatic and intestinal processing of proglucagon in man. *Diabetologia* **30**:874-881.
- Orskov C, Wettergren A and Holst JJ (1993) Biological effects and metabolic rates of glucagon-like peptide-1(7–36) amide and glucagon-like peptide-1(7–37) in healthy subjects are indistinguishable. *Diabetes* **42**:658–661.
- Ozaki N, Shibasaki T, Kashima Y, Miki T, Takahashi K, Ueno H, Sunaga Y, Yano H, Matsuura Y, Iwanaga T, Takai Y and Seino S (2000) cAMP-GEFII is a direct target of cAMP in regulated exocytosis. *Nat Cell Biol* **2**:805–811
- Paetzel M, Karla A, Strynadka NC and Dalbey RE (2002) Signal peptidases. *Chem Rev.* **102**:4549-4580.
- Palczewski K, Kumasaka T, Hori T, Behnke CA, Motoshima H, Fox BA, Le Trong I, Teller DC, Okada T, Stenkamp RE, Yamamoto M and Miyano M (2000) Crystal structure of rhodopsin: a G-protein-coupled receptor. *Science.* **289**:739-745.
- Pang, R, Ng S, Cheng C, Holtmann M, Miller L and Chow B (1999) Role of N-linked glycosylation on the function and expression of the human secretin receptor. *Endocrinology* **140**:5102-5111
- Pantazaka E and Taylor CW (2009). Targeting of inositol 1,4,5-trisphosphate receptor to the endoplasmic reticulum by its first transmembrane domain. *Biochem J.* **425**:61-69.
- Park SY, Ye H, Steiner DF, Bell GI (2010) Mutant proinsulin proteins associated with neonatal diabetes are retained in the endoplasmic reticulum and not efficiently secreted. *Biochem Biophys Res Commun.* **391**:1449-1454.
- Patuzzo C, Castellani C, Sagramoso C, Gomez-Lira M, Bonamini D, Belpinati F, Dehecchi MC, Assael BM and Pignatti PF (2003) Cationic trypsinogen and pancreatic secretory trypsin inhibitor gene mutations in neonatal hypertrypsinemia. *Eur J Hum Genet.* **11**:93-96.
- Pelkmans L, Kartenbeck J and Helenius A (2001) Caveolar endocytosis of simian virus 40 reveals a new two-step vesicular-transport pathway to the ER. *Nat Cell Biol.* **3**:473-483.
- Perley MJ and Kipnis DM (1967) Plasma Insulin Responses to Oral and Intravenous Glucose – Studies in Normal and Diabetic Subjects. *Journal of Clinical Investigation* **46**:1954-1962.
- Perret BG, Wagner R, Lecat S, Brillet K, Rabut G, Bucher B and Pattus F (2003) Expression of EGFP-amino-tagged human mu opioid receptor in Drosophila Schneider 2 cells: a potential expression system for large-scale production of G-protein coupled receptors. *Protein Expr Purif.* **31**:123-132.
- Pitonzo D, Yang Z, Matsumura Y, Johnson AE and Skach WR (2009) Sequence-specific retention and regulated integration of a nascent membrane protein by the endoplasmic reticulum Sec61 translocon. *Mol Biol Cell.* **20**:685-698.

- Plewczynski D, Slabinski L, Ginalska K and Rychlewski L (2008) Prediction of signal peptides in protein sequences by neural networks. *Acta Biochim Pol.* **55**:261-267.
- Pratley RE (2008). Overview of glucagon-like peptide-1 analogs and dipeptidyl peptidase-4 inhibitors for type 2 diabetes. *Medscape J Med.* **10**:171
- Pratley RE and Salsali A (2007) Inhibition of DPP-4: a new therapeutic approach for the treatment of type 2 diabetes. *Curr Med Res Opin.* **23**:919-931.
- Prentki M and Nolan CJ (2006) Islet β -cell failure in type 2 diabetes. *J Clin Invest.* **116**:1802-1812.
- Quoyer J, Longuet C, Broca C, Linck N, Costes S, Varin E, Bockaert J, Bertrand G and Dalle S (2010) GLP-1 mediates antiapoptotic effect by phosphorylating Bad through a beta-arrestin 1-mediated ERK1/2 activation in pancreatic beta-cells. *J Biol Chem.* **285**:1989-2002.
- Rahbar S, Blumenfeld O and Ranney HM (1969) Studies of an unusual hemoglobin in patients with diabetes mellitus. *Biochem. Biophys. Res. Commun.* **36**:838-843.
- Rands E, Candelore MR, Cheung AH, Hill WS, Strader CD and Dixon RA (1990) Mutational analysis of beta-adrenergic receptor glycosylation. *J Biol Chem* **265**:10759-10764.
- Ratner R, Nauck M, Kapitza C, Asnaghi V, Boldrin M and Balena R (2010) Safety and tolerability of high doses of taspoglutide, a once-weekly human GLP-1 analogue, in diabetic patients treated with metformin: a randomized double-blind placebo-controlled study. *Diabet Med.* **27**:556-562.
- Rayner CK, Samsom M, Jones KL and Horowitz M (2001) Relationships of upper gastrointestinal motor and sensory function with glycemic control. *Diabetes Care* **24**:371-381.
- Reed BC, Ronnett GV and Lane MD (1981) Role of glycosylation and protein synthesis in insulin receptor metabolism by 3T3-L1 mouse adipocytes. *Proc Natl Acad Sci U S A.* **78**: 2908-2912.
- Reimann F (2010) Molecular mechanisms underlying nutrient detection by incretin-secreting cells. *Int Dairy J.* **20**:236-242.
- Rhodes CJ and White MF (2002) Molecular insights into insulin action and secretion (2002) *Eur J Clin Invest.* **32**:S3-13.
- Risérus U, Willett WC, Hu FB (2009). Dietary fats and prevention of type 2 diabetes. *Progress in Lipid Research* **48**:44-51.
- Ritter SL and Hall RA (2009) Fine-tuning of GPCR activity by receptor-interacting proteins. *Nat Rev Mol Cell Biol.* **10**:819-830.
- Robben JH, Kortenoeven ML, Sze M, Yae C, Milligan G, Oorschot VM, Klumperman J, Knoers NV and Deen PM (2009) Intracellular activation of vasopressin V2 receptor mutants in nephrogenic diabetes insipidus by nonpeptide agonists. *Proc Natl Acad Sci U S A.* **106**:12195-12200.
- Robles GI and Singh-Franco D (2009) A review of exenatide as adjunctive therapy in patients with type 2 diabetes. *Drug Des Devel Ther.* **21**:219-240.

- Robson A and Collinson I (2006) The structure of the Sec complex and the problem of protein translocation. *EMBO Rep.* **7**:1099-1103.
- Rodrigues AR, Pignatelli D, Almeida H and Gouveia AM (2009) Melanocortin 5 receptor activates ERK1/2 through a PI3K-regulated signaling mechanism. *Mol Cell Endocrinol.* **303**:74-81
- Rosenthal W, Schülein R, Hermosilla R, Oueslati M, Donalies U, Schönenberger E, Krause E and Oksche A (2004) Disease-causing V(2) vasopressin receptors are retained in different compartments of the early secretory pathway. *Traffic.* **5**:993-1005.
- Rouille Y, Westermark G, Martin S and Steiner D (1994) Proglucagon is processed to glucagon by prohormone convertase PC2 in alpha TC1-6 cells. *PNAS* **91**:3242–3246.
- Roux PP, Shahbazian D, Vu H, Holz MK, Cohen MS, Taunton J, Sonenberg N and Blenis J (2007) RAS/ERK signaling promotes site-specific ribosomal protein S6 phosphorylation via RSK and stimulates cap-dependent translation. *J Biol Chem.* **282**:14056-14064.
- Roy S, Perron B and Gallo-Payet N (2010) Role of Asparagine-Linked Glycosylation in Cell Surface Expression and Function of the Human Adrenocorticotropin Receptor (Melanocortin 2 Receptor) in 293/FRT Cells *Endocrinology* **151**: 660-670.
- Rung J, Cauchi S, Albrechtsen A, Shen L, Rocheleau G, Cavalcanti-Proença C, Bacot F, Balkau B, Belisle A, Borch-Johnsen K, Charpentier G, Dina C, Durand E, Elliott P, Hadjadj S, Järvelin MR, Laitinen J, Lauritzen T, Marre M, Mazur A, Meyre D, Montpetit A, Pisinger C, Posner B, Poulsen P, Pouta A, Prentki M, Ribel-Madsen R, Ruukonen A, Sandbaek A, Serre D, Tichet J, Vaxillaire M, Wojtaszewski JF, Vaag A, Hansen T, Polychronakos C, Pedersen O, Froguel P and Sladek R (2009) Genetic variant near IRS1 is associated with type 2 diabetes, insulin resistance and hyperinsulinemia. *Nat Genet.* **41**:1110-1115.
- Runge S, Thøgersen H, Madsen K, Lau J and Rudolph R (2008) Crystal structure of the ligand-bound glucagon-like peptide-1 receptor extracellular domain. *J Biol Chem* **283**:11340-11347.
- Rutz, C., Renner, A., Alken, M., Schulz, K., Beyermann, M., Wiesner, B., Rosenthal, W. and Schülein, R. (2006) The corticotropin-releasing factor receptor type 2a contains an N-terminal pseudo signal peptide. *J. Biol. Chem.* **281**:24910-24921.
- Ruvinsky I, Sharon N, Lerer T, Cohen H, Stolovich-Rain M, Nir T, Dor Y, Zisman P and Meyuhas O (2005) Ribosomal protein S6 phosphorylation is a determinant of cell size and glucose homeostasis. *Genes Dev.* **19**:2199-2211.
- Ruvolo VR, Kurinna SM, Karanjeet KB, Schuster TF, Martelli AM, McCubrey JA and Ruvolo PP (2008). PKR regulates B56 α -mediated BCL2 phosphatase activity in acute lymphoblastic leukemia-derived REH cells. *J Biol Chem* **283**:35474–35485.
- Sadka T and Linial M (2005) Families of membranous proteins can be characterized by the amino acid composition of the transmembrane domains *Bioinformatics.* **21 Suppl 1**:i378-386.

- Sadlish H, Pitonzo D, Johnson AE and Skach WR (2005) Sequential triage of transmembranesegments by Sec61alpha during biogenesis of a native multispanning membrane protein. *Nat Struct Mol Biol.* **12**(10):870-878.
- Salapatek AMF, MacDonald PE, Gaisano HY and Wheeler MB 1999 Mutations to the third cytoplasmic domain of the glucagon-like peptide 1 (GLP-1) receptor can functionally uncouple GLP-1-stimulated insulin secretion in HIT-T15 cells. *Mol Endocrinol* **13**:1305–1317
- Salehi M, Aulinger B, Prigeon RL and D'Alessio DA (2010). Effect of endogenous GLP-1 on insulin secretion in type 2 diabetes. *Diabetes.* **59**:1330-1337.
- Samama P, Cotecchia S, Costa T and Lefkowitz RJ (1993) A mutation-induced activated state of the beta 2-adrenergic receptor. Extending the ternary complex model. *J Biol Chem.* **268**:4625-4636.
- Sambrook and Russell (2001). *Molecular Cloning: A Laboratory Manual*, 3rd edition, Cold Spring Harbor Laboratory Press.
- Sandvig K, Torgersen ML, Raa HA and van Deurs B (2008) Clathrin-independent endocytosis: from nonexisting to an extreme degree of complexity. *Histochem Cell Biol.* **129**:267-276.
- Sawutz DG, Lanier SM, Warren CD and Graham RM (1987) Glycosylation of the mammalian α 1-adrenergic receptor by complex type N-linked oligosaccharides. *Mol. Pharmacol.* **32**:565-571.
- Schirra J, Katschinski M, Weidmann C, Schäfer T, Wank U, Arnold R and Göke B (1996) Gastric emptying and release of incretin hormones after glucose ingestion in humans, *J Clin Invest* **97**:92–103.
- Schlatter P, Beglinger C, Drewe J and Gutmann H (2007). Glucagon-like peptide 1 receptor expression in primary porcine proximal tubular cells. *Regul Pept.* **141**:120-128.
- Schneider G, Fechner U. (2004) Advances in the prediction of protein targeting signals. *Proteomics.* **4**:1571-1580.
- Schröder B and Saftig P. (2010) Molecular insights into mechanisms of intramembrane proteolysis through signal peptide peptidase (SPP). *Biochem J.* **427**:e1-3.
- Schrul B, Kapp K, Sinning I and Dobberstein B (2010) Signal peptide peptidase (SPP) assembles with substrates and misfolded membrane proteins into distinct oligomeric complexes. *Biochem J.* **427**:523-534.
- Schulz K, Rutz C, Westendorf C, Ridelis I, Vogelbein S, Furkert J, Schmidt A, Wiesner B, Schüle R (2010) The pseudo signal peptide of the corticotropin-releasing factor receptor type 2a decreases receptor expression and prevents Gi-mediated inhibition of adenylyl cyclase activity. *J Biol Chem.* **285**:32878-32887.
- Schwartz TW and Holst B (2006) Ago-allosteric modulation and other types of allosterism in dimeric 7TM receptors. *J Recept Signal Transduct Res.* **26**:107-128.
- Schwartz TW and Holst B (2007) Allosteric enhancers, allosteric agonists and ago-allosteric modulators: where do they bind and how do they act? *Trends Pharmacol Sci.* **28**:366-373.

- Schwarz PE, Reimann M, Li J, Bergmann A, Licinio J, Wong ML and Bornstein SR (2007) The Metabolic Syndrome - a global challenge for prevention. *Horm Metab Res.* **39**:777-780.
- Sloop KW, Cao JX, Siesky AM, Zhang HY, Bodenmiller DM, Cox AL, Jacobs SJ, Moyers JS, Owens RA, Showalter AD, Brenner MB, Raap A, Gromada J, Berridge BR, Monteith DK, Porksen N, McKay RA, Monia BP, Bhanot S, Watts LM, and Michael MD (2004) Hepatic and glucagon-like peptide-1-mediated reversal of diabetes by glucagon receptor antisense oligonucleotide inhibitors. *J Clin Invest.* **113**:1571-1581.
- Sequeira M, Jasani B, Fuhrer D, Wheeler M and Ludgate M (2002) Demonstration of reduced in vivo surface expression of activating mutant thyrotrophin receptors in thyroid sections. *Eur J Endocrinol.* **146**:163-171.
- Serre, V., Dolci, W., Schaerer, E., Scrocchi, L., Drucker, D., Efrat, S., and Thorens, B. (1998) *Endocrinology* **139**: 4448-4454.
- Setacci C, de Donato G, Setacci F and Chisci E (2009) Diabetic patients: epidemiology and global impact. *J Cardiovasc Surg (Torino).* **50**:263-273.
- Shaw JE, Sicree RA and Zimmet PZ (2010) Global estimates of the prevalence of diabetes for 2010 and 2030. *Diabetes Res Clin Pract.* **87**:4-14.
- Shimada M, Chen X, Cvrk T, Hilfiker H, Parfenova M and Segre GV (2002) Purification and characterization of a receptor for human parathyroid hormone and parathyroid hormone-related peptide. *J Biol Chem* **277**:31774–31780.
- Short Clinical Guidelines Technical Team (2009). Type 2 diabetes: newer agents. NICE short clinical guideline 87. <http://www.nice.org.uk/nicemedia/pdf/CG87NICEGuideline.pdf>. Accessed 23 June, 2010.
- Shu L, Matveyenko AV, Kerr-Conte J, Cho JH, McIntosh CH and Maedler K (2009). Decreased TCF7L2 protein levels in type 2 diabetes mellitus correlate with downregulation of GIP- and GLP-1 receptors and impaired beta-cell function. *Hum Mol Genet.* **18**:2388-2399.
- Shukla AK, Reinhart C and Michel H (2006) Biochem Comparative analysis of the human angiotensin II type 1a receptor heterologously produced in insect cells and mammalian cells. *Biophys Res Commun.* **349**:6-14.
- Smit MJ, Leurs R, Alewijnse AE, Blauw J, Van Nieuw Amerongen GP, Van De Vrede Y, Roovers E and Timmerman H (1996) Inverse agonism of histamine H2 antagonist accounts for upregulation of spontaneously active histamine H2 receptors. *Proc Natl Acad Sci U S A.* **93**:6802-6807.
- Sniderman, AD, Bhopal R, Prabhakaran D, Sarrafzadegan N and Tchernof A (2007) Why might South Asians be so susceptible to central obesity and its atherogenic consequences? The adipose tissue overflow hypothesis. *International journal of epidemiology* **36**:220–225.
- Stewart RS, Drisaldi B and Harris DA. A transmembrane form of the prion protein contains an uncleaved signal peptide and is retained in the endoplasmic Reticulum. *Mol Biol Cell.* **12**:881-889.

- Stoffel M, Espinosa R III, Le Beau MM and Bell GI (1993) Human glucagon-like peptide-1 receptor gene: localization to chromosome band 6p21 by fluorescence in situ hybridization and linkage of a highly polymorphic simple tandem repeat DNA polymorphism to other markers on chromosome 6. *Diabetes* **42**:1215-1218
- Stoner GD (2005) Hyperosmolar hyperglycemic state. *Am Fam Physician*. **71**:1723-1730.
- Strachan RT, Sheffler DJ, Willard B, Kinter M, Kiselar JG and Roth BL (2009) Ribosomal S6 kinase 2 directly phosphorylates the 5-hydroxytryptamine 2A (5-HT2A) serotonin receptor, thereby modulating 5-HT2A signalling. *J Biol Chem*. **284**:5557-5573.
- Stulc T and Sedo A (2010) Inhibition of multifunctional dipeptidyl peptidase-IV: is there a risk of oncological and immunological adverse effects? *Diabetes Res Clin Pract*. **88**:125-131.
- Su H, He M, Li H, Liu Q, Wang J, Wang Y, Gao W, Zhou L, Liao J, Young AA and Wang MW (2008) Boc5, a non-peptidic glucagon-like Peptide-1 receptor agonist, invokes sustained glycemic control and weight loss in diabetic mice. *PLoS One*. **3**:e2892.
- Swinnen SG, Hoekstra JB and DeVries JH (2009) Insulin therapy for type 2 diabetes. *Diabetes Care*. **32**:S253-259.
- Syme CA, Zhang L and Bisello A (2006) Caveolin-1 regulates cellular trafficking and function of the glucagon-like peptide 1 receptor. *Mol Endocrinol* **20**:3400–3411.
- Takhar S, Gyomory S, Su RC, Mathi SK, Li X and Wheeler MB (1996) The third cytoplasmic domain of the tGLP-1 (7–36 amide) receptor is required for coupling to the adenylyl cyclase system. *Endocrinology* **137**:2175–2178.
- Tansky MF, Pothoulakis C and Leeman SE (2007) Functional consequences of alteration of N-linked glycosylation sites on the neurokinin 1 receptor *Proc Natl Acad Sci U S A*. **104**:10691-10696.
- Thim L and Moody AJ (1981) The Primary Structure of Porcine Glicentin (Proglucagon). *Regulatory Peptides* **2**:139-150.
- Thomas L, Leduc R, Thorne BA, Smeekens SP, Steiner DF and Thomas G (1991) Kex2-like endoproteases PC2 and PC3 accurately cleave a model prohormone in mammalian cells: evidence for a common core of neuroendocrine processing enzymes. *Proc Natl Acad Sci USA* **88**:5297-5301
- Thorens B (1992) Expression cloning of the pancreatic β -cell receptor for the glucagon-like peptide 1. *Proc Natl Acad Sci U S A*. **89**:8641-8645.
- Thorens B and Widmann C (1996) Signal transduction and desensitization of the glucagon-like peptide-1 receptor. *Acta Physiol Scand* **157**:317-319.
- Thorens B, Porret A, Bühler L, Deng SP, Morel P and Widmann C (1993) Cloning and functional expression of the human islet GLP-1 receptor. Demonstration that exendin-4 is an agonist and exendin-(9-39) an antagonist of the receptor. *Diabetes* **42**:1678-1682.

- Tierney LM, McPhee SJ and Papadakis MA (2002) Current medical Diagnosis & Treatment. International edition. New York: Lange Medical Books/McGraw-Hill, pp1203-1215.
- Tobin AB (2008) G-protein-coupled receptor phosphorylation: where, when and by whom. *Br J Pharmacol.* **153** (Suppl 1):S167-176.
- Tomas E and Habener JF (2010) Insulin-like actions of glucagon-like peptide-1: a dual receptor hypothesis. *Trends Endocrinol Metab.* **21**:59-67.
- Tornehave D, Kristensen P, Rømer J, Knudsen LB and Heller RS (2008) Expression of the GLP-1 receptor in mouse, rat, and human pancreas. *J Histochem Cytochem.* **56**:841-851.
- Tovey SC and Willars GB (2004) Single-cell imaging of intracellular Ca²⁺ and phospholipase C activity reveals that RGS 2, 3, and 4 differentially regulate signaling via the Galphaq/11-linked muscarinic M3 receptor. *Mol Pharmacol.* **66**:1453-1464.
- Tuteja N (2009) Signaling through G-protein coupled receptors. *Plant Signal Behav.* **4**:942-947.
- Underwood CR, Garibay P, Knudsen LB, Hastrup S, Peters GH, Rudolph R and Reedtz-Runge S (2010) Crystal structure of glucagon-like peptide-1 in complex with the extracellular domain of the glucagon-like peptide-1 receptor. *J Biol Chem.*; **285**:723-30.
- Unger J and Parkin CG (2010) Type 2 diabetes: an expanded view of pathophysiology and therapy. *Postgrad Med.* **122**:145-157.
- Urban JD, Clarke WP, von Zastrow M, Nichols DE, Kobilka B, Weinstein H, Javitch JA, Roth BL, Christopoulos A, Sexton PM, Miller KJ, Spedding M and Mailman RB (2007). Functional selectivity and classical concepts of quantitative pharmacology. *Pharmacol Exp Ther.* **320**:1-13.
- Vahl TP, Tauchi M, Durler TS, Elfers EE, Fernandes TM, Bitner RD, Ellis KS, Woods SC, Seeley RJ, Herman JP and D'Alessio DA. (2007) Glucagon-like peptide-1 (GLP-1) receptors expressed on nerve terminals in the portal vein mediate the effects of endogenous GLP-1 on glucose tolerance in rats. *Endocrinology* **148**:4965-4973.
- van Eyll B, Lankat-Buttgereit B, Bode HP, Göke R and Göke B (1994) Signal transduction of the GLP-1-receptor cloned from a human insulinoma. *FEBS Lett.* **348**:7-13.
- van Genugten RE, van Raalte DH and Diamant M (2009) Does glucagon-like peptide-1 receptor agonist therapy add value in the treatment of type 2 diabetes? Focus on exenatide. *Diabetes Res Clin Pract.* **86** (Suppl 1):S26-34.
- van Koppen CJ and Nathanson NM (1990) Site-directed mutagenesis of the m2 muscarinic acetylcholine receptor. Analysis of the role of N-glycosylation in receptor expression and function. *J. Biol. Chem.* **265**:20887-2082.
- Varki A, Cummings RD, Esko JD, Freeze HH, Stanley P, Bertozzi CR, Hart GW and Etzler ME, editors (2009) Essentials of Glycobiology. 2nd edition. Cold Spring Harbor (NY): Cold Spring Harbor Laboratory Press.

- Vázquez P, Roncero I, Blázquez E and Alvarez E (2005a) The cytoplasmic domain close to the transmembrane region of the glucagon-like peptide-1 receptor contains sequence elements that regulate agonist-dependent internalisation. *J Endocrinol* **186**:221–231.
- Vázquez P, Roncero I, Blázquez, and Alvarez E (2005b) Substitution of the cysteine 438 residue in the cytoplasmic tail of the glucagon-like peptide-1 receptor alters signal transduction activity. *J Endocrinology* **185**:35–44.
- Venables MC and Jeukendrup AE (2009) Physical inactivity and obesity: links with insulin resistance and type 2 diabetes mellitus. *Diabetes Metab Res Rev.* **25** (Suppl 1): S18-23.
- Vezzosi D, Bennet A, Fauvel J and Caron P (2007) Insulin, C-peptide and proinsulin for the biochemical diagnosis of hypoglycaemia related to endogenous hyperinsulinism. *Eur J Endocrinol.* **157**:75-83.
- Villardaga JP, Bünemann M, Feinstein TN, Lambert N, Nikolaev VO, Engelhardt S, Lohse MJ and Hoffmann C (2009) GPCR and G-proteins: drug efficacy and activation in live cells. *Mol Endocrinol.* **23**:590-599.
- VilSB, Il T, Krarup T, Madsbad S and Holst JJ (2002) Defective amplification of the late phase insulin response to glucose by GIP in obese Type II diabetic patients. *Diabetologia* **45**:1111-1119.
- Virk MS, Arttamangkul S, Birdsong WT and Williams JT (2009) Buprenorphine is a weak partial agonist that inhibits opioid receptor desensitization. *J Neurosci.* **29**:7341-7348.
- von Heijne G (1990) The signal peptide. *J. Membr. Biol.* **115**:195–201.
- Wallin E and von Heijne G (1995) Properties of N-terminal tails in G-protein coupled receptors: a statistical study. *Protein Eng.* **8**: 693–698.
- Walter P and Lingappa VR. 1986. Mechanism of protein translocation across the endoplasmic reticulum membrane. *Annu. Rev. Cell Biol.* **2**:499-516.
- Wang L, Martin B, Brennehan R, Luttrell LM and Maudsley S.J (2009) Allosteric modulators of g protein-coupled receptors: future therapeutics for complex physiological disorders. *Pharmacol Exp Ther.* **331**:340-348.
- Wang Q, Li L, Xu E, Wong V and Rhodes C (2004) Brubaker PL. Glucagon-like peptide-1 regulates proliferation and apoptosis via activation of protein kinase B in pancreatic INS-1 beta cells. *Diabetologia.* **47**:478-487.
- Wei Y and Mojsov S (1995) Tissue-specific expression of the human receptor for glucagon-like peptide 1: brain, heart and pancreatic forms have the same deduced amino acid sequences. *FEBS Lett* **358**:219-224.
- White SH, Ladokhin AS, Jayasinghe S and Hristova K (2001) How membranes shape protein structure. *J Biol Chem.* **276**:32395-32398.
- White SH and von Heijne G (2005) Transmembrane helices before, during, and after insertion. *Curr Opin Struct Biol.* **15**:378-386
- Wideman RD, Covey SD, Webb GC, Drucker DJ and Kieffer TJ (2007) A switch from prohormone convertase (PC)-2 to PC1/3 expression in transplanted alpha-cells is

- accompanied by differential processing of proglucagon and improved glucose homeostasis in mice. *Diabetes*. **56**:2744-2752.
- Wideman RD, Gray SL, Covey SD, Webb GC, and Kieffer TJ (2009) Transplantation of PC1/3-Expressing α -cells Improves Glucose Handling and Cold Tolerance in Leptin-resistant Mice. *Mol Ther*. **17**:191–198.
- Wideman RD, Yu IL, Webber TD, Verchere CB, Johnson JD, Cheung AT and Kieffer TJ (2006) Improving function and survival of pancreatic islets by endogenous production of glucagon-like peptide 1 (GLP-1). *Proc Natl Acad Sci U S A*. **103**:13468-13473.
- Widmann C, Dolci W and Thorens B (1995) Agonist-induced internalization and recycling of the glucagon-like peptide-1 receptor in transfected fibroblasts and in insulinomas. *Biochem J* **310**:203–214.
- Widmann C, Dolci W and Thorens B (1996) Desensitization and phosphorylation of the glucagon-like peptide-1 (GLP-1) receptor by GLP-1 and 4-phorbol 12-myristate 13-acetate. *Mol Endocrinol*. **10**:62-75.
- Widmann C, Dolci W and Thorens B (1997) Internalization and homologous desensitization of the GLP-1 receptor depend on phosphorylation of the receptor carboxyl tail at the same three sites. *Mol Endocrinol* **11**:1094-1102.
- Widmann C, Dolci W and Thorens B (1995) Agonist-induced internalization and recycling of the glucagon-like peptide-1 receptor in transfected fibroblasts and in insulinomas. *Biochem J* **310**:203–214.
- Willars GB, Royall JE, Nahorski SR, El Gehani F, Everest H and McArdle CA (2001). Rapid down-regulation of the type I inositol 1,4,5-trisphosphate receptor and desensitization of gonadotropin-releasing hormone-mediated Ca²⁺ responses in alpha T3-1 gonadotropes. *J Biol Chem* **276**:3123–3129.
- Wilmen A, Van EB, Goke B and Goke R (1997) Five Out of Six Tryptophan residues in the N-terminal extracellular domain of the rat GLP-1 receptor are essential for its ability to bind GLP-1. *Peptides* **18**:301-305.
- Witt H, Luck W and Becker M (1999) A signal peptide cleavage site mutation in the cationic trypsinogen gene is strongly associated with chronic pancreatitis. *Gastroenterology*. **117**:7-10.
- Wolfe BL and Trejo J (2007) Clathrin-dependent mechanisms of G-protein-coupled receptor endocytosis. *Traffic*. **8**:462-470.
- Woodcock DM, Crowther PJ, Doherty J, Jefferson S, DeCruz E, Noyer-Weidner M, Smith SS, Michael MZ and Graham MW (1989) Quantitative evaluation of Escherichia coli host strains for tolerance to cytosine methylation in plasmid and phage recombinants. *Nucleic Acids Res*. **17**:3469-3478.
- World Health Organization (1999) Definition, Diagnosis and Classification of Diabetes Mellitus and Its Complications: Report of a WHO Consultation. WHO/NCD/NCS/99.2. Geneva: WHO.
http://www.staff.ncl.ac.uk/philip.home/who_dmc.htm
- World Health Organization (2006) Definition, diagnosis and classification of diabetes mellitus and its complications: Report of a WHO Consultation. Part 1. Diagnosis

and classification of diabetes mellitus".
<http://www.who.int/diabetes/publications/en/>.

- Wright EE Jr. (2009) Overview of insulin replacement therapy. *J Fam Pract.* **58**(Suppl):S3-9.
- Xiao Q, Jeng W and Wheeler MB (2000) Characterization of glucagon-like peptide-1 receptor-binding determinants. *J Mol Endocrinol* **25**(3): 321-335
- Xu G, Kaneto H, Laybutt DR, Duvivier-Kali VF, Trivedi N, Suzuma K, King GL, Weir GC and Bonner-Weir S (2007) Downregulation of GLP-1 and GIP receptor expression by hyperglycemia: possible contribution to impaired incretin effects in diabetes. *Diabetes.* **56**:1551-1558..
- Yu DM, Yao TW, Chowdhury S, Nadvi NA, Osborne B, Church WB, McCaughan GW and Gorrell MD (2010) The dipeptidyl peptidase IV family in cancer and cell biology. *FEBS J.* **277**:1126-1144.
- Zander M, Madsbad S, Madsen JL and Holst JJ (2002) Effect of 6-week course of glucagon-like peptide 1 on glycaemic control, insulin sensitivity and beta-cell function in type 2 diabetes: a parallel-group study. *Lancet* **359**:824-830
- Zhang R, Kim TK, Qiao ZH, Cai J, Pierce WM Jr and Song ZH (2007) Biochemical and mass spectrometric characterization of the human CB2 cannabinoid receptor expressed in *Pichia pastoris*--importance of correct processing of the N-terminus. *Protein Expr Purif.* **55**:225-235.
- Zhang X, Schaffitzel C, Ban N and Shan SO (2009). Multiple conformational switches in a GTPase complex control co-translational protein targeting. *Proc Natl Acad Sci U S A.* **106**:1754-1759.
- Zhang Y, Wang Q, Zhang J, Lei X, Xu GT and Ye W. (2009) Protection of exendin-4 analogue in early experimental diabetic retinopathy. *Graefes Arch Clin Exp Ophthalmol.* **247**:699-706.
- Zhang Z and Henzel WJ (2004) Signal peptide prediction based on analysis of experimentally verified cleavage sites. *Prot. Sci.* **13**:2819-2824.
- Zhao JH, Liu HL, Lin HY, Huang CH, Fang HW, Chen SS, Ho Y, Tsai WB and Chen WY (2007) Chemical chaperone and inhibitor discovery: potential treatments for protein conformational diseases. *Perspect Medicin Chem.* **1**:39-48.
- Zheng D, Ionut V, Mooradian V, Stefanovski D and Bergman RN (2009) Exenatide sensitizes insulin-mediated whole-body glucose disposal and promotes uptake of exogenous glucose by the liver. *Diabetes.* **58**:352-359.
- Zhou, A, Assil I, Abou-Samra AB (2000) Role of asparagine-linked oligosaccharides in the function of the rat PTH/PTHrP receptor. *Biochemistry* **39**:6514-6520.
- Zimmet P, Alberti KG and Shaw J (2001) Global and societal implications of the diabetes epidemic. *Nature.* **414**:782-787.